

Modelling of a Natural-Gas-Based Clean Energy Hub

by

Abduslam Sharif

A thesis

presented to the University of Waterloo

in fulfillment of the

thesis requirement for the degree of

Master of Applied Science

in

Chemical Engineering

Waterloo, Ontario, Canada, 2012

©Abduslam Sharif 2012

AUTHOR'S DECLARATION

I hereby declare that I am the sole author of this thesis. This is a true copy of the thesis, including any required final revisions, as accepted by my examiners.

I understand that my thesis may be made electronically available to the public.

ABSTRACT

The increasing price of fuel and energy, combined with environmental laws and regulations, have led many different energy producers to integrate renewable, clean energy sources with non-renewable ones, forming the idea of *energy hubs*. Energy hubs are systems of technologies where different energy forms are conditioned and transformed. These energy hubs offer many advantages compared to traditional single-energy sources, including increased reliability and security of meeting energy demand, maximizing use of energy and materials resulting in increasing the overall system efficiency.

In this thesis, we consider an energy hub consisting of natural gas (NG) turbines for the main source of energy— electricity and heat— combined with two renewable energy sources—wind turbines and PV solar cells. The hub designed capacity is meant to simulate and replace the coal-fired Nanticoke Generating Station with NG-fired power plant. The generating station is integrated with renewable energy sources, including wind and solar. The hub will also include water electrolysers for hydrogen production. The hydrogen serves as an energy storage vector that can be used in transportation applications, or the hydrogen can be mixed into the NG feed stream to the gas turbines to improve their emission profile. Alkaline electrolysers' technology is fully mature to be applied in large industrial applications. Hydrogen, as an energy carrier, is becoming more and more important in industrial and transportation sectors, so a significant part of the thesis will focus on hydrogen production and cost.

In order to achieve the goal of replacing the Nanticoke Coal-fired Power Plant by introducing the energy hub concept, the study investigates the modeling of the combined system of the different technologies used in terms of the total energy produced, cost per kWh, and emissions. This modeling is done using GAMS® in order to make use of the optimization routines in the software. The system is modeled so that a minimum cost of energy is achieved taking into account technical and thermodynamic constraints. Excess energy produced during off-peak demand by wind turbines and PV solar cells is used to feed the electrolyser to produce H₂ and O₂. Through this method, a significant reduction in energy cost and greenhouse gas (GHG) emissions are achieved, in addition to an increased overall efficiency.

ACKNOWLEDGEMENTS

It is a pleasure to thank those without their support, encouragement, and advice, this thesis would never have been possible.

I would like to express my sincere thanks to my supervisors, Prof. Ali Elkamel, and Prof. Michael Fowler, for their guidance, encouragement, and patience throughout this study. It is my honour to be under their supervision, and it is my honour to be one of their students.

I owe my deepest gratitude to my family: my father, my sisters, and my brothers for their support and encouragement. I am very grateful to those friends who gave support and encouragement throughout my study; my strength in need.

I would like to thank Prof. Peter Douglas and Prof. Evgueniy Entchev for their time to review this work and the useful suggestions and comments they provided.

My thanks go to those who have contributed to this work, particularly the Libyan Ministry of Higher Education for sponsoring me throughout this program.

Abduslam Sharif

April 2012

DEDICATION

I dedicate this thesis to my father and my siblings. Without their support, patience, and help, the completion of this work would not have been possible.



TABLE OF CONTENTS

LIST OF FIGURES	x
LIST OF TABLES.....	xiii
GLOSSARY	xiv
CHAPTER 1	1
1.1 Model Overview.....	1
1.2 Research Motivations.....	3
1.3 Research Objectives	5
1.4 The Project’s Scope and Scale	6
1.5 The Modeling Approach	7
CHAPTER 2	8
2.1 Energy Hubs.....	8
2.1.1 Energy hubs overview.....	8
2.1.2 Motivations	9
2.1.3 Power generation	10
2.1.4 Hub modeling.....	12
2.1.5 Illustrative case studies	14
2.1.6 Environmental benefits	17
2.2 Gas Turbines Power Plants	19
2.2.1 Simple cycle power plants (SCPPs).....	21
2.2.2 Combined cycle power plants (CCPPs).....	24
2.2.3 Hydrogen-NG turbines.....	26
2.2.4 Gas emissions.....	26
2.3 Wind Energy	27
2.3.1 Wind energy overview	27

2.3.2	Wind turbines.....	31
2.3.3	Economics and growth of wind energy	31
2.4	Solar Energy.....	33
2.4.1	Solar energy overview	33
2.4.2	PV solar cells	36
2.4.3	Economics of solar energy.....	38
2.5	Electrolysers.....	40
2.5.1	Electrolysers overview.....	40
2.5.2	Electrolyser selected, advantages, and challenges.....	44
2.6	Hydrogen Economy.....	45
2.6.1	Hydrogen production	45
2.6.2	Hydrogen infrastructures	48
2.6.3	Motivations for hydrogen economy.....	49
2.6.4	Challenges and barriers to hydrogen economy.....	50
2.7	Ontario and Nanticoke Region Overview	51
2.7.1	Province of Ontario.....	51
2.7.2	Nanticoke region.....	54
CHAPTER 3		56
3.1	Parameters and Design Variables.....	56
3.1.1	Gas turbine power plant.....	56
3.1.2	Wind turbines.....	63
3.1.3	PV solar cells	69
3.1.4	Electrolysers.....	72
3.2	Modeling Logic	76
3.2.1	NG turbines ML.....	76

3.2.2	Wind turbines ML.....	76
3.2.3	PV solar cells ML	81
3.2.4	Electrolysers ML.....	81
CHAPTER 4	84
4.1	GAMS® Overview	84
4.2	Model Scenarios.....	85
4.2.1	Scenario A: NG stand-alone power plant	85
4.2.2	Scenario B: NG-renewable energy hub	86
4.2.3	Scenario C: Hydrogen economy	87
4.3	Scenarios Development.....	88
4.3.1	Scenario A: NG stand-alone power plant	88
4.3.2	Scenario B: NG-renewable energy hub	91
4.3.3	Scenario C: Hydrogen economy	94
CHAPTER 5	98
5.1	Scenario A: NG Stand-Alone Power Plant	98
5.1.1	Electricity generation.....	98
5.1.2	Electricity cost	100
5.1.3	GHG emissions.....	101
5.1.4	Summary.....	102
5.2	Scenario B: NG-Renewable Energy Hub.....	103
5.2.1	Electricity generation.....	103
5.2.2	Electricity cost	107
5.2.3	Summary.....	110
5.3	Scenario C: Hydrogen Economy.....	111
5.3.1	Electricity generation.....	112

5.3.2	Hydrogen and oxygen production.....	115
5.3.3	Electricity cost	116
5.3.4	Summary	118
5.4	Comparison between Scenarios	120
CHAPTER 6	122
6.1	Conclusion.....	122
6.2	Recommendations for Future Work.....	123
REFERENCES	125
APPENDICES	135
APPENDIX A	135
APPENDIX B	137
Scenario A	: NG stand-alone power plant.....	137
Scenario B	: NG-renewable energy hub.....	140
Scenario C	: Hydrogen economy.	143
APPENDIX C	146

LIST OF FIGURES

Figure 1.1 Schematic block diagram of the proposed energy hub.....	3
Figure 2.1 Block diagram features of energy hubs.	9
Figure 2.2 An example of an energy hub (Favre-Perrod et al., 2005).	13
Figure 2.3 Predicted cost of electricity (Sirikitputtisak et al., 2009).	15
Figure 2.4 Schematic of systems and energy interactions in the clean energy hub model (Syed et al., 2009).	16
Figure 2.5 Simple cycle power plant flowchart.	22
Figure 2.6 Brayton ideal cycle for GT engines, $T-s$ diagram.	23
Figure 2.7 Combined cycle power plant flowchart.	24
Figure 2.8 Rankine ideal cycle for GT engines, $T-s$ diagram.	25
Figure 2.9 Wind rose plot of Nanticoke region at 42.791N & -80.168W.	30
Figure 2.10 Probability distribution of wind speed and power at Nanticoke region at 42.791N & -80.168W.	30
Figure 2.11 World cumulative production of wind energy.....	32
Figure 2.12 Overview of the different solar cell technologies.....	34
Figure 2.13 Solar-gas turbine hybrid system.	35
Figure 2.14 Current-voltage characteristics of SunPower-400 model.....	37
Figure 2.15 World annual market of PV energy (2000–2009).	39
Figure 2.16 Schematic diagram of SPE water electrolyser.....	41
Figure 2.17 Mechanism of PEM water electrolysis.....	42
Figure 2.18 Alkaline electrolyzers operating principles.	43
Figure 2.19 Main technological routes to hydrogen production from renewable sources.....	46
Figure 2.20 Ontario electricity supply generation and transmission highlights.	51
Figure 2.21 Ontario’s existing installed generation capacity by fuel type as of 2011.....	53
Figure 2.22 Assumed hydrogen transition in Ontario.....	54
Figure 2.23 Nanticoke Region overview, the proposed site for the energy hub (Google Map, 2010).	55
Figure 3.1 The proposed CCPP process flow diagram.	58
Figure 3.2 NG turbine ML block diagram.	78
Figure 3.3 Onshore wind power ML block diagram.....	79

Figure 3.4 Offshore wind power ML block diagram.....	80
Figure 3.5 PV solar cells ML block diagram.....	82
Figure 3.6 Alkaline electrolyzers ML block diagram.....	83
Figure 4.1 Scenario B ML block diagram.....	93
Figure 4.2 Scenario C ML block diagram.....	97
Figure 5.1 Net hourly energy produced from the power plant, Scenario A.....	99
Figure 5.2 Hourly number of combined cycle units (1x1) in operation, Scenario A.....	99
Figure 5.3 Hourly costs of electricity from the power plant, Scenario A.....	100
Figure 5.4 Hourly gas emissions from the CCPP, Scenario A.....	101
Figure 5.5 Energy produced from the hub, Scenario B.....	104
Figure 5.6 Hourly efficiency of PV solar modules, Scenario B.....	105
Figure 5.7 Monthly total energy produced from the hub, Scenario B.....	106
Figure 5.8 Cost of energy from the energy hub components, Scenario B.....	108
Figure 5.9 Monthly average cost of energy produced from the hub, Scenario B.....	109
Figure 5.10 Energy produced and consumed from the hub, Scenario C.....	113
Figure 5.11 Monthly total energy produced and consumed by the hub, Scenario C.....	114
Figure 5.12 Hydrogen and oxygen produced from the electrolyser units.....	115
Figure 5.13 Hourly number of electrolyzers in operation and their turndown factors.....	115
Figure 5.14 Cost of energy produced from the energy hub components, Scenario C.....	117
Figure 5.15 Hydrogen and oxygen cost profiles, Scenario C.....	118
Figure A.1 Seasonal average onshore and offshore wind speed, Nanticoke, ON.....	135
Figure A.2 Hourly temperature and solar radiation (Maniyali, 2009).....	135
Figure A.3 Ontario's hourly electricity demand in 2009.....	136
Figure A.4 Ontario's hourly electricity cost in 2009.....	136
Figure A.5 Average monthly NG price.....	136
Figure A.6 Hourly energy produced from the power plant, a ten-day sample.....	137
Figure A.7 Total monthly energy production from 3,150 MW CCPP.....	137
Figure A.8 Hourly operating capacity of combined cycle units.....	138
Figure A.9 Hourly costs of the power plant, a ten-day sample.....	138
Figure A.10 Hourly gas emissions from the CCPP, a ten-day sample.....	139
Figure A.11 Hourly number of CCPP units in operation.....	140

Figure A.12 Energy produced from the hub, a ten-day sample.....	140
Figure A.13 PV solar cells operation status: [0] OFF, [1] ON.....	141
Figure A.14 Sample hourly PV solar energy produced at the beginning of each month.	141
Figure A.15 Hourly cost of PV solar energy.....	141
Figure A.16 Hourly cost of electricity, Scenario B.....	142
Figure A.17 Hourly number of CCPP units in operation.....	143
Figure A.18 Energy produced from the hub, a ten-day sample, 1-10 January.....	143
Figure A.19 Monthly average cost of energy produced and consumed by the hub, Scenario C.....	144
Figure A.20 Hourly cost of electricity, a ten-day sample, 1-10 January.....	145

LIST OF TABLES

Table 2.1 Canadian’s current installed and projected capacity by province.....	33
Table 2.2 Overview of PV solar technologies	36
Table 2.3 Nuclear hydrogen production technologies overview.	47
Table 2.4 Total annual Ontario energy demand.....	52
Table 3.1 NG turbine parameters and specifications.	57
Table 3.2 Onshore wind data for Nanticoke, ON (Environment Canada, 2003).....	64
Table 3.3 GE1.5 SLE model wind turbine parameters and specifications.	64
Table 3.4 Offshore wind data for Nanticoke, ON (Environment Canada, 2003).	67
Table 3.5 Siemens SWT2.3-93 model wind turbine parameters and specifications (Siemens AG, 2009).	68
Table 3.6 SPR-400 model PV module parameters and specifications (Sunpower Cor., 2010)....	70
Table 3.7 Specifications of the alkaline electrolyser.	73
Table 4.1 Scenario A: NG stand-alone power plant key inputs and outputs.	86
Table 4.2 Scenario B: NG-renewable energy key inputs and outputs.	87
Table 4.3 Scenario C: Hydrogen economy key inputs and outputs.....	88
Table 5.1 Summary of results: Scenario A.	102
Table 5.2 Summary of results: Scenario B.	110
Table 5.3 Seasonal and annual hydrogen production and cost.	116
Table 5.4 Summary of results: Scenario C.	118
Table 5.5 Comparison between scenarios.....	121

GLOSSARY

CANWEA	Canadian Wind Energy Association
CCGT	Combined cycle gas turbine
CCP	Combined heat and power
CCPP	Combined cycle power plant
CHP	Combined heat and power
EH	Energy hub
EPA	U.S. Environmental Protection Agency
EPIA	European Photovoltaic Industry Association
FC	Fuel cell
FCVs	Fuel cell vehicles
GAMS	General Algebraic Modeling System
GHG	Greenhouse gas
GT	Gas turbine
HCS	Hydrocarbons
HHV	Higher heating value
Hythane	A name given to the mixture of hydrogen and methane
ICC	Installed capital cost
ICE	Internal combustion engine
IEA	International Energy Agency
IESO	Independent Electricity System Operator
IGCC	Integrated gasification combined cycle
LHV	Lower heating value

LP	Linear programming
MIP	Mixed integer programming
NG	Natural gas
NGPP	Natural gas power plant
NLP	Non-linear programming
O&M	Operations and maintenance
OME	Ontario Ministry of Energy
OPG	Ontario Power Generation
PCS	Power conditioning system
PEM	Polymer electrolyte material
PM	Particulate matter
PV	photovoltaic
R&D	Research and development
SCPP	Simple cycle power plant
SMR	Steam-methane reforming
SPE	Solid polymer electrolyte
ST	Steam turbine
U.S. DOE	U.S. Department of Energy
UHCs	Unburned hydrocarbons
VOCs	Volatile organic compounds
WT	Wind turbine

CHAPTER 1

Introduction

1.1 Model Overview

In this chapter, an overview of the proposed energy hub, the technologies to be employed for the various components are shown. A schematic diagram represents the general flow of energy and materials and displays the major units in the hub, is suggested. The motivations and the objectives behind establishing such research are discussed in Sections 1.2 and 1.3. The project scale and the modeling procedures are explored in this chapter, as well. The remainder of the chapter reviews the energy profile of the proposed site in Nanticoke, Ontario, and closes by discussing the potential environmental benefits of this research.

There have been few studies that show the integrated system of the renewable and non-renewable energy sources compared to the independent systems. The integrated energy systems have received extra diligence for their environmental benefits against controversial power plants with their dependency on fossil fuels (Giannakoudis et al., 2010). Such integrated and interconnected energy systems where multiple energy carriers can be converted, conditioned and stored (Geidl et al., 2007), are called *energy hubs*.

Energy carriers (including electricity, natural gas [NG], hydrogen, and district heat) are of major importance in commercial and residential use. This study focuses on production, exchange and conversion of energy between several types of energy generators with a natural gas power plant (NGPP) as a key energy producer within the hub. In a combined cycle power plant (CCPP), or combined cycle gas turbine (CCGT) plant, a gas turbine generator generates electricity, and the heat of its exhaust is used to make steam, which in turn drives a steam turbine to generate additional electricity.

For further improvement, NG-enhanced-H₂ gas turbines can be considered in further studies as they offer higher combustion rate, more complete combustion and hence more efficiency than NG alone, and lower urban air emissions (specifically NO_x). In a study done by Pawlowski

(2009) on implementing Hythane as an alternative to NG combustion has been found that adding hydrogen to NG resulted in a cleaner and more efficient combustion. Moreover, energy produced increased and the emissions reduced. More discussions and work on H₂-NG are presented in (Phillips & Roby, 2000; Sierens & Rosseel, 2000; Chiesa et al., 2005; & Cheng et al., 2009).

The NGPP will ensure a reliable, non-intermittent supply of electricity, while wind turbines (WTs) and photovoltaic (PV) solar cells provide an emission free (both criteria emissions and greenhouse gases) renewable supply of electricity. Alkaline electrolyzers use water and excess electricity from the WTs and the PV solar cells during off-peak times to generate hydrogen and pure oxygen. Hydrogen and pure oxygen could be fed to the NGPP to enhance performance and ensure efficient combustion, or could be sold to local markets. A power conditioning system (PCS), that is, inverters, converters, and/or transformers, is used to enhance electricity interchanges between the hub units and to secure high quality power to the transmission lines.

The proposed model will investigate the benefits, both economic and environmental; barriers; and challenges of energy hubs by developing several scenarios. The proposed energy hub would be in Nanticoke Region, ON; however, it can be applied to any place, taking into account fuel prices, solar and wind data, and potential hydrogen markets.

A detailed study done by Y. Maniyali (2009) was aimed to replace a 4,000 MW coal fired plant in Nanticoke region with an energy hub comprising of a nuclear power plant as the main energy supplier. This study, on the other hand, is devoted to an alternative solution where a natural gas power plant is the principal energy producer. This avoids the high costs related to constructing a new nuclear plant, and the concerns about radioactive wastes. Figure 1.1 shows the schematic diagram of the proposed energy hub.

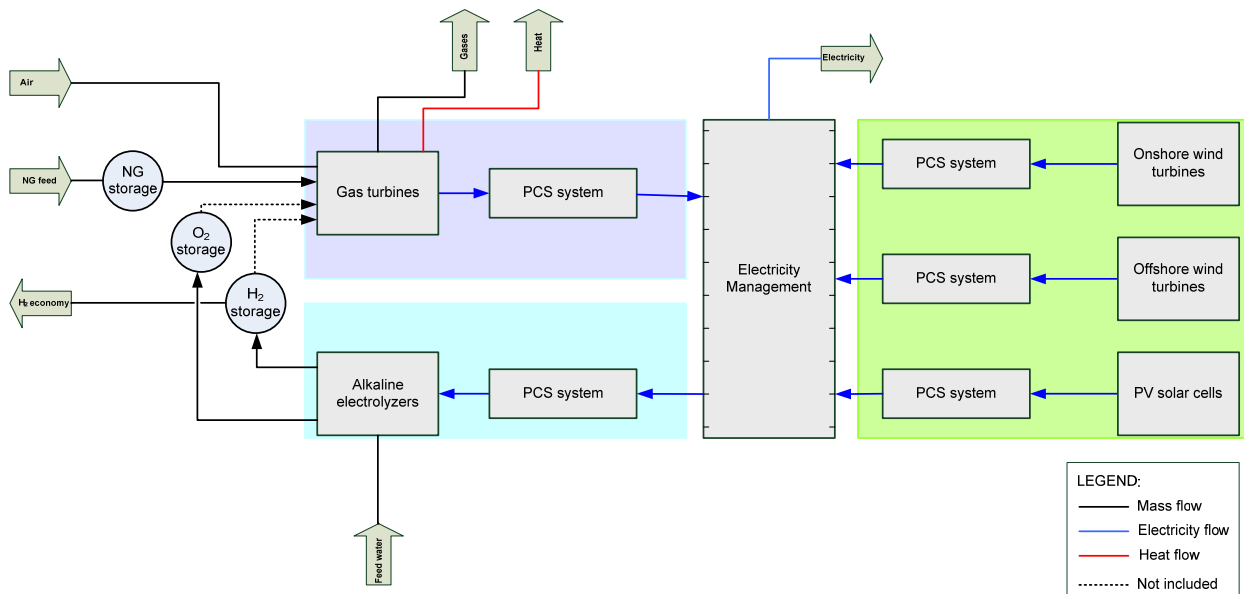


Figure 1.1 Schematic block diagram of the proposed energy hub.

1.2 Research Motivations

The need for more integrated power plants is a necessity pushed by new strict environmental regulations, volatile oil prices, and the move toward a more stable and sustainable systems. Such power plants or energy hubs would produce, transform, and condition energy as required for residential or industrial use. The fundamental motivation behind this research is the need to find an alternative solution to the closing down of the coal-fired power plant in Nanticoke region, and the need to meet Ontario’s increasing-demand for electricity.

The motivations behind establishing this thesis are summarized by the following points:

- The volatile prices of oil and some of its derivatives are of major concern. This study would reduce the dependency on non-renewable energy sources and shift the energy sector into a more sustainable, diverse, and clean system.
- The need for integrating renewable and non-renewable energy sources due to the intermittency nature of renewable resources. Because the stand-alone renewable energy sources, with the exception of hydropower, do not provide adequate availability for commercial-production, such integration would reduce the intermittency of these systems.

- The need for various forms of energy, such as electricity and heat, for commercial and residential use. The hub is designed to meet electricity demand, as well as being easily implementable to meet district heat and compressed air demand for industrial and residential use.
- The recommendations of Ontario Ministry of Energy (OME) regarding the alternatives to replace coal-fired plants either by NGPPs or by nuclear-NG power plants (DSS Management Consultants, 2005). In addition, Ontario's policies toward reducing the environmental impact of the electricity sector, by increasing the penetration of renewable energy sources (Ontario's Smart Grid Forum, 2009), make it necessary to include solar and power energy with NGPPs.
- Energy security. The rising costs of energy resources and its limited amount have changed the way power generation systems look. Finding alternative ways to meet the increasing power demand is an imperative for a more sustainable economy. Diversity in power supply insures a reliable and secure system and puts less pressure on natural resources. This research study would offer a more stable and secure energy supply through the use of local energy resources, that is, NG, wind, and solar.
- New sources have natural gas, specifically unconventional natural gas from shale gas or tight gas, have developed in the past three years. Development of these resources will keep the price of natural gas low for a generation and make natural gas a viable power generation alternative.
- Meeting hydrogen demand. The "hydrogen economy" has been expanding over the last decades; moreover, there is an expectation that hydrogen powered fuel cell vehicles will be commercialized in 2015. Beside hydrogen-consuming processes, such as ammonia production, new paths for hydrogen consumption have appeared in the last few years. Water electrolysis presents an alternative way to produce hydrogen from the current steam methane reforming fossil fuel-based production method. A significant part of this thesis is devoted to hydrogen production from renewable resources to meet the increased hydrogen demand for power back up, chemical and petrochemical industry, and automotive industry, specifically hydrogen vehicles.
- Climate change and the Government initiative toward cutting the GHGs by 17% by 2020, based on 2005 predictions (Government of Canada, 2010). One of the main objectives of

this study is to eliminate GHG emissions that pose a significant global warming potential from coal generation power plants. Coal generation also has many other undesirable environmental impacts specifically criteria emission (NO_x , SO_x , VOCs, N_2O , and particulate matter), mercury emissions and impacts associated with mining operations.

- Increased-electricity demand. With an annual average electricity demand growth of 1.2% ("Energy sources," 2009), Canada's increasing population, combined with economic growth, has put extra pressure on the electricity sector. A diverse electricity system is proposed to eliminate the reliance on fossil fuels and to meet the increasing electricity demand.
- This study would give an insight to the challenges and the technical barriers of establishing such integrated power projects in the real world.

1.3 Research Objectives

The main objective of this thesis is to examine the combination of a conventional non-renewable power generation unit (NGPP), with renewable power generation units (wind turbines and PV solar cells), and hydrogen as an energy vector. The result of this combination can be implemented from both economic and environmental points of view. The economic objective is to produce electricity with a minimum cost per unit of energy generated. This can be achieved by considering some factors such as increasing the system efficiency, minimizing the fuel required, minimizing the O&M costs, and integrating the overall system operation. The environmental objective, on the other hand, is to produce the required electricity with minimum negative environmental impact. This can be implemented by using clean renewable energy sources, using alternative or upgraded fuels that generate less emissions (H_2 -NG mixture in pure O_2 environment), and a proper design of the combustion process.

The main objectives of the model are summarized by the following points:

- Development of a model of an energy hub comprising of NGPP, onshore and offshore wind turbines, PV solar cells, alkaline electrolysers, and PEM fuel cells, for a minimum cost per kilowatt of electricity generated in order to understand the potential for implementation of such energy hubs. The investigation includes the profile of hourly cost

of energy produced, hourly GHG emissions, performance and efficiency of the gas turbine.

- Develop an understanding the concept of energy hubs by proposing different operation scenarios. Each scenario investigates the project from a different point of view. Economic-based and environmental-based scenarios are a base of comparison.
- Optimization of an energy hub comprising of NGPP, onshore and offshore wind turbines, PV solar cells, alkaline electrolyzers, and PEM fuel cells, for a minimum cost per kilo watt generated.
- Studying the energy hub system as a new concept and evaluating the economic and environmental benefits.
- Improving the overall system performance and reliability by eliminating the intermittency and dispatchability problems of wind and solar energy. The excess energy of wind and solar generated can be converted to hydrogen to be stored or sold to local markets. As such a model of technology supports the development of the hydrogen economy.

1.4 The Project's Scope and Scale

- **The Gas turbines.** The overall energy hub capacity is targeted to meet the current energy generation provided through the Nanticoke Generating Station. As such this technology could be used to replace the coal based power production currently at the station. Depending on the scenario being investigated, the capacity is either generated entirely by GTs, or it is shared among GT units, wind turbines, and solar cells.
- **The wind farm.** The wind farm is proposed to include both onshore and offshore wind turbines. The onshore wind farm is assumed to have GE 1.5 SLE wind turbines, with a nominal capacity of 1.5 MW. The offshore wind farm, on the other hand, is assumed to have SWT 2.3-93 wind turbines, with a nominal capacity of 2.3 MW.
- **The solar energy farm.** The PV solar cells used are SPR-400 model (Sunpower Cor., 2010), with a maximum power of 400 W at standard test condition (STC), and a total of 20 MW.
- **The alkaline electrolyzers.** Alkaline electrolyzers are fully mature technology that is being commercially used, and alkaline electrolyzers are suitable for large-scale hydrogen production. The type used is HySTAT™-60, which has a maximum hydrogen generation

of 60 Nm³/h, with purity around 99.998% (Hydrogenics Cor., 2009). The number of electrolyzers used depends on the targeted hydrogen production, which is different for each scenario.

1.5 The Modeling Approach

In this study, the modeling process is based on economic and environmental aspects. The economic aspects are associated with capital costs, O&M costs, and gas emission costs. The environmental aspects are implemented in renewable energy and hydrogen economy scenarios.

The energy hub system is investigated by proposing three different operation scenarios: (a) NG stand-alone power plant scenario, (b) NG-renewable energy scenario, and (c) hydrogen economy scenario. The scenarios are discussed in detail in Chapter 3.

GAMS has been used to formulate the optimization problems. Each of the technologies being used has been modelled separately, and then, all models are put together according to each scenario's orientation. The results are implemented in: hourly gas emissions, hourly cost of electricity, hourly production and cost of hydrogen, as well as to the annual averages of emissions, cost, and production. All data used is based on the year 2009 to ensure consistent results. Hourly data is used whenever possible. Temperature, solar irradiance, NG prices, and electricity demand are taken on hourly data. However, seasonal wind data is used as it is not always possible to have a full data profile for a specific region. Accordingly, an hourly output is generated in each of the scenarios in terms of electricity production, cost, hydrogen production, and gas emissions.

CHAPTER 2

Literature Review

2.1 Energy Hubs

2.1.1 Energy hubs overview

“An energy hub is considered a unit where multiple energy carriers can be converted, conditioned, and stored” (Geidl et al., 2007). It is also an interface between energy producers and consumers (Frik & Favre-Perrod, 2004). The energy hub is a new concept, where coupling of different energy producers and consumers occurs. Energy can be obtained from different sources, can be delivered in various forms, and can be stored in a chemical, thermal or mechanical form. Exchange of energy and material streams from multiple energy sources within the same hub are some characteristics that distinguish energy hubs from conventional energy systems.

The main features of energy hubs are represented in Figure 2.1 and are summarized by the following points (Geidl & Andersson, 2005) :

- **Energy conversion.** One of the main features of energy hubs is energy conversion. Energy can be converted easily between electricity, chemical, and thermal forms (Geidl & Andersson, 2005). Gas turbines, for example, convert the chemical energy of NG to mechanical energy and then to electricity. Hydrogen FCs, on the other hand, convert the chemical energy of hydrogen directly into electricity. At low electricity demand periods, electrolyzers are used to convert excess energy back into chemical energy—hydrogen.
- **Energy conditioning.** In energy hub system, energy is conditioned to meet certain needs. An example of energy conditioning systems is electric inverters where the direct current (DC) from FCs is inverted to alternating current (AC). Step-up and step-down transformers are also used to transform voltage between the hub units and the grid.
- **Energy storage.** One of the main features of energy hubs is energy storage. Excess wind and solar energy during the high-production times can be transformed into an energy vector form such as hydrogen. Hydrogen is stored and can be converted back into electricity, used as transportation fuel, or it can be fed to other industrial processes.

Energy can also be stored in a mechanical form, such as compressed air or pumped water. Thermal energy storage is an effective way to store solar energy during day-time, in the form of hot water or molten salt, to be used for space heating during the night.

- **Inputs and outputs.** Energy hubs consume electricity, heat, and chemicals at their inputs, and, at the same time, they could produce electricity, heat, compressed air, and by-products, such as hydrogen, at their outputs (Geidl et al., 2007).

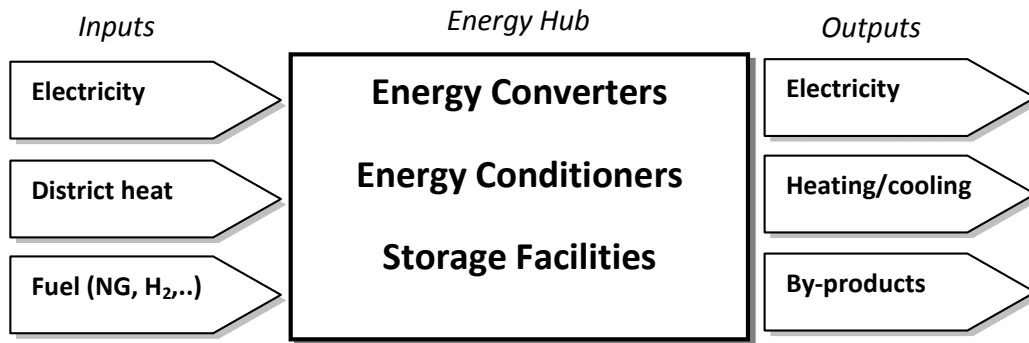


Figure 2.1 Block diagram features of energy hubs.

However, the concept is not fully mature and is still in the early stages of forming its fundamentals. Most of the technologies forming the energy hub system such as gas turbines are well addressed in the literature, both technically and economically. However, technical and operational issues regarding combining these technologies under one firm are not well addressed. This research study would be an introductory study to address these issues and give preliminary evaluations of the economic and environmental benefits of combining these technologies.

2.1.2 Motivations

Energy hubs have the potential to offer many advantages compared to conventional energy systems today. The introduction of renewable energy into traditional energy systems has overcome the intermittent nature of wind and solar power, for example. The diversity and integration of supply have offered a better overall environmental profile, more reliable supply, and, most importantly, increased system performance. Motivation and benefits of establishing energy hubs are summarized by the following points (Geidl et al., 2007):

- **Reliability of supply.** The reliability of generation in energy hub systems is increased through the integration of renewable and non-renewable energy systems. Because the electricity produced is no longer dependent on one source, energy hubs are more reliable and offer more stable and a reliable supply.
- **Increasing the system performance.** The intermittency of wind and solar power can be overcome by conversion of electricity during times of excess capacity and the off-peak hours to hydrogen. Hydrogen can be stored and used later during the high-demand hours, either by fuel cells (FC) or by combustion turbines. The performance is increased through insuring an efficient and secure energy storage system, in addition to the high quality of the electricity produced.
- **Various forms of energy can be utilized.** Since residential and commercial energy needs are not limited to electricity (Favre-Perrod et al.,2005), energy hubs can manage and deliver several forms of energy. District heat, NG, hydrogen and compressed air are some energy forms that can be easily transported to the required use, which most of conventional energy systems lack today.
- **Optimization of supply.** Energy hubs offer an additional degree of freedom especially in the planning and design stage.
- **Improving the efficiency.** Energy hubs can offer higher efficiency through extensive use of energy and minimization of heat and energy loss. Efficiency can also be increased by energy storage in the form of hydrogen.

2.1.3 Power generation

An effective power generation and delivery system is a combination of maximizing energy efficiency and minimizing overall energy cost. Power dispatch seeks energy generation taking into account economic and environmental consideration. The economic dispatch of the power generation industry is defined by the EPA Act Section 1234 (2005) as “the operation of generation facilities to produce energy at the lowest cost to reliability serve consumers, recognizing any operational limits of the generation and transmission facilities.”

A proper and a reliable operation of power plants requires detailed specifications of the units and their limits, their maximum inputs and outputs, fuel cost, and load forecast to keep a smooth operation of the units taking into account the environmental and economic constraints. In this

section, a review of the power generation technologies that were used in the early stages of power industry, the transitional systems or state-of-art technologies, and future systems are briefly reviewed.

The twentieth century witnessed an obvious development of the internal combustion engines. The simplicity and durability of these engines, which used gases from burning coal as a working fluid, were the reason for the fast-spread of their applications. However, compared to today's state-of-art technologies of the power industry, the traditional systems lacked efficiency, environmental constraints, and renewable fuel resources. Coal has been used extensively in the past few decades as a cheap, abundant fuel source for power generation. Yet, severe environmental problems have been witnessed due to its high rate of PM and SO_x emissions, and coal is the most intensive power generation sources of greenhouse gas emissions (GHGs), specifically CO₂.

Power energy systems today are more reliable, capable of meeting changing demands, and most importantly more efficient. Combined heat and power (CHP) power plants have significantly improved the overall plant efficiency, and offered a heat recovery system that is capable of supplying heat for industrial and commercial use. The introduction of wet-burning technologies, such as water-injected and steam-injected cycles (Jonsson & Yan, 2005) as well as the dry low-NO_x gas turbines, combined with sophisticated chamber design and control, have enhanced the burning efficiency and minimized VOC and NO_x emissions. Shifting toward NG and partially abandoning coal, as well as engaging renewable and clean-burning fuels in the power industry, are some characteristics of today's energy sector.

The environmental impact of the power industry, along with rising fuel prices and increased power consumption, all led to the consideration of more sustainable and clean technologies. Future power generation systems would be mostly gas-fired integrated with wind and solar energy to partially eliminate the dependency on fossil fuel and to overcome the intermittency of renewable energy systems. Shifting to hydrogen-based economy is also a notable transfer to more sustainable and clean power systems. As issues arise, from resource depletion to and high fuel costs, the energy sector will be witnessing a high share of renewable energy, such as wind, solar, and hydro. Energy systems are being developed to accommodate these changes.

Future energy systems would address some key characteristics that today's systems lack. Some of these characteristics include:

- A diverse power generation system that employs multi-energy sources.
- A power generation system that is more efficient and sustainable.
- Power generation system that is dependent upon more renewable resources instead of relying only on fossil fuel resources.

In conclusion, power dispatch is affected by scheduling frequency, ease of communication and accurate exchange of information between independent energy generators.

2.1.4 Hub modeling

Energy hubs are a relatively new concept and most of the modeling and optimization literature in the past has focused only on energy generation systems that include independent energy carriers. Few studies have included multi-generation energy systems (Favre-Perrod et al., 2005; Geidl & Andersson, 2005; Geidl et al., 2007). The complexity of the modelling process comes from the decision that has to be made regarding the trade-off between maximizing energy production from renewable sources, the cost of energy produced, and the reliability of system. The interaction between different multi-generation units and multi-energy forms and carriers adds a complexity to the optimization process, and hence, decision making.

In general, the modelling process is governed by both material and energy balance. The input L , the output P , and the accumulated or the power stored \dot{E} from the energy hub in terms of heat, electricity or any other form of energy are related by the following relation (Carradore & Bignucolo, 2008):

$$L = CP - S\dot{E} \quad (2.1)$$

Where; C is a coupling matrix represents the relationship between energy systems and S is the coupling accumulation or storage matrix.

$$\begin{bmatrix} L_\alpha \\ L_\beta \\ \vdots \\ L_\omega \end{bmatrix} = \begin{bmatrix} c_{\alpha\alpha} & c_{\beta\alpha} & \dots & c_{\omega\alpha} \\ c_{\alpha\beta} & c_{\beta\beta} & \dots & c_{\omega\beta} \\ \vdots & \vdots & \ddots & \vdots \\ c_{\alpha\omega} & c_{\beta\omega} & \dots & c_{\omega\omega} \end{bmatrix} \begin{bmatrix} P_\alpha \\ P_\beta \\ \vdots \\ P_\omega \end{bmatrix} - S \begin{bmatrix} \dot{E}_\alpha \\ \dot{E}_\beta \\ \vdots \\ \dot{E}_\omega \end{bmatrix} \quad (2.2)$$

The elements of the power storage vector \dot{E}) are further defined by (Carradore & Bignucolo, 2008):

$$\dot{e}_\alpha = \begin{cases} e_{\alpha^+} & \text{if } Q_\alpha \geq 0 \\ 1 & \\ e_{\alpha^-} & \text{else} \end{cases} \quad (2.3)$$

Where Q_α is the amount of power exchanged for the vector α .

An example of an integrated energy hub comprised of different energy carriers is shown in Figure 2.2 (Favre-Perrod et al., 2005).

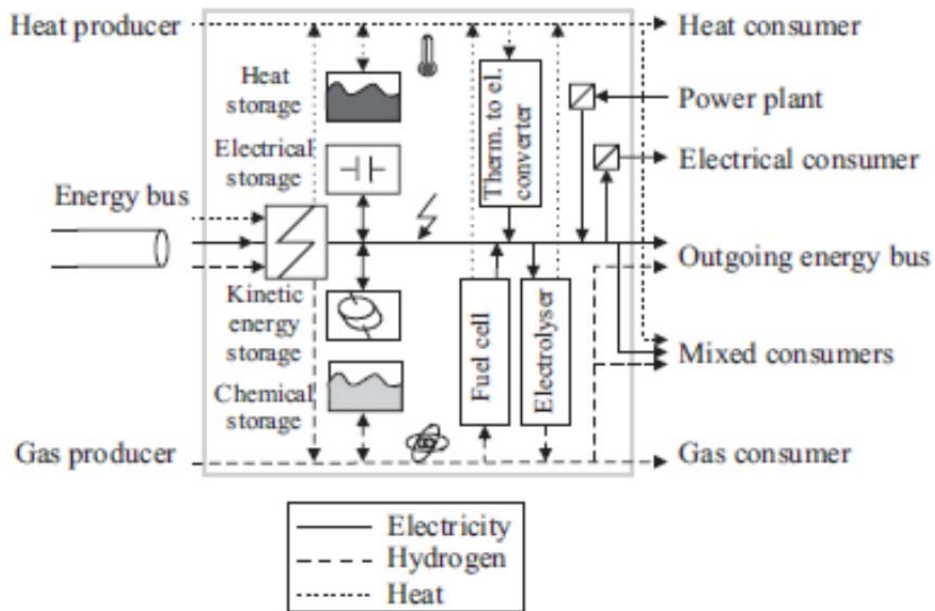


Figure 2.2 An example of an energy hub (Favre-Perrod et al., 2005).

2.1.5 Illustrative case studies

Energy hub concept was implemented in some previous studies (Sirikitputtisak et al., 2009; & Mirzaesmaeeli et al., 2010) that seek generation of electricity under constrained conditions of CO₂ emissions and capacity limits. Ordorica-Garcia *et al.* (2009) investigated the optimal infrastructure required for oil sands in Alberta in the year 2030 where exchange of energy (power, steam, and process heat) and materials (hydrogen and CO₂) were involved. Syed *et al.* (2009) used a different approach in implementing energy hubs by introducing a fleet of plug-in fuel cell vehicles. Both works are reviewed and discussed as they hold similar ideas to this research specifically what is concerning the production and use of hydrogen, and exchange of steam and power.

Sirikitputtisak *et al.* developed a multi-period optimization model considering CO₂ emissions. The study deals with an energy hub comprising of coal-fired power station, NG combined cycle, hydroelectric, carbon capture and storage (CCS), nuclear, and wind power. This configuration is meant to meet Ontario's predicted demand from 2006 to 2020, while reducing the emissions of CO₂ by introducing the CCS technology. A number of scenarios were investigated with and without CO₂ emission limits. A time constrained variables such as construction time and fluctuating fuel prices were included. The model included a minimization of multi-period MINLP optimization function using GAMS. The objective function represents the O&M costs of existing and new power plants, fuel costs, total investment costs, carbon credit costs, and CCS costs. Moreover, the CPLEX 10 solver was used with over 11,470 variables and 14,900 equations. Figure 2.3 summarizes the results of the study in terms of the cost of electricity per kilowatt over a period of 14 years. Each of the lines in the figure represents a reduction target of CO₂ compared to the year of 1990. The base case line represents the cost with no CO₂ emission limits are applied. The study has proven that NG results in lower overall O&M costs and less emission compared to coal although the latter is cheaper in price.

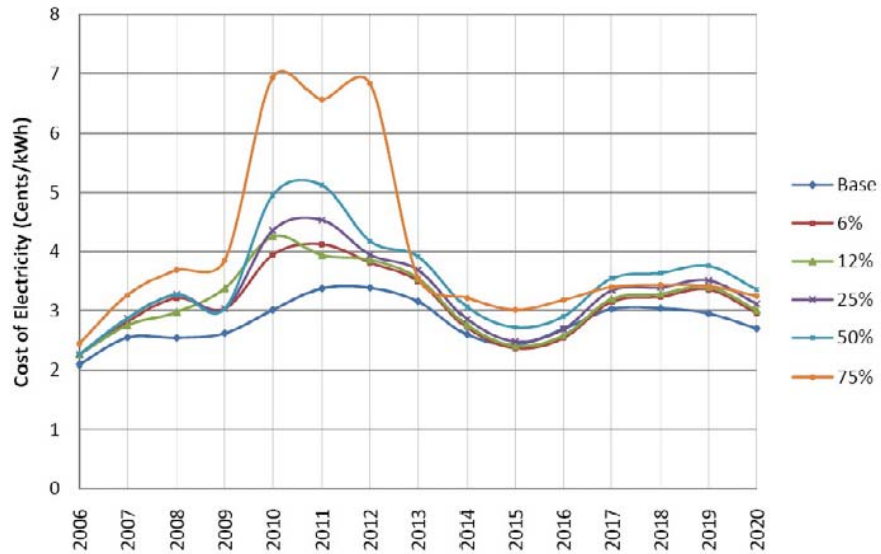


Figure 2.3 Predicted cost of electricity (Sirikitputtisak et al., 2009).

Although this study included comprehensive details regarding the process costs and a predicted data for demand and fuel prices, more technologies including but not limited to PV solar energy, biomass, and energy storage should be implemented in order to give more generalized results and more accuracy for decision making.

Another similar work was done by Ordorica-Garcia et al. (2009). Work is concerned with minimizing energy consumption and environmental impacts of the Canadian oil sands in 2030. The investigated technologies include coal and NG power plants, IGCC, and oxyfuel plants. The extraction of oil from sand requires the use of different forms of energy and materials ranging from power and diesel fuel to hydrogen, steam, and process heat, resulting in considerable amounts of CO₂ emissions. The objective of the study was to find the optimal combination of energy units that satisfy the demand while meeting the CO₂ emission limits. The objective function is of MILP type in which GAMS was used as a tool to formulate the problem. The objective function was presented in terms of the annual overall costs of producing steam, hot water, hydrogen, and power taking into account CO₂ capturing. It has been found that for the baseline of comparison where no carbon capture is applied, 9 NGCC power plants and 109 SMR units were required to meet electricity and hydrogen demand. Compared to the baseline scenario,

12 oxyfeul power plants, 106 SMR units, and 1 gasification units were required to meet electricity and hydrogen demand with 38.6% CO₂ capture.

This study investigated the optimal infrastructure required to meet energy and material demand of extracting oil from tar sands. Some issues, however, need to be addressed such as hydrogen storage and energy conditioning and storage as they form an important part of any energy system.

Syed *et al.* investigated a system of energy supply and demand units comprising of hybrid plug-in fuel cell vehicles that work on hydrogen and electricity, a commercial building, hydrogen production and storage facility, and wind turbines as shown in Figure 2.4. The energy hub was modeled on hourly basis based on 24 hours cycle. The outcome of the study was an hourly profile of wind energy supply, hourly demand of the charging fleet, hourly demand of the commercial building, and the hourly excess electricity. This study gives an example of distributed energy production systems in which renewable energy sources are used to meet a commercial building’s electricity demand and to produce hydrogen during the off-peak hours. Such systems could be more improved by implementing solar energy and hydrogen management facility to be sold to local markets. Moreover, an economic study predicting the cost of electricity and hydrogen generated would be of great importance in helping to make the right decision to choose among the most suitable technologies.

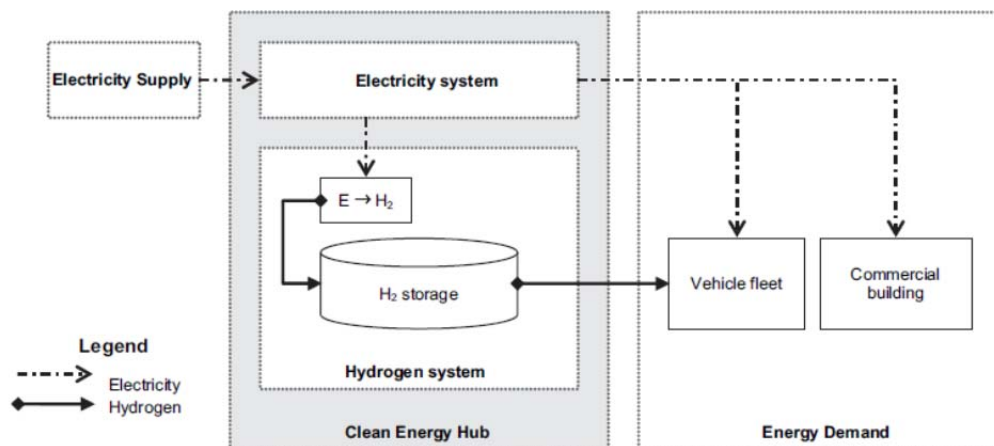


Figure 2.4 Schematic of systems and energy interactions in the clean energy hub model (Syed et al., 2009).

2.1.6 Environmental benefits

The idea of energy hubs has come to light from both economic and environmental points of views. The negative environmental impact of the electricity production sector has limited future plans for some technologies (e.g., coal-fuelled power plants). On the other hand, the penetration of renewable energy, in the energy sector, is expected to rise in the future.

Energy hubs offer a dramatic change in both the performance and gas emissions of conventional energy sectors. In this study, a NGPP combined with wind farm and solar energy station eliminates gas emissions related to the combustion of NG, and, at the same time, increases the reliability of wind and solar energy supply. For example, the stored hydrogen during the off-peak hours is added to the NG to increase the performance and decrease the formation of VOCs and NO_x . The environmental benefits of establishing energy hubs, in general, and hythane turbines can be summarized by the following points:

- **Reduction of GHG emissions and particulate matter (PM).**

CO_2 as GHG is a major contributor to global warming. In Canada, CO_2 accounts for about 78% of all emissions according to Environment Canada (Greenhouse Gas Division, 2010). CO_2 is produced in power generation units during the combustion of hydrocarbons and coal. Hydrogen-based fuel emits no CO_2 , with water vapour being the only by-product. NG has a higher hydrogen-carbon ratio compared to liquid fuels or coal, which means the CO_2 emitted per unit of energy produced is lower.

CO and VOCs are the result of incomplete combustion of fuel due to incomplete mixing or low residence time. CO is an odourless, toxic pollutant. VOCs have high global warming potentials and can combine with NO_x to form ground ozone. NG gas combustion is more efficient than coal or kerosene resulting less CO and VOCs emissions. When mixed with hydrogen, the combustion efficiency increases even more.

NO_x is a mix of NO and NO_2 . NO_x results either from burning nitrogen-containing fossil fuels or from atmospheric nitrogen when burning is performed at high temperatures. NO_2 can cause serious health problems, along with its global warming potentials. Burning of fuel performed in oxygen-rich environment, in addition to using hydrogen as fuel would reduce NO_x emissions dramatically.

SO_x are the oxides of sulfur. SO₂, sulfur dioxide, results from burning fuels containing sulfur compounds. SO₂ is the main cause of acid rain and other health effects, such as asthma and eye irritation. Including renewable energy sources would dramatically decrease SO_x emissions. In addition, NG has very low concentration of sulfur compounds compared to coal and petroleum.

Particulate matter (PM). Particulate matter is tiny particles suspended in the atmosphere. PM causes major health problems and can cause asthma and lung cancer. Combustion of coal and heavy fuels containing a considerable amount of metals, such as Hg and Va, contribute to significant PM concentrations in the atmosphere. Combustion of NG completely eliminates PMs, since these pollutants are associated with heavy HCs and coal combustion.

Mercury is emitted to the atmosphere due to burning of heavy fuels, such as coal and petroleum coke, cement, and steel production. Mercury deposits in fish and shellfish tissues are causing serious health problems to humans. Large amounts of mercury compounds are released to the environment because of the massive combustion of fossil fuels especially coal. A study, in 2000, showed that stationary combustion of fossil fuels are responsible for about 65% of the emitted mercury worldwide (Pacyna et al., 2006). In this project, a cleaner fossil fuel, NG, is used instead of coal, which would entirely eliminate mercury emissions.

- **Improving urban air quality.** Ground level ozone and PM are the main cause of smog. Ground ozone is a secondary pollutant results when NO_x reacts with VOCs in the presence of sunlight. Such pollutants cause serious health problems, smog, and acid rain. Shifting to a cleaner fossil fuel (NG) and renewable sources (wind and solar) eliminates PM emission and other pollutants. Hydrogen, as a by-product in this project, could be used in transportation, instead of gasoline, to generate electricity, or in chemical processes. The only products of hydrogen combustion are heat and water vapour. Moving toward renewable and hydrogen-based fuels eliminates PM, NO_x, SO_x, and CO emissions leading to better overall air quality.
- **Retrieving hydrogen economy.** Although hydrogen plays a major role in today's economy, securing a reliable and clean source of hydrogen is still a concern. Fossil fuel,

which is of a limited amount, is still the dominant source of hydrogen. Energy hubs offer a secure and clean source of hydrogen. They would reduce the cost of centralized hydrogen, and they offer the advantage of a more distributed hydrogen production. This is especially important in the transportation sector (hydrogen vehicles), where a lack of constructing proper and greater distribution of refueling stations is still a barrier.

2.2 Gas Turbines Power Plants

Power plants are the backbone of today's growing economy and industrial development. Gas turbines have improved dramatically since the first appearance of commercial gas turbines in 1938. In the early stages of power generation, gas turbines were unable to meet fluctuating demands and emission limits. Coal-fuelled gas turbines offered inexpensive and an abundant electricity supply. The massive environmental impact, however, such as SO₂ emissions and the costs related to eliminating GHG emissions, have limited their use by today's power industry. NG-powered turbines have offered inexpensive and clean electricity generation in today's standards. With many coal and diesel-fired power plants having switched to NG as fuel, NG-fuelled gas turbines offer an alternative technology to generate electricity in the near to midterm future for the power industry.

A gas turbine is an internal combustion engine that offers low emissions and reliable supply of electricity. The efficiency of the CHP turbines has exceeded 60%, while the average production capacity has reached up to 570 MW according to Siemens SGT5-8000H new gas turbine product (2010). There have been several advancements regarding gas turbine technology. Technologies such as cooling of turbine fins, pre-mixing, and sophisticated control systems have made it possible for gas turbines to accommodate several types of fuels and to operate at high temperatures.

Any gas turbine consists of three main sections:

- **Air compressor.** There are two configurations of air compressors: (a) axial flow and (b) centrifugal flow design. Axial design is the most common type in the power industry. The power required for compression is given by the general relationship:

$$W_c = NRT_i * \frac{n}{n-1} * \left[\left(\frac{P_o}{P_i} \right)^{\frac{n-1}{n}} - 1 \right] \quad (2.4)$$

Where; W_c is the work required for compression, N number of moles, R ideal gas constant, T_i and P_i inlet conditions, T_o and P_o outlet conditions, and n is the expansion-compression index.

The relationship between temperature and pressure both at the inlet and outlet is given by:

$$T_o = T_i * \left(\frac{P_o}{P_i} \right)^m \quad (2.5)$$

Where m is the polytropic temperature coefficient.

- **Combustor.** The combustor or the combustion chamber can be classified into three categories: (a) tubular, (b) annular, and (c) turbo-annular. Fuel combustion takes place in three zones, the primary zone, the intermediate zone, and the dilution zone. The combustor chamber is equipped with units, such as air filtration, an air control system, and a fuel injection system to help achieve high-combustion efficiency and therefore, low pollutant emissions.
- **Gas turbine.** There are many configurations and layouts of power or combustion turbines based on their intended use. The most common and commercially available type is axial flow with dry combustion system. The power turbine is comprised of many auxiliary units including cooling unit and control system. The work output of a gas turbine is given by a similar relationship to that of the air compressor as following:

$$W_t = NRT_i * \frac{n}{n-1} * \left[\left(\frac{P_i}{P_o} \right)^{\frac{n-1}{n}} - 1 \right] \quad (2.6)$$

Where W_t is the work done by the expander.

The performance of a gas turbine is governed by its design parameters, in addition to fuel type, ambient temperature and pressure, and humidity. The efficiency of the power turbine is given by (Giampaolo, 2006):

$$\eta_t = \frac{1 - T_{EXH}/T_{TIT}}{1 - \left(\frac{1}{r_c}\right)^\sigma} \quad (2.7)$$

Where; η_t efficiency of power turbine, T_{EXH} and T_{TIT} exhaust and inlet temperatures respectively, r_c pressure ratio, and σ isentropic temperature coefficient.

2.2.1 Simple cycle power plants (SCPPs)

Simple cycle power plants (SCPPs) or the open circuit gas turbines are the simplest and the earliest gas turbine cycles in operation. A schematic process flow diagram of the SCPP is shown in Figure 2.5 which represents the simplest configuration of this cycle. There have been many configurations and modifications made on SCPPs since their first appearance. Reversible intercooled cycle, reheating cycle, and the ultimate gas turbine cycle are some of the attempts to improve the performance and reliability of the SCPPs. A typical SCGT can generate over 208 MW on average, with an overall thermal efficiency exceeding 38%.

SCPPs are suitable for peak demand since they have a high response to the changing demand and shorter start-up time. On the other hand, SCPPs' efficiency is very low especially at part-load operation, since heat at the exhaust is not recovered, and the engine delivers high-grade exhaust to the environment.

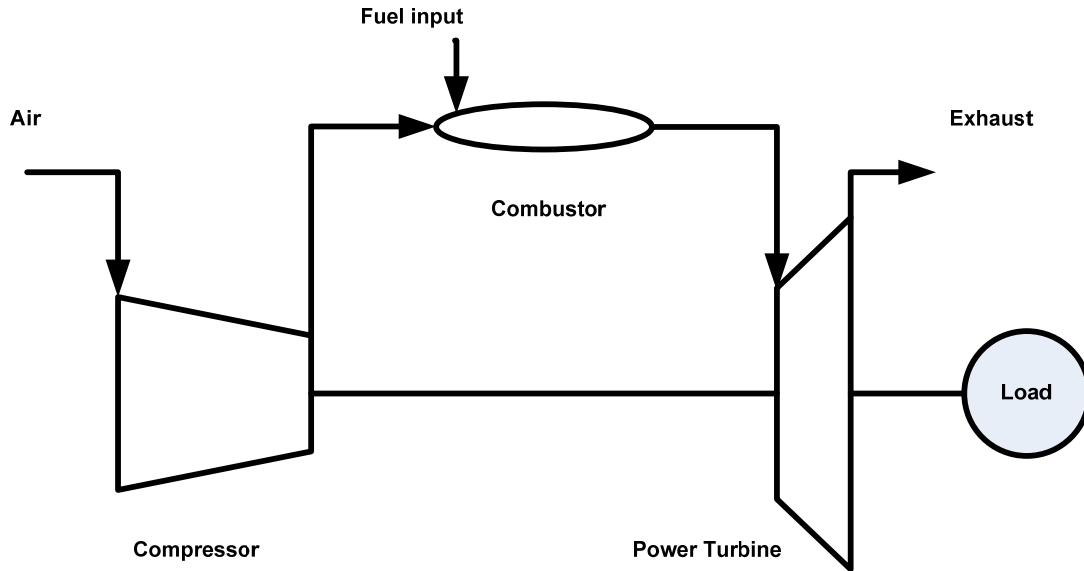


Figure 2.5 Simple cycle power plant flowchart.

Brayton cycle:

Brayton cycle is the ideal cycle that represents SCGTs operation and the backbone of power generation applications. The cycle is described by the first law of thermodynamics:

$$dU = \delta Q - \delta W \quad (2.8)$$

Where; U is the internal energy, Q is the heat added to the system, and W work done by the system. The cycle efficiency is given by the following equation:

$$\eta = \frac{\text{net work output}}{\text{heat supply}} = 1 - \left(\frac{1}{r_c}\right)^{(k-1)/k} \quad (2.9)$$

Where; r_c is the pressure ratio, and k depends on the gas nature.

Brayton cycle is best represented by temperature–entropy diagram in Figure 2.6. Some modifications can include inter-cooling, reheating, and closed cycles. The four main steps of Brayton cycle are:

- **Adiabatic compression.** The compression is reversible with no heat is added or removed from the system. Work from compressor causes the air temperature to rise from T_1 to T_2 , and the air pressure from P_1 to a higher pressure P_2 . This step is represented by the line 1–2 in Figure 2.6.
- **Isobaric combustion.** Fuel is injected to the combustion chamber and the combustion process occurs. The combustion process is assumed to proceed under a constant pressure P_2 . The heat added by the fuel Q causes the gas temperature to rise from T_2 to T_3 . This step is represented by the line 2–3 in Figure 2.6.
- **Adiabatic expansion.** The combustion mixture enters the expansion turbine at a temperature T_3 and a pressure P_2 . Work extracted by the gas turbine W causes the temperature and pressure to fall to T_4 and P_3 driving the air compressor and generating electricity. This step is represented by the line 3–4 in Figure 2.6.
- **Isobaric cooling.** Heat rejection under constant pressure where temperature falls back to T_1 . The dashed line 4–1 represented in Figure 2.6 indicates that the cycle is an open cycle.

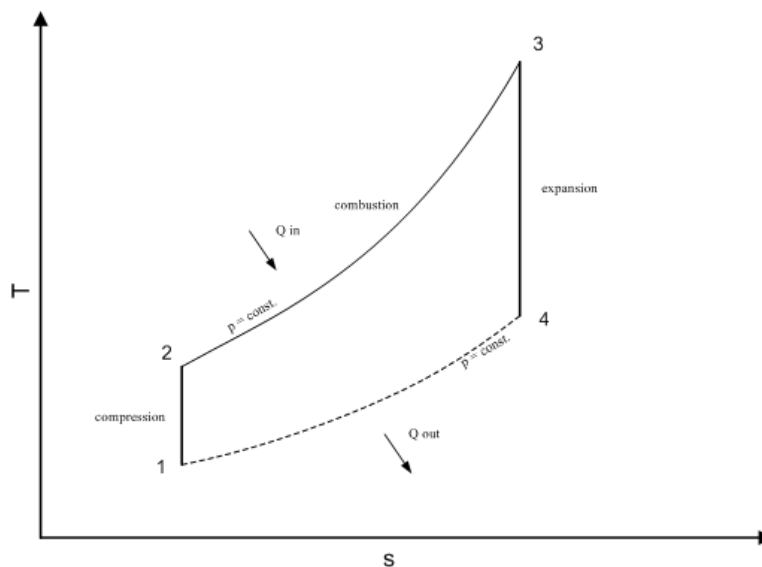


Figure 2.6 Brayton ideal cycle for GT engines, T – s diagram.

2.2.2 Combined cycle power plants (CCPPs)

A combined cycle power plant (CCPP) is the integration of the SCPPs or Brayton cycle—the gas turbine with an upper-stream steam turbine or Rankine cycle—and the steam cycle to generate electricity. In the upper-stream steam cycle, heat waste from the gas turbine’s exhaust is used to generate steam at temperatures between 540–570 °C, and a pressure of 22 MPa as stated by the Office of Air Quality Planning and Standards (2010). The generated steam is classified according to pressure into: high pressure, intermediate pressure, and low pressure steam. Increasing the pressure and temperature of the steam increases the efficiency and power output of the cycle. If the steam is used directly for heating, the process is called cogeneration—heat and power. The combined heat and power cycle minimizes heat loss leading to an enhanced overall efficiency and better fuel economy. A schematic diagram of the CCPP is shown in Figure 2.7.

The CCPPs are classified further into (a) unfired operation, where only the heat from the exhaust is extracted without any additional input, and (b) fired operation, where extra fuel is added to the exhaust to increase the power output. Fired operation is used where extra power is required or when the temperature of the steam is not high enough to meet the external requirements. Steam, which can reach up to 500 °C, is used in many residential and industrial applications.

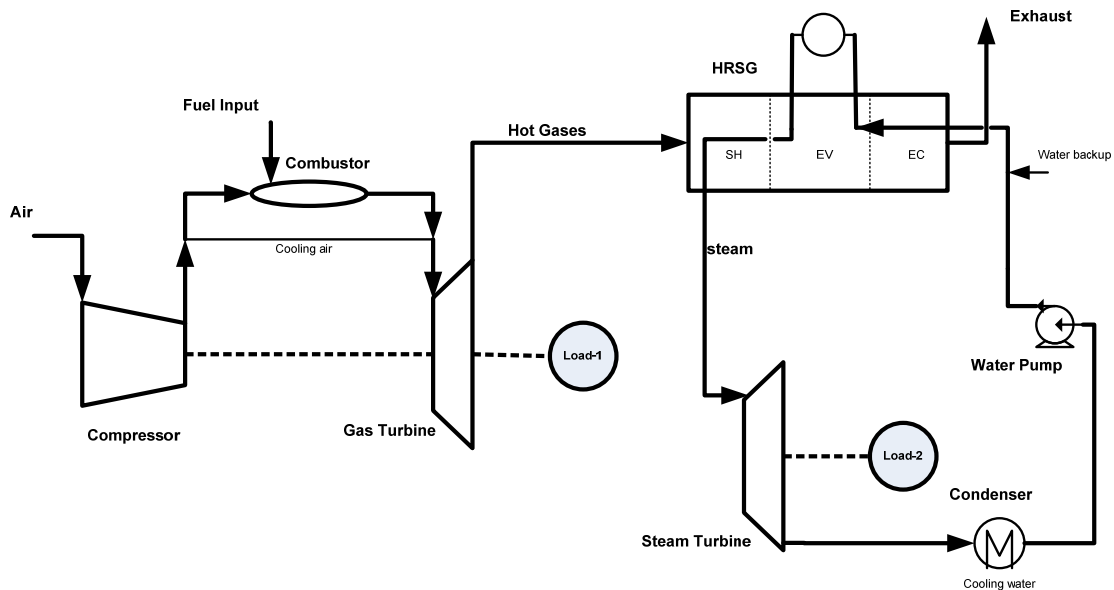


Figure 2.7 Combined cycle power plant flowchart.

A typical CCPP can generate between 350–500 MW, with a total achievable efficiency exceeding 58% (Poullikkas, 2001). In today’s power industry, CCPPs are the dominant technology as they offer the highest total efficiencies among the other cycles. They are more flexible, in both design and operation, in meeting energy demand. The efficiency of CCPP is given by Equation 2.10, where it is obvious that the efficiency of CCPP is higher than the efficiency of SCPP.

$$\eta_{cc} = \frac{\text{net GT work} + \text{net ST work}}{\text{fuel energy input}} \quad (2.10)$$

Figure 2.8 shows the relationship between temperature T and the entropy s of Rankine steam cycle. CCPP is simply the combination of Brayton and Rankine cycles.

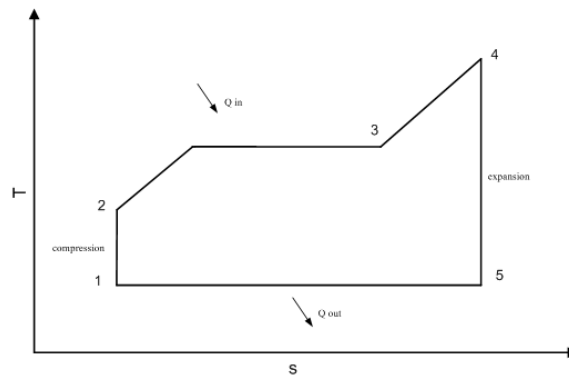


Figure 2.8 Rankine ideal cycle for GT engines, T – s diagram.

Compared to SCPPs, CCPPs are more efficient since the wasted heat is used to generate steam and electricity. The high efficiency is interpreted in terms of low operating costs–fuel savings, as well as a reduction in GHG emissions. The technology offers high availability, about 95%, and operates longer times without any shutdown. The overall system efficiency is higher, leading to lower operating costs as a direct cause of fuel saving. The cogeneration capability enables using low pressure steam, which cannot be used to generate electricity, for district or process heating. The well-developed technology, high efficiency, and short construction time are some key factors of spreading SCPPs technology.

2.2.3 Hydrogen-NG turbines

Combustion of NG is performed under controlled temperatures and in an excess air environment to eliminate GHG emissions. However, considerable amounts of CO₂, CO, VOCs, and NO_x are emitted in the combustion process. Under strict environmental regulations, many technologies have been used to control these emissions. Among these technologies is water or steam injection, selective catalyst, dry, low NO_x (DLN) technology, or other gas turbine exhaust cleanup systems. Although many of these technologies are an effective way to control GHG emissions, some limitations related to lowering the flame temperature and cost are still a barrier.

In recent years, hydrogen is being used as an alternative fuel to—fully or partially—replace conventional fuels. In the automotive industry, hydrogen is either used directly in internal combustion engines or in fuel cells vehicles. In the power industry, several studies show the possibility of improving gas turbines performance and diminishing GHG emissions (Cheng et al., 2009; Termaath et al., 2006). Integrated H₂-NG turbine systems offer the following advantages over turbines fuelled only by NG:

- Adding hydrogen to NG lowers NO_x and CO emissions. Some studies show that the reduction of NO_x emission can be done economically by adding from 10 to 15% of hydrogen to NG (Phillips & Roby, 2000).
- Adding hydrogen increases NG combustion ability leading to improved overall combustion efficiency.
- Hydrogen-enriched NG eliminates the need for post-combustion cleanup units.

A reliable supply of hydrogen is still needed. Currently steam methane reforming (SMR) process and coal gasification are the dominant sources of hydrogen; however, extra costs and emissions are added to the hydrogen produced from these processes. Some solutions could include integrating conventional power plants with renewable energy technologies and converting excess electricity to hydrogen during the off-peak hours to be mixed with NG.

2.2.4 Gas emissions

- **CO₂ and CO.** CO₂ is a natural product of fuel combustion containing carbon. CO₂ emissions caused by the combustion of NG are affected by fuel type. The higher carbon content of the fuel, the higher CO₂ emission per kilowatt-hour of electricity produced. NG combustion

releases on average 117 lb CO₂ per MMBtu as stated by the Office of Air Quality Planning and Standards (2010). CO emission, on the other hand, is affected by fuel-to-air ratio and the combustor design. It is also a product where combustion proceeds at low temperatures in very lean fuel–air mixture environment.

- **VOCs.** VOCs emission is a direct result of incomplete combustion. Usually, VOCs emission is controlled by a well-design of the combustor in excess air environment.
- **NO_x.** Nitrogen oxides in combustion engines are formed by three different paths. The first type is thermal NO_x, which is formed by the reaction of N₂ from the air with O₂ molecules. The reaction is enhanced by high temperatures and excess air. The second type is prompt NO_x, which is formed at the early stages of the combustion process. The last type is NO_x results from nitrogen compounds contained in the fuel or organic NO_x. Thermal NO_x is the dominant path, so controlling flame temperature is a critical to eliminate NO_x emissions.
- **SO_x.** Sulfur oxides emission depends on sulfur content in the fuel. Usually, NG is sweetened before being used as fuel. Therefore, SO_x emissions can be avoided before the combustion process. Typically, SO_x emission from NG turbines is negligible compared to coal or other heavy fuels when used as fuels.
- **PM.** Particulate matter emission depends on fuel composition. Heavy fuels such as crude oil, contain considerable amounts of salts and metals, such as Va and Pd, which cause PM emission. In the combustion process of NG, the presence of PM in the emitted gases is negligible compared to liquid and solid fuels.

2.3 Wind Energy

2.3.1 Wind energy overview

Wind energy is the kinetic energy caused by air motion as a result of the natural convection happening in the atmosphere between high pressure areas and low pressure areas. The early use of wind energy was in the form of small wind mills and small-scale water pumping systems for processing crops and for other farming purposes.

The extracted power P of wind passing through a circular area πr^2 is given by:

$$P = 0.5 \pi \cdot \rho \cdot V^3 \cdot r^2 \quad (2.11)$$

Where; V is the wind speed, ρ is the air density, and r is the rotor radius.

Although wind energy is an intermittent resource and has noise and visual impacts, its benefits exceed the barriers. Environmental, social and economic characteristics of wind energy can be summarized by the following points:

- Wind energy is renewable; it is plentiful, free and sustainable.
- Wind energy is a clean energy and emissions-free technology. By 2020, power from wind is estimated to avoid 1500 mega tonnes of CO₂ every year (Zervos, Teske, & Sawyer, 2008).
- Wind energy improves the air quality and eliminates the costs associated with GHG emissions.
- Wind energy reserves natural resources, such as water, and conserves conventional energy sources such as oil and NG as stated by the Canadian Wind Energy Association (2008b).
- Wind energy offers jobs and employment opportunities.

Challenges:

- Cost is still a concern especially in terms of capital costs. Compared with electricity from NG and coal, electricity from wind can be as high as 12.0 ¢/kWh at low wind speeds (Zervos et al., 2008).
- Wind energy is not completely reliable unless it is coupled with other forms of energy.
- Public acceptability, due to noise concerns and visual impacts, especially in urban areas is still an ongoing issue.
- It cannot be used for base-loads due to its intermittent nature, which is uncontrolled. Also it cannot be used directly for power backup during peak hours unless it has been transformed to another form of energy–hydrogen, for example.

Integration with other energy sources:

The intermittent nature of wind power is one of the main challenges for supplying a reliable energy source. However, this problem, in commercial scales, is overcome by increasing the

number of turbines involved in the project and, most importantly, large-scale integration with other energy resources such as nuclear, gas, or hydro power plants. One of the aims of this study is to merge renewable energy technologies with conventional energy resources. That is, to not only reduce the problems associated with the intermittency nature of wind energy, but to also lower the cost of electricity per kilowatt produced and increase the quality of energy, compared to stand-alone wind farms.

Penetration of wind power in the electricity system can be increased by converting excess electricity into other forms of energy during high availability hours. There are many storage options in large-scale production. Excess energy can be stored in a chemical form, mainly hydrogen, through the use of electrolyzers or in a mechanical form, for example compressed air or pumped water. Storage is vitally important to maintain high penetration and, at the same time, keeping the reliability and security of the electricity supply.

Representation of wind data:

The wind data for a particular region can be represented by a wind rose graph. The graph is a circle divided into eight or twelve sectors, and represents the direction, speed, and frequency of wind. Figure 2.9 shows a representation of Nanticoke region's wind data (Environment Canada, 2003). The data could also be represented by a probability distribution curve as shown in Figure 2.10 which gives the frequency and magnitude of wind speed or power (Environment Canada, 2003).

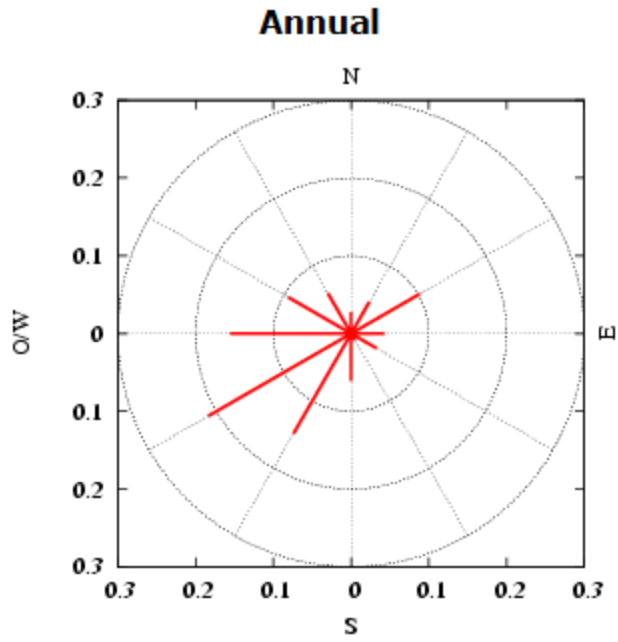


Figure 2.9 Wind rose plot of Nanticoke region at 42.791N & -80.168W.

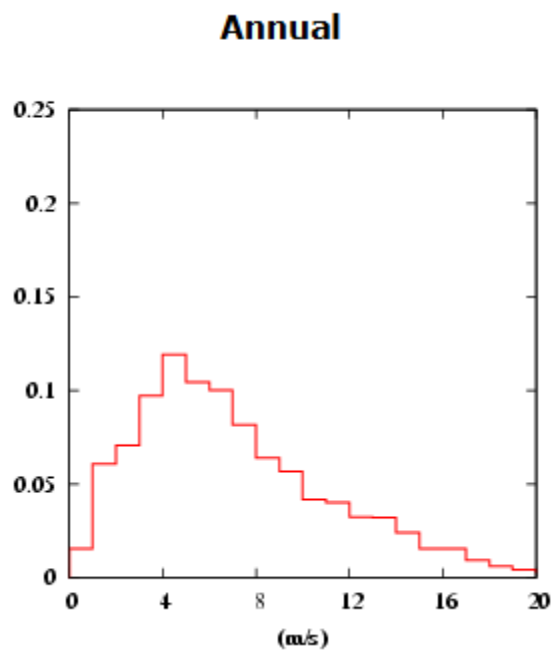


Figure 2.10 Probability distribution of wind speed and power at Nanticoke region at 42.791N & -80.168W.

2.3.2 Wind turbines

Wind turbines extract wind energy and convert it to a more useful form, specifically electricity. The advances in wind turbines sector have offered many choices of turbines from which to choose ranging from micro-turbines producing a few kilowatts, to large-scale commercial turbines connected to the local electric transmission networks. Wind turbines can be classified according to the following criteria:

- **Yaw system.** Because wind changes in direction, a control system is needed to ensure the turbine is perpendicular to the direction of wind. This is necessary to maximize the energy captured by the turbine. The mechanism of yawing can occur naturally by wind “passive”, or using a control system “active” as stated by the Danish Wind Industry Association (2003). Active yawing turbines are considered in this project, as they are used in commercial large-scale turbines.
- **Vertical versus horizontal axes.** Wind turbines can be classified into vertical axis and horizontal axis layouts. The vertical axis type is perpendicular to the wind flow. Although a yaw mechanism is not needed in this layout, horizontal axis wind turbines, in which the rotation of the rotor is parallel to the direction of wind flow, have the advantages of being more efficient and suitable for large-scale power generation (Danish Wind Industry Association, 2003). The vertical axis layout is chosen for this work.
- **Number of blades.** Wind turbines can be classified based on the number of blades as one, two, and three-bladed. One and two-bladed types are not as commercial as 3-bladed type, which offers stability, balance, and efficiency over the other two designs (Danish Wind Industry Association, 2003). Only 3-bladed designs are considered in this work.
- **Nameplate capacity (nominal power).** Depending on the purpose of the wind turbine, they range from small-scale turbines ranging from 2–10 kW for farm and individual homes use (American Wind Energy Association, 2009), to commercial-scale starting at 1 MW. Only large-scale turbines are considered in this work, since they are the choice for utility energy hubs.

2.3.3 Economics and growth of wind energy

Arising from volatile fuel prices and the accompanying environmental issues of conventional energy production systems, the wind energy sector has seen as unexpected growth in the last

decade. Worldwide electricity production from wind has risen up from 6.1 GW worldwide in 1996, to 120.8 GW in 2008 (Zervos & Sawyer, 2008). Figure 2.11 shows wind power production of the top ten countries and the rest of the world between 1990 and 2008 (Tanaka, 2009). By 2014, wind energy is expected to account for 447 GW of global electricity production and is expected to rise to 1000 GW by 2019 (BTM Consult ApS, 2010).

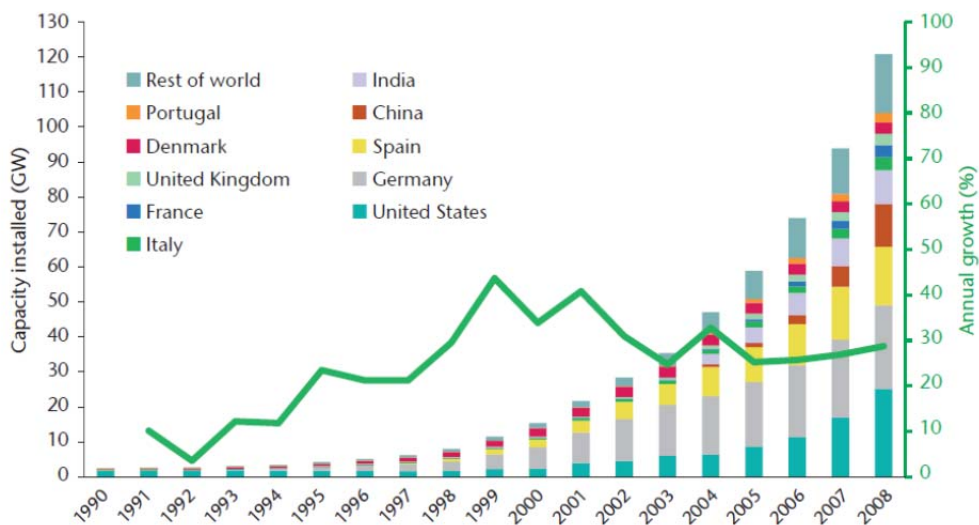


Figure 2.11 World cumulative production of wind energy.

Canada generates 1% of its electricity from wind, or about 2,360 MW as of 2008 (Zervos & Sawyer, 2008). Among Canadian provinces, Ontario is a leader in wind power sector with seven large-scale wind farms in operation. In Ontario alone, about 780 MW was produced from wind in 2008. This accounts for 3% of the total energy produced, or almost 1100 MW of installed capacity. Another six large-scale farms are expected to add more than 490 MW of installed capacity between 2010 and 2012 (IESO, 2010). Table 2.4 shows the installed and projected capacity in Canadian provinces as of 2010.

Table 2.1 Canadian’s current installed and projected capacity by province.

Province	Existing capacity^a (MW)	Under construction^b (MW)	Projects completion^b
Ontario	1,457	4,032.1	2010–2016
Alberta	806	1,029.6	2010–2013
Quebec	663	2,361	2011–2015
New Brunswick	249	163.5	2010–2011
Nova Scotia	235	1,634.1	2010–2012
Saskatchewan	171.2	54.75	2011–2013
PEI	164	10	2011
Manitoba	104	138	2011
British Columbia	103.5	711.2	2011–2014
Other^c	55.51	-	-
Total	4,008	10,134.25	-

(a) Source: (Canadian Wind Energy Association, 2008a). (b) Source: (Canadian Wind Energy Association, 2010).

(c) Newfoundland = 54.7 MW, and Yukon = 0.810 MW.

2.4 Solar Energy

2.4.1 Solar energy overview

Solar energy is the most abundant renewable energy on earth. Ultimately, there are three technologies to harvest energy from the sun: (a) solar thermal, (b) solar chemical, and (c) photovoltaic (PV) solar technology. Solar thermal is based on the collection of sun energy to heat a fluid to a high temperature. Heat is used to generate steam or hot water for space heating or some industrial applications. Excess energy from solar thermal systems during the day can be stored in the form of hot oil or molten salt to eliminate intermittency. Solar chemical energy uses lenses to drive photochemical reactions to split water to its components. Coupled with other technologies, the temperature can exceed 2200 °C, which is the temperature required to obtain a good degree of dissociation (Kodama, 2003). The advantage of this technology is the ability to produce a portable fuel and the diversity of feedstock used (e.g., NG).

Among the technologies mentioned, PV is the most promising technology. Today, PV solar is used for stationary applications for both isolated and grid-connected systems. Over the last thirty years, this technology has been developing steadily; yet, further development is required to compete with conventional energy systems. Figure 2.12 shows an overview of different solar power technologies (Raugei & Frankl, 2009).

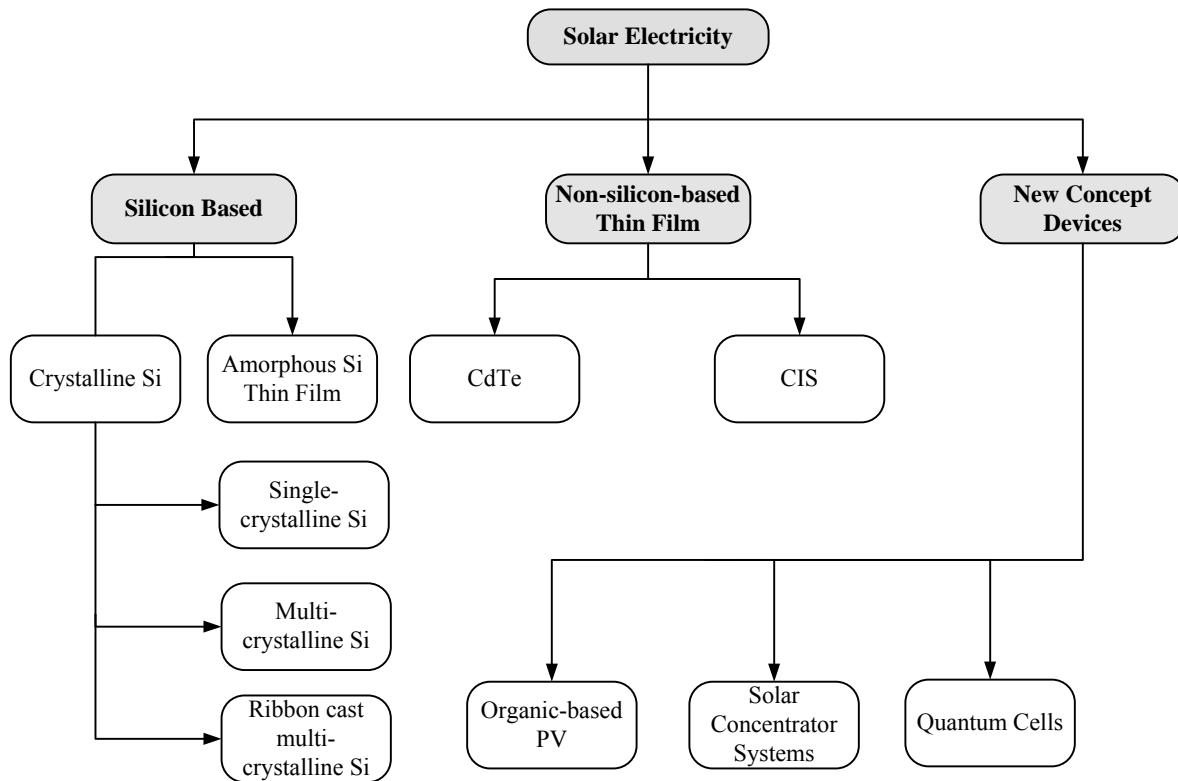


Figure 2.12 Overview of the different solar cell technologies.

Integration with other energy sources:

Solar energy is an intermittent source of electricity that is not completely reliable if it is not coupled with other technologies. Using solar energy effectively means using either an energy storage system, or connection and integration with other energy production systems. There are many storage options for energy, such as batteries and mechanical storage in the form of compressed air or pumped water. These technologies, however, are either expensive or only suitable for small-scale electricity generation.

A more effective way is to use electricity during the daytime to generate hydrogen to be used for power or other industrial applications. Another method is to couple solar heat with conventional power systems, such as gas turbines. A performance assessment done by Schwarzbözl *et al.* (2006) shows the economic and technical perspectives of solar–gas turbine hybrid system. Energy from solar concentrators is used directly to heat the pressurized air upon its entrance to the combustion chamber. The elevated air temperature can reach up to 1,000 °C which reduces the fuel required for generation dramatically. Figure 2.13 shows a schematic diagram of the system (Heller et al., 2006). A conversion efficiency of solar heat in the range of 40–50% was obtained. Some advantages that solar–fossil hybrid systems are expected to offer are high efficiency, lower cost, and increased reliability. The solar-fossil hybrid systems are promising technology, yet it is still in the early stages.

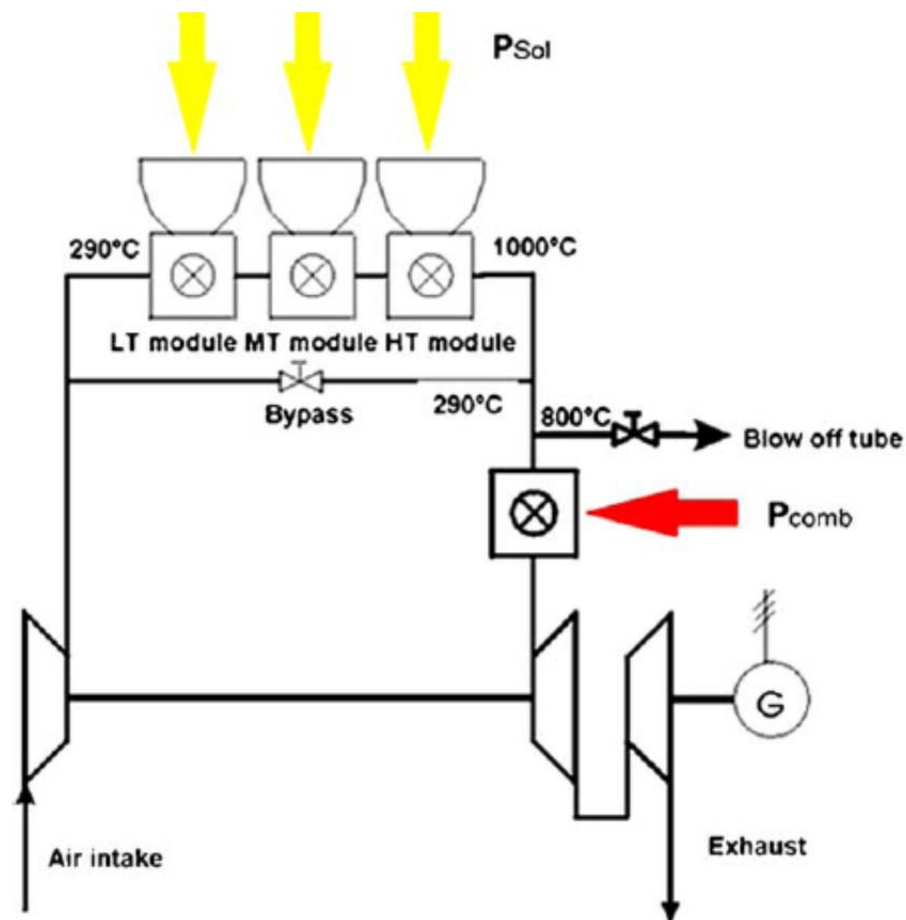


Figure 2.13 Solar–gas turbine hybrid system.

2.4.2 PV solar cells

PV solar cells are the basic units for the PV system and the dominant technology in solar power. PV solar cells convert sunlight directly into electricity via PV effect. A group of cells are combined to form a module. Modules, on the other hand, are connected together in series to form an array. Connecting modules in a series increases the system voltage, while connecting arrays in parallel ensures a high-current system. Despite the high manufacturing costs, PV solar cells are commercially available, reliable, and dominating the marketplace. As shown in Figure 2.12, silicon-based PV solar cells are classified into amorphous (a-Si) and crystalline silicon (c-Si). The most common type is c-Si which is further classified into single-crystalline silicon (sc-Si), multi-crystalline silicon (mc-Si), and ribbon silicon (ribbon-Si). Table 2.2 shows a comparison between different PV technologies in terms of efficiency, lifetime, and market share (EPIA, 2011). Among c-Si technologies available today, sc-Si technology has the highest market penetration (89.5%), with an efficiency reaching up to 22% the highest among c-Si technologies.

PV solar system components:

- PV array (modules) to collect sunlight.
- DC–AC inverter and step-up transformer for grid-connected systems.
- Storage facilities for stand-alone and off-grid systems.

Table 2.2 Overview of PV solar technologies^(a).

Technology	Crystalline Si			Thin films		
	sc-Si	mc-Si	ribbon-Si	a-Si	CIS	CdTe
Module efficiency, %	16–22	14–18	14–16 ^a	4–8	7–12	10–11
Module power, W	120–300			60–350		
Area needed per kW, m ²	7	8	-	15	10	10

(a) Source : (Agrawal & Tiwari, 2010)

Theory:

The theoretical maximum power P_{max} of a PV solar cell is dependent on the characteristics of the PV cell, and is given by the following equation:

$$P_{max} = P_o * [1 + (\alpha + \beta)\Delta T] \quad (2.12)$$

Where; α and β are the coefficients for a specific PV solar cell, ΔT is the temperature difference between the cell and the reference cell temperature, and P_o is given by:

$$P_o = I_o \cdot V_o \quad (2.13)$$

Where; I_o and V_o are the short-circuit current and the open-circuit voltage for a specific PV solar cell respectively.

The power generated by a PV solar cell depends on the amount of yearly sunlight or solar irradiance, the efficiency of the PV cell, as well as the ambient air temperature. Figure 2.14 shows the I - V characteristics of PV system proposed for the energy hub (Sunpower Cor., 2010).

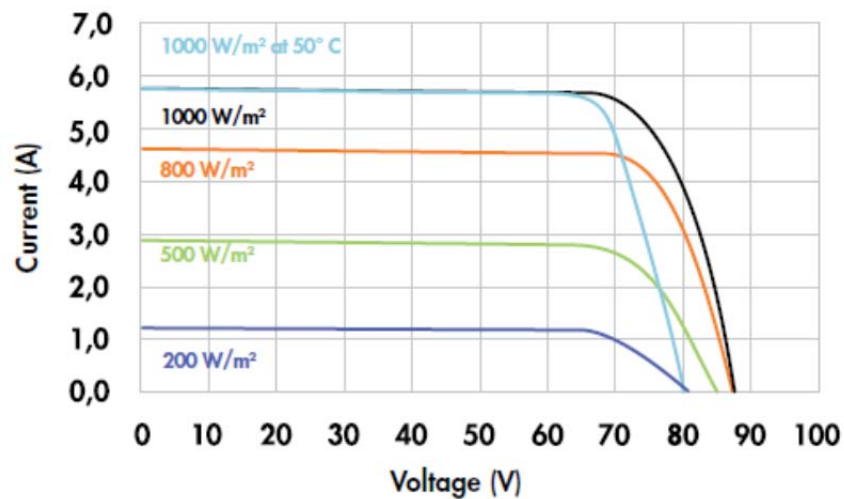


Figure 2.14 Current-voltage characteristics of SunPower-400 model.

Solar energy in general and PV technology have been chosen for the following reasons:

- solar energy is clean power and emissions-free technology;
- it is renewable and plentiful;
- it has wide applications—satellite and communication stations;
- it is suitable for rural areas—it can operate independently;
- it is flexible, where it can be used directly for heating or to generate electricity; and,
- it has very low maintenance costs.

Challenges:

- Solar energy is intermittent; that is, it is only available during day time;
- PV solar technology has low energy density—requires large area; and,
- the investment costs are still very high, due to the expensive manufacturing materials.

2.4.3 Economics of solar energy

As of 2009, solar energy provided more than 22.8 GW of energy worldwide compared to 1.4 GW in 2000 (EPIA, 2010); yet, this represents less than 1% of the world's produced electricity. The share is expected to grow up to 30 GW by 2014. According to the Department of Natural Resources Canada Report on Canadian PV solar energy, the total installed capacity of PV solar is 94.57 MW in 2009 (Ayoub, Dignard-Bailey, & Poissant, 2010). About 87% of the generated electricity is grid-connected, while the off-grid applications account for 13%. Figure 2.15 shows the world annual market of PV solar energy (EPIA, 2010).

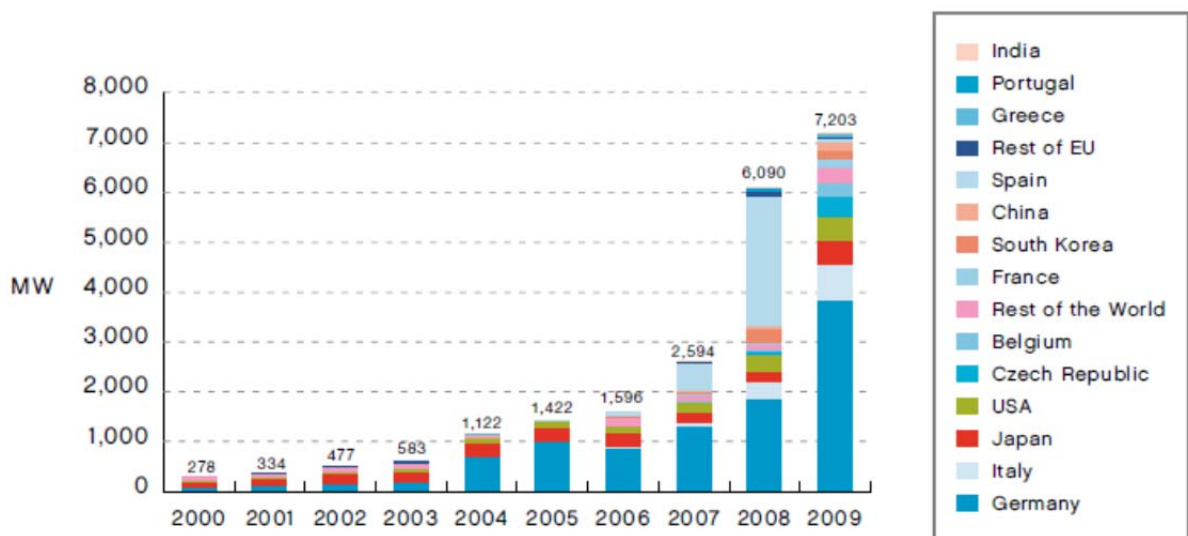


Figure 2.15 World annual market of PV energy (2000–2009).

Although electricity price from solar energy has been decreasing over the past few years, relatively high costs are still a barrier for PV systems to invade the power industry. As PV technology improves, the cost of produced electricity is expected to fall to the current average cost (35 ¢/kWh). According to EPIA (2011), low and competitive PV electricity costs can be achieved by addressing the following issues:

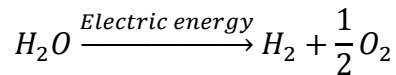
- Technological advancement.
- Production optimization.
- Increasing the market share.
- Improving the system efficiency.
- Increasing the lifetime of PV cells
- Developing unified standards and codes.

Finally, as the price of fossil fuels rise, solar energy shows great promise for the future, driven by public support of renewable energy resources and the increasing efficiencies and reliabilities of this technology.

2.5 Electrolysers

2.5.1 Electrolysers overview

Hydrogen is produced from water electrolysers by passing an electric current through electrodes in the presence of electrolyte. This technology has been used successfully to produce hydrogen in rural areas and in some applications related to wind and solar power. The purity of hydrogen produced can reach up to 99.999% in some technologies. Hydrogen is produced at the cathode, while oxygen is produced at the anode side and the overall electrolysis reaction is described by:



There are three main technologies developed for water electrolysis today: solid electrolyte electrolysers, proton exchange membrane electrolysers, and alkaline electrolysers.

Solid polymer electrolyte (SPE) electrolysers. SPE electrolysers are composed of a membrane as a solid electrolyte with anode and cathode. The cell operates at high temperatures which reduces the energy required to produce hydrogen. SPE electrolysers, compared with alkaline technology, are safer in operation since they do not include KOH. Because of their simplicity and safety, SPE technologies are used in some applications, such as in submarine and space applications. SPE electrolysers, however, have not been commercialized yet due to their short operating life; besides, they are not yet well-proven technology and they still at the R&D stage.

The dissociation reaction into oxygen and hydrogen is described by the general water electrolysis chemical equation. Figure 2.16 shows the working principles of SPE electrolysers (Choi, Bessarabov, & Datta, 2004).

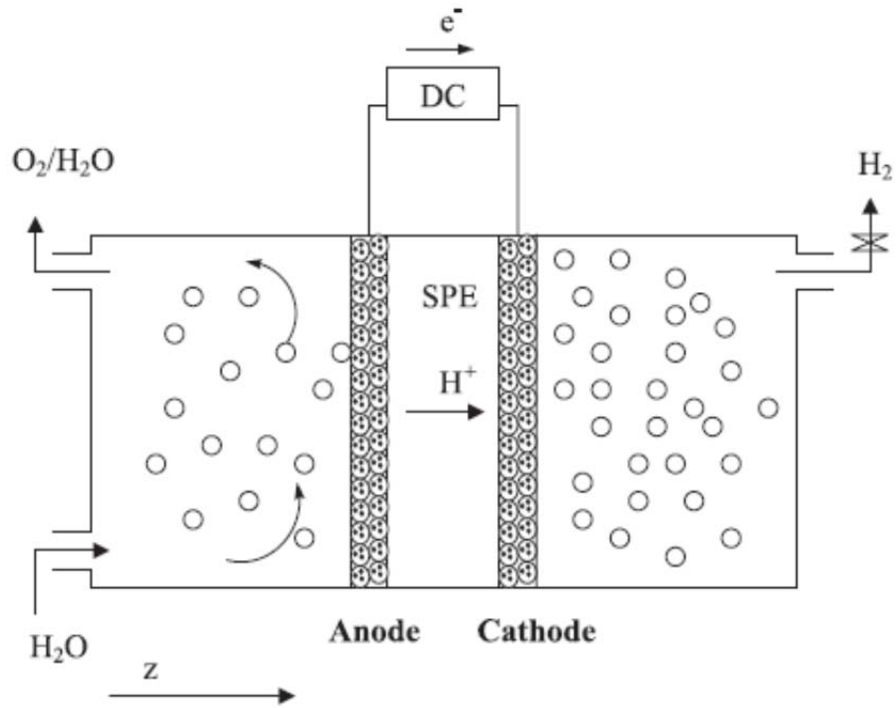
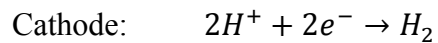
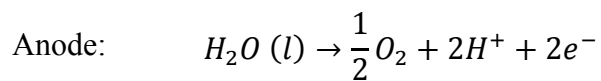


Figure 2.16 Schematic diagram of SPE water electrolyser.

Proton exchange membrane (PEM) electrolysers. PEM water electrolysis technology is similar to that of the PEM fuel cells, but, with reverse working principles. Figure 2.17 shows the mechanism of PEM water electrolysis (Barbir, 2005). Water electrolysis in PEM electrolysers proceeds according to the following equations:



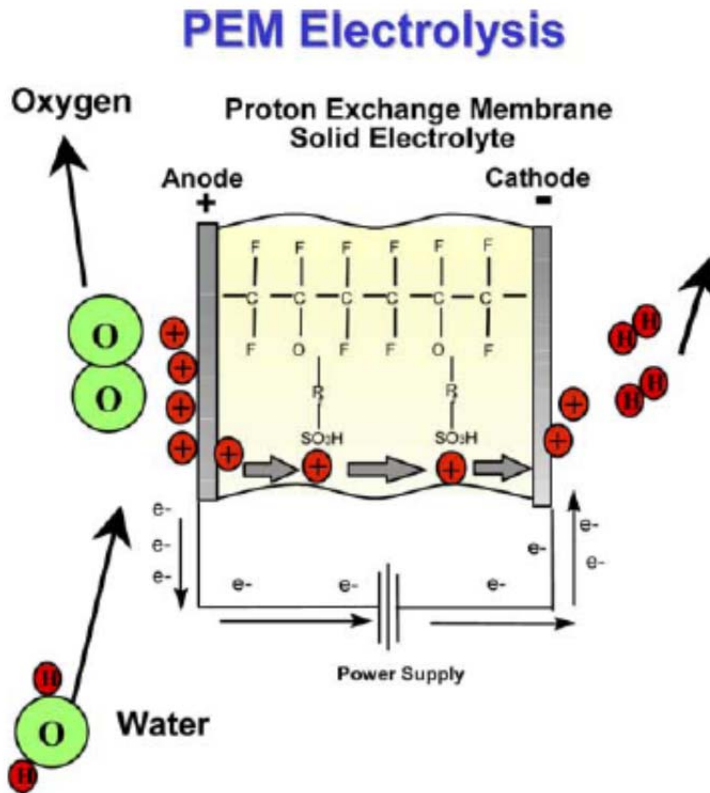
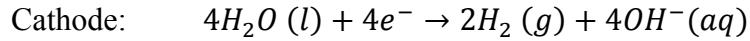


Figure 2.17 Mechanism of PEM water electrolysis.

PEM electrolyzers operate at very high current density. The hydrogen is produced at high purity 99.999% and high pressure. PEM electrolyzers compact design and flexibility in operation, make them suitable whenever intermittent electricity sources are applied (e.g., wind and solar). However, the cost of this technology is still high, and it has not been applied commercially on a large scale. Moreover, this technology is not suitable for large scale electricity production.

Alkaline electrolyzers. In alkaline electrolyzers the electrolyte is usually KOH solution 20–30 wt%, with operating pressure 1–30 bar and temperature 70–100 °C (Ulleberg, 2003). Alkaline electrolyzers generate hydrogen at good purity with conversion efficiency exceeds 60% based on LHV of hydrogen. Hydrogen is produced at the cathode side, while oxygen is produced at the anode side as shown in (Ulleberg, 2003), and by the following reactions:



Basically, alkaline electrolyzers are classified according to the type of electrodes: unipolar and bipolar. Bipolar alkaline electrolyzers are more efficient than the unipolar type, and they are commercially available. Recent studies showed that alkaline electrolyzers of bipolar filter-press type are the most applicable water electrolysis technology used today (Gandía et al., 2007). The pressurized hydrogen produced without need to external compressors reduces the cost associated with compression utilities. Moreover, alkaline electrolysis is well-proven technology, and it dominates water electrolysis with a large number of units in operation today.

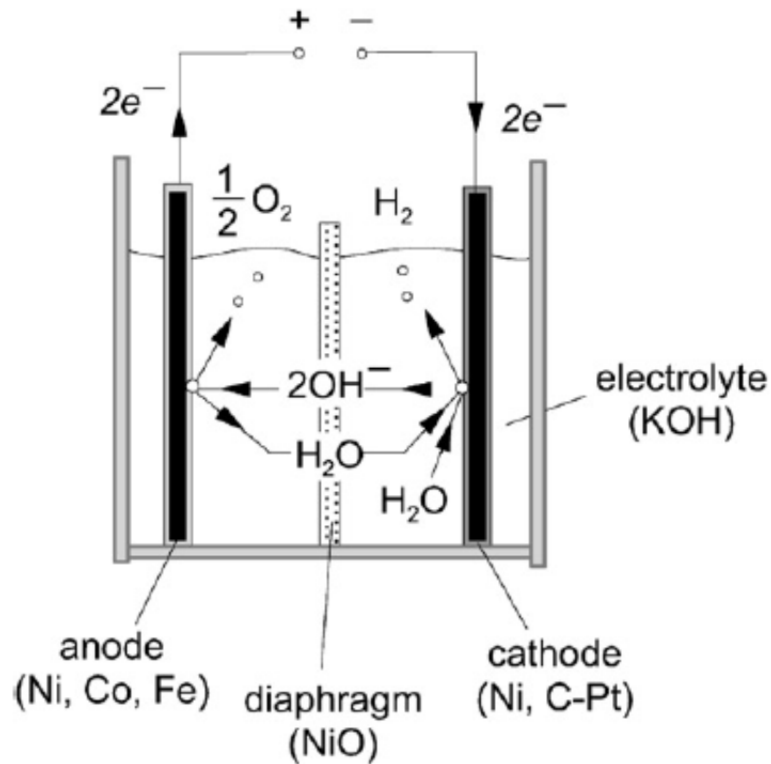


Figure 2.18 Alkaline electrolyzers operating principles.

2.5.2 Electrolyser selected, advantages, and challenges

Water electrolysers offer many advantages over conventional hydrogen production, although the cost of hydrogen produced is still high:

- Electrolysers operate at high efficiency up to 70% (Diéguez et al., 2008).
- Electrolysers have the ability to operate in distributed and small scale systems.
- They can operate in rural areas and be integrated with renewable energy (such as wind and solar), where excess energy can be converted to hydrogen.
- O&M costs are very low, since no moving parts are included (Diéguez et al., 2008).
- They are clean source for hydrogen if used in conjunction with renewable sources.
- High purity hydrogen can be produced—up to 99.9999%.

In addition to the advantages of using water electrolysis as the hydrogen source, alkaline electrolysers have been chosen over PEM and SPE technologies for the following reasons:

- There is no need to use noble-metal catalysts, so alkaline electrolysers are cheaper than PEM electrolysers.
- This type is a well-proven technology, and there are hundreds of units in operation worldwide today, compared to SPE electrolysers.
- Suitable for large scale production compared to PEM electrolysers.

Challenges:

- Production capacity is still small since shifting to the hydrogen economy will require a production capacity 10–100 times the production size today (National Renewable Energy Laboratory, 2004).
- Cost of hydrogen produced from electrolysis is still high compared to hydrogen from SMR and coal gasification units.
- In the long-term, issues such as improving efficiency and durability are needed to be addressed in order to produce hydrogen with competitive prices.

2.6 Hydrogen Economy

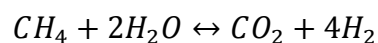
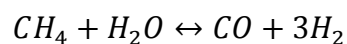
Hydrogen plays a major role in today's economy. Large quantities of hydrogen are used in refinery processes, hydro-cracking, to crack the heavy undesirable fractions to lighter, more valuable products. Ammonia-based fertilizers consume a significant amount of hydrogen, as well. The hydrogen economy is a hydrogen-based system concerned with hydrogen production, distribution, storage, and applications. The hydrogen economy is becoming a necessity in the transition from non-renewable fossil fuel-based economy to a more sustainable hydrogen-based economy.

2.6.1 Hydrogen production

There are different paths for hydrogen production. Currently, the dominant hydrogen source is fossil fuels (natural gas, petroleum, and coal). Steam–methane reforming (SMR) process, for example, account for about 40% of hydrogen produced worldwide. Fossil fuels are the cheapest and the most widely used in hydrogen production in large scales. Hydrogen is also produced via water electrolysis from renewable energy—wind, solar and hydro—and nuclear power in considerable amount. Hydrogen annual production is expected to rise to 150 million tons by 2040 which could replace 18.3 million barrels per day of petroleum according to the National Commission on Energy Policy (2004).

Figure 2.19 shows the technological paths for hydrogen production from different routes (Muradov & Veziroglu, 2008).

SMR process is the dominant process for hydrogen production in efficient and cost effective way. The technology is fully mature to produce hydrogen in a large scale with competitive prices. Nearly 80% of hydrogen produced in the U.S is from SMR process ("Roadmap on manufacturing R&D for the hydrogen economy," 2005). The process includes the reforming of natural gas or other light hydrocarbons with steam. The reforming process is carried out in the presence of a nickel-based catalyst at a temperature 1000 °C and a pressure 20 atm (Barelli et al., 2008). The reaction is highly endothermic and is described by the following reactions:



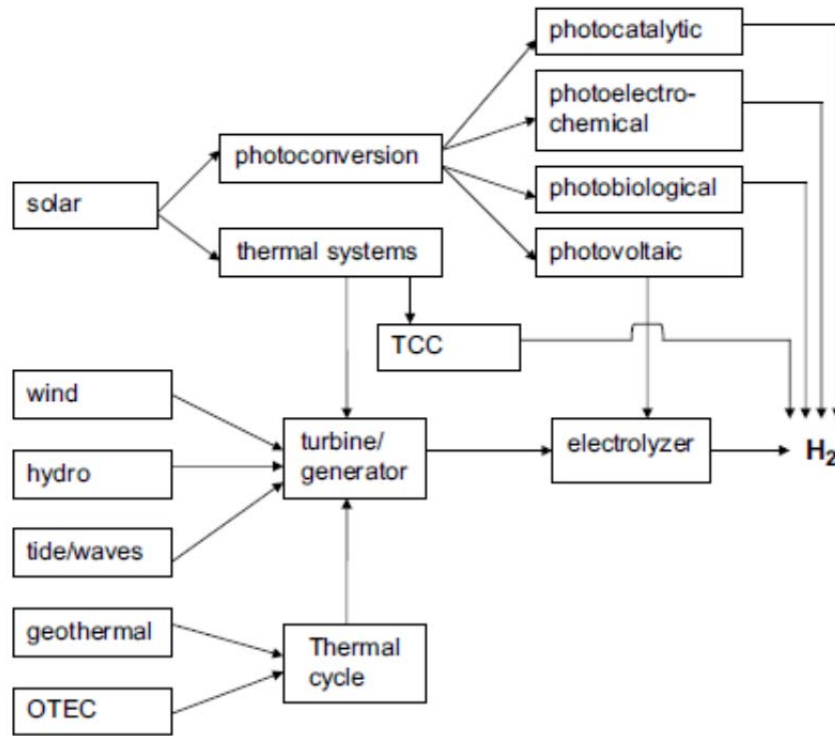
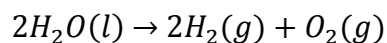


Figure 2.19 Main technological routes to hydrogen production from renewable sources.

The reformed gas mixture contains about 76% of hydrogen (Kirk-Othmer, 1998). Hydrogen purity can reach up to 99% either by using pressure swing adsorption (PSA) technology or amine scrubbing (Barelli et al., 2008). The coal gasification process also accounts for high hydrogen production share. The gasification process is carried out by burning coal at high temperatures. The gas produced (syngas) is a mixture of hydrogen, methane and heavier HCs, carbon dioxide and other pollutants. Although fossil fuels are the lowest-cost option for today’s hydrogen production, source depletion and carbon footprint require seeking an alternative, sustainable way for hydrogen production.

Water electrolysis is another form for hydrogen production from water. Water electrolyzers can be integrated with nuclear, wind, solar, or hydro power systems to eliminate some of these technology barriers such as intermittency. The overall electrolysis reaction of water is:



The technology is not fully mature and only represents a small share compared with the SMR process. Electrolysis is energy-intensive process and on average it consumes about 4.5–5 kWh/m³ H₂ (Stojic et al., 2003), making hydrogen produced from this technology more expensive than fossil fuel-based hydrogen.

Nuclear energy is an emission-free technology that can generate electricity and hydrogen as an energy carrier. Nuclear energy is a mature technology, relatively not costly. The technology can be coupled with water electrolyzers and thermochemical processes to produce hydrogen in mass quantities. The disadvantage of nuclear energy regarding its limits to base-load demand can be partially overcome by producing hydrogen as an energy carrier. Various hydrogen production technologies from nuclear are summarized in Table 2.3 as stated by the Committee on Alternatives and Strategies for Future Hydrogen Production and Use (2005).

Table 2.3 Nuclear hydrogen production technologies overview.

Feature	Electrolysis		Thermochemistry	
	Water	High temperature steam	Methane reforming	Water splitting
Required temperature, °C	>0	300–600	>700	600–850
Efficiency	75–80	85–90	70–80	>45
Advantages	- Proven technology. - No CO ₂ emissions.	- No CO ₂ emissions.	- Proven chemistry. - 40% reduction in CO ₂ emission.	- No CO ₂ emissions.
Disadvantages	- Low efficiency	- Requires high temperature reactors.	- CO ₂ emissions. - Dependent on CH ₄ prices.	- Aggressive chemistry. - Requires development.

Hydrogen end-use:

- Major feedstock for ammonia production and some other chemicals.
- Hydro-cracking and hydrogenation units in refining industries.
- Stationary power generation: FCs and H₂-rich gas turbines.
- Automotive sector as fuel: internal combustion engines and hydrogen FCVs.

2.6.2 Hydrogen infrastructures

Hydrogen distribution and transportation plays a key role in the final cost of hydrogen. Because of its very low energy density by volume, hydrogen distribution can be very costly. Basically, there are three methods of hydrogen transportation: pipelines, trucks, trains and ships. Pipelines are the most energy efficient for hydrogen transportation, especially on a mass-scale. However, the high capital costs and some technical issues are still a barrier for hydrogen distribution inside urban cities and rural areas. Trucks are used to deliver relatively small amounts of hydrogen between central production facilities and demanding sectors. Trains and ships, on the other hand, are suitable for medium to large hydrogen transportation, although transportation by ships can be costly due to compression and low temperature requirements.

Hydrogen storage is a vital step in hydrogen economy. Hydrogen gas has a very low energy density by volume; therefore, storage can be a costly process. There are many technologies for hydrogen storage depending on the scale and the end-use of hydrogen.

- **Pressurized hydrogen storage.** This is the most common technology. Hydrogen is pressurized and stored under 350–700 bar at ambient temperature ("Roadmap on manufacturing R&D for the hydrogen economy," 2005). This method, however, has its limitations due to the very low hydrogen density. The problem is obvious when hydrogen is used as fuel for portable applications (i.e., hydrogen FCVs).
- **Underground hydrogen storage.** Hydrogen is stored in underground depleted oil and gas wells, caverns, and salt domes. Underground hydrogen storage is a promising technology especially in processes involving large-scale hydrogen production or use. The technology has been used successfully to store large amounts of NG. However, extra care must be taken with hydrogen as it is more expensive and any leakage or loss will be translated into storage costs.
- **Liquid hydrogen storage.** Hydrogen can be stored at very low temperature, up to 20 K, and near ambient pressure ("Roadmap on manufacturing R&D for the hydrogen economy," 2005). This technology offers higher energy density per volume than pressurized hydrogen technology which makes it more convenient in automotive industry. However, liquefaction and keeping hydrogen under low temperatures is an intensive energy-consuming process—

about 40% of hydrogen LHV are consumed during the liquefaction process (Aceves et al., 2006).

- **Metal hydride storage.** Metal hydrides such as those of Mg and Li have the ability to absorb hydrogen and form weak bonds. Metal hydride then heated to release hydrogen. This method has very high storage capacity compared to pressurized and liquid hydrogen storage; besides, it offers safer design and more stability (Melnichuk, Silin, & Peretti, 2009). However, this technology is still under development and more research and development are needed before commercialization.

2.6.3 Motivations for hydrogen economy

Transition from conventional-fuel based economy to hydrogen-based economy is the only visible way to decrease the environmental effects of burning fossil fuels. Although the infrastructure for widely distributed hydrogen economy is immature today, moving toward clean, renewable sources of hydrogen is a necessity to overcome the environmental issues in a cost effective way. Combined technological, economical, and social drivers for hydrogen-based economy can be summarized by the following points:

- **Local air quality.** The negative effects of certain pollutants such as NO_x, PM, and SO_x on health have been raising concerns in urban and industrialized cities. The vast majority of these pollutants come from both the transportation and power generation sectors. A hydrogen-based economy would reduce these emissions through its implementation in the transportation sector; that is, hydrogen-powered fuel cell vehicles, and, in the power generation sector, through FCs technology or in H₂-NG turbines.
- **Intermittency of renewable energy.** The intermittent nature of wind and solar power has limited their applications and has become one of the major barriers for implementing these technologies for many vital applications. However, hydrogen can be used as an energy carrier and storage vector. For example, excess power from solar energy during the daytime can be converted to hydrogen and stored. Hydrogen, then, can be converted back to electricity by fuel cells eliminating the need for the costly storage technologies, and presenting energy on demand systems.
- **Energy security.** The limited amount of oil and NG, increasing cost of fossil fuels in general, and vulnerability to attack (McDowall & Eames, 2006), makes shifting to a more

sustainable and distributed system, such hydrogen-based economy, a necessity in the near to midterm future. Note that recently the potential for NG has developed to become a larger component of the energy security solution, as more supply has come on line with the development of shale gas reserves.

- **Economic development.** The last few years have witnessed many technological progresses and shifts in the energy sector. In terms of green economy growth, hydrogen is seen as the future for sustainable and clean economy, especially in transportation and power generation sectors. There are many potential new markets for hydrogen-related industries including FCVs, hydrogen internal combustion engine ICEs vehicles, and power backups (McDowall & Eames, 2006).
- **Resource depletion.** Today, over 97% of global liquid fuels are provided from oil and gas sources, and this number is expected to drop only to 90% by 2030 (Tanaka, 2008). The limited oil and gas availability, and the expectancy of oil peak in the near-term future, imposes the necessity of finding alternative ways to replace fossil fuels with sustainable resources. Hydrogen can be produced from completely renewable energy sources, such as wind and solar energy, which would substitute the demand for fossil fuels in the near-term future and to replace them in the long term.
- **Climate change.** The rising concern regarding industrial gas emissions and their direct effects on global warming and climate change means hydrogen is regarded as the energy vector of the future for energy storage and for an urban transportation fuel. Hydrogen produces zero emissions if used in fuel cells, and only small amounts of NO_x if burned directly with air (Sherif, Barbir, & Veziroglu, 2005). Besides, hydrogen economy can be implemented for the most two energy consumers, power generations and transportation sectors which could save billions of tonnes of VOCs, CO₂, CO, PMs and other pollutants.

2.6.4 Challenges and barriers to hydrogen economy

Hydrogen economy still has many barriers to be overcome. The key barriers to hydrogen economy penetration can be summarized by the following points:

- The high costs related to hydrogen production from renewable energy, and the high costs related to its applications such as FCVs (McDowall & Eames, 2006).

- Many technological issues are still a barrier for hydrogen economy penetration. Effective hydrogen storage, transportation, and conversion structures are still not mature for distributed hydrogen-based economy. The very low energy density of hydrogen by volume makes costs related to storage and transportation of major concern.
- Lack of infrastructure, especially in a more distributed system; for example, absence of refuelling stations for FCVs (McDowall & Eames, 2006).

2.7 Ontario and Nanticoke Region Overview

2.7.1 Province of Ontario

Ontario is home to more than 13,422,000 million people, making it the largest province by population according to the Statistics Canada report “*Quarterly Demographic Estimates*” (2011). The high population, combined with economic and industrial growth, put major stress on the energy sector in the province. The province is trying to build an energy infrastructure that is diverse, reliable, and more sustainable. Figure 2.20 shows power generation stations in Ontario in addition to the transmission lines infrastructure (IESO, 2009).



Figure 2.20 Ontario electricity supply generation and transmission highlights.

The annual energy demand in Ontario is fluctuating. While total demand in 2006 was 151 TWh, this had been lowered to 139 TWh by the end of 2009. Table 2.4 shows Ontario's demand pattern over the last six years ("Demand overview,," 2012). Demand in a specific year is affected by weather conditions, the time of the year, and the time of day. Usually, demand peaks between 4 p.m. and 7 p.m. during the daytime and reaches a minimum at midnight.

Table 2.4 Total annual Ontario energy demand.

Year	Total TWh	Increase over previous year
2011	141.5	-0.35%
2010	142	2.2%
2009	139	-6.1%
2008	148	-2.3%
2007	152	0.7%
2006	151	-3.8%

Ontario has a total installed capacity of 34,079 MW ("Supply overview," 2012). This existing capacity is shared between nuclear, coal, gas and renewable including hydro and wind energy. The share of wind and solar power is very low, as shown in Figure 2.21 ("Supply overview," 2012). Nuclear energy's share is 11,446 MW as of January 2012, or about 56.9% of the total generated electricity. Although nuclear power is emissions free with low operating costs, the high capital costs required to construct new reactors, along with the problem of radioactive wastes, are still of major concern. Hydroelectric power is the lowest-cost power source and the most visible renewable energy. In Ontario alone, the 65 hydroelectric stations operated by OPG generated about 36 terawatt-hours in 2009 alone ("Power generation,," 2010).

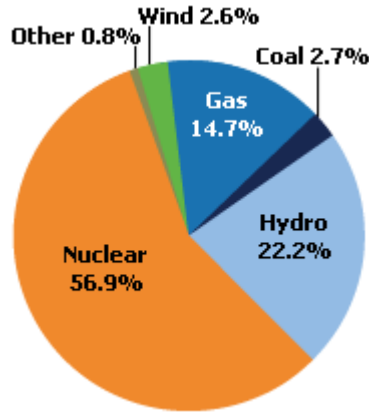


Figure 2.21 Ontario’s existing installed generation capacity by fuel type as of 2011.

Coal-fired power plants are being replaced by NG fuel due to the high negative environmental footprint of coal combustion, and the cost related to gas emissions control and mitigation. OPG currently runs four coal-fuelled power stations with a combined capacity of 4,000 MW. Because of new government regulations, these coal-fuelled power plants will be phased out by 2014 ("Thermal power," 2010).

Hydrogen economy in Ontario:

Hydrogen plays a significant role in the Ontario fuel economy and is expected to have an increasing demand over the next few years, as shown in Figure 2.22 (Hajimiragha et al., 2009). The introduction of hydrogen vehicles is expected to shift the transportation fuel pattern from gasoline-based to hydrogen-based. However, the lack of infrastructure for gas refuelling stations, concerns about hydrogen safety, and the costs related to HVs are still a barrier for applying hydrogen-based technologies in commercial scales.

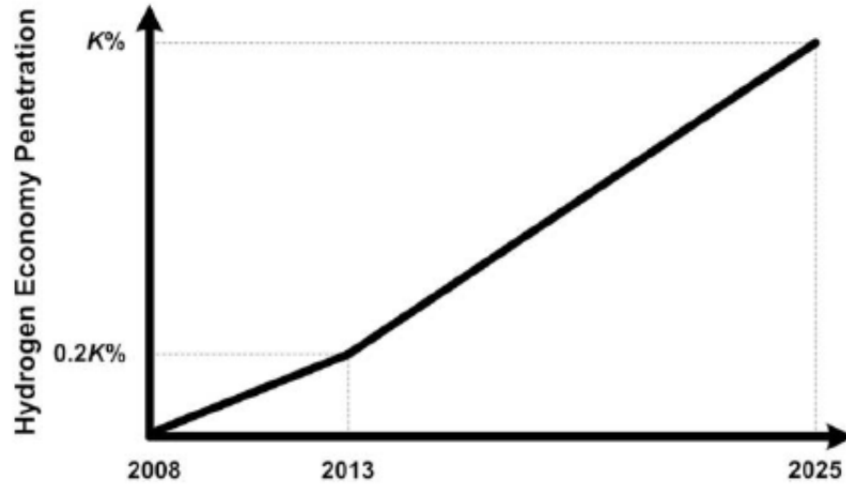


Figure 2.22 Assumed hydrogen transition in Ontario.

2.7.2 Nanticoke region

Nanticoke is located in Haldimand Country, on the north shore of Lake Erie, Ontario, Canada and has a population of 45,200 according to Census Canada (2006).

Lake Erie Industrial Park is in the heart of Nanticoke region and is one of the largest industrial parks in Ontario. There are three main major employers in the area: US Steel Canada Lake Erie works, Imperial Oil, and Nanticoke Generating Station. The Nanticoke Generating Station, a coal-fired power plant operated by OPG, started operation in 1972 and is capable of generating 2,760 MW of electricity. This represents more than 50% of the total coal-fired generated electricity operated by OPG. A screen shot of from the region Google Map® with major employers is shown in Figure 2.23. The 500 kV transmission lines, as shown in Figure 2.20, connect the area to the main generating stations and major cities. The area has been chosen for the project as it has the infrastructure for power generation, a 3,000 MW transmission station with a 500 kV transmission line, is close to a major highway and railway, and has high potential wind energy.



Figure 2.23 Nanticoke Region overview, the proposed site for the energy hub (Google Map, 2010).

CHAPTER 3

Model Development

3.1 Parameters and Design Variables

The modeling process is dependent on assuming certain values to be constant. These values or parameters work as the starting point for the modeling process. The parameters used are either: physical properties, standard and operating conditions, manufacturer's specifications, or cost factors. The model, however, which has been written in GAMS, made it easy to alter these parameters in order to accommodate some improvements on the model or to update certain values, such as cost factors. Sections below summarize the key design variables that have been used in each of the three scenarios.

3.1.1 Gas turbine power plant

The power plant configuration selected is of a combined cycle type. The key parameters for air compressor, combustion chamber, gas and steam turbines are shown in Table 3.5. Some of these parameters are standards, such as design ambient temperature and pressure, others, such as efficiencies, are taken as what was most common in literature.

Figure 3.1 shows the process flow diagram for the proposed CCPP with stream numbers used to identify parameters and variables at certain points. Parameters and variables, such as temperature and pressure, are used to develop a technical and an economic model for the hub, are identified by numbers each represents a stream number in Figure 3.1.

Table 3.1 NG turbine parameters and specifications.

Specification	Value	Source
Ambient temp. (°C)	15	(ISO 2314, 2009)
Ambient pressure (bar)	1.013	(ISO 2314, 2009)
Nominal power (MW)	200	assumed
Pressure ratio	15.6	(Lazzaretto & Toffolo, 2010)
Mechanical efficiency turbine to compressor (%)	98.5	(Lazzaretto & Toffolo, 2010)
Turbine entry temperature, TET (°C)	1120	(Lazzaretto & Toffolo, 2010)
Polytropic efficiencies (%)		
Air compressor	92	(Godoy, Benz, & Scenna, 2011)
Gas turbine	90	(Godoy et al., 2011)
Steam turbine	92	(Godoy et al., 2011)
Boiler feed pump (isentropic)	84	(Baghernejad & Yaghoubi, 2011)
Burner pressure loss (%)	3	(Lazzaretto & Toffolo, 2010)
Compressor inlet pressure loss (%)	2	(Lazzaretto & Toffolo, 2010)
Electric generator efficiency (%)	98	(Lazzaretto & Segato, 2002)
NG LHV (kJ/kmol)	802,279	Assumed for pure CH ₄
Exhaust final exit temperature (°C)	≥105	(Lazzaretto & Toffolo, 2004)
Maintenance factor (% of IC)	1.1	(Naughten, 2003)
Overall heat transfer coefficient of the condenser W/(m².K)	1250	(Sinnott, 2005)

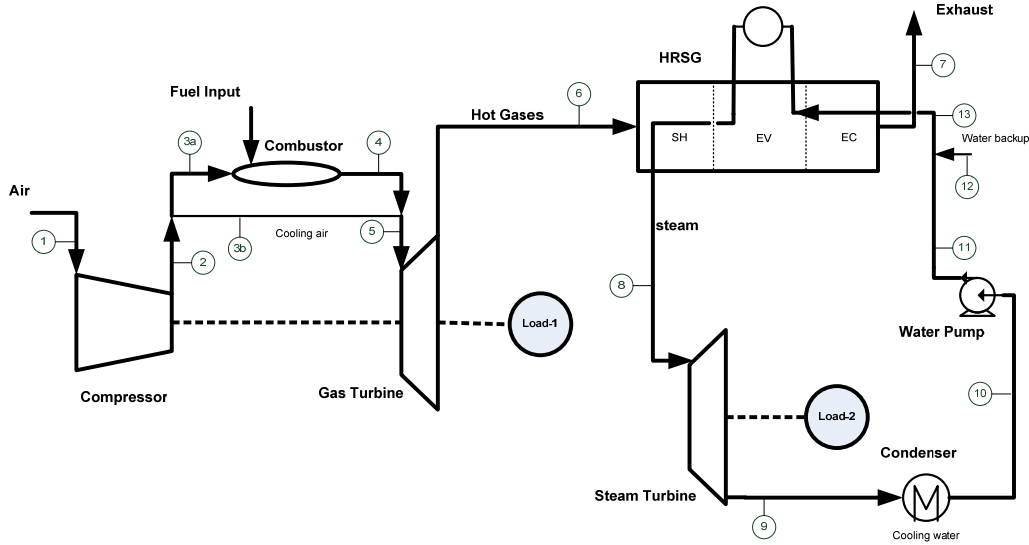


Figure 3.1 The proposed CCPP process flow diagram.

The mathematical model starts with estimating the energy required by the air compressor $E_{AC,i}$ in MWh during the compression. Equation 2.4 in Chapter 2 is applied in a new form to give:

$$E_{AC,i} = N_{1,i}RT_{1,i} * \frac{n}{n-1} * \left[\left(\frac{P_{2,i}}{P_{1,i}} \right)^{\frac{n-1}{n}} - 1 \right] . t \quad (3.1)$$

Where $T_{1,i}$ is assumed to equal the ambient temperature T_0 . $P_{1,i} = P_0 - \Delta P_{0-1}$; where P_0 is the ambient pressure, and ΔP_{0-1} is the pressure drop at the compressor inlet. It is assumed to be $2\% \cdot P_0$ as shown in Table 3.1.

The second major component of power plant modeling is the combustion chamber. The modeling is based on a lean, pre-mixed combustion chamber type. The first step is to define a relationship between the inlet and the outlet gases as it passes through the combustor. Pressure drops as air and fuel passes through the combustion chamber. Pressure at the combustion chamber exit, stream (4) in Figure 3.1, is given by: $P_{4,i} = P_{3a} - \Delta P_{3a-4}$, where ΔP_{3a-4} is the pressure drop at the combustion chamber and is assumed to be $3\% \cdot P_{3a}$ as shown in Table 3.1. The temperature of gases leaving the combustion chamber is determined by the energy balance

around the combustor. The *adiabatic flame temperature* or the combustion temperature, $T_{4,i}$ in Figure 3.1, is a key variable in designing a combustion chamber. A general relation given by Smith (2005) can be used to give an approximate value for $T_{4,i}$ as shown by Equation 3.2. A trial and error method is applied in order to get an approximate value of $T_{4,i}$.

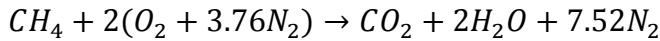
$$\Delta H_p = \Delta H_R - \Delta H_C^o \quad (3.2)$$

Where; ΔH_p and ΔH_R are the enthalpy change of products and reactants respectively, and ΔH_C^o is the standard heat of combustion at 298 K. Enthalpy change ΔH_j of a component j is a function of heat capacity ($\Delta H_j = \int_{T_i}^{T_o} C_{p,j} \cdot dT$), where the heat capacity $C_{p,j}$ is given by:

$$C_{p,j} = \alpha_j + \beta_j \cdot T + \gamma_j \cdot T^2 + \delta_j \cdot T^3 \quad (3.3)$$

In Equation 3.3, α_j , β_j , γ_j and δ_j are heat capacity constants for a given component j .

ΔH_C^o of NG is assumed for that of methane according to the following combusting reaction:



Another key parameter that should be considered in the combustion chamber modeling is the mathematical representation of gas emissions. Although a direct factor such as a percentage from the outlet gases could be used, this assumption lacks accuracy due to the variability of emissions according to the temperature and pressure drop through the combustor. Rizk and Mongia (1993), on the other hand, developed a semi-empirical relationship to estimate gas emissions as a function of the operating conditions as shown by the following equations:

$$NO_{x,i} = \frac{0.15E16 \cdot \tau^{0.5} \exp(-71100/T_{pz,i})}{p_{3,i}^{0.05} (\Delta p_{3a-4}/p_{3,i})^{0.5}} \quad (3.4)$$

$$CO_i = \frac{0.18E9 \cdot \exp(7800/T_{pz,i})}{p_{3,i}^2 \tau (\Delta p_{3a-4}/p_{3,i})^{0.5}} \quad (3.5)$$

$$UHC_i = \frac{0.755E11 \cdot \exp(9756/T_{pz,i})}{p_{3,i}^{2.3} \tau^{0.1} (\Delta p_{3a-4}/p_{3,i})^{0.6}} \quad (3.6)$$

Where; $NO_{x,i}$, CO_i , and UHC_i are emissions at any time i in g/kg of fuel, and τ is the residence time in the primary zone and is assumed 2 ms (Lazzaretto & Toffolo, 2004), and $T_{pz,i}$ is the primary zone temperature and is assumed to equal $T_{4,i}$. It is also of importance to highlight that incomplete combustion causes the formation of CO and UHCs, while the dissociation reactions are the cause for NO_x in the exhaust.

The third major component in modeling of combined cycles is the gas turbine or the expander. Equation 2.6, used to estimate work done by the gas turbine, is newly defined by Equation 3.7 to estimate the gross power from the device, and hence, the hourly electricity output.

$$E_{GT,i} = N_{5,i}RT_{5,i} * \frac{n}{n-1} * \left[\left(\frac{P_{5,i}}{P_{6,i}} \right)^{\frac{n-1}{n}} - 1 \right] . t \quad (3.7)$$

Where; $E_{GT,i}$ is the hourly energy from the turbine given in MWh, and t time interval given in hours. The relationship between inlet and outlet conditions is governed by the adiabatic compression-expansion relations.

The fourth major component in the combined cycle modeling is the heat recovery steam generator (HRSG). HRSG is the main unit that generates steam from the waste heat from the gas cycle to be delivered later to the steam expander. From the technical point of view, HRSG is divided into three zones: economizer, evaporator, and super-heater. The total energy transferred to the steam, stream (8) in Figure 3.1, is given by the general energy balance:

$$Q_{HRSG,i} = \int_{T_{7,i}}^{T_{6,i}} \sum_j (N_{j,i} \cdot C_{p,j}) \cdot dT_i \quad (3.8)$$

Where; $Q_{HRSG,i}$ heat transferred from the exhaust to the steam, $N_{j,i}$ molar flow of component j at any time i , and $C_{p,j}$ is previously defined by Equation 3.3. This relationship will be used later to determine the purchased cost of the HRSG, and to determine the hourly flow of steam can be generated and its temperature.

The fifth main component of the combined cycle modeling is the steam turbine or expander. The same relationship for the gas turbine is use for steam considering the inlet and outlet conditions. Similarly, the hourly energy production from the steam turbine $E_{ST,i}$ in MWh is given by:

$$E_{ST,i} = N_{8,i}RT_{8,i} * \frac{n}{n-1} * \left[\left(\frac{P_{8,i}}{P_{9,i}} \right)^{\frac{n-1}{n}} - 1 \right] . t \quad (3.9)$$

This relation will be used later to determine the overall electricity of the combined cycle.

The sixth major component in the combined cycle modeling is the steam condenser. Modeling of the condenser is assumed for that of a shell-and-tube type with an overall heat transfer coefficient U_{CON} of 1000–1500 W/(m².°C) (Sinnott, 2005). An average value of 1250 W/(m².°C) is assumed for this process. The design equation for the condenser is:

$$Q_{CON,i} = U_{CON} \cdot A \cdot LMTD_{CON,i} \quad (3.10)$$

Where; $Q_{CON,i}$ heat transferred at time i , A heat transfer area, $LMTD_{CON,i}$ log mean temperature difference at time i and is given by:

$$LMTD = \frac{\Delta T_h - \Delta T_c}{\ln(\Delta T_h / \Delta T_c)} \quad (3.11)$$

Where ΔT_h the temperature difference at the hot terminal, and ΔT_c is the temperature difference at the cold terminal. These relations will be used to rate the condenser and to estimate the cost of the condenser.

The last major component of the combined cycle modeling is the boiler feed pump or simply the water pump. Work required by the pump is given by Bernoulli's equation for incompressible fluids:

$$W_{PMP,i} = 9.81\dot{m}_{11,i} \cdot \Delta z_{10-11} + \frac{\dot{m}_{11,i}}{\rho_{H_2O}} \cdot \Delta P_{10-11,i} + \frac{\dot{m}_{11,i}}{\rho_{H_2O}} \cdot \Delta P_{f10-11,i} \quad (3.12)$$

Where; $W_{PMP,i}$ work required by the pump at any time i given in W, $\dot{m}_{11,i}$ steam mass flow rate given in kg/s, Δz_{10-11} difference in elevation given in m, $\Delta P_{10-11,i}$ pressure drop between point 10 and 11 in Figure 3.1 given in N/m², and $\Delta P_{f10-11,i}$ pressure drop due to friction given in N/m².

Similarly, hourly energy consumed by the water pump $E_{PMP,i}$ in Wh is given by:

$$E_{PMP,i} = \frac{W_{PMP,i}}{\eta_{PMP}} \cdot t \quad (3.13)$$

This relation will be used in the calculation of the net electricity produced from the steam cycle and the pump installed capital costs.

The last part of modeling the combined cycle is cost estimation. Cost estimation is dependent on the purchased cost of equipment as well as the O&M costs. For power plant equipment, the following relations are adopted to estimate the purchased costs, and hence the installed capital costs in US dollars (Attala, Facchini, & Ferrara, 2001).

$$IC_{GT,o} = 3,832 Np_{GT}^{0.71} \quad (3.14)$$

$$IC_{gGT,o} = 3,082 \left(\frac{Np_{GT}}{\eta_{gGT}} \right)^{0.58} \quad (3.15)$$

$$IC_{HRSG,o} = 17,000 \sum_k \left(\frac{Q_k}{\Delta T_k} \right)^{0.6} \quad (3.16)$$

$$IC_{ST,o} = 3,197,280 A_{ST}^{0.261} + 823.7 Np_{ST}^{1.543} \quad (3.17)$$

$$IC_{gST,o} = 3,082 \left(\frac{Np_{ST}}{\eta_{gST}} \right)^{0.58} \quad (3.18)$$

$$IC_{CON,o} = 162 A_{CON}^{1.01} \quad (3.19)$$

$$IC_{PMP,o} = 1,293.44 Np_{PMP}^{0.8} \left(1 + \left[\frac{0.3}{1 - \eta_{PMP}} \right]^{-0.46} \right) \quad (3.20)$$

Where:

$IC_{j,o}$: The initial installed capital costs of equipment j , \$.

Np_j : Nominal power of equipment j , kW.

A_j : Heat transfer area of equipment j , m².

Q_k : Heat flow at section k in the condenser, W.

ΔT_k : Temperature difference through section k , °C.

η_j : Efficiency of equipment j .

Annuity is then applied to estimate the value of installed capital costs over the entire life of the project. The general formula of annuity is given by:

$$A = P \cdot \frac{I(1 + I)^N}{(1 + I)^N - 1} \quad (3.21)$$

Where; A annual payments given in \$/y, P present value given in \$, N number of payments—assumed to be the project lifetime given in y, and I interest rate—assumed 5% for all the technologies used.

The annual installed capital cost IC_j of equipment j is given by:

$$IC_j = IC_{j,o} \cdot \frac{I(1 + I)^N}{(1 + I)^N - 1} \quad (3.22)$$

Derivation of the total annual costs of the power plant and the average annual cost per kilowatt are illustrated in Scenario A in Chapter 4.

3.1.2 Wind turbines

The proposed wind farm in Nanticoke region is based on Port Dover and Nanticoke Wind Project. In late 2009, a plan was announced to build a 110 MW wind farm holding up to 70 wind turbines with up to 8,900 acres of land available for the project, as stated by Capital Power (Stantic Consulting Ltd., 2009). The location of the project offers a stable and a strong wind profile, in addition to the easy access to the national transmission lines.

Onshore wind farm:

Data for the onshore wind farm is taken from Environment Canada at 42.791 N, -80.168 W, and 80 m above ground level. Table 3.2 gives the seasonal wind profile of the proposed onshore wind project.

Table 3.2 Onshore wind data for Nanticoke, ON (Environment Canada, 2003).

Period	Mean wind speed	Mean wind energy	Weibull scale
Annual	6.96	374.00	7.81
Winter (DJF)	8.26	536.75	9.32
Spring (MAM)	6.91	348.88	7.78
Summer (JJA)	5.53	178.94	6.22
Fall (SON)	7.26	400.50	8.17
Range	5.53–8.26	178.94–536.75	6.22–9.32

The design parameters for the onshore wind turbines are adopted for that of the GE 1.5 SLE model (GE Energy, 2009). Table 3.3 summarizes the key parameters needed for the modeling of onshore wind farm.

Table 3.3 GE1.5 SLE model wind turbine parameters and specifications.

Specification	Value	Source
Model	GE 1.5 SLE	(GE Energy, 2009)
Nominal power (MW)	1.5	(GE Energy, 2009)
Type	3-bladed, horizontal axis	(GE Energy, 2009)
Position	Up-wind	(GE Energy, 2009)
Yaw system	Active	(GE Energy, 2009)
Rotor diameter (m)	77	(GE Energy, 2009)
Swept area (m²)	4,657	(GE Energy, 2009)
Hub height (m)	80	(GE Energy, 2009)
Voltage (V)	690	(GE Energy, 2009)
Frequency (Hz)	50	(GE Energy, 2009)
Cut-in wind speed (m/s)	3.5	(GE Energy, 2009)
Cut-out wind speed (m/s)	25	(GE Energy, 2009)
Coefficient of performance	35	(Kurtulan & Sevgi, 2009)
Generator efficiency (%)	90	(Kurtulan & Sevgi, 2009)
Mechanical efficiency of the	95	(Kurtulan & Sevgi, 2009)
Installed costs (\$USD/MW)	1,700,000	(Blanco, 2009)
O&M costs (US\$/kWh)	0.007	(NREL, 2006)
Service life (y)	20	assumed

The first step in modeling a wind farm is to estimate the power output from each turbine as wind speed varies. The power of a wind turbine at a given wind speed is approximated by (Wizelius, 2007):

$$P_i = 0.5\rho \cdot A \cdot C_p \cdot \eta_g \cdot \eta_m \cdot w_{s,i}^3 \quad (3.23)$$

Where; P_i power produced given in W, A swept area given in m^2 , C_p the power coefficient or coefficient of performance, and $w_{s,i}$ average hourly wind speed given in m/s.

Power coefficient accounts for the maximum power can be captured by a wind turbine. According to Betz's law: $C_{p,max} = 0.59$, (Wizelius, 2007); and for a good design: $C_p = 0.35$, (Kurtulan & Sevgi, 2009). The generator efficiency coefficient η_g varies with load and turbine size—90% is acceptable in most commercial turbines. The mechanical efficiency η_m accounts for energy loss in the bearings and the gear box. For modern wind turbines, the mechanical efficiency can reach up to 95% (Kurtulan & Sevgi, 2009).

The equivalent captured energy can be expressed by:

$$E_i = P_i(w_s) \cdot t \quad (3.24)$$

This equation gives an approximate relationship between the hourly electricity E_i given in Wh produced from a wind turbine and the average hourly wind speed $w_{s,i}$. The total annual energy from onshore wind $E_{WTON,y}$ in Wh can be estimated by:

$$E_{WTON,y} = \sum_{i=1}^n P_{WTON,i}(w_s) \cdot t \quad (3.25)$$

The second step of modeling the wind farm is cost estimation. Cost of energy produced from wind turbines is governed by capital costs, wind speed, O&M costs, life time, and other auxiliary costs. The cost of onshore wind per installed capacity ranges from 1100 to 1400 €/kW (Blanco, 2009). An average value of 1250 €/kW ($c_1 = 1700 \$/kW$) is assumed for this model. Annual installed capital cost is defined over the equations:

$$IC_{WTON,o} = c_1 \cdot Np_{WTON} \quad (3.26)$$

$$IC_{WTON,y} = IC_{WTON,o} \cdot \frac{I(1+I)^N}{(1+I)^N - 1} \quad (3.27)$$

Where; $IC_{WTON,o}$ purchased costs of onshore wind turbines, Np_{WTON} nominal power, and $IC_{WTON,y}$ the annual payment.

O&M costs vary with the size of wind farm and the company's policy. O&M costs include costs for maintenance, spare parts, and administration. According to the National Renewable Energy Laboratory in 2006, the O&M costs of onshore wind farms has an average value of 0.7 ¢/kWh (Fingersh, Hand, & Laxson, 2006), and is assumed constant despite the farm size.

$$OMC_{WTON,y} = \sum_{i=1}^n c_2 \cdot E_{WTON,i} \quad (3.28)$$

Where $OMC_{WTON,y}$ is the annual O&M costs of onshore wind, and c_2 is given a value of 0.7 ¢/kWh.

The total annual costs of wind turbines $Ct_{WTON,y}$ can be divided into installed capital costs and O&M costs and are given by the following equation:

$$Ct_{WTON,y} = OMC_{WTON,y} + IC_{WTON,y} \quad (3.29)$$

The average annual cost of producing one unit of onshore wind energy $C_{kWh,y}$ is given by Equation 3.30. The farm capacity factor which is the annual produced electricity to the maximum annual that could be produced CF_{WTON} is given by Equation 3.31.

$$C_{kWh,y} = \frac{IC_{WTON,y} + OMC_{WTON,y}}{E_{WTON,y}} \quad (3.30)$$

$$CF_{WTON} = 100 \cdot \frac{E_{WTON,y}}{Np \cdot n} \quad (3.31)$$

Offshore wind farm:

The location of onshore wind turbines is in Nanticoke region, Lake Erie. Data shown in Table 3.4 is taken from Environment Canada at 42.772 N, 80.116 W, and 80 m above ground level.

Table 3.4 Offshore wind data for Nanticoke, ON (Environment Canada, 2003).

Period	Mean wind speed (m/s)	Mean wind energy (W/m²)	Weibull scale parameter A (m/s)
Annual	7.47	462.88	8.39
Winter (DJF)	8.83	660.00	9.96
Spring (MAM)	7.38	427.25	8.30
Summer (JJA)	5.97	228.31	6.72
Fall (SON)	7.78	495.75	8.76
Range	5.97–8.83	228.31–660.00	6.72–9.96

The design parameters for the offshore wind farm, however, are selected for that model SWT 2.3-93 (Siemens AG, 2009). The turbine with a nominal power of 2.3 MW is suitable for large-scale production since it is superior for moderate wind speeds as described by Siemens AG. Table 3.5 summarizes the key parameters used to build the offshore wind model.

Cost estimation for offshore wind is similar to that of onshore wind. Equations from 3.24 to 3.29 can be used to estimate the cost of electricity produced from offshore wind turbines with different c_1 and c_2 values. The cost of offshore wind turbines per installed capacity ranges from 1800 to 2500 €/kW (Blanco, 2009). An average value of 2150 €/kW ($c_1 = 2,924 \$/kW$) is assumed for this model.

Table 3.5 Siemens SWT2.3-93 model wind turbine parameters and specifications (Siemens AG, 2009).

Specification	Value	Source
Model	SWT 2.3-93	(Siemens AG, 2009)
Nominal power (MW)	2.3	(Siemens AG, 2009)
Type	3-bladed, horizontal axis	(Siemens AG, 2009)
Position	Up-wind	(Siemens AG, 2009)
Yaw system	Active	(Siemens AG, 2009)
Rotor diameter (m)	93	(Siemens AG, 2009)
Swept area (m²)	6,800	(Siemens AG, 2009)
Hub height (m)	80	(Siemens AG, 2009)
Voltage (V)	690	(Siemens AG, 2009)
Frequency (Hz)	50	(Siemens AG, 2009)
Cut-in wind speed (m/s)	4	(Siemens AG, 2009)
Cut-out wind speed (m/s)	25	(Siemens AG, 2009)
Coefficient of performance (%)	35	(Kurtulan & Sevgi, 2009)
Generator efficiency (%)	90	(Kurtulan & Sevgi, 2009)
Mechanical efficiency of the gearbox and bearings (%)	95	(Kurtulan & Sevgi, 2009)
Installed costs (\$USD/MW)	2,924,000	(Blanco, 2009)
O&M costs (US\$/kWh)	2	(NREL, 2006)
Service life (y)	20	assumed

Because of the uneasy access and the special equipment needed for the offshore wind turbines, the O&M costs of offshore wind farms are higher than the onshore wind farms. According to the National Renewable Energy Lab Report, c_2 is estimated to be 2 ¢/kWh (Fingersh et al., 2006).

The average annual costs of offshore wind energy per unit of energy produced can be expressed by:

$$C_{kWh,y} = \frac{IC_{WTOF,y} + OMC_{WTOF,y}}{E_{WTOF,y}} \quad (3.32)$$

$$CF_{WTOF} = 100 \cdot \frac{E_{WTOF,y}}{Np \cdot n} \quad (3.33)$$

Where; $E_{WTOF,y}$, $IC_{WTOF,y}$, and $OMC_{WTOF,y}$ are defined by equations 3.25, 3.27, 3.28 respectively with $c_1 = 2,924$ \$/kW, and $c_2 = 2$ ¢/kWh. CF_{WTOF} is the capacity factor of the wind farm.

3.1.3 PV solar cells

The model chosen for PV solar farm is SPR-400 from Sunpower Corporation (2010). The solar panel uses 128-back contact monocrystalline solar cells, with an efficiency of 18.5% and a peak power of 400 W. An inverter and a step-up transformer are needed in order to connect the PV system to the grid. Inverter lifetimes range from 5 to 10 years (Borenstein, 2008). An average value of 8 years is assumed, meaning that the inverters have to be replaced twice during the project lifetime of 25 years. According to Solarbuzz (2011), the cost of the inverter is 71.4 ¢/W as of September 2011. Table 3.6 summarizes the key parameters of the PV model.

The first step in modeling a PV solar farm is to estimate the hourly power efficiency. The power efficiency $\eta_{p,i}$ is a function of the operating cell temperature $T_{cl,i}$ and is given by (Russell & Bergman, 1986):

$$\eta_{p,i}(T_{cl}) = \eta_{cl} \cdot [1 + \eta_{p,T_o}(T_{cl,i} - NOCT)] \quad (3.34)$$

Where η_{p,T_o} is the power efficiency at the reference temperature—for this model equals to 0.0038 K⁻¹ (Sunpower Cor., 2010).

Table 3.6 SPR-400 model PV module parameters and specifications (Sunpower Cor., 2010).

Type	Type	Type
Model	SPR-400	(Sunpower Cor., 2010)
Max power at STC, watt	400	(Sunpower Cor., 2010)
Type	All-back monocrystalline	(Sunpower Cor., 2010)
Module efficiency, %	18.5	(Sunpower Cor., 2010)
Operating temperature, °C	-40 to 85	(Sunpower Cor., 2010)
NOCT, °C	45	(Sunpower Cor., 2010)
Max voltage, V	600	(Sunpower Cor., 2010)
Open circuit voltage, V	85.3	(Sunpower Cor., 2010)
Short circuit current, A	5.87	(Sunpower Cor., 2010)
Temperature power coefficient, K⁻¹	-0.38%	(Sunpower Cor., 2010)
Dimensions, mm	1046x2067x54	(Sunpower Cor., 2010)
No. of cells in the module	128(8*16)	(Sunpower Cor., 2010)
Life span (warranted), y	25	(Sunpower Cor., 2010)
Installed costs, CAD/kW	7,000	(Ayoub et al., 2010)
O&M costs, \$/kW	0.01	("PV cost factors," 2010)
Inverter efficiency, %	95	assumed
Inverter cost, \$/W	0.714	(Solarbuzz, 2011)
Inverter life span, y	8	assumed
Transformer efficiency, %	99	assumed

From Table 3.6 the nominal operating cell temperature $NOCT$ is $45\text{ }^{\circ}\text{C}$. According to the ASME standards, $NOCT$ is estimated at irradiance ($G_{NOCT} = 800\text{ w/m}^2$), an air temperature ($T_{a,NOCT} = 20\text{ }^{\circ}\text{C}$), and a wind speed ($w_s = 1\text{ m/s}$). $NOCT$ is used to predict $T_{cl,i}$ by the following equation (Duffie & Beckman, 2006):

$$T_{cl,i} = \frac{G_i}{G_{NOCT}}(NOCT - T_{a,NOCT}) + T_{a,i} \quad (3.35)$$

Where; G_i is the hourly solar radiation and $T_{a,i}$ the hourly ambient air temperature. Both G_i and $T_{a,i}$ are taken on hourly bases. Figure A.2 shows the hourly profile of the solar farm.

The second step is to evaluate energy captured by the solar modules. The hourly energy captured by a PV solar module $E_{PV,i}$, and the total annual $E_{PV,y}$ is a function of G_i and $\eta_{p,i}$ and is given by (Russell & Bergman, 1986):

$$E_{PV,i} = G_i \cdot A \cdot \eta_{p,i} \quad (3.36)$$

$$E_{PV,y} = \sum_{i=1}^n E_{PV,i} \quad (3.37)$$

The last step is to evaluate the production costs of the solar farm. The total annual costs $Ct_{PV,y}$ of a PV solar farm could be split among annual O&M costs $OMC_{PV,y}$, annual installed capital costs $IC_{PV,y}$, and the inverter costs $IC_{Inv,y}$. The installed costs of grid-connected modules ranges from 6000 to 8000 CAD/kW (Ayoub et al., 2010). An average value of 7000 CAD/kW is assumed for this model. The annual installed capital costs of the module $IC_{PV,y}$ and the inverter $IC_{Inv,y}$ are given by:

$$IC_{PV,y} = IC_{PV,o} \cdot \frac{I(1+I)^{N_{PV}}}{(1+I)^{N_{PV}} - 1} \quad (3.38)$$

$$IC_{Inv,y} = IC_{Inv,o} \cdot \frac{I(1+I)^{N_{Inv}}}{(1+I)^{N_{Inv}} - 1} \quad (3.39)$$

Where; $IC_{PV,o} = c_{11} \cdot Np_{PV}$, with $c_{11} = 7000 \text{ \$/kW}$, and $IC_{Inv,o} = c_{12} \cdot Np_{Inv}$, with $c_{12} = 0.714 \text{ \$/W}$.

The O&M costs of PV solar cells are as low as \$0.01 per kilowatt ("PV cost factors," 2010). The annual O&M costs are given by:

$$OMC_{PV,y} = \sum_{i=1}^n c_2 \cdot E_{PV,i} \quad (3.40)$$

Now the annual costs of the PV solar cells $Ct_{PV,y}$ can be estimated by:

$$Ct_{PV,y} = OMC_{PV,y} + IC_{PV,y} + IC_{Inv,y} \quad (3.41)$$

Finally, the annual average cost of the PV solar energy $C_{kWh,y}$, and its capacity factor CF_{PV} are expressed by:

$$C_{kWh,y} = \frac{IC_{PV,y} + IC_{Inv,y} + OMC_{PV,y}}{E_{PV,y}} \quad (3.42)$$

$$CF_{PV} = 100 \cdot \frac{E_{PV,y}}{Np \cdot n} \quad (3.43)$$

3.1.4 Electrolysers

The model HySTAT-60 from Hydrogenics® has been chosen for the electrolyser's technology. Table 3.7 summarizes the key design variables of the HySTAT-60 model (Hydrogenics Cor., 2009).

Table 3.7 Specifications of the alkaline electrolyser.

Specification	Value	Source
Model	HySTAT™-60	(Hydrogenics Cor., 2009)
Type	H ₂ O + 30% wt. KOH	(Hydrogenics Cor., 2009)
Voltage, V AC 3-ph	400	(Hydrogenics Cor., 2009)
Frequency, Hz	50	(Hydrogenics Cor., 2009)
Power consumption, kWh/Nm³	5.2	(Hydrogenics Cor., 2009)
Max H₂ generated, Nm³/h	60	(Hydrogenics Cor., 2009)
H₂ purity, %	99.998	(Hydrogenics Cor., 2009)
H₂ output pressure, bar (g)	10	(Hydrogenics Cor., 2009)
O₂ generated	50% H ₂	(Hydrogenics Cor., 2009)
O₂ output pressure, bar (g)	8	(Hydrogenics Cor., 2009)
Temperature range, °C	(-20) — (+40)	(Hydrogenics Cor., 2009)
Electrolyser running capacity range, (Nm³/h of H₂)	24—60	(Hydrogenics Cor., 2009)
Operating range, %	40—100	(Hydrogenics Cor., 2009)
Electrolyser lifespan, y	10	assumed
Electrolyser capital costs, \$/unit	$224.49E3 \times N_{CELZ}^{0.6156}$	(Saur, 2008)
Electrolyser O&M costs (% of IC)	5	
Inverter efficiency, %	95	assumed
Inverter cost, \$/W	0.714	(Solarbuzz, 2011)

The maximum H₂ could be produced per stack is 60 Nm³/h. Both O₂ produced $\dot{m}_{O_2,i}$ and H₂O consumed $\dot{m}_{H_2O,i}$ per hour can be determined from the following relations:

$$\dot{m}_{H_2,i} = Nc \cdot N_{ELZ,i} \quad (3.44)$$

$$\dot{m}_{O_2,i} = \frac{M_{wt,O_2}}{2 M_{wt,H_2}} \times \dot{m}_{H_2,i} \quad (3.45)$$

$$\dot{m}_{H_2O,i} = \frac{M_{wt,H_2O}}{M_{wt,H_2}} \times \dot{m}_{H_2,i} \quad (3.46)$$

Total annual productions are the sum of the hourly product throughout the year and are given by:

$$\dot{m}_{H_2,y} = \sum_{i=1}^n Nc \cdot N_{ELZ,i} \quad (3.47)$$

$$\dot{m}_{O_2,y} = \frac{M_{wt,O_2}}{2 M_{wt,H_2}} \sum_{i=1}^n Nc \cdot N_{ELZ,i} \quad (3.48)$$

$$\dot{m}_{H_2O,y} = \frac{M_{wt,H_2O}}{M_{wt,H_2}} \sum_{i=1}^n Nc \cdot N_{ELZ,i} \quad (3.49)$$

Where $N_{ELZ,i}$ is the number of electrolyzers in operation per hour.

The cost of hydrogen produced via water electrolysis is affected significantly by the capital costs of the electrolyser and the price of electricity. Capital costs of the electrolyser y in dollars are given by: $y = 224.49 \cdot 10^3 x^{0.6156}$ where x is the production capacity in kg H₂/h (Saur, 2008).

The annual installed capital costs of the electrolyser $IC_{ELZ,y}$ and the inverter $IC_{Inv,y}$ are given by:

$$IC_{ELZ,y} = IC_{ELZ,o} \cdot \frac{I(1+I)^{N_{ELZ}}}{(1+I)^{N_{ELZ}} - 1} \quad (3.50)$$

$$IC_{Inv,y} = IC_{Inv,o} \cdot \frac{I(1+I)^{N_{Inv}}}{(1+I)^{N_{Inv}} - 1} \quad (3.51)$$

Where $IC_{ELZ,o} = 224.49E3 \cdot Nc_{ELZ}^{0.6156}$, and $IC_{Inv,o} = c_{12} \cdot Np_{Inv}$, with $c_{12} = 0.714$ \$/W.

The O&M costs $OMC_{ELZ,y}$ are assumed as a percentage (5%) of the total IC costs of the electrolyser (Saur, 2008). The cost is given by:

$$OMC_{ELZ,y} = 0.05 IC_{ELZ,y} \quad (3.52)$$

The total annual electricity and the cost of electricity consumed by the electrolysers are given by Equation 3.53 and 3.54 as follow:

$$E_{ELZ,y} = \sum_{i=1}^n E_{ELZ,i} \quad (3.53)$$

$$C_{E,y} = \sum_{i=1}^n c_i \cdot E_{ELZ,i} \quad (3.54)$$

Where $E_{ELZ,i} = c_1 N_{ELZ,i}$ the hourly electricity consumed by electrolysers with $c_1 = 312$ kWh, and c_i is the hourly price of electricity per kWh as illustrated in Figure A.4.

Finally, the total annual costs of electrolysers include the annual expense and scheduled payments in addition to O&M costs:

$$Ct_{ELZ,y} = OMC_{ELZ,y} + IC_{ELZ,y} + IC_{Inv,y} + C_{E,y} + C_{H_2O,y} \quad (3.55)$$

Where $C_{H_2O,y}$ the annual costs of demineralized water and is defined by:

$$C_{H_2O,y} = \sum_{i=1}^n c_1 \cdot \dot{m}_{H_2O,i} \quad (3.56)$$

Hourly and average hydrogen cost per kilogram is pointed out in Scenario C, Chapter 4.

3.2 Modeling Logic

3.2.1 NG turbines ML

The modeling logic (ML) of NG power plant, as shown in Figure 3.2, starts with inputting the hourly electricity data $E_{D,i}$. First, the hourly demand is checked to ensure that it is higher than the minimum designed production capacity of the power plant. If the required energy production is within the range, then, the next step is to start the design process by applying the design parameters of the power plant (Table 3.1) to the material and energy balances based on Figure 3.1 after setting an initial number of turbine units $N_{GT,i}$. After that, the net energy from the power plant based on equations 3.1, 3.7, 3.9, and 3.12 is estimated. The turbine units are then checked to determine whether they are within the allowed operating range, and whether demand is met. If both conditions are met, then the next step is to estimate the hourly energy cost $C_{kWh,i}$ based on hourly fuel consumed, capital costs, and O&M costs. Hourly gas emissions $em_{j,i}$ of a component j can also be estimated from equations 3.4, 3.5, and 3.6 based on the operating conditions and the hourly fuel consumed. Finally, the average annual cost of energy $C_{kWh,y}$, total annual energy produced $E_{PP,y}$, and the total emissions per year $em_{j,y}$ can be estimated.

This model logic diagram will be implemented in Chapter 4 in scenarios A, B, and C.

3.2.2 Wind turbines ML

a. Onshore wind turbines:

Figure 3.3 shows a modeling logic diagram proposed for onshore wind energy. The model starts with entering the hourly or seasonal average wind speed $w_{s,i}$. Wind speed is checked with the operation range of the onshore turbines, 3.5–25 m/s. If it is within the range, then the next step is to set the turbine parameters, illustrated in Table 3.3 and the number of turbines N_{WTON} . Based on the power equation of wind turbines, Equation 3.24, the total hourly electricity from the farm $E_{WTON,i}$ can be estimated. If the targeted load is met, then, the next step is to perform the hourly and annual cost calculations; if not, a new number of turbines are set. The annual average cost of electricity from onshore wind turbines $C_{kWh,y}$, which is a function of the annual total cost $C_{tWTON,y}$, and the total energy produced $E_{WTON,y}$, is estimated from Equation 3.25. This modeling logic will be

implemented later in both Scenario B and Scenario C for estimating the total energy produced and the total cost of energy hub.

b. Offshore wind turbines:

The modeling logic of the offshore wind farm is similar to that illustrated for the onshore wind farm. Seasonal average wind speed $w_{s,i}$ profile, Figure A.1b, is used to estimate the hourly offshore wind electricity $E_{WTOF,i}$. Wind speed is first checked to ensure it is within the operating range of the offshore turbines, 4–25 m/s. A number of turbines N_{WTOF} are set, and if the target load is met, then the next step is to go through the cost estimation process. The annual average cost $C_{kWh,y}$, Equation 3.32, is based on the total cost per year $Ct_{WTOF,y}$ and total electricity generated $E_{WTOF,y}$ —equations 3.29 and 3.25. Parameters illustrated in Table 3.5 are used as an input, while the output is implemented as part of Scenario B and Scenario C in Chapter 4.

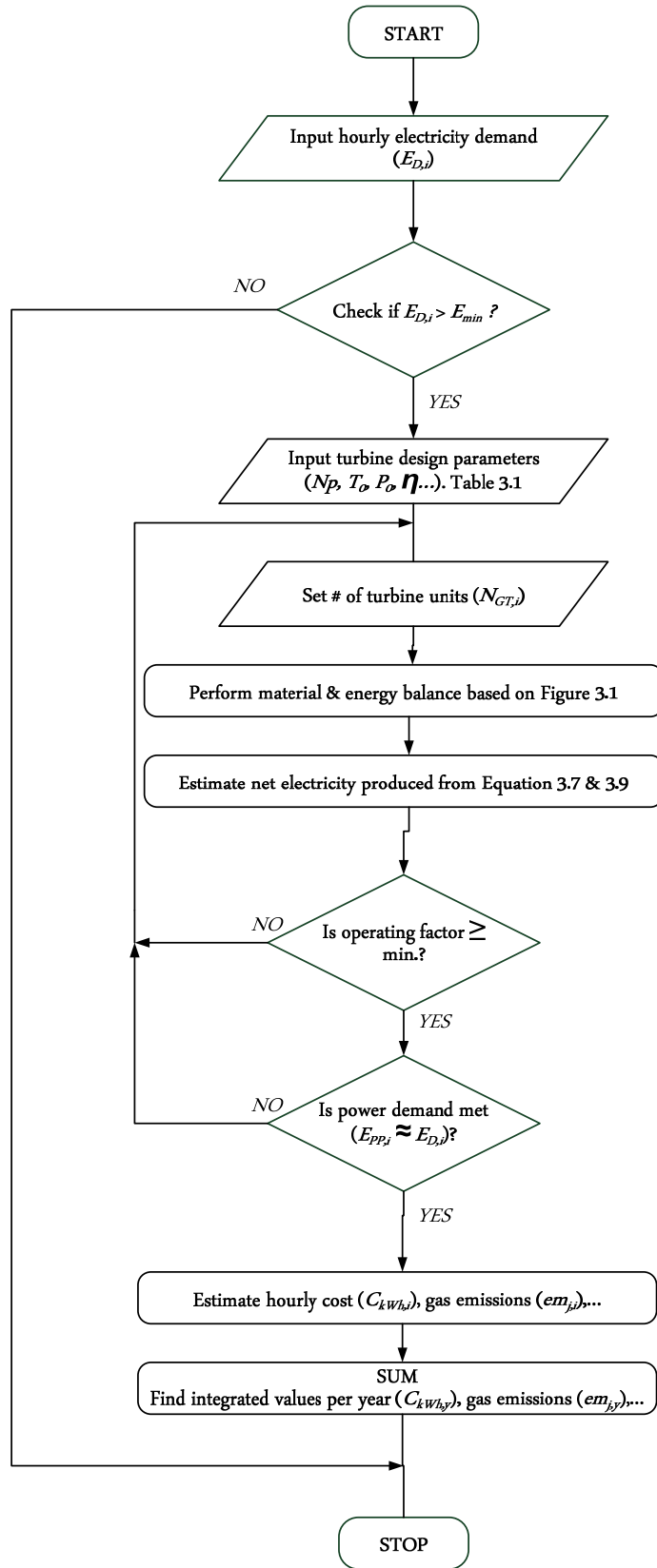


Figure 3.2 NG turbine ML block diagram.

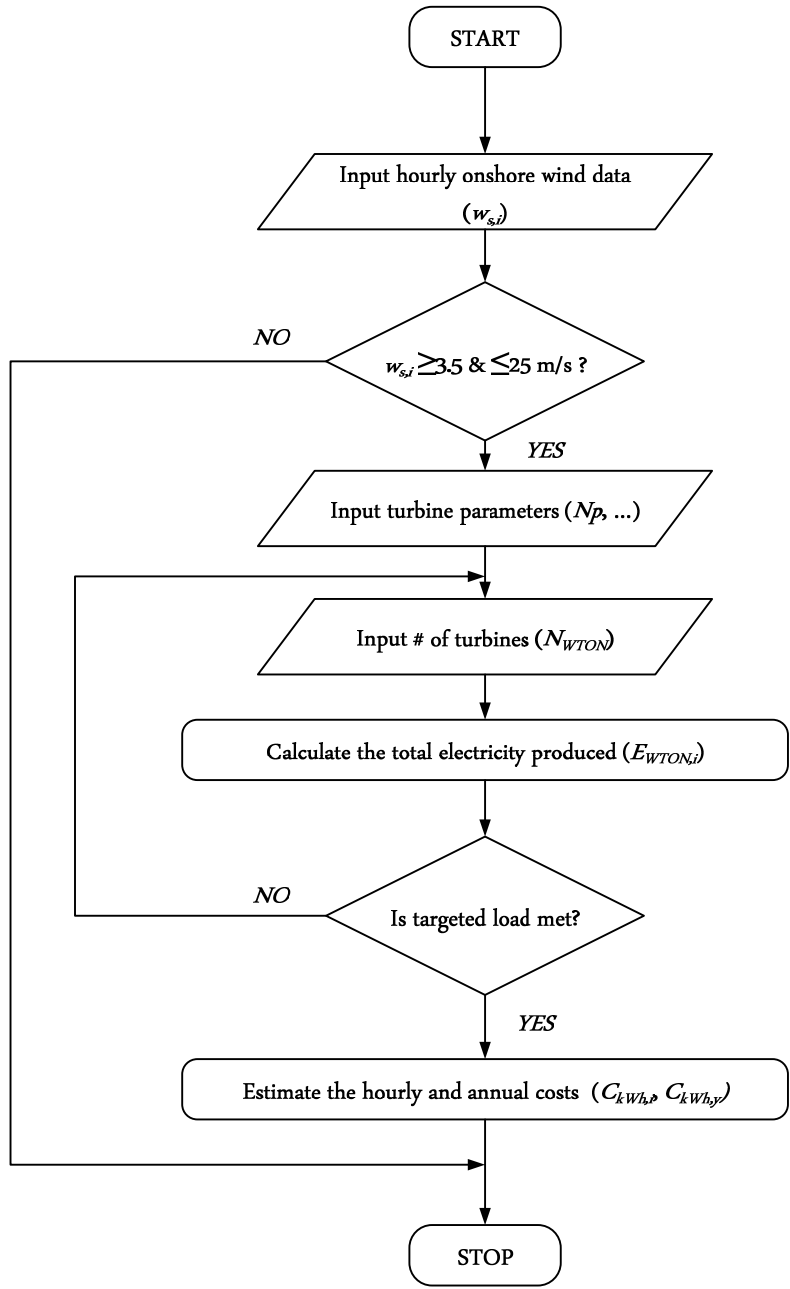


Figure 3.3 Onshore wind power ML block diagram.

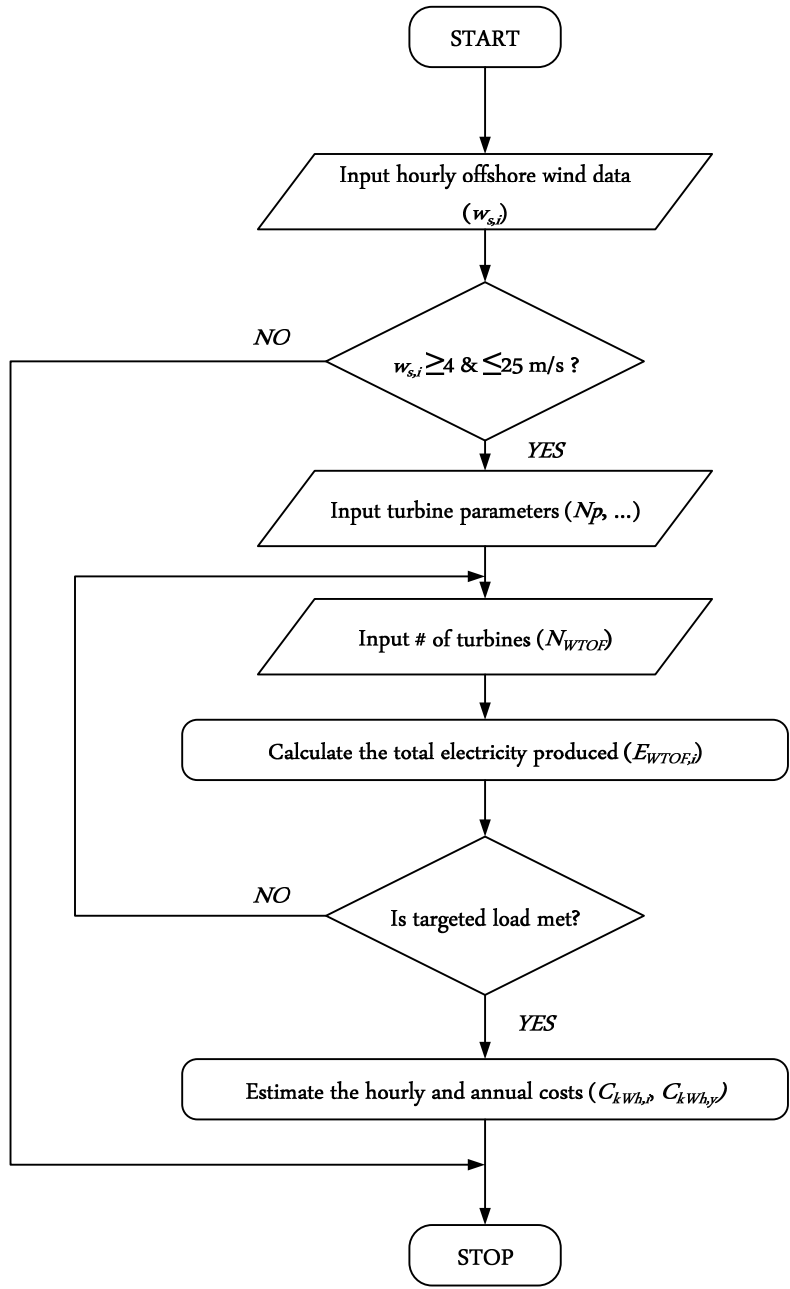


Figure 3.4 Offshore wind power ML block diagram.

3.2.3 PV solar cells ML

Modeling of a PV solar farm starts with applying the hourly ambient temperature $T_{a,i}$, Figure A.2a, and the hourly radiation G_i , Figure A.2b, to the power equation. First, G_i is checked if it is greater than the minimum radiation G_{min} required to operate the solar cell. The second step is to ensure that the cell operating temperature T_{cl} , Equation 3.35, is within the range. Cell efficiency $\eta_{p,i}$ is then estimated as a function of $T_{a,i}$ and G_i —Equation 3.34. A number of PV modules are set, and from Equation 3.36, the hourly electricity produced from PV $E_{PV,i}$ is estimated. An iteration loop as shown in Figure 3.5 is applied to ensure that the energy produced is within the range. The total annual energy produced $E_{PV,y}$ and the annual average cost $C_{kWh,i}$ calculations are then followed. This model logic is then implemented in the NG-renewable energy and the hydrogen economy scenarios in Chapter 4.

3.2.4 Electrolysers ML

The electrolysers' modeling logic is derived so that it can handle excess electricity from the hub E_{EXC} . The model starts by checking whether there is excess electricity or not. If there is enough electricity E_{EXC} to operate one or more electrolyser units, then a number of electrolyser units $N_{ELZ,i}$ is set and checked if they can accommodate the excess energy, where $N_{ELZ,i}$ represents the hourly electrolyser units required to be in operation. Then, hourly H₂ produced $\dot{m}_{H_2,i}$, hourly O₂ produced $\dot{m}_{O_2,i}$, and the hourly water consumed $\dot{m}_{H_2O,i}$ are estimated from equations 3.44, 3.45, and 3.46 respectively. Design parameters required for the input are taken from Table 3.7, while the output variables such as $\dot{m}_{H_2,y}$, $\dot{m}_{O_2,y}$, $C_{H_2,y}$, and $C_{O_2,y}$ are implemented in Scenario C in Chapter 4.

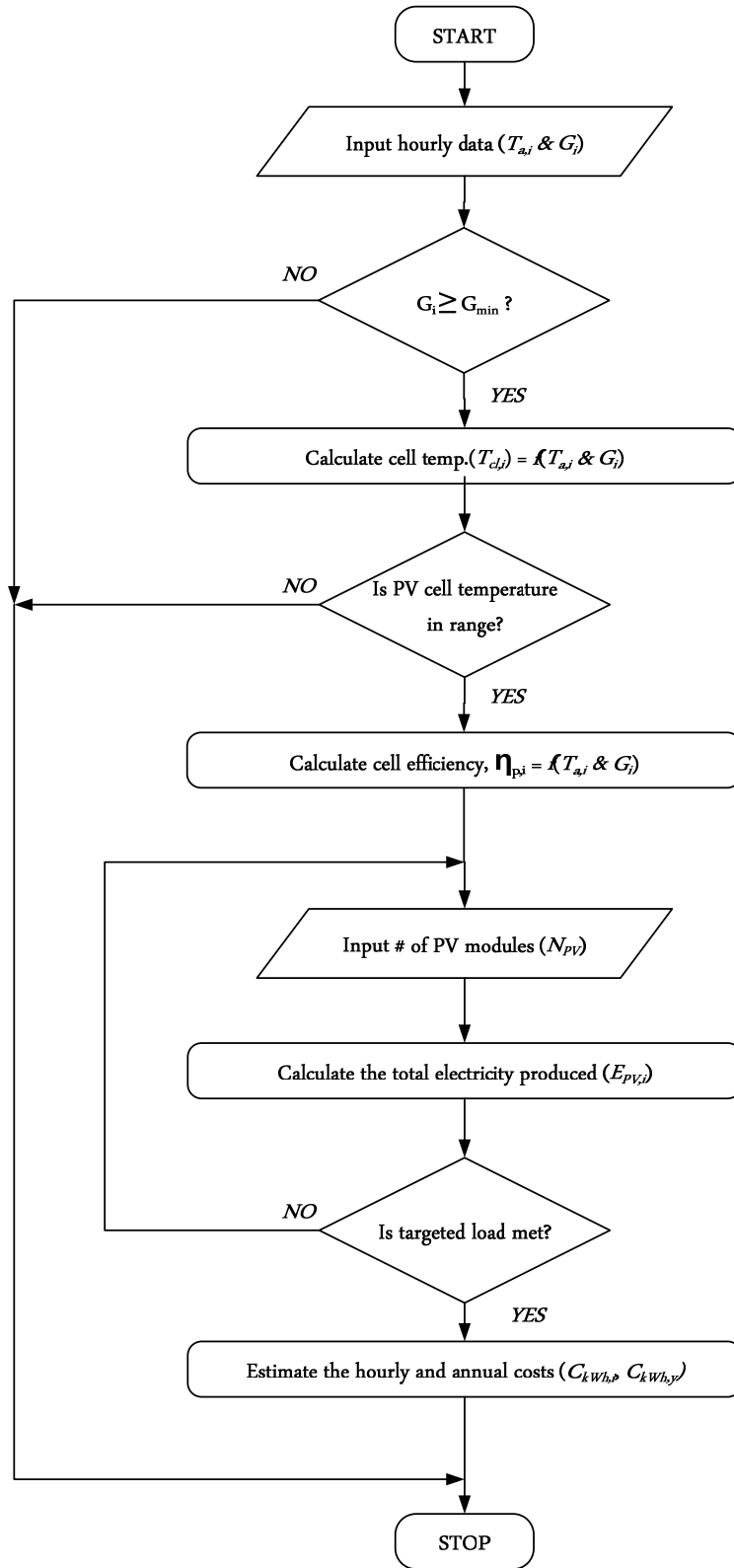


Figure 3.5 PV solar cells ML block diagram.

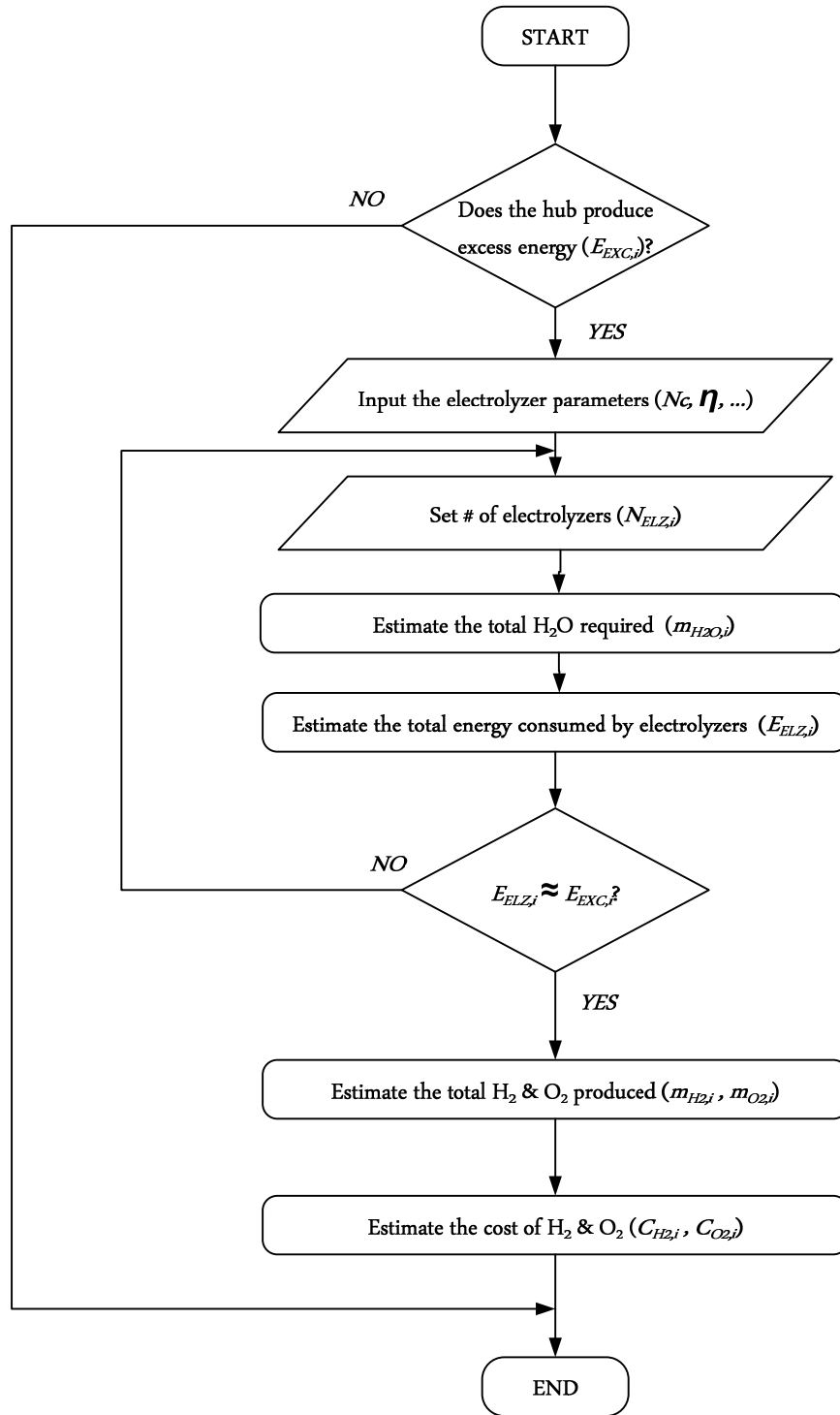


Figure 3.6 Alkaline electrolyzers ML block diagram.

CHAPTER 4

Model Derivation

4.1 GAMS® Overview

The modeling system “General Algebraic Modeling System” or GAMS is a high-level programming language that enables the modeller to write the modeling problem in a simple, logical way. The idea first came to light in 1950s and 1960s when the need arose to solve large and complex mathematical problems (Brooke et al., 1998).

Basic Features of GAMS:

Despite the many high-level modeling systems available today, GAMS offers the advantage of being a user-friendly environment since it does not require the modeller to have a lot of experience to be able to write a program. In addition, GAMS is capable of handling large-scale and complex optimization problems making it a very suitable tool in real-life industrial and economical applications. Most importantly, GAMS is an open system that has the ability to use different types of solvers depending on the mathematical model type.

With over fifty solvers, GAMS can be used to handle a wide range of modeling systems from basic linear mathematical problems to more sophisticated non-linear and integer problems. Developing a more sophisticated model from a basic model and switching between solvers can be done easily. GAMS is adapted by many modelers for its ability to handle complex optimization problems, flexibility to interface, and capability to detect errors and verifying the model correctness.

The model which is built in GAMS is defined over parameters, variables, and functions. In GAMS, each type of input-output should be declared over one of these commands:

Scalars: scalars represent single-value parameters such as nominal power, equipment efficiency, physical properties, and cost factors.

Sets: Sets in this project define the equipment operation hours per year, n .

Parameters: Parameters are defined over sets which represent hourly data such as hourly ambient temperature, hourly fuel cost, hourly demand and production.

Variables: variables in this project are mainly assigned for capital costs, O&C costs, and total costs.

Equations: Equations give the relationship between parameters, variables, and data. Equations in this project represent objective functions, cost and production.

4.2 Model Scenarios

This research study depends mainly on three scenarios, each concerned with simulation of an issue. The design capacity of renewable energy sources is assumed based on average values of the existing technologies. For future work, an optimization problem could be added to find the optimum values that generate electricity with lower cost. Electricity cost, GHG emissions, renewable energy, and hydrogen economy are the main concerns of the today's energy sector. The following three scenarios are proposed for the study of energy hubs:

4.2.1 Scenario A: NG stand-alone power plant

This scenario is the baseline for comparison in terms of electricity production, average cost, and gas emissions. This scenario serves as the baseline for comparison in terms of power cost and emissions. In this scenario, CCPP is proposed to simulate the Nanticoke Generating Station's output, replacing the coal-fired steam turbines with NG-operated gas and steam turbines. The simulation is based on plant production data for 2009 provided by IESO. Demand is taken based on one hour intervals for one year. NG is assumed to be widely available at a stable price (monthly average) and sulfur-free. With the further development of non-convention natural gas deposits (e.g. 'tight gas' and shale gas), natural gas is expected to be a stable resource for, at least, the next couple of decades. The output data for electricity is implemented in hourly energy production, hourly cost per kWh, and hourly gas emissions. Performance of NG turbines in terms of availability and efficiency is estimated as well. In addition to the hourly output, average annual values for production, cost, and emissions are estimated and considered as the baseline for comparison between other scenarios. The objective of this scenario is to be the reference point for the subsequent scenarios in terms of energy cost, GHG emissions, and efficiency.

While Figure 3.2 illustrates the logic of modeling this scenario, Table 4.1 summarizes the main inputs-outputs parameters and design variables for this scenario.

Table 4.1 Scenario A: NG stand-alone power plant key inputs and outputs.

Level: NG turbines	
Input	Hourly targeted load $E_{D,i}$ given in MWh.
	NG monthly average cost $c_{f,i}$ given in \$/kg.
	Design parameters: $T_0, P_0, Np, r_c, \eta_{AC}, \eta_{GT}, \eta_{ST}$, and TET .
	Gases properties: $C_p, \Delta H, M_{wt}$...etc.
Output	Hourly energy produced $E_{PP,i}$ given in MWh.
	Hourly energy cost $C_{kWh,i}$ given in \$/kWh.
	Average simple cycle and combined cycle efficiencies, $\eta_{GT,i}$ and $\eta_{PP,i}$.
	Hourly CO ₂ , CO, NO _x , and UHCs emissions $em_{j,i}$ in kg/h.
	Average annual production $E_{PP,y}$, cost $C_{kWh,y}$, and gas emissions $em_{j,y}$.

4.2.2 Scenario B: NG-renewable energy hub

In this scenario, the objective is to add onshore wind, offshore wind, and PV solar energies to Scenario A. The objective is to meet demand by implementing renewable energy sources to the conventional CCPP in Scenario A. The scenario is modeled to read the hourly electricity demand and generate an hourly output. In addition to the inputs in Scenario A, hourly wind speed, air temperature, specifications of wind turbines and PV modules are needed to be entered as inputs. Outputs are implemented in terms of hourly generation, hourly cost, and hourly emitted and saved gases. Average annual values for each of the outputs are estimated to facilitate comparison between the different operating scenarios and to avoid the fluctuations during the on-and-off peak hours. Table 4.2 summarizes the essential inputs and output of this scenario.

Table 4.2 Scenario B: NG-renewable energy key inputs and outputs.

Level: NG-renewable energy	
Input	Scenario A input data.
	Onshore wind: hourly wind speed $w_{s,i}$, nominal power Np_{WTON} , number of turbines N_{WTON} , and turbine specifications.
	Offshore wind: hourly wind speed $w_{s,i}$, nominal power Np_{WTOF} , number of turbines N_{WTOF} , and turbine specifications.
	PV solar: hourly temperature $T_{a,i}$, hourly solar radiation $G_{a,i}$, nominal power Np_{PV} , number of turbines N_{PV} , and PV module specifications.
Output	Hourly energy produced: $E_{PP,i}$, $E_{WTON,i}$, $E_{WTOF,i}$, $E_{PV,i}$, and $E_{EH,i}$ given in MWh.
	Hourly energy cost: $C_{PP(kWh),i}$, $C_{WTON(kWh),i}$, $C_{WTOF(kWh),i}$, $C_{PV(kWh),i}$, and $C_{EH(kWh),i}$ in \$/kWh.
	Hourly CO ₂ , CO, NO _x , and UHCs emissions $em_{j,i}$ in kg/h.
	Average annual production: $E_{PP,y}$, $E_{WTON,y}$, $E_{WTOF,y}$, $E_{PV,y}$, and $E_{EH,y}$ in MWh.
	Average annual cost: $C_{PP(kWh),y}$, $C_{WTON(kWh),y}$, $C_{WTOF(kWh),y}$, and $C_{EH(kWh),y}$ in \$/kWh.

4.2.3 Scenario C: Hydrogen economy

The hydrogen economy scenario focuses on maximizing hydrogen production from electrolyzers while meeting the electricity demand. The excess power during off-peak hours is used to feed electrolyzers to produce hydrogen, which then can be sold into the market to power fuel cell vehicles expected to start to be marketed in 2015. The scenario includes, in addition to CCPP, onshore and offshore wind turbines, PV solar cells, and alkaline electrolyzers. In addition to the hourly inputs for Scenario B, hourly excess electricity and price are added to set a limit for the maximum hydrogen that could be produced. Outputs, besides that in Scenario B, include hourly hydrogen and pure oxygen production and their cost. Average annual electricity generated, average cost, hydrogen and oxygen production, in addition to gas emissions are included in this

scenario as well. Table 4.3 summarizes the main inputs and outputs of Scenario C. This scenario allows for greater availability and utility of the power generation assets.

Table 4.3 Scenario C: Hydrogen economy key inputs and outputs.

Level: Hydrogen economy	
Input	Scenario B input data.
	Electrolyser parameters.
	Hourly excess electricity in MWh.
	Hourly electricity cost in \$/kWh.
Output	Hourly H ₂ produced $\dot{m}_{H_2,i}$ and hourly O ₂ produced $\dot{m}_{O_2,i}$ in kg/h.
	Hourly cost of H ₂ $C_{H_2,i}$ and O ₂ $C_{O_2,i}$ produced in \$/kg.
	Hourly energy produced: $E_{PP,i}$, $E_{WTON,i}$, $E_{WTOF,i}$, $E_{PV,i}$, and $E_{EH,i}$ in MWh.
	Hourly energy cost: $C_{PP(kWh),i}$, $C_{WTON(kWh),i}$, $C_{WTOF(kWh),i}$, $C_{PV(kWh),i}$, and $C_{EH(kWh),i}$ in \$/kWh.
	Hourly CO ₂ , CO, NO _x , and UHCs emissions $em_{j,i}$ given in kg/h.
	Average annual production: $E_{PP,y}$, $E_{WTON,y}$, $E_{WTOF,y}$, $E_{PV,y}$, and $E_{EH,y}$ in MWh, and $\dot{m}_{H_2,y}$, and $\dot{m}_{O_2,y}$ given in kg/y.
	Average annual cost: $C_{PP(kWh),y}$, $C_{WTON(kWh),y}$, $C_{WTOF(kWh),y}$, and $C_{EH(kWh),y}$ in \$/kWh, $C_{H_2,y}$, and $C_{O_2,y}$ given in \$/kg.

4.3 Scenarios Development

4.3.1 Scenario A: NG stand-alone power plant

Scenario assumptions:

- Scenario's parameters and design points are as given in Table 3.1.
- The power plant model is developed for a single-shaft, combined cycle power plant.
- Air compressor is of axial-flow type with no intercooler.
- Combustion chamber is assumed to be lean, premixed type, with mixing assumed to be ideal.
- NG is treated as pure CH₄ in the calculation of mass and energy balance.

- NG is assumed sulfur free, so there is no SO_x at the exhaust outlet. Further, PMs are not included as they are highly connected to heavy fuels such as diesel and coal.
- Gas turbines are not allowed to operation less than 40% (i.e. turndown ≥ 40%).
- NO_x, CO, and UHCs emissions are a function of pressure drop ΔP_{3a-4} and the adiabatic flame temperature $T_{4,i}$.
- Electricity demand data is based on the year of 2009.
- Interest rate for cost estimation is assumed 5%.
- Exchange rates for cost and cost factors are as of September 2011.

Mathematical model:

Developing a mathematical model for this scenario is based on the relationships developed for the gas turbine in Chapter 3. The overall net energy from the power plant $E_{PP,i}$ is a combination of energy produced from the gas and steam turbines minus that required by the air compressor and the water pump as shown by the following equation:

$$E_{PP,i} = E_{GT,i} - E_{AC,i} + E_{ST,i} - E_{PMP,i} \quad (4.1)$$

Where $E_{AC,i}$, $E_{GT,i}$, $E_{ST,i}$, and $E_{PMP,i}$ are defined by equations 3.1, 3.7, 3.9, and 3.12 respectively.

The hourly thermal efficiency $\eta_{PP,i}$, at which the power plant is being operated, is the ratio of the hourly electricity produced to the total heating value of NG.

$$\eta_{PP,i} = \frac{E_{PP,i}}{LHV_f \cdot \dot{m}_{f,i}} \quad (4.2)$$

Where LHV_f is the lower heating value of NG, and $\dot{m}_{f,i}$ is the hourly mass flow rate of NG.

Equation 4.1 represents the hourly power production in MWh. The total annual electricity production for this scenario in MWh is therefore:

$$E_{PP,y} = \sum_{i=1}^n E_{PP,i} \quad (4.3)$$

In order to estimate the average cost per unit of electricity produced, it is necessary to evaluate the equipments' annual installed capital costs $IC_{PP,y}$, annual fuel cost $C_{f,y}$, and annual O&M costs $OMC_{PP,y}$. These annual costs are given by the following equations:

$$IC_{PP,y} = \sum_j IC_j \quad (4.4)$$

$$C_{f,y} = \sum_{i=1}^n c_{f,i} \cdot \dot{m}_{f,i} \quad (4.5)$$

Where; IC_j is defined by Equation 3.22, $c_{f,i}$ average monthly cost of NG as shown in Figure A.5.

The O&M costs are divided into fixed and variable costs. The fixed O&M costs are function of the power plant installed capacity Np_{PP} , while the variable O&M costs are a function of the total produced electricity $E_{PP,y}$.

$$OMC_{PP,y} = c_1 \cdot Np_{PP} + c_2 \cdot E_{PP,y} \quad (4.6)$$

Where $c_1 = 20 \text{ \$/}(kW \cdot y)$, and $c_2 = 0.002 \text{ \$/}kWh$ (Mansouri et al., 2012).

Annual NO_x , CO and UHC emissions are based on equations 3.4, 3.5, and 3.6 and are defined by:

$$em_{j,y} = \sum_{i=1}^n em_{j,i} \quad (4.7)$$

Finally, the average annual electricity cost per kWh of electricity for a power plant with capacity factor CF is given by:

$$C_{kWh,y} = \frac{IC_{PP,y} + OMC_{PP,y} + C_{f,y}}{E_{PP,y}} \quad (4.8)$$

$$CF = 100 \cdot \frac{E_{PP,y}}{Np_{PP} \cdot n} \quad (4.9)$$

Modeling logic:

In order to meet the targeted electricity load, the first scenario is proposing to meet the demand only from NG-fired power plant. The primary steps for meeting demand are discussed in Section 3.2.1 and the modeling logic is shown in Figure 3.2. Developing a modeling algorithm for this scenario was based mainly on assumptions that have been already made: thermodynamic of power cycles, mass and energy balances, and the economic evaluations of the project.

A detailed code for this scenario is presented in Appendix C.

4.3.2 Scenario B: NG-renewable energy hub

Scenario assumptions:

In addition to the assumptions of the NG turbine scenario, Scenario B is based on a number of other assumptions as follow:

- Scenario parameters and design points are as given in Table 3.1, 3.2, 3.3, 3.4, 3.5, and 3.6.
- Onshore and offshore wind speed data is taken as the seasonal average.
- The operating range of onshore wind turbines is 3.5–25 m/s, and for the offshore is 4–25 m/s.
- Air density involved in wind power calculations are assumed constant, 1.225 kg/m³.
- Ambient air temperature and solar irradiance data is taken on hourly basis.
- The minimum irradiance G_{min} required to operate the PV solar cells is assumed 100 W/m².
- Electricity demand data is based on the year of 2009.

Mathematical model:

Derivation of a mathematical model for the whole energy hub is based on its individual components derived models. Equations derived in Chapter 3 are used here to implement the overall relationships.

The total energy produced $E_{EH,i}$ at any time i is the sum of energy from power plant, onshore wind farm, offshore wind farm, and the PV solar modules.

$$E_{EH,i} = E_{PP,i} + E_{WTON,i} + E_{WTOF,i} + E_{PV,i} \quad (4.10)$$

Where $E_{PP,i}$, $E_{WTON,i}$, $E_{WTOF,i}$, and $E_{PV,i}$ are defined by equations 4.1, 3.24 and 3.36. The only controllable output here is that from the power plant $E_{PP,i}$ where it would be adjusted in order to accommodate the hourly fluctuation of the demand. The annual production is simply the sum of the hourly output for the whole year and is expressed by:

$$E_{EH,y} = \sum_i^n (E_{PP,i} + E_{WTON,i} + E_{WTOF,i} + E_{PV,i}) \quad (4.11)$$

The total hourly cost of the energy hub is the sum of its individual technologies' costs. Which include the hourly costs of the power plant $Ct_{PP,i}$, hourly costs of onshore wind $Ct_{WTON,i}$, hourly costs of offshore wind $Ct_{WTOF,i}$, and the hourly costs of PV solar energy $Ct_{PV,i}$.

$$Ct_{EH,i} = Ct_{PP,i} + Ct_{WTON,i} + Ct_{WTOF,i} + Ct_{PV,i} \quad (4.12)$$

As a result, the total annual costs of the energy hub in Scenario B are:

$$Ct_{EH,y} = \sum_i^n (Ct_{PP,i} + Ct_{WTON,i} + Ct_{WTOF,i} + Ct_{PV,i}) \quad (4.13)$$

The average hourly cost of electricity per kWh $C_{kWh,i}$, and the annual average cost $C_{kWh,y}$ are given by:

$$C_{kWh,i} = \frac{Ct_{EH,i}}{E_{EH,i}} \quad (4.14)$$

$$C_{kWh,y} = \frac{Ct_{EH,y}}{E_{EH,y}} \quad (4.15)$$

Modeling logic:

In this scenario, in order to meet the electricity demand shown in Figure 5.1, renewable energy in the form of onshore wind, offshore wind, and PV solar technologies have been added to Scenario A. The modeling logic developed here is based on the assumptions that have been already made, energy balance, and economic evaluations. Modeling of onshore wind turbines, offshore wind

turbines, and the PV solar cells are part of this scenario and are based on what was discussed in Section 3.1 and 3.2. A graphical representation of this model is illustrated in Figure 4.1.

A detailed code for this scenario is presented in Appendix C.

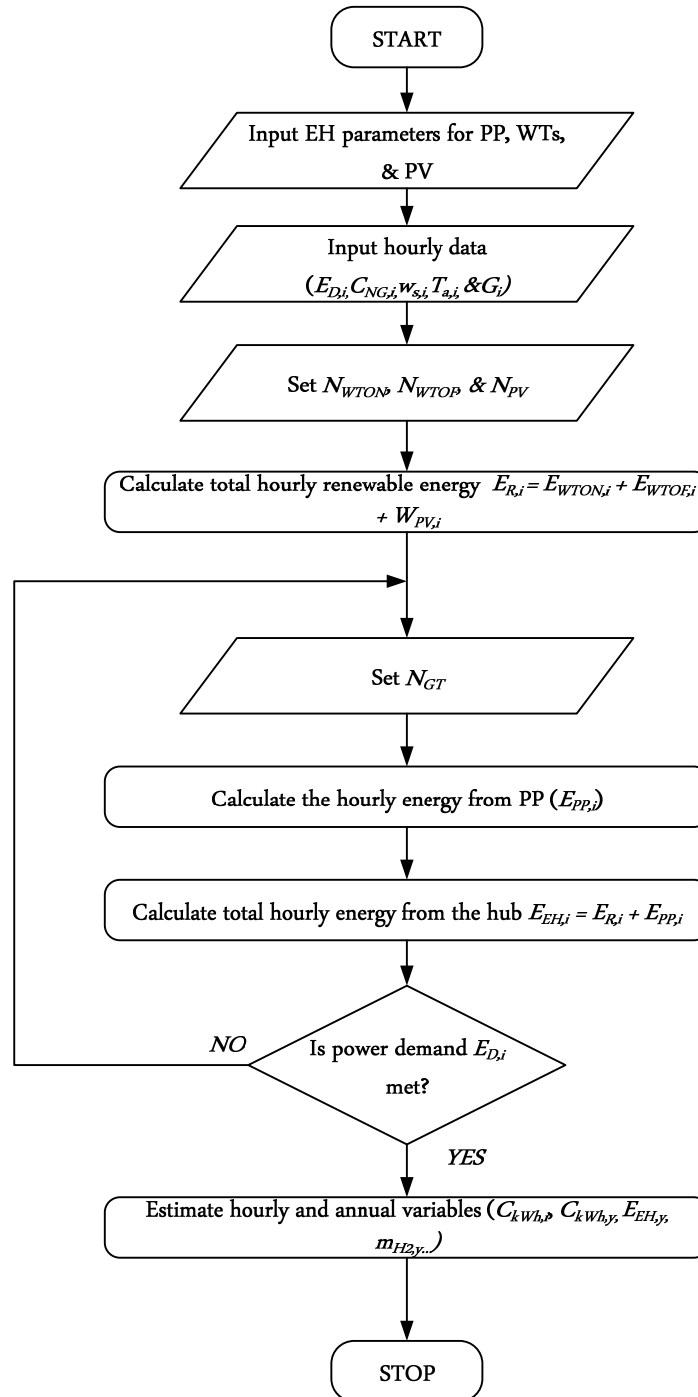


Figure 4.1 Scenario B ML block diagram.

4.3.3 Scenario C: Hydrogen economy

Scenario assumptions:

Adding to the assumptions of scenarios A and B:

- Electrolyser parameters and design variables are given in Table 3.7.
- The operation range of the electrolyser units is 40–100%.
- The minimum number of electrolyser units allowed is one electrolyser with operating capacity $\geq 40\%$.
- Hydrogen is generated at 10 bar at the electrolyser's output.
- Cost of electricity consumed by electrolyser units is based on the year of 2009.

Mathematical model:

The hourly energy produced from the entire hub $E_{EH,i}$ for this scenario at any time i is the sum of energy produced from the power plant $E_{PP,i}$, onshore wind farm $E_{WTON,i}$, offshore wind farm $E_{WTOF,i}$, and PV solar modules $E_{PV,i}$, minus energy consumed by electrolyzers $E_{ELZ,i}$.

$$E_{EH,i} = E_{PP,i} + E_{WTON,i} + E_{WTOF,i} + E_{PV,i} - E_{ELZ,i} \quad (4.16)$$

Where $E_{PP,i}$, $E_{WTON,i}$, $E_{WTOF,i}$, $E_{PV,i}$ and $E_{ELZ,i}$ are previously defined by equations in Chapter 3 and 4. Similarly, the annual electricity production from the hub is the sum of the hourly production for each of the technologies for the whole year and is expressed by:

$$E_{EH,y} = \sum_i^n (E_{PP,i} + E_{WTON,i} + E_{WTOF,i} + E_{PV,i} - E_{ELZ,i}) \quad (4.17)$$

The total hourly cost of the energy hub is the sum of its individual technologies' costs. The total energy costs at any hour i are given by:

$$Ct_{EH,i} = Ct_{PP,i} + Ct_{WTON,i} + Ct_{WTOF,i} + Ct_{PV,i} + Ct_{ELZ,i} \quad (4.18)$$

Whereas the total annual costs:

$$Ct_{EH,y} = \sum_i^n (Ct_{PP,i} + Ct_{WTON,i} + Ct_{WTOF,i} + Ct_{PV,i} + Ct_{ELZ,i}) \quad (4.19)$$

The average hourly and annual cost of electricity per kWh can be expressed by:

$$C_{kWh,i} = \frac{Ct_{EH,i} - Ct_{ELZ,i}}{E_{EH,i} + E_{ELZ,i}} \quad (4.20)$$

$$C_{kWh,y} = \frac{Ct_{EH,y} - Ct_{ELZ,y}}{E_{EH,y} + E_{ELZ,y}} \quad (4.21)$$

On the other hand, the average cost of hydrogen and oxygen produced $C_{H_2,y}$ and $C_{O_2,y}$ respectively given in \$/kg are assigned as a percentage, X_1 and X_2 , of the total annual costs. The cost factors X_1 and X_2 are determined by minimizing an objective function Z . The objective function Z needs to be optimized is the total hydrogen and oxygen cost:

$$\text{Minimize } Z = C_{H_2,y} + C_{O_2,y} \quad (4.22)$$

Subject to:

$$\dot{m}_{H_2,y} \cdot C_{H_2,y} - X_1 \cdot Ct_{ELZ,y} = 0 \quad (4.23)$$

$$\dot{m}_{O_2,y} C_{O_2,y} - X_2 \cdot Ct_{ELZ,y} = 0 \quad (4.24)$$

$$X_1 \cdot \sum_1^k C_{k,y} + X_2 \cdot \sum_1^k C_{k,y} = Ct_{ELZ,y} \quad (4.25)$$

$$X_1 + X_2 = 1 \quad (4.26)$$

$$X_1 \text{ and } X_2 \geq A \quad (4.27)$$

Where $C_{k,y}$ is the annual cost of component k , k represents the installed capital costs, O&M costs, electricity costs, and water costs, and A represents a fraction from zero to one.

Finally, the capacity factor CF_{ELZ} of the electrolyser unit is expressed as the percentage of hydrogen produced to the maximum can be produced and is given by:

$$CF_{ELZ} = 100 \cdot \frac{\dot{m}_{H_2,y}}{N_C \cdot N_{ELZ} \cdot n} \quad (4.28)$$

Modeling logic:

The hydrogen economy scenario is based on the idea that during the excess electricity periods, hydrogen can be generated and sold to local markets. As shown in Figure 4.2, the modeling starts with setting a design capacity for onshore and offshore wind energy, and the PV solar farm. Design parameters such as NG cost, hourly air temperature, and solar radiation are entered as an input to the model. The next step is to assume a number of NG turbines and calculation of the energy produced from the CCPP. The output is, then, checked with the hourly load whether the demand is met. The total hourly electricity from CCPP, onshore wind, offshore wind, and PV solar is then estimated. The next step is to find whether there is an excess production of electricity or not. If there is electricity to operate at least one electrolyser with an operation capacity at least 40%, then the next step is find the number of electrolysers required to accommodate this excess energy (Figure 3.6). The last step is to estimate the hourly gross energy output, energy cost, and hydrogen and oxygen output, in addition to their annual averages as well.

A detailed code for this scenario is presented in Appendix C.

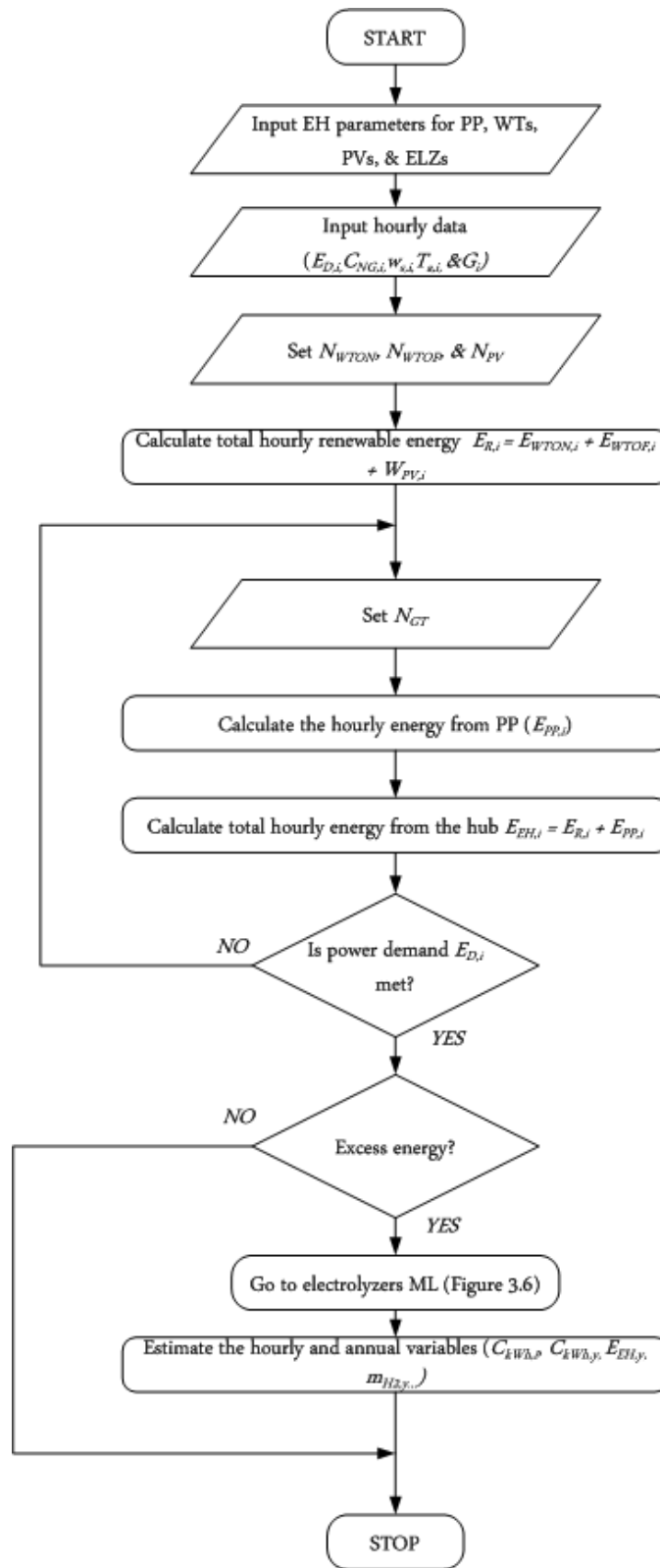


Figure 4.2 Scenario C ML block diagram.

CHAPTER 5

Results and Discussion

5.1 Scenario A: NG Stand-Alone Power Plant

After the scenarios were proposed and the modeling logic and assumptions were discussed in sections 4.2.1 and 4.3.1, the model is now executed. Results are implemented, and hence discussed, in terms of energy produced profile, production costs, and gas emissions. The section ends with a summary of the key outputs and average values of outputs over one year.

5.1.1 Electricity generation

This scenario, as discussed in Chapter 4, is the baseline for comparison, where only a conventional CCPP is used to meet the electricity demand. The production data for Nanticoke Generating Station, with a maximum output of 3,138 MW in 2009, as shown in Figure 5.1d, was taken as the design point for the CCPP. Figure 5.1a shows the energy output from the simple cycle power plant, with a maximum production of 1,898 MW, and a production efficiency of 37.7%, based on the LHV of NG. The output from the steam cycle as shown in Figure 5.1b, however, is found to be lower than the simple cycle—1,240 MW. The overall power plant hourly profile is represented by Figure 5.1c, with a peak production of 3,150 MW, which corresponds to the Nanticoke production profile shown in Figure 5.1d. A sample of a ten-day profile is shown in Figure A.6.

The CCPP was designed to handle up to 3,150 MW, with an overall efficiency up to 62.3%, based on the LHV of NG. The maximum number of combined cycle units needed to meet the demand is found to be 8 units. Each unit is comprised of a gas and a steam turbine.

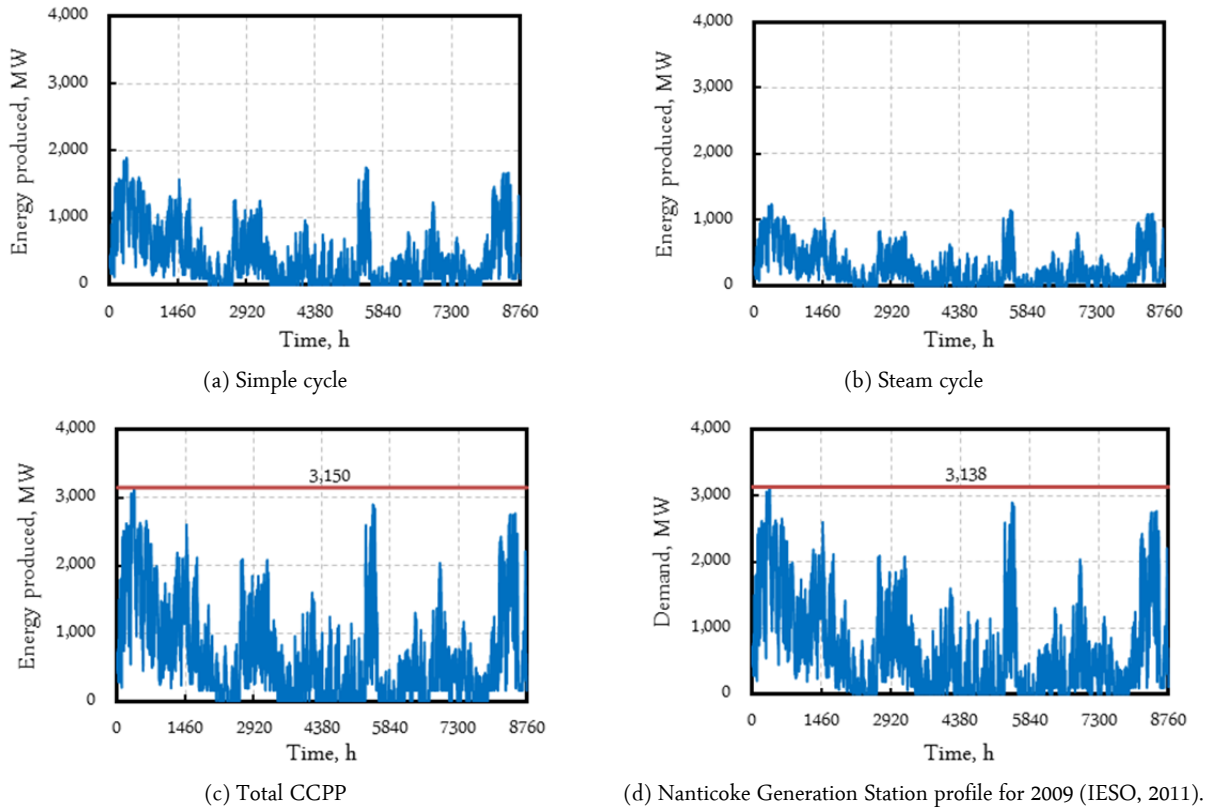


Figure 5.1 Net hourly energy produced from the power plant, Scenario A.

Figure 5.2 shows the hourly number of turbine units (gas and steam) in operation in order to meet demand. As shown in the figure, the minimum number of turbines in operation is found to be one turbine unit with a minimum production capacity of 40%. This state corresponds to the low production profile of Nanticoke Power Station. The hourly operating capacity (turndown) is illustrated in Appendix B, Figure A.8.

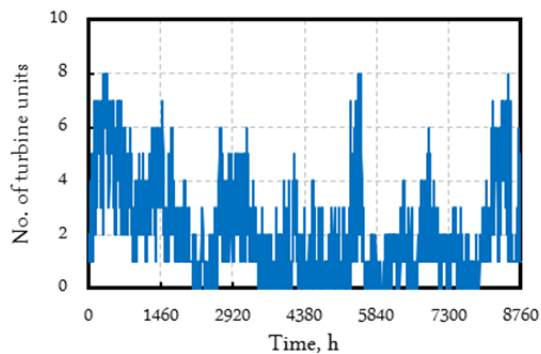


Figure 5.2 Hourly number of combined cycle units (1x1) in operation, Scenario A.

5.1.2 Electricity cost

The total cost of the CCPP—as illustrated by equations 4.4, 4.5, and 4.6, and implemented in Figure 5.3a—is a function of the capital costs, O&M costs, and fuel costs. The total cost is found to be very sensitive to fuel prices. The high cost rates in Figure 5.3a corresponds to the high production rate in Figure 5.1a. The cost per kilowatt-hour of energy produced, however, decreases as the production rate increases, as it is illustrated in Figure 5.3b. The cost of energy in this scenario is found to have a minimum value of 3.3 ¢/kWh which corresponds to high production rates and low NG prices. A maximum value of 14.3 ¢/kWh, on the other hand, corresponds to low production rates and high NG prices. Figure 5.3c outlines the average monthly prices of the electricity produced where the overall average cost is found to be 7.4 ¢/kWh. Figure A.9 shows a plot of a ten-day sample of the electricity cost.

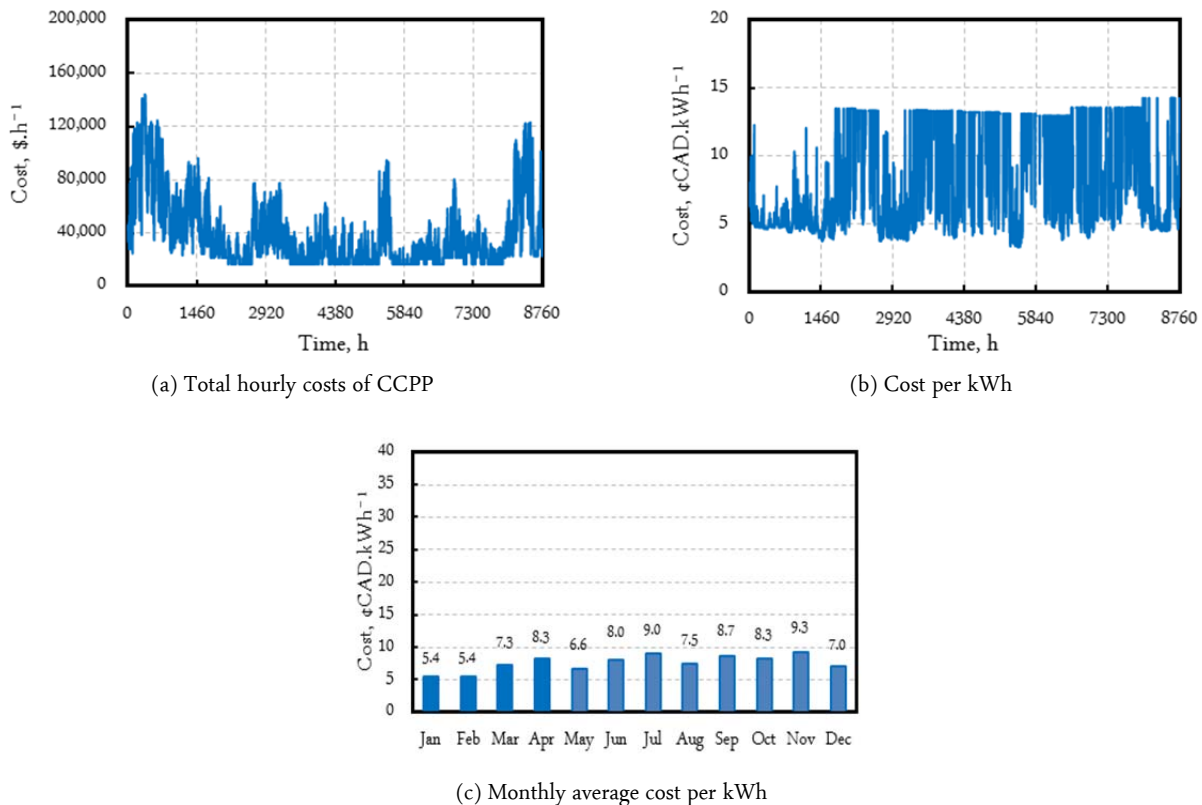


Figure 5.3 Hourly costs of electricity from the power plant, Scenario A.

5.1.3 GHG emissions

Finally, the emission profile of CO₂ is represented by Figure 5.4a, with the output profile of NO_x, CO, and UHCs based on equations 3.4, 3.5, and 3.6 respectively, which are represented in Figure 5.4b, -c, and -d. CO₂ emissions reaches a maximum value of 994,235 kg/h, which corresponds to a maximum production rate of 3,138 MWh. NO_x, CO, and UHCs show a similar CO₂ behaviour where emissions reach a maximum at peak productions, while they hit the minimum boundaries at low-production rates. The specific emissions, on the other hand, showed a steady profile. Among emitted gases, CO₂ emissions were the highest at 316.8 kg/MWh, while NO_x, CO, and UHCs showed lower limits residing at 14.6, 4.4, and 1.6 kg/MWh respectively. Figure A.10 shows a ten-day sample profile of the emitted gases.

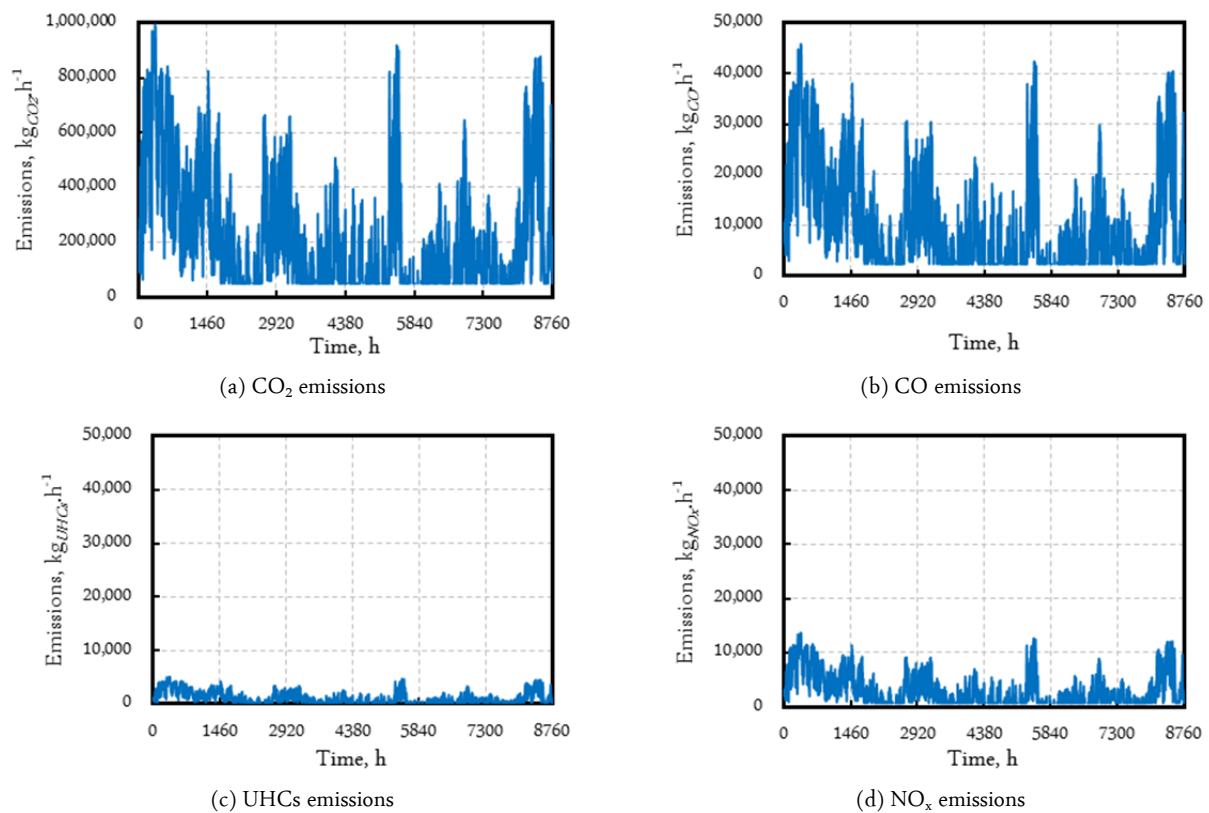


Figure 5.4 Hourly gas emissions from the CCPP, Scenario A.

5.1.4 Summary

To summarize, a CCPP was proposed to simulate the Nanticoke Generating Station electrical output with a design capacity of 3,150 MW operating at a maximum overall efficiency of 62.3% based on the LHV of NG. The required combined cycle units was found to be 8, producing energy at an average cost of 7.4 ¢/kWh at a specific NG cost and capacity factor. The power plant, in general, works at a low operation range with a capacity factor of 21% and total operating hours of 7,304 per year. Availability, which is the number of working hours per year divided by the total number of hours per year, was relatively high hitting 83.4% with 1,456 h/y for maintenance and repair. Table 5.1 summarizes the results of Scenario A.

Table 5.1 Summary of results: Scenario A.

Parameter	Value
Design capacity	
Simple cycle (MW per turbine)	238
Steam cycle (MW per turbine)	156
CCPP (MW per unit)	394
Total capacity for the plant (MW)	3,150
Total number of CCPP units	8
Efficiency (% based on LHV)	
Simple cycle	37.7
Combined cycle	62.3
Total energy produced (MWh/y)	5,883,650
Average cost of energy unit (¢CAD/kWh)	7.4
Total costs per year(\$CAD/y)	343,437,681
Emissions	
CO ₂ (kg/MWh)	316.8
CO(kg/MWh)	14.6
NO _x (kg/MWh)	4.4
UHCs(kg/MWh)	1.6
Operating hours per year(h/y)	7,304
Capacity factor (%)	21
Availability (%)	83.4

5.2 Scenario B: NG-Renewable Energy Hub

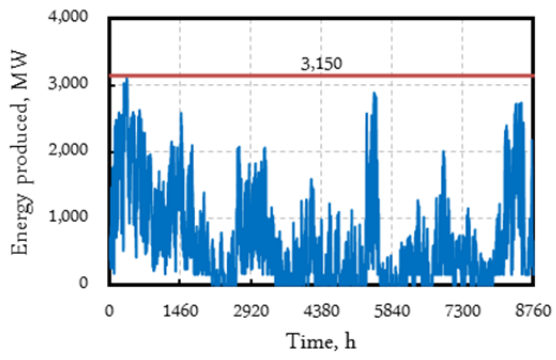
In this scenario, as illustrated in Chapter 4, onshore and offshore wind energy, as well as PV solar cells, were added to the CCPP to meet the hourly demand represented by Figure 5.1d. As there is no control over renewable energy outputs, the CCPP is used to handle the hourly fluctuation and fill the gap between what is produced from renewable sources and demand.

5.2.1 Electricity generation

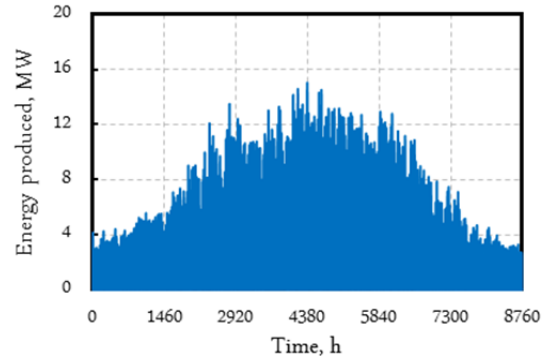
Figure 5.5a illustrates the output from the CCPP as it varies according to hourly demand. The power plant is found to have 8 units in operation with a maximum capacity of 3,150 MW in order to meet a peak demand of 3,138 MW. The hourly number of the CCPP units in operation is illustrated in Figure A.11, where the overall efficiency of the plant is found to be 62.3% based on the LHV.

The PV solar farm, with a design capacity of 20 MW and 50,000 modules in operation, is found to cover 108,100 m² of land. The PV solar technology share over one year, as shown in Figure 5.5b, is estimated to be 23,969 MWh, with a capacity factor 13.7% and annual operating hours reach up to 3,837 h.

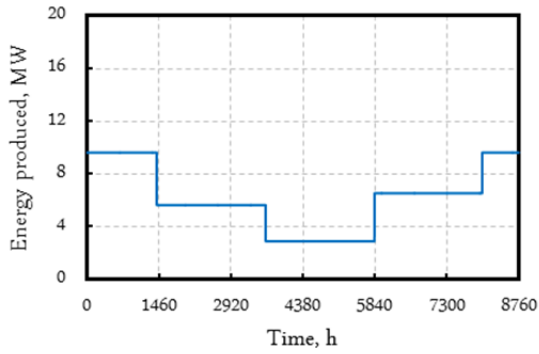
The cell efficiency, as well as energy production, reaches its highest level (18%) during summer, while in winter it falls to 14.4%, as shown in Figure 5.6. The operation status of the PV solar farm, as well as a sample of the energy profile at the beginning of each month, is illustrated in Appendix B, Figure A.13 and Figure A.14 respectively.



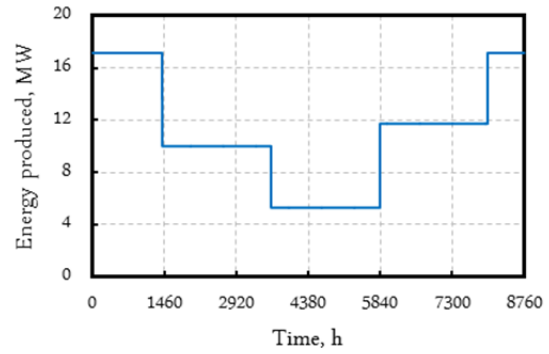
(a) CCPP, 3150 MW



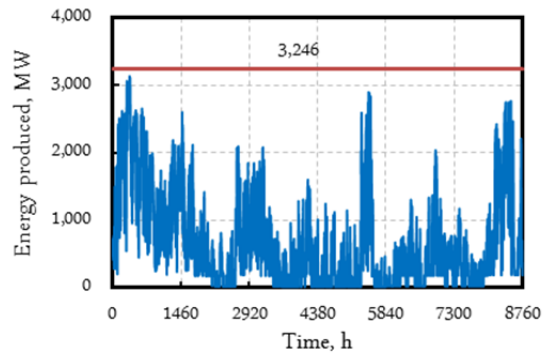
(b) PV solar farm, 20 MW



(c) Onshore wind farm, 30 MW



(d) Offshore wind farm, 46 MW



(e) Total energy hub, 3246 MW

Figure 5.5 Energy produced from the hub, Scenario B.

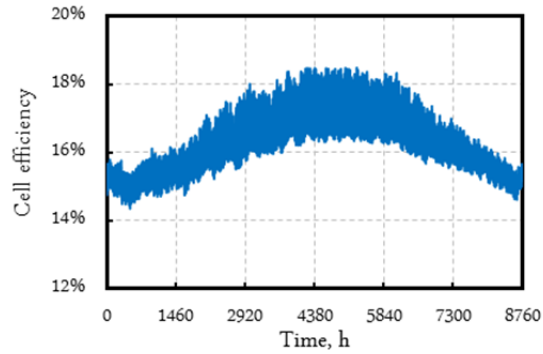
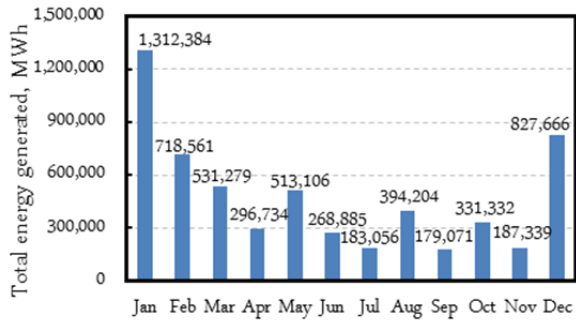


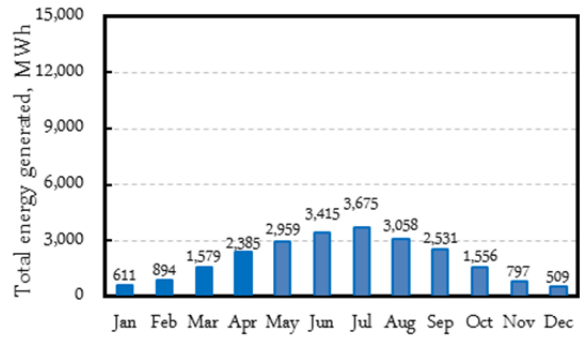
Figure 5.6 Hourly efficiency of PV solar modules, Scenario B.

The wind energy profile varies by season as wind speed is taken as a seasonal average. The onshore wind farm is designed to provide up to 30 MW an hour with 20 turbines in operation. The total energy produced over one year is 53,860 MWh, with a capacity factor of 20.5%. The offshore wind farm, however, offers a higher profile than the onshore wind farm, due to the fact that wind speed on the water's surface is than is greater than it is on the ground. The offshore wind farm is designed with a maximum capacity of 46 MW with 20 turbines in operation. Energy produced is estimated to be 96,541 MWh, over the period of one year, with a capacity factor 24%. Wind availability is estimated to be 100% due to the assumption of average seasonal wind speed. In reality, however, wind speed fluctuates causing energy and availability to be lower than the ideal operation. This point is addressed as a potential future work. Figure 5.5c and Figure 5.5d show the energy produced from onshore and offshore wind, respectively, over the period of one year.

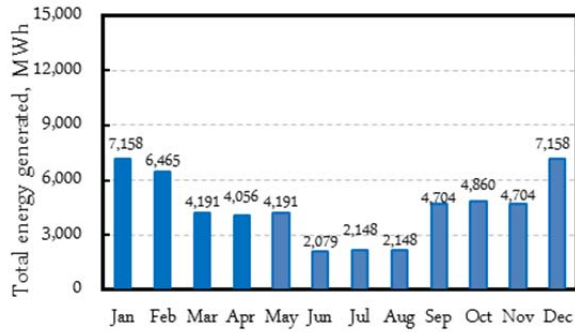
The overall design capacity of the energy hub in order to meet the demand in Scenario B is found to be 3,246 MW. The total profile is shown in Figure 5.5e with an overall 5,917,986 MWh produced over the course of one year. The total monthly energy production is illustrated in Figure 5.7 with CCPP technology has the highest share, followed by offshore and onshore wind energies.



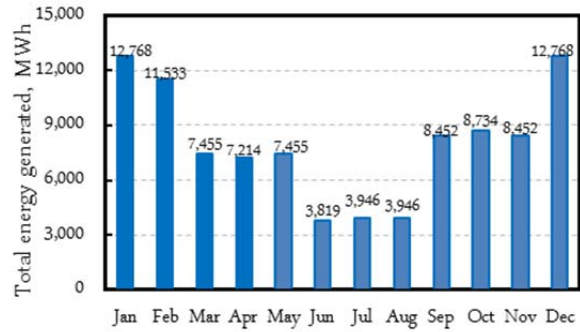
(a) CCPP, 3150 MW



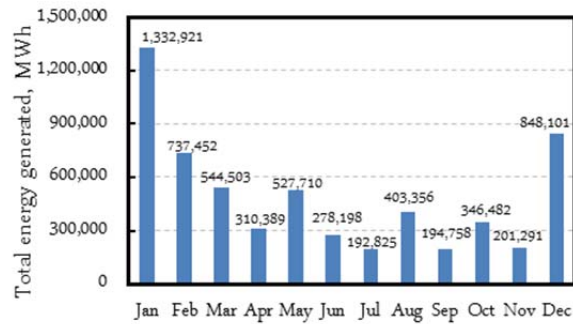
(b) PV solar farm, 20 MW



(c) Onshore wind farm, 30 MW



(d) Offshore wind farm, 46 MW



(e) Total energy from the hub

Figure 5.7 Monthly total energy produced from the hub, Scenario B.

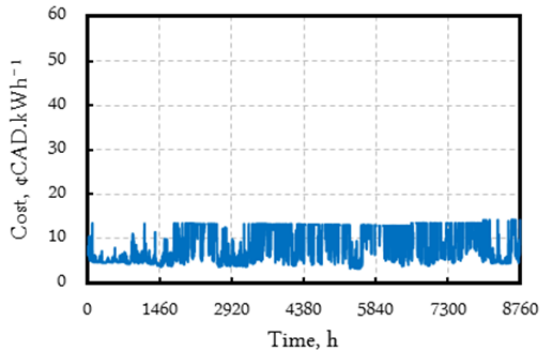
5.2.2 Electricity cost

Cost of energy from the hub, as shown in Figure 5.8, was estimated on an hourly basis for each of the technologies used. Among the technologies used, PV solar energy cost was the highest, at 18 ¢/kWh. A low cost of 13.1 ¢/kWh came in July, due to the high temperature and solar radiation. On the other hand, the highest average monthly cost, 32.8 ¢/kWh, was recorded in December, as both air temperature and solar radiation decreased. Figure A.15 in Appendix B shows a ten-day and a twenty-four-hour sample of PV energy cost profile in January.

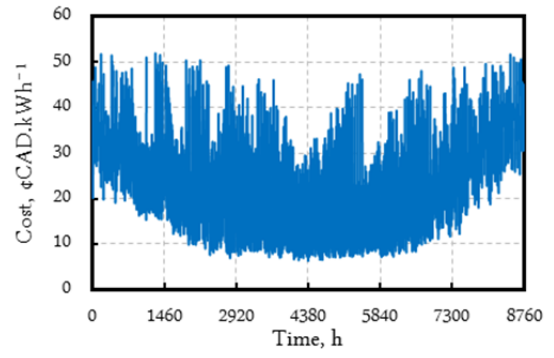
The cost of offshore wind energy was higher than onshore wind energy 15.8 ¢/kWh on average. On the other hand, onshore wind energy was the lowest among renewable energy technologies, giving an average of 10.2 ¢/kWh. Although offshore wind turbines were higher in production rate, high installation costs reflected negatively on the final cost per kilowatt-hour compared with onshore wind turbines. Figure 5.8c and d outline the seasonal average costs of onshore and offshore wind energies.

CCPP energy cost was the lowest among the technologies used, recording an average of 7.5 ¢/kWh. The highest cost is estimated to be 14.3 ¢/kWh, and the lowest cost is found to be 3.3 ¢/kWh.

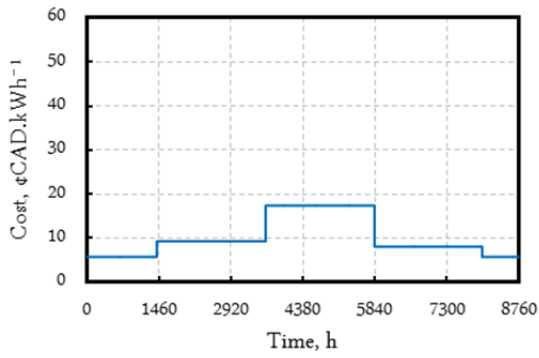
Finally, the average cost of energy produced from the hub is illustrated in Figure 5.8e. The average cost is found to be 9.2 ¢/kWh, which accounts the cost of energy from the CCPP, PV solar, onshore and offshore wind energies. A ten-day sample of the cost profile for both CCPP and the energy hub is shown in Figure A.16. The monthly average costs are shown in Figure 5.9.



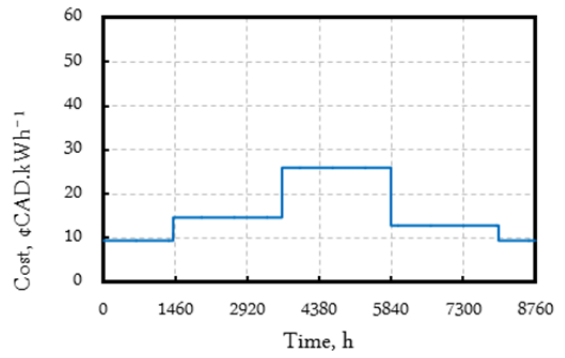
(a) CCPP, 3150 MW



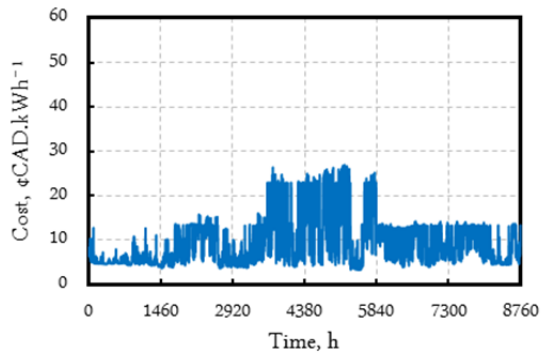
(b) PV solar farm, 20 MW



(c) Onshore wind farm, 30 MW

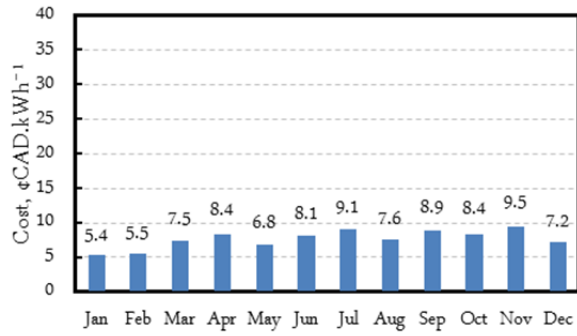


(d) Offshore wind farm, 46 MW

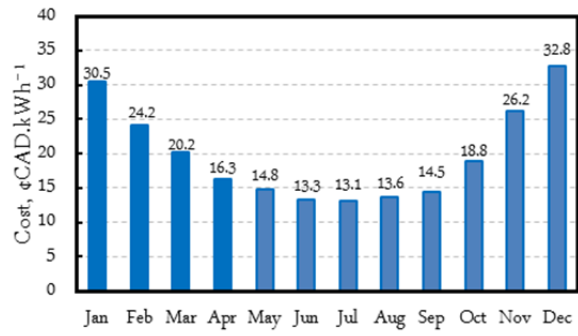


(e) Energy hub, 3246

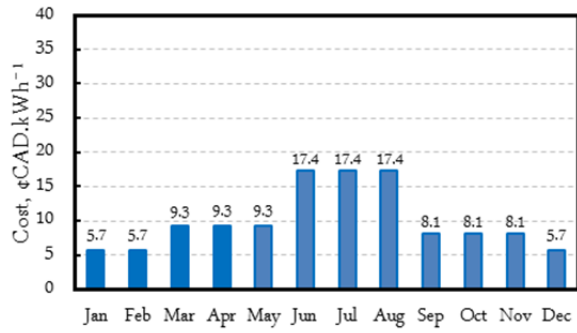
Figure 5.8 Cost of energy from the energy hub components, Scenario B.



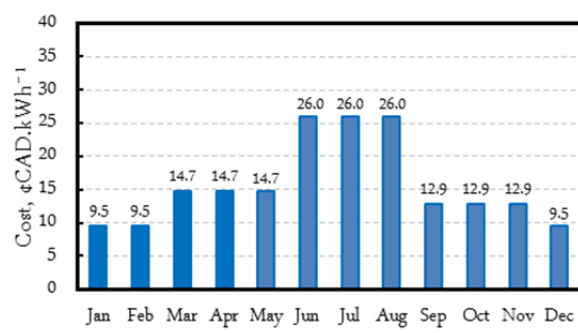
(a) CCPP, 3150 MW



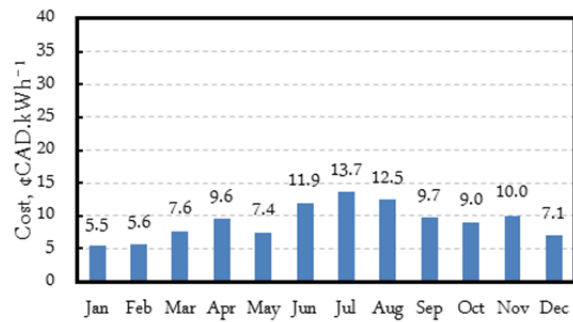
(b) PV solar farm, 20 MW



(c) Onshore wind farm, 30 MW



(d) Offshore wind farm, 46 MW



(e) Energy hub, 3246 MW

Figure 5.9 Monthly average cost of energy produced from the hub, Scenario B.

5.2.3 Summary

To summarize, an energy hub comprised of CCPP, PV solar cells, and onshore and offshore wind turbines is designed to meet electricity demand. The required design capacity is found to be 3,246 MW, with an overall 20.8% capacity factor and an average cost of 9.2 ¢/kWh. The total energy produced from the hub over one year is found to be 5,917,987 MWh. The use of renewable energy sources resulted in an emission reduction from 316.8 kg_{CO2}/MWh to 307.5 kg_{CO2}/MWh. The key outputs from Scenario B are summarized in Table 5.2.

Table 5.2 Summary of results: Scenario B.

Parameter	Value
Design capacity (MW)	
CCPP	3,150
Onshore wind turbines	30
Offshore wind turbines	46
PV solar cells	20
Energy hub	3,246
Number of units	
CCPP	8
Onshore wind turbines	20
Offshore wind turbines	20
PV solar cells	50,000
Energy produced (MWh/y)	
CCPP	5,743,617
Onshore wind turbines	53,860
Offshore wind turbines	96,541
PV solar cells	23,969
Energy hub	5,917,987
Average cost per energy unit (¢CAD/kWh)	
CCPP	7.5
Onshore wind turbines	10.2
Offshore wind turbines	15.8
PV solar cells	18
Energy hub	9.2
Total costs per year (\$CAD/y)	
CCPP	338,803,498
Onshore wind turbines	4,603,472

Table 5.2 cont'd.

Offshore wind turbines	13,105,480
PV solar cells	7,219,639
Energy hub	363,732,090
Emissions (kg_{CO2}/MWh)	
CCPP	316.8
Onshore wind turbines	-
Offshore wind turbines	-
PV solar cells	-
Energy hub	307.5
Operating hours per year (h/y)	
CCPP	7,252
Onshore wind turbines	8,760
Offshore wind turbines	8,760
PV solar cells	3,837
Energy hub	8,760
Capacity factor (%)	
CCPP	21
Onshore wind turbines	20.5
Offshore wind turbines	23.9
PV solar cells	13.7
Energy hub	20.8
Availability (%)	
CCPP	82.8
Onshore wind turbines	100
Offshore wind turbines	100
PV solar cells	43.8
Energy hub	100

5.3 Scenario C: Hydrogen Economy

In this scenario, as outlined in Chapter 4, an energy hub comprising of CCPP, onshore and offshore wind farm, PV solar cells, and alkaline electrolyzers is used to meet the electricity demand shown in Figure 5.1d. As was discussed in Section 4.3.3, CCPP is assumed to meet electricity demand, while electricity from renewable sources is utilized for hydrogen production.

5.3.1 Electricity generation

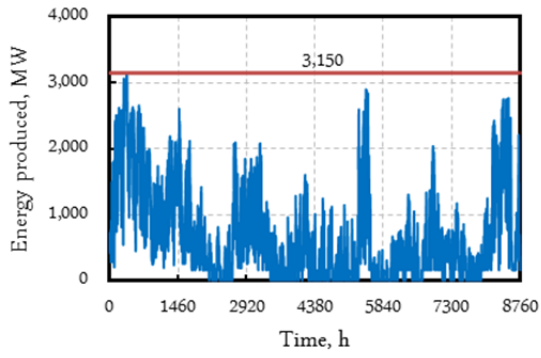
In order to meet electricity demand and produce hydrogen, the CCPP is found to have 8 units in operation with a maximum capacity 3,150 MW, as shown in Figure 5.10a. The CCPP is estimated to generate 5,883,650 MWh per year. Moreover, the power plant is found to operate at an efficiency of 62.3% based on the LHV of NG. The hourly number of turbines in operation is shown in Figure A.17.

The design capacity of the PV solar farm is set at 20 MW, with 50,000 solar cells in operation. The solar farm is found to operate at 3,837 h/y, with an overall annual production of 23,969 MWh and operates at 13.7% of its maximum design capacity. The hourly output from the PV solar cells is shown in Figure 5.10b. The farm also shows a similar profile to that illustrated in Figure A.13 and Figure A.14.

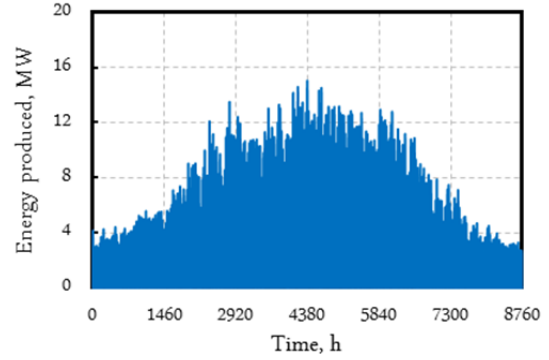
The onshore and offshore wind profiles as shown in Figure 5.10c, on the other hand, are found to have higher production rates—53,860 and 96,541 MWh/y respectively. The onshore wind farm operates at 1,795 full load hours per year with a capacity factor of 20.5%, while the offshore wind farm operates at 2,099 full load hours per year, with a capacity factor of 24%.

Energy consumed by electrolyzers (i.e., the excess electricity available) is represented by Figure 5.10d. In order to accommodate the excess electricity, the number of electrolyser units is found to be 493. This number of electrolyzers consumes about 229,220 MWh of electricity per year. Most of the electricity consumed comes from wind and solar farms, since the CCPP is set to meet only the fluctuating demand.

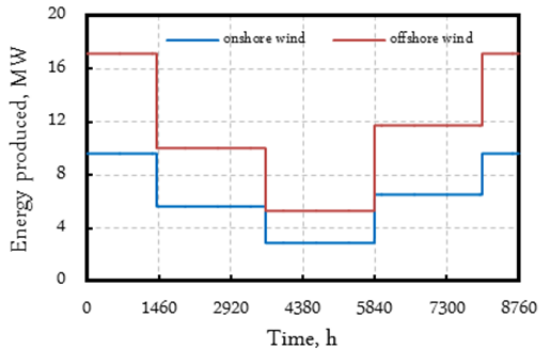
The overall energy hub, as shown in Figure 5.10e, is simulated to meet electricity demand as well as hydrogen production. The overall design capacity of Scenario C is found to be 3,246 MW. Overall, the energy hub generates 6,058,019 MWh of electricity per year. The net output, however, is found to be 5,828,799 MWh of electricity per year. Figure 5.11 shows the total monthly energy produced from the hub, while a ten-day sample of electricity produced from 1–10 January is shown in Figure A.18.



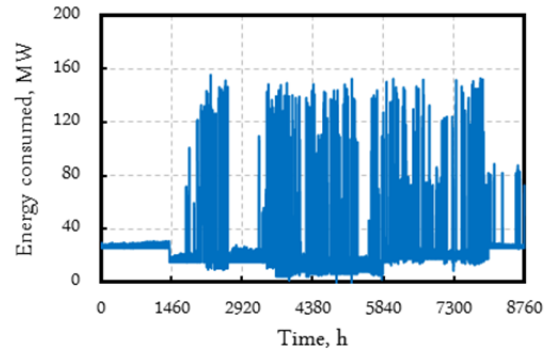
(a) CCPP, 3150 MW



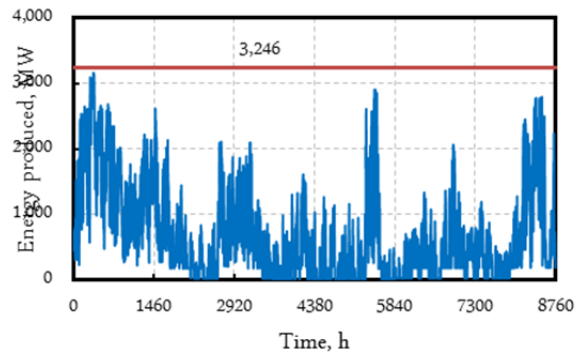
(b) PV solar farm, 20 MW



(c) Wind farm, 30 and 46 MW

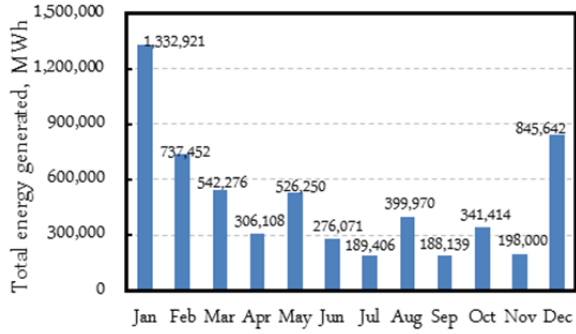


(d) Electrolyzers, 2,677 kg_{H2}/h

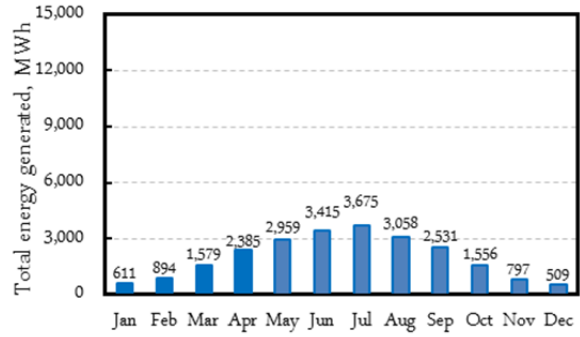


(e) Total gross energy from the hub, 3246 MW

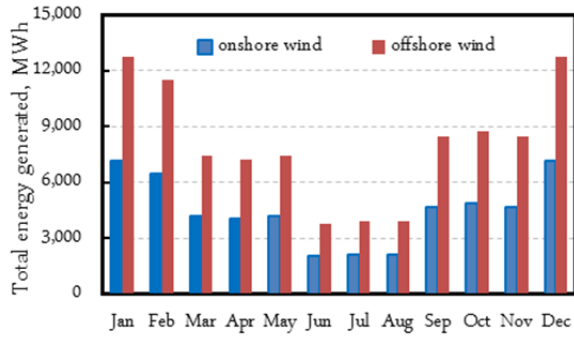
Figure 5.10 Energy produced and consumed from the hub, Scenario C.



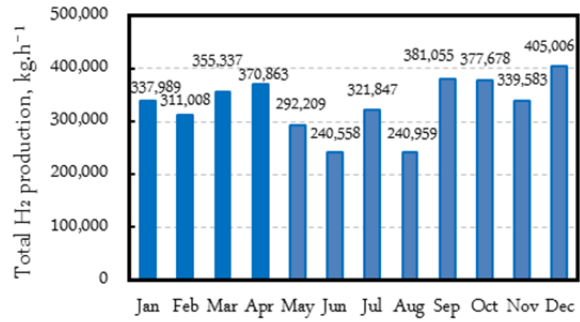
(a) CCPP, 3150 MW



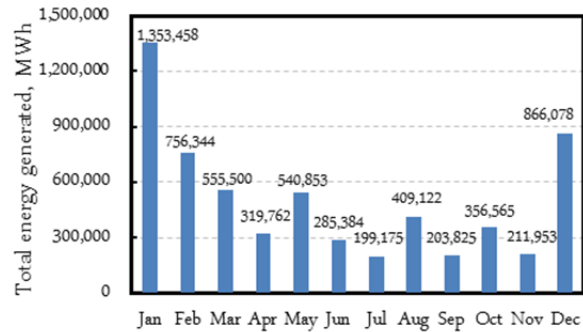
(b) PV solar farm, 20 MW



(c) Wind farm, 30 and 46 MW



(d) Electrolysers, 2677 kg_{H2}/h



(e) Total gross energy from the hub, 3246 MW.

Figure 5.11 Monthly total energy produced and consumed by the hub, Scenario C.

5.3.2 Hydrogen and oxygen production

As the main purpose of this scenario is to produce hydrogen while meeting the electricity demand, it has been found that the total production capacity of the electrolyzers is 2,677 kg_{H₂}/h (29,580 Nm³/h), with an efficiency of 68.3%, based on HHV of H₂. Over a year, the electrolyzers generate 3,974 ton of hydrogen and about 31,477 ton of pure oxygen. The hourly profile of hydrogen and oxygen produced is shown in Figure 5.12, while the hourly number of electrolyzers in operation and their turndown factors are illustrated by Figure 5.13.

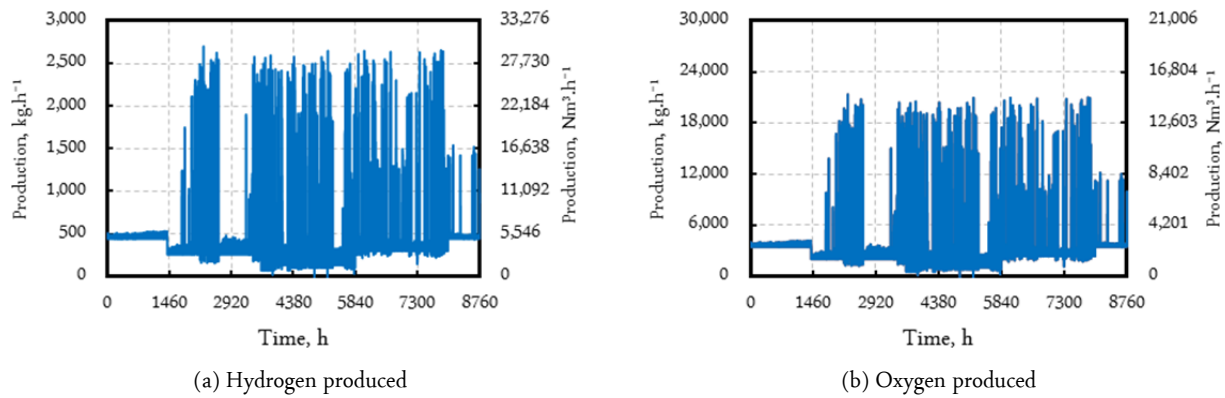


Figure 5.12 Hydrogen and oxygen produced from the electrolyser units.

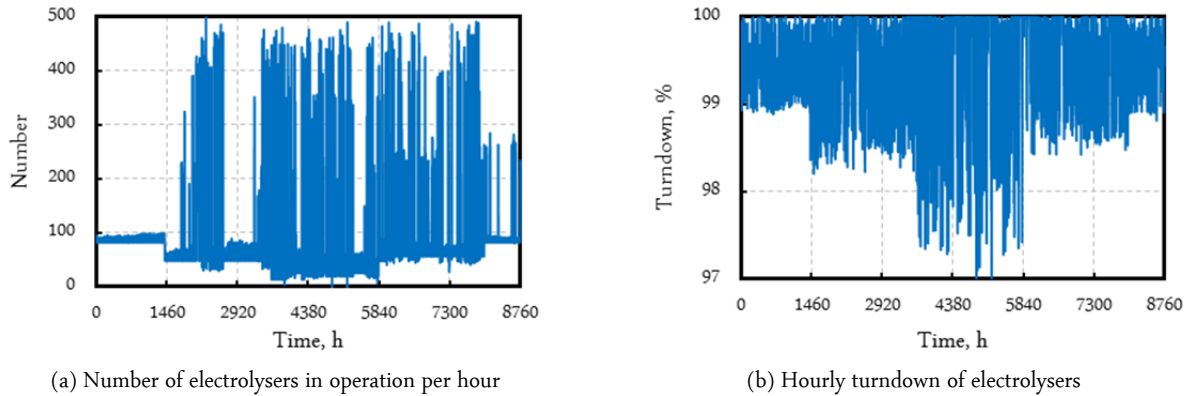


Figure 5.13 Hourly number of electrolyzers in operation and their turndown factors.

5.3.3 Electricity cost

In this scenario, hourly and annual costs of electricity, generated and consumed, are investigated. Hourly and annual costs of hydrogen and oxygen are determined as well, for both the estimated and optimal values.

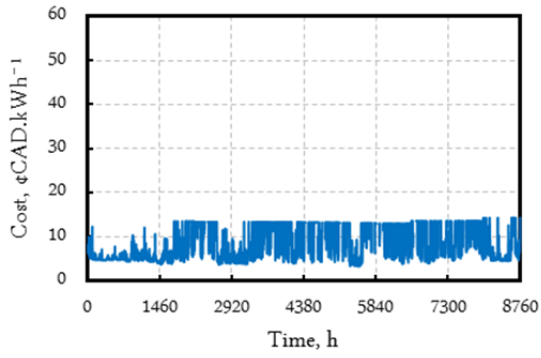
As shown in Figure 5.14a, the average annual cost of electricity from the CCPP is 7.4 ¢/kWh. PV solar cost, as it is illustrated in Scenario B and shown in Figure 5.14b, is the highest 18 ¢/kWh. On the other hand, onshore and offshore costs are slightly lower, recording 10.1 and 15.8 ¢/kWh respectively. The average overall cost of electricity from the hub is 9.0 ¢/kWh. The overall cost profile of the energy hub is illustrated by Figure 5.14e. The average monthly cost of electricity generated from the hub, on the other hand, is shown in Figure A.19.

Hydrogen and oxygen cost:

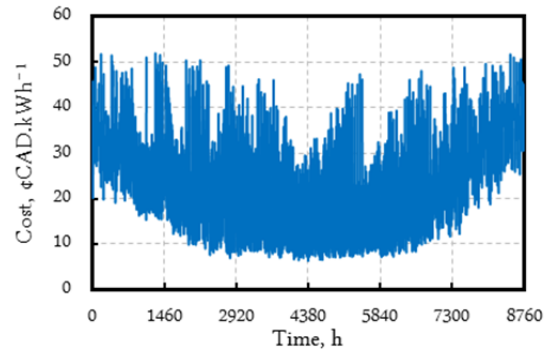
The cost of hydrogen generated from the electrolyzers is a function of excess electricity and the hourly cost of consumed electricity. As shown in Figure 5.15a, the average estimated cost of hydrogen is 17.2 \$/kg. The optimum value (minimum cost), however, is estimated to be 2.1 \$/kg. Oxygen cost, as shown in Figure 5.15b, is 1.45 \$/kg. The optimum value that results in a higher overall revenue is estimated to be 2.38 \$/kg. Table 5.3 shows the monthly production of hydrogen as well as the corresponding cost.

Table 5.3 Seasonal and annual hydrogen production and cost.

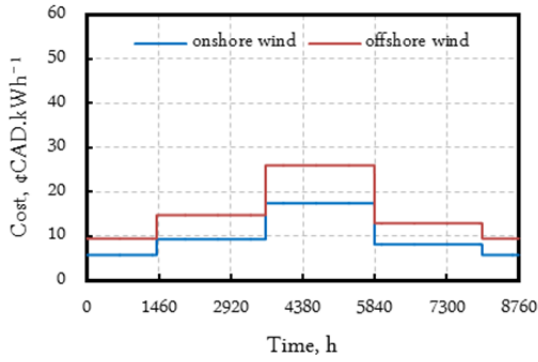
Season	H ₂ production (kg)	H ₂ average cost (\$/kg)
Winter	1,054,003	11.07
Spring	1,018,409	15.83
Summer	803,364	26.87
Autumn	1,098,316	14.80
Annual	3,974,092	17.14



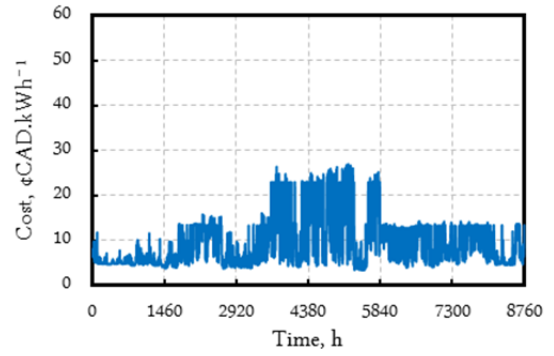
(a) CCPP, 3150 MW



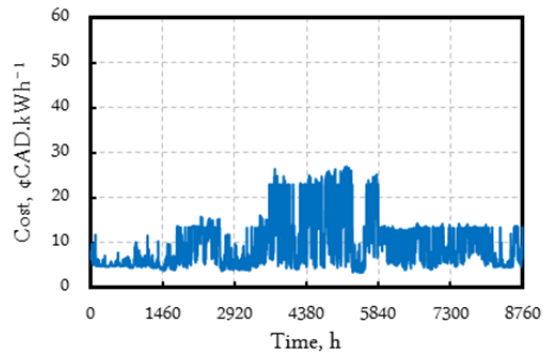
(b) PV solar farm, 20 MW



(c) Wind farm, 30 and 46 MW



(d) Electrolyzers, 2,677 kg_{H2}/h



(e) Energy hub, 3246

Figure 5.14 Cost of energy produced from the energy hub components, Scenario C.

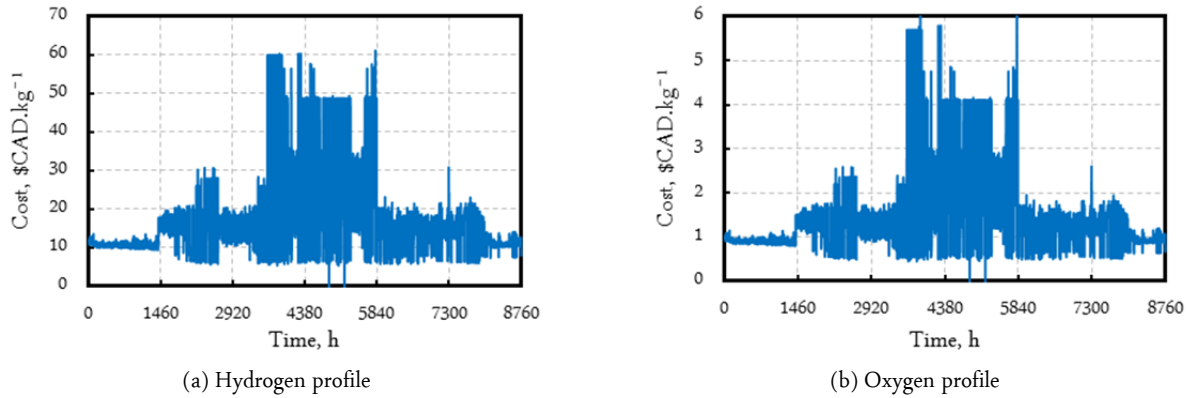


Figure 5.15 Hydrogen and oxygen cost profiles, Scenario C.

5.3.4 Summary

To summarize, an energy hub with a design capacity of 3,246 MW is used to generate hydrogen while meeting electricity demand. The gross energy produced from the hub is found to be 6,058,019 MWh per year. The energy hub operates at 21.3% of its full design capacity with overall annual costs of \$451,682,161. CO₂ emissions are found to drop from 316.8 kg/MWh to 307.7 kg/MWh, compared to the base-load scenario (Scenario A). Table 5.4 summarizes the key results of Scenario C.

Table 5.4 Summary of results: Scenario C.

Parameter	Value
Design capacity (MW)	
CCPP	3,150
Onshore wind turbines	30
Offshore wind turbines	46
PV solar cells	20
Electrolysers (Nm ³ /h)	29,580
Energy hub	3,246
Number of units	
CCPP	8
Onshore wind turbines	20
Offshore wind turbines	20
PV solar cells	50,000
Electrolysers	493

Table 5.4 cont'd.

Energy produced (MWh/y)	
CCPP	5,883,650
Onshore wind	53,860
Offshore wind	96,541
PV solar	23,969
Electrolysers (consumed)	229,220
Energy hub (gross)	6,058,019
Energy hub (net)	5,828,799
Average cost per energy unit (¢CAD/kWh)	
CCPP	7.4
Onshore wind	10.2
Offshore wind	15.8
PV solar	18
Energy hub	9
Annual hydrogen produced (ton/y)	
	3,974
Average cost of hydrogen produced (\$/kg)	
	17.14
Total costs per year (\$CAD/y)	
CCPP	343,437,681
Onshore wind turbines	4,603,472
Offshore wind turbines	13,105,480
PV solar cells	7,219,639
Electrolysers	83,315,889
Energy hub	451,682,161
Emissions (kg_{CO2}/MWh)	
CCPP	316.8
Onshore wind turbines	-
Offshore wind turbines	-
PV solar cells	-
Electrolysers	-
Energy hub	307.7
Operating hours per year (h/y)	
CCPP	7,304
Onshore wind turbines	8,760
Offshore wind turbines	8,760
PV solar cells	3,837
Electrolysers	8,758
Energy hub	8,760

Table 5.4 cont'd.

Capacity factor (%)	
CCPP	21
Onshore wind turbines	20.5
Offshore wind turbines	23.9
PV solar cells	13.7
Electrolysers	17
Energy hub	21.3
Availability (%)	
CCPP	83
Onshore wind turbines	100
Offshore wind turbines	100
PV solar cells	43.8
Electrolysers	99.98
Energy hub	100

5.4 Comparison between Scenarios

Among the three scenarios proposed, the CCPP scenario is found to give the lowest cost of electricity. The scenario meets demand with a design capacity of 3,150 MW, producing an overall 5,883,650 MWh of electricity per year at 7.4 ¢/kWh. Scenario B, on the other hand, shows a 307.5 kg_{CO2}/MWh reduction in CO₂ emissions, compared to Scenario A which gives 316.8 kg_{CO2}/MWh. The design capacity of Scenario B is found to be 3,246 MW with 5,917,987 MWh of electricity per year at 9.2 ¢/kWh. Finally, Scenario C meets electricity demand and generates hydrogen at 3,246 MW design capacity. The annual gross of energy produced is 5,828,799 MWh at 9.0 ¢/kWh. The reason why the electricity cost in Scenario C is lower than in Scenario B is to the fact that total annual energy produced in A is higher than it is in B although the design capacity is the same (the same investment cost). Availability of the overall hub is estimated to be a maximum value (100%) as a direct effect of the assumed averages of wind speed. In reality, availability should be lower than that as wind turbines would not operate 8,760 h/y.

Based on this comparison, Scenario C is the most convenient renewable and non-renewable combination as it produces hydrogen, and, at the same time, the electricity produced comes at a relatively low price. A summary of comparisons between the scenarios are outlined in the following table:

Table 5.5 Comparison between scenarios.

Parameter	Scenario A	Scenario B	Scenario C
Design capacity	3,150	3,246	3,246
Number of units			
CCPP	8	8	8
Onshore wind turbines	-	20	20
Offshore wind turbines	-	20	20
PV solar cells	-	50,000	50,000
Electrolysers	-	-	493
Gross power output, MWh	5,883,650	5,917,987	6,058,019
Net power output, MWh/y	5,883,650	5,917,987	5,828,799
Total annual costs, \$/y	343,437,681	363,732,090	451,682,161
Average cost of electricity, ¢/kWh	7.4	9.2	9.0
CO₂ emissions, kg/MWh	316.8	307.5	307.7
Operation hours, h/y	7,304	8,760	8,760
Capacity factor, %	21	20.8	21.3
Availability, %	83.4	100	100

CHAPTER 6

Conclusion and Recommendations

6.1 Conclusion

The concept of an energy hub has been applied to the Nanticoke Generating Station in Nanticoke, Ontario, specifically a model considering a replacement of the coal-fired power plant with NG-based gas and steam turbines. The energy hub concept has been investigated by proposing three main scenarios, representing three different combinations of renewable and conventional energy systems. The mathematical model for the various technologies has been developed based on theories, material and energy balances, thermodynamics relations, and economic evaluations.

The first scenario, a natural gas combined cycle, or *NG Stand -Alone Power Plant*, represents a conventional CCPP to meet electricity demand. This scenario is used as a reference point for comparison in terms of the total energy production, total efficiency, energy cost, GHG emissions, and availability. The scenario is found to meet the demand with a design capacity of 3,150 MW, producing a total electricity of 5,883,650 MWh/y, with an average cost 7.4 ¢/kWh and a capacity factor of 21%.

The second proposed scenario, *NG-Renewable Energy Hub*, represents a CCPP coupled with onshore wind turbines, offshore wind turbines, and PV solar cells. Both of the CCPP and the renewable energy technologies were used to meet the electricity demand with no excess electricity produced. The required design capacity of the hub was found to be 3,246 MW, producing a total electricity of 5,917,987 MWh/y, with an average cost 9.2 ¢/kWh and a capacity factor of 20.8 %. However, this scenario resulted in a reduction of 2.9 % of CO₂ emissions.

The last proposed scenario, *Hydrogen Economy*, represents a CCPP, onshore wind turbines, offshore wind turbines, and PV solar cells, in addition to alkaline electrolysers. The scenario's aim was to meet electricity demand and produce hydrogen from the excess electricity during off-peak hours. The hub design capacity is found to be 3,246 MW, producing a total gross electricity

of 6,058,019 MWh/y, with an average cost 9.0 ¢/kWh and a capacity factor of 21.3%. In this scenario, 3 974 kg/y of hydrogen would also be produced that could be sold into the market.

In conclusion, conventional power plants offer lower costs per unit of energy produced. Emissions and environmental footprints, on the other hand, are higher than energy hubs incorporated the use of solar and wind energy production. As such the combined NG-renewable energy system offers energy production at lower gas emissions. The higher costs of electricity produced, however, are still a barrier in adopting the energy hub concept in today's economy. In order to overcome these barriers, a tremendous development of today's renewable energy extractors is required, both, in terms of cost and performance.

6.2 Recommendations for Future Work

This project gives an introduction to energy hub layout comprising of renewable and non-renewable technologies, and basic models in GAMs that could be used for further investigations. A broader, yet more complicated, concept could be established by introducing more industrial sectors. During some discussions in this research, however, some ideas came to light that could be of interest to any future studies on the NG-renewable energy system.

Alternative scenarios could be developed for maximum use of the electrical transmission assets at Nanticoke, specifically, rather than meeting the current profile of transmission (which is limited because the high emission from the coal plant), but to produce maximum profile close to 3,000 MW at all times providing base-load electricity. A related scenario could investigate the economic feasibility of hydrogen fuel cells as part of energy hubs, that is, whether it is economical to convert hydrogen energy directly into electricity via fuel cells for load following and peak shaving, or if it would be more beneficial to have it sold to external markets.

The model for the combined cycle natural gas unit can be modified for various types of advanced technologies that have been proposed or trialed, including:

- With the electrolyzers there is the production of hydrogen, and thus studying the effects of adding hydrogen to NG on the combustion process and on the overall power plant efficiency and emissions. A general relationship could be developed to investigate the optimum H₂-NG ratio that gives the minimum NO_x emissions considering the cost.

- Although normal off gasses from the electrolyser, studying the effects of capture adding pure oxygen to NG on the combustion process and on the overall power plant efficiency, could be investigated. A general relationship could be developed to investigate the optimum H₂-NG ratio that gives the minimum emissions considering the cost. This option may have to include the consideration of pressure swing absorption (PSA) unit for additional production of oxygen. This option is likely best explored with the consideration of carbon capture and sequestration. Such consideration would have to consider the location and if sequestration opportunities are available.
- The combined heat of power unit could include the addition of a thermal solar farm (concentrated thermal heat technology) to generate a preheated stream of heated water or steam to add to Rankin Cycle to increase the efficiency in an emission free manner.
- With the addition of electrolysers the cost of hydrogen storage as a compressed gas in tanks or underground should be further explored.
- Initial studies could use to model to with an optimization function that optimizes the overall design and operation for a weighted balance between cost of electricity and emission reductions. The model could be used to develop designs that meet specific emission targets for either reduction of criteria emissions or reduction of GHG emissions.
- The energy hub could be investigated more by including different wind turbines sizes (e.g., 1, 1.5, 2, 2.5, 3, and 3.5 MW), different PV solar cells nominal power (e.g., 100, 200, 300, 400 W), and different electrolysers' capacities (e.g., 30, 60, 90, and 120 Nm³/h). An optimization problem could be formed to select among the most economic combinations of these technologies.
- The model can be developed by predicting data for weather conditions, sensitivity to NG prices, and equipment costs. Hourly wind data could be used instead of the average seasonal to take into account the sensitivity of production and availability to wind speed variations.
- Ultimately the model can be converted to a mixed integer model so that the individual units of the various energy generation technologies can be added to meet the various optimization scenarios.

REFERENCES

- Aceves, S. M., Berry, G. D., Martinez-Frias, J., & Espinosa-Loza, F. (2006). Vehicular storage of hydrogen in insulated pressure vessels. *International Journal of Hydrogen Energy*, 31(15), 2274-2283.
- Agrawal, B., & Tiwari, G. N. (2010). Life cycle cost assessment of building integrated photovoltaic thermal (BIPVT) systems. *Energy and Buildings*, 42(9), 1472-1481.
- American Wind Energy Association. (2009). FAQ for small wind systems. Retrieved January 1st, 2010, from <http://www.awea.org/>
- Attala, L., Facchini, B., & Ferrara, G. (2001). Thermoeconomic optimization method as design tool in gas-steam combined plant realization. *Energy Conversion and Management*, 42(18), 2163-2172.
- Ayoub, J., Dignard-Bailey, L., & Poissant, Y. (2010). National survey report of PV power applications in Canada. Québec: Canmet Energy.
- Baghernejad, A., & Yaghoubi, M. (2011). Multi-objective exergoeconomic optimization of an Integrated Solar Combined Cycle System using evolutionary algorithms. *International Journal of Energy Research*, 35(7), 601-615.
- Barbir, F. (2005). PEM electrolysis for production of hydrogen from renewable energy sources. *Solar Energy*, 78(5), 661-669.
- Barelli, L., Bidini, G., Gallorini, F., & Servili, S. (2008). Hydrogen production through sorption-enhanced steam methane reforming and membrane technology: A review. *Energy*, 33(4), 554-570.
- Blanco, M. I. (2009). The economics of wind energy. *Renewable and Sustainable Energy Reviews*, 13(6-7), 1372-1382.

- Borenstein, S. (2008). The market value and cost of solar photovoltaic electricity production. California: Center for the Study of Energy Markets (CSEM).
- Brooke, A., Kendrick, D., Meeraus, A., Raman, R., & Rosenthal, R. E. (1998). *GAMS: A user's guide*. Washington, DC: GAMS Development.
- BTM Consult ApS. (2010). World market update 2010 report.
- Canadian Wind Energy Association. (2008a). Canadian wind farms. Retrieved October 1st, 2010, from http://www.canwea.ca/farms/index_e.php
- Canadian Wind Energy Association. (2008b). Wind facts. Retrieved July 25th, 2010, from http://www.canwea.ca/wind-energy/index7_e.php
- Canadian Wind Energy Association. (2010). Canadian wind energy projects. Retrieved October 1st, 2010, from http://www.canwea.ca/farms/future_e.php
- Carradore, L., & Bignucolo, F. (2008). *Distributed multi-generation and application of the energy hub concept in future networks*. Paper presented at the 43rd International UPEC, Padova.
- Census Canada. (2006). Retrieved January 15th, 2012, from <http://www12.statcan.gc.ca/census-recensement/index-eng.cfm>
- Cheng, R. K., Littlejohn, D., Strakey, P. A., & Sidwell, T. (2009). Laboratory investigations of a low-swirl injector with H₂ and CH₄ at gas turbine conditions. *Proceedings of the Combustion Institute*, 32(2), 3001-3009.
- Chiesa, P., Lozza, G., & Mazzocchi, L. (2005). Using hydrogen as gas turbine fuel. *Journal of Engineering for Gas Turbines and Power*, 127(1), 73-80.
- Choi, P., Bessarabov, D. G., & Datta, R. (2004). A simple model for solid polymer electrolyte (SPE) water electrolysis. *Solid State Ionics*, 175(1-4), 535-539.
- Danish Wind Industry Association. (2003). Retrieved July 25th, 2010, from <http://www.talentfactory.dk/en/tour/wres/index.htm>

- Demand overview. (2012). Retrieved February 1st, 2012, from http://www.ieso.ca/imoweb/media/md_demand.asp
- Diéguez, P. M., Ursúa, A., Sanchis, P., Sopena, C., Guelbenzu, E., & Gandía, L. M. (2008). Thermal performance of a commercial alkaline water electrolyzer: Experimental study and mathematical modeling. *International Journal of Hydrogen Energy*, 33 (24), 7338-7354.
- DSS Management Consultants. (2005). Cost benefit analysis: Replacing Ontario's coal-fired electricity generation. Ontario: Ontario Ministry of Energy.
- Duffie, J. A., & Beckman, W. A. (2006). *Solar engineering of thermal processes* (3rd ed.). Hoboken, NJ: John Wiley & Sons.
- Energy sources. (2009). Retrieved October 1st, 2010, from <http://www.nrcan.gc.ca/eneene/sources/eleele/abofai-eng.php>
- Environment Canada. (2003). Retrieved July 25th, 2010, from <http://www.windatlas.ca/en/nav.php?field=EU&height=80&season=ANU&lat=42.791&lon=-80.168&postal=&no=24>
- EPIA. (2010). Global market outlook for photovoltaics until 2014 report. Brussels, Belgium: EPIA.
- EPIA. (2011). Solar generation 6: Solar photovoltaic electricity empowering the world report. Brussels, Belgium: EPIA.
- Favre-Perrod, P., Geidl, M., Klockl, B., & Koepfel, G. (2005, 11-15 July). *A vision of future energy networks*. Paper presented at the Power Engineering Society Inaugural Conference and Exposition in Africa, 2005 IEEE, Durban, South Africa.
- Fingersh, L., Hand, M., & Laxson, A. (2006). Wind turbine design cost and scaling model report. Golden, Colorado: National Renewable Energy Laboratory.

- Frik, R., & Favre-Perrod, P. (2004). *Proposal for a multifunctional energy bus and its interlink with generation and consumption*. Diploma, Swiss Federal Institute of Technology, Zurich.
- Gandía, L. M., Oroz, R., Ursúa, A., Sanchis, P., & Diéguez, P. M. (2007). Renewable hydrogen production: Performance of an alkaline water electrolyzer working under emulated wind conditions. *Energy & Fuels*, *21*(3), 1699-1706.
- GE Energy. (2009). 1.5 MW Wind Turbine brochure. In G. Energy (Ed.). Atlanta, GA.
- Geidl, M., & Andersson, G. (2005, 27-30 June). *A modeling and optimization approach for multiple energy carrier power flow*. Paper presented at the Power Tech., 2005 IEEE Russia, St. Petersburg, Russia.
- Geidl, M., Koeppel, G., Favre-Perrod, P., Klockl, B., Andersson, G., & Frohlich, K. (2007, Jan-Feb). Energy hubs for the future. *IEEE Power & Energy Magazine*, *5*, 24-30.
- Giampaolo, T. (2006). *Gas turbine handbook: Principles and practices* (3rd ed.). Lilburn, GA: The Fairmont Press, Inc.
- Giannakoudis, G., Papadopoulos, A. I., Seferlis, P., & Voutetakis, S. (2010). Optimum design and operation under uncertainty of power systems using renewable energy sources and hydrogen storage. *International Journal of Hydrogen Energy*, *35*(3), 872-891.
- Godoy, E., Benz, S. J., & Scenna, N. J. (2011). A strategy for the economic optimization of combined cycle gas turbine power plants by taking advantage of useful thermodynamic relationships. *Applied Thermal Engineering*, *31*(5), 852-871.
- Government of Canada. (2010). Canada's action on climate change. Retrieved December 1st, 2010, from <http://www.climatechange.gc.ca/default.asp?lang=En&n=72F16A84-1>
- Greenhouse Gas Division. (2010). National inventory report 1990–2008: Greenhouse gas sources and sinks in Canada.

- Hajimiragha, A., Fowler, M. W., & Cañizares, C. A. (2009). Hydrogen economy transition in Ontario - Canada considering the electricity grid constraints. *International Journal of Hydrogen Energy*, 34(13), 5275-5293.
- Heller, P., Pfänder, M., Denk, T., Tellez, F., Valverde, A., Fernandez, J., & Ring, A. (2006). Test and evaluation of a solar powered gas turbine system. *Solar Energy*, 80(10), 1225-1230.
- Hydrogenics Cor. (2009). HySTAT alkaline electrolyser brochure. In H. Cor. (Ed.). Mississauga, Ontario: Hydrogenics Cor.
- IESO. (2010). Wind power in Ontario. Retrieved August 1st, 2010, from <http://www.ieso.ca/imoweb/marketdata/windpower.asp>
- ISO 2314. (2009). Gas turbines: acceptance tests.
- Jonsson, M., & Yan, J. (2005). Humidified gas turbines: A review of proposed and implemented cycles. *Energy*, 30(7), 1013-1078.
- Kirk-Othmer. (1998) *Kirk-Othmer Concise Encyclopedia of Chemical Technology* (4th ed.). New York: John Wiley & Sons Inc.
- Kodama, T. (2003). High-temperature solar chemistry for converting solar heat to chemical fuels. *Progress in Energy and Combustion Science*, 29(6), 567-597.
- Kurtulan, S., & Sevgi, L. (2009). A village house energy supply system: Fundamentals of energy conversion. *Antennas and Propagation Magazine, IEEE*, 51(4), 233-237.
- Lazzaretto, A., & Segato, F. (2002). A thermodynamic approach to the definition of the HAT cycle plant structure. *Energy Conversion and Management*, 43(9-12), 1377-1391.
- Lazzaretto, A., & Toffolo, A. (2004). Energy, economy and environment as objectives in multi-criterion optimization of thermal systems design. *Energy*, 29(8), 1139-1157.
- Lazzaretto, A., & Toffolo, A. (2010). Analytical and neural network models for gas turbine design and off-design simulation. *International Journal of Thermodynamics*, 4(4), 173-182.

- Maniyali, Y. A. (2009). *Modeling of a clean energy hub with hydrogen as energy vector using Nanticoke region as a case study*. MAsc, University of Waterloo, Waterloo, ON.
- McDowall, W., & Eames, M. (2006). Forecasts, scenarios, visions, backcasts and roadmaps to the hydrogen economy: A review of the hydrogen futures literature. *Energy Policy*, 34(11), 1236-1250.
- Melnichuk, M., Silin, N., & Peretti, H. A. (2009). Optimized heat transfer fin design for a metal-hydride hydrogen storage container. *International Journal of Hydrogen Energy*, 34(8), 3417-3424.
- Mirzaesmaeeli, H., Elkamel, A., Douglas, P. L, Croiset, E., & Gupta, M. (2010). A multi-period optimization model for energy planning with CO₂ emission consideration. *Journal of Environmental Management*, 91(5), 1063-1070.
- Muradov, N. Z., & Veziroglu, T. N. (2008). "Green" path from fossil-based to hydrogen economy: An overview of carbon-neutral technologies. *International Journal of Hydrogen Energy*, 33(23), 6804-6839.
- National Commission on Energy Policy. (2004). *Ending the energy stalemate: A bipartisan strategy to meet America's energy challenges*. Washington, DC: Bipartisan Policy Center.
- National Renewable Energy Laboratory. (2004). *Technology brief: Analysis of current-day commercial electrolyzers*. Golden, Colorado: NREL.
- National Research Council. (2005). *The hydrogen economy: Opportunities, costs, barriers, and R&D needs*. Washington, DC: The National Academies Press.
- Naughten, B. (2003). Economic assessment of combined cycle gas turbines in Australia: Some effects of microeconomic reform and technological change. *Energy Policy*, 31(3), 225-245.

- Office of Air Quality Planning and Standards. (2010). Available and emerging technologies for reducing greenhouse gas emissions from coal-fired electric generating units. North Carolina: U.S. Environmental Protection Agency.
- Ontario's Smart Grid Forum. (2009). Enabling tomorrow's electricity system: Report of the Ontario Smart Grid Forum. Toronto, ON: Independent Electricity System Operator.
- Ordorica-Garcia, G., Elkamel, A., Douglas, P. L., Croiset, E., & Gupta, M. (2009). Optimizing energy production with integrated CCS technology for CO₂ emissions mitigation in the Canadian oil sands industry. *Energy Procedia*, 1(1), 3985-3992.
- Pacyna, E. G., Pacyna, J. M., Steenhuisen, F., & Wilson, S. (2006). Global anthropogenic mercury emission inventory for 2000. *Atmospheric Environment*, 40(22), 4048-4063.
- Pawlowski, C. (2009). Hythane: Implementing an alternative method to natural gas combustion. Waterloo, ON: Green Energy and Fuel Cell Laboratory, University of Waterloo.
- Phillips, J. N., & Roby, R. J. (2000). Hydrogen-enriched natural gas offers economic NO_x reduction alternative. *Power Engineering*, 104(5), 36-40.
- Poullikkas, A. (2001). A technology selection algorithm for independent power producers. *The Electricity Journal*, 14(6), 80-84.
- Power generation. (2010). Retrieved October 1st, 2010, from <http://www.opg.com/power/>
- PV cost factors. (2010). Retrieved December 15th, 2011, from <http://www.repartners.org/solar/pvcost.htm>
- Raugei, M., & Frankl, P. (2009). Life cycle impacts and costs of photovoltaic systems: Current state of the art and future outlooks. *Energy*, 34(3), 392-399.
- Rizk, N. K., & Mongia, H. C. (1993). Semianalytical correlations for NO_x, CO, and UHC emissions. *Journal of Engineering for Gas Turbines and Power*, 115(3), 612-619.
- Roadmap on manufacturing R&D for the hydrogen economy. (2005). Washington, DC: U.S. Department of Energy.

- Russell, M. C., & Bergman, D. A. (1986). Photovoltaic flat-plate array and insolation measurements. *Solar Cells*, 18(3-4), 353-362.
- Saur, G. (2008). Wind-to-hydrogen project: Electrolyzer capital cost study.
- Schwarzbozl, P., Buck, R., Sugarmen, C., Ring, A., Marcos Crespo, M., Altwegg, P., & Enrile, J. (2006). Solar gas turbine systems: Design, cost and perspectives. *Solar Energy*, 80(10), 1231-1240.
- Sherif, S. A., Barbir, F., & Veziroglu, T. N. (2005). Wind energy and the hydrogen economy: Review of the technology. *Solar Energy*, 78(5), 647-660.
- Siemens AG. (2009). Siemens wind turbine SWT 2.3-93 brochure. Germany: Siemens AG.
- Siemens AG. (2010). Siemens SGT5-8000H brochure. Germany: Siemens AG.
- Sierens, R., & Rosseel, E. (2000). Variable composition hydrogen/natural gas mixtures for increased engine efficiency and decreased emissions. *Journal of Engineering for Gas Turbines and Power*, 122(1), 135-140.
- Sinnott, R. K. (2005). *Coulson and Richardson's chemical engineering: Chemical engineering design* (4th ed. Vol. 6). Oxford, UK: Butterworth-Heinemann.
- Sirikittittisak, T., Mirzaesmaeli, H., Douglas, P. L., Croiset, E., Elkamel, A., & Gupta, M. (2009). A multi-period optimization model for energy planning with CO₂ emission consideration. *Energy Procedia*, 1(1), 4339-4346.
- Smith, R. (2005). *Chemical process design and integration*. New York: Wiley Ltd.
- Solarbuzz. (2011). Inverter prices. Retrieved September 15th, 2011, from <http://www.solarbuzz.com/facts-and-figures/retail-price-environment/inverter-prices>
- Stantic Consulting Ltd. (2009). Port Dover and Nanticoke Wind Project: Draft project description.
- Statistics Canada. (2011). Quarterly demographic estimates. Ottawa, ON.

- Stojic, D. L., Marceta, M. P., Sovilj, S. P., & Miljanic, S. S. (2003). Hydrogen generation from water electrolysis: Possibilities of energy saving. *Journal of Power Sources*, 118(1-2), 315-319.
- Sunpower Cor. (2010). Sunpower 400 solar panel brochure. California: Sunpower Cor.
- Supply overview. (2012). Retrieved February 1st, 2012, from http://www.ieso.ca/imoweb/media/md_supply.asp
- Syed, F., Fowler, M., Wan, D., & Maniyali, Y. (2009). An energy demand model for a fleet of plug-in fuel cell vehicles and commercial building interfaced with a clean energy hub. *International Journal of Hydrogen Energy*, 35(10), 5154-5163
- Tajik Mansouri, M., Ahmadi, P., Ganjeh Kaviri, A., & Jaafar, M. N. M. (2012). Exergetic and economic evaluation of the effect of HRSG configurations on the performance of combined cycle power plants. *Energy Conversion and Management*, 58, 47-58.
- Tanaka, N. (2008). Energy technology perspectives: Scenarios & strategies to 2050. Paris: International Energy Agency (IEA).
- Tanaka, N. (2009). Technology roadmap: Wind energy. Paris: International Energy Agency (IEA).
- Termaath, C., Skolnik, E., Schefer, R., & Keller, J. (2006). Emissions reduction benefits from hydrogen addition to midsize gas turbine feedstocks. *International Journal of Hydrogen Energy*, 31 (9), 1147-1158.
- Thermal power. (2010). Retrieved October 1st, 2010, from <http://www.opg.com/power/thermal/>
- Ulleberg, Ø. (2003). Modeling of advanced alkaline electrolyzers: A system simulation approach. *International Journal of Hydrogen Energy*, 28(1), 21-33.
- US Department of Energy. (2005). *Energy policy act of 2005*. Retrieved from <http://www.doi.gov/pam/EnergyPolicyAct2005.pdf>.
- Wizelius, T. (2007). *Developing wind power projects: Theory and practice*. London: Earthscan.

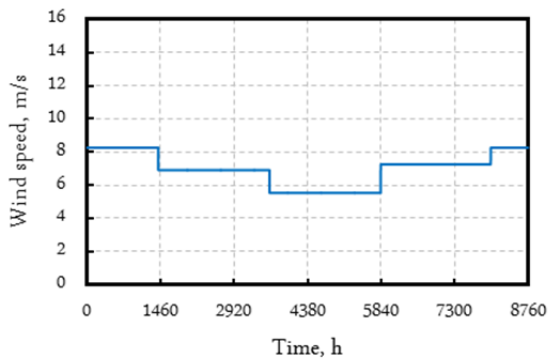
Zervos, A., & Sawyer, S. (2008). Global wind 2008 report. Belgium: Global Wind Energy Council (GWEC).

Zervos, A., Teske, S., & Sawyer, S. (2008). Global wind energy outlook 2008. Belgium: Global Wind Energy Council (GWEC).

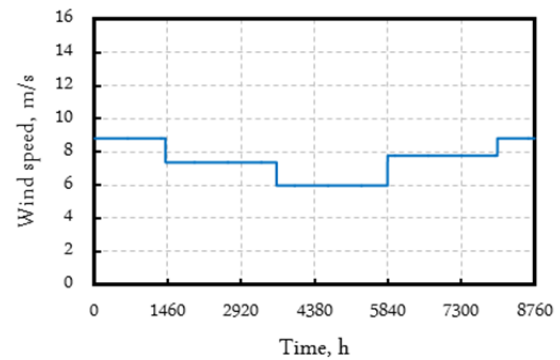
APPENDICES

APPENDIX A

Charts & Diagrams

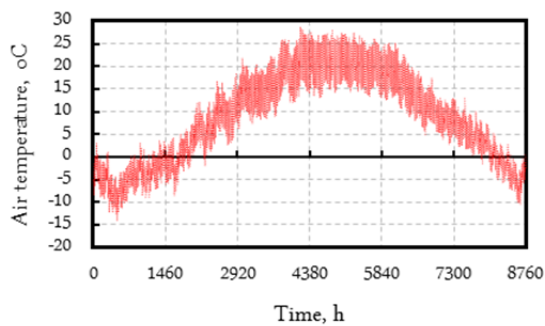


(a) Onshore wind profile at 42.791 N & -80.168 W.

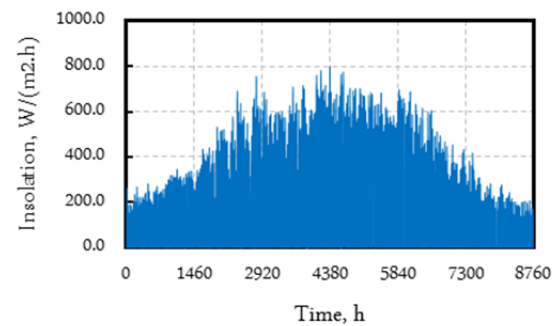


(b) Offshore wind profile at 42.772 N & -80.116 W.

Figure A.1 Seasonal average onshore and offshore wind speed, Nanticoke, ON.



(a) Hourly air temperature, °C



(b) Hourly solar radiation, W.m⁻².h⁻¹

Figure A.2 Hourly temperature and solar radiation (Maniyali, 2009).

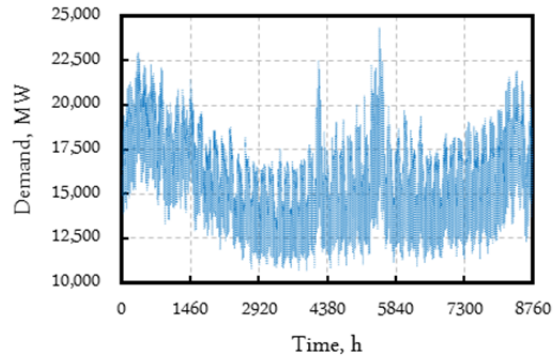


Figure A.3 Ontario's hourly electricity demand in 2009.

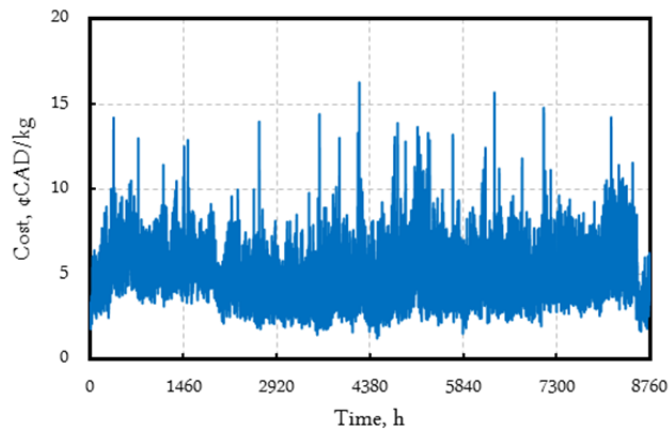


Figure A.4 Ontario's hourly electricity cost in 2009.

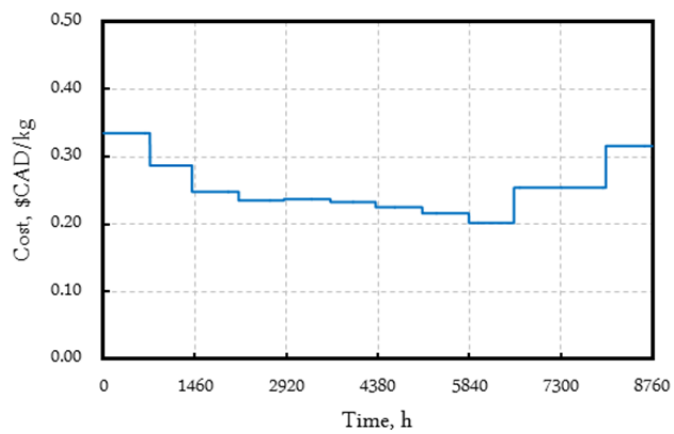


Figure A.5 Average monthly NG price.

APPENDIX B

GAMS® Results

Scenario A : NG stand-alone power plant.

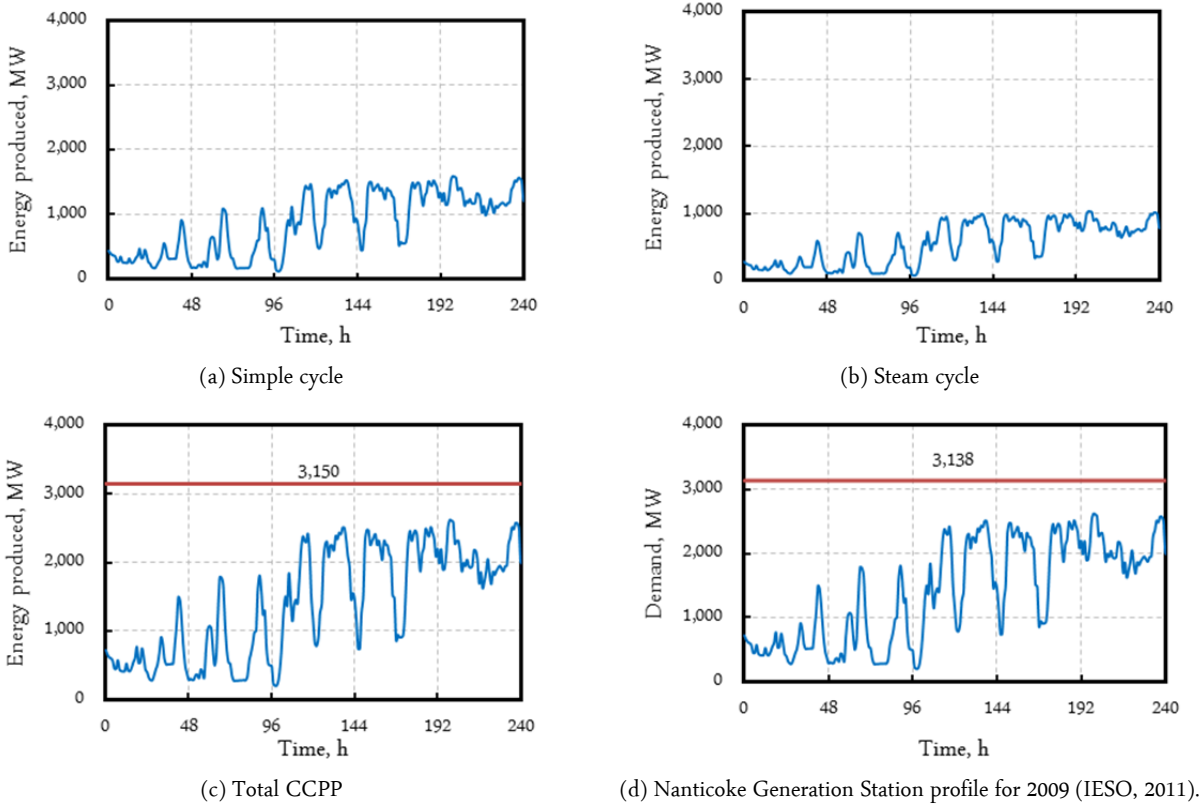


Figure A.6 Hourly energy produced from the power plant, a ten-day sample.

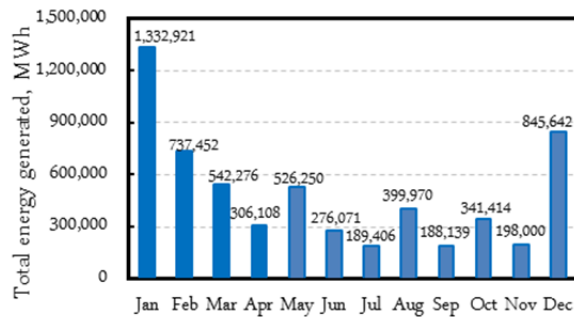
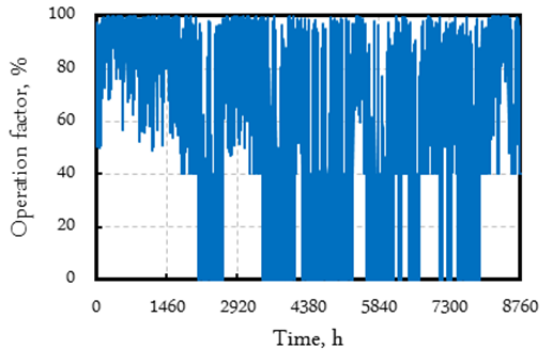
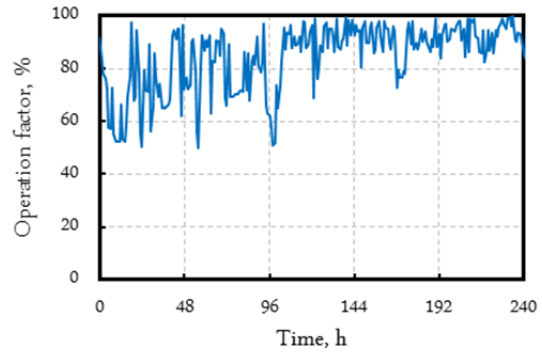


Figure A.7 Total monthly energy production from 3,150 MW CCPP.

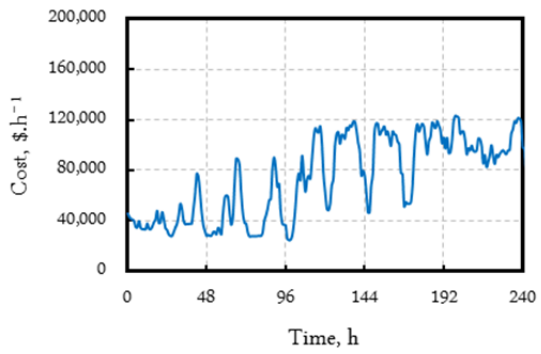


(a) Over one year

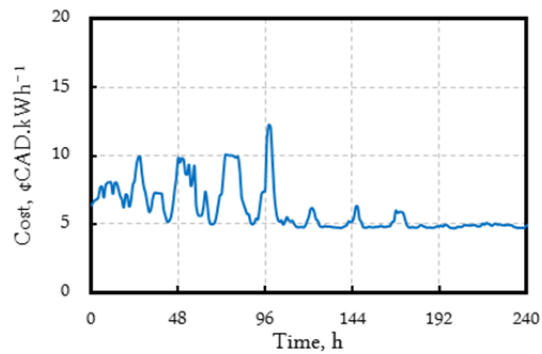


(b) A 10-day sample, 1-10 January.

Figure A.8 Hourly operating capacity of combined cycle units.

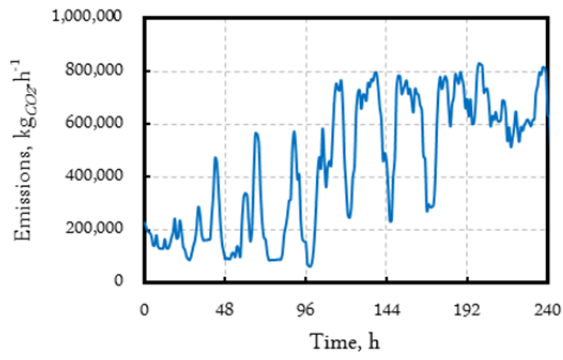


(a) Total hourly costs of CCPP

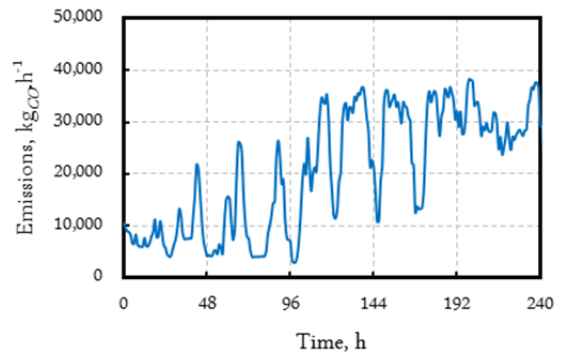


(b) Cost per kWh

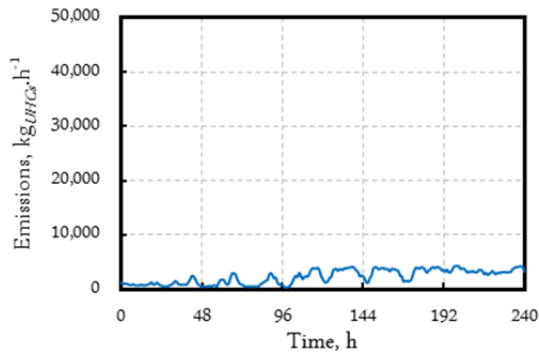
Figure A.9 Hourly costs of the power plant, a ten-day sample.



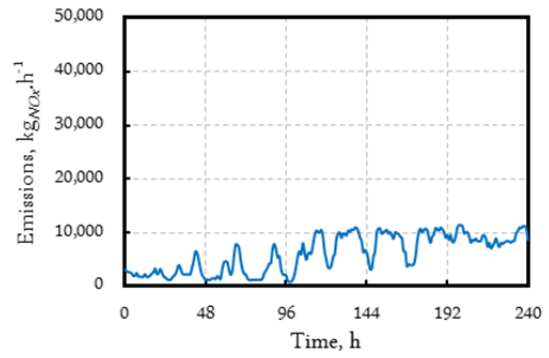
(a) CO₂ emissions



(b) CO emissions



(c) UHCs emissions



(d) NO_x emissions

Figure A.10 Hourly gas emissions from the CCPP, a ten-day sample.

Scenario B : NG-renewable energy hub.

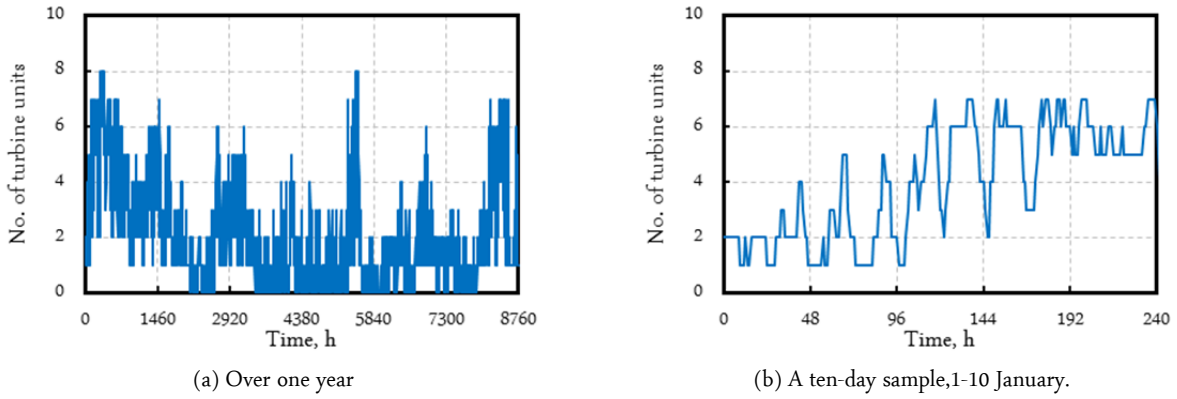


Figure A.11 Hourly number of CCPP units in operation.

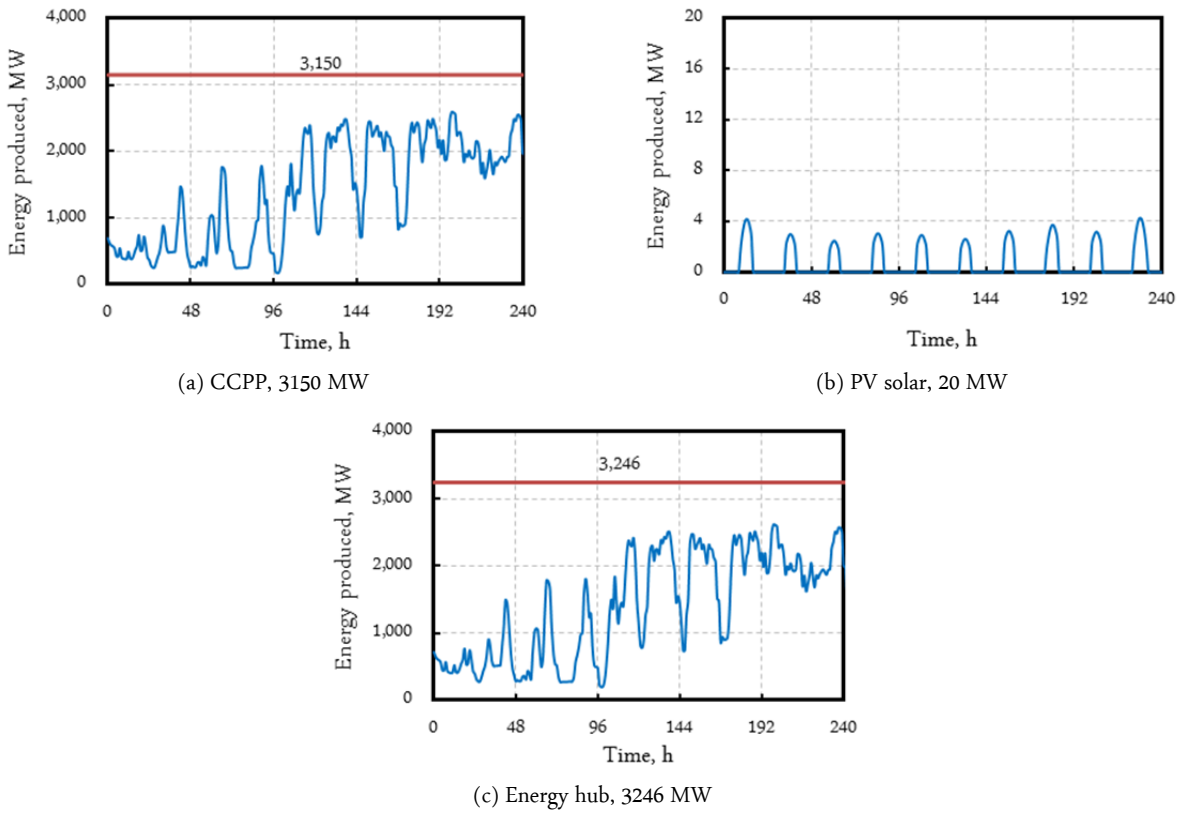
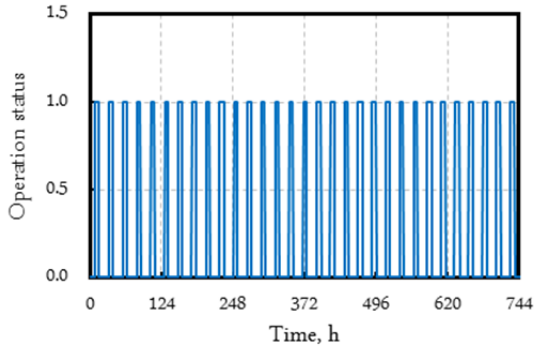
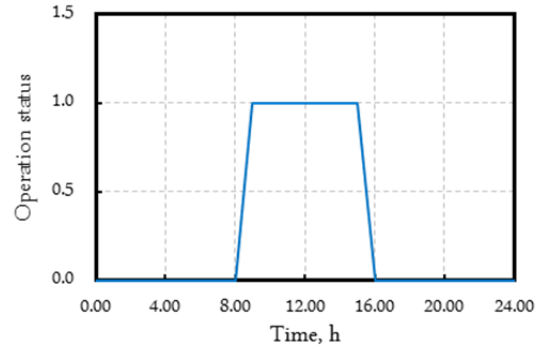


Figure A.12 Energy produced from the hub, a ten-day sample.



(a) sample operation status in January



(b) sample operation status on January 1

Figure A.13 PV solar cells operation status: [0] OFF, [1] ON.

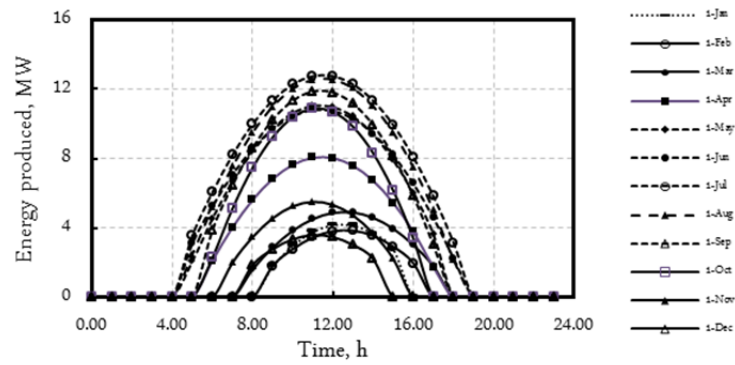
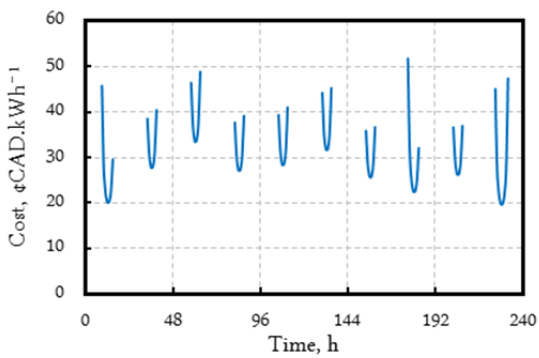
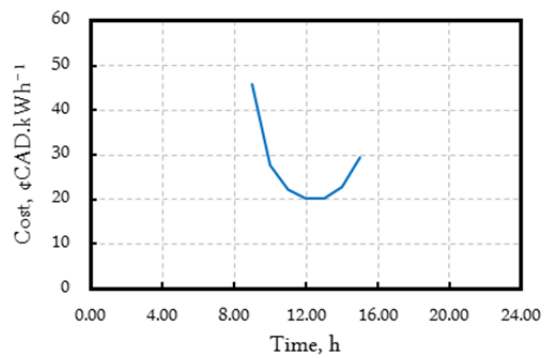


Figure A.14 Sample hourly PV solar energy produced at the beginning of each month.

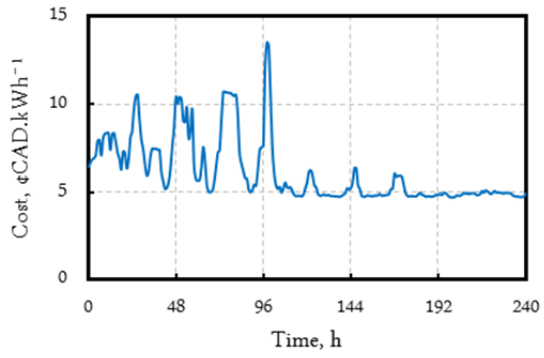


(a) A ten-day sample, 1-10 January

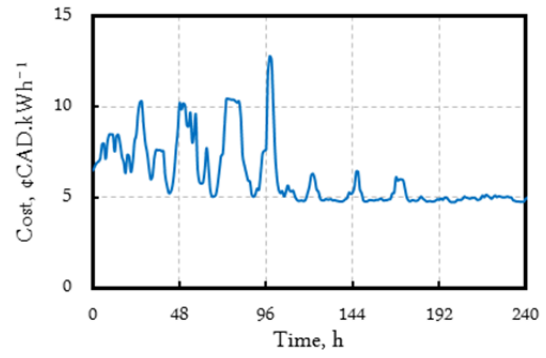


(b) A twenty-four-hour sample, January 1

Figure A.15 Hourly cost of PV solar energy.



(a) CCPP electricity cost: A ten-day sample, 1-10 January



(b) EH electricity cost: A ten-day sample, 1-10 January

Figure A.16 Hourly cost of electricity, Scenario B.

Scenario C : Hydrogen economy.

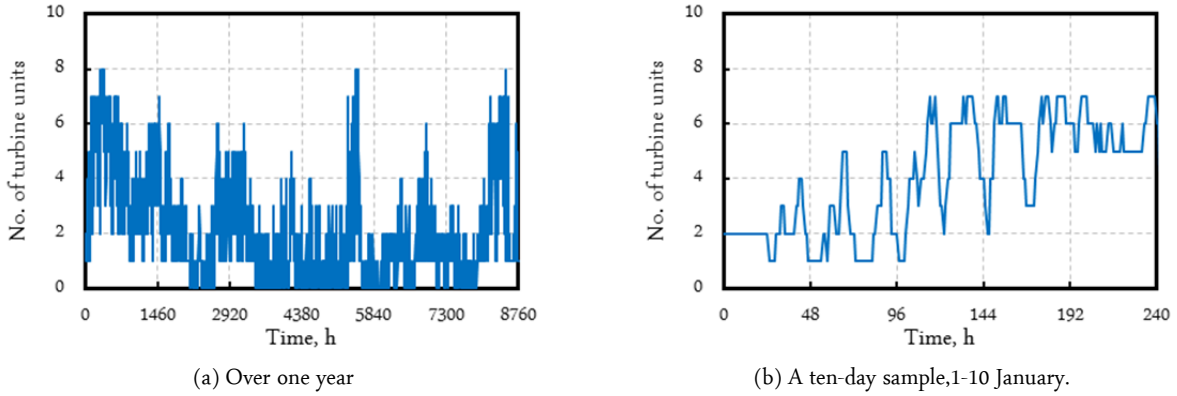


Figure A.17 Hourly number of CCPP units in operation.

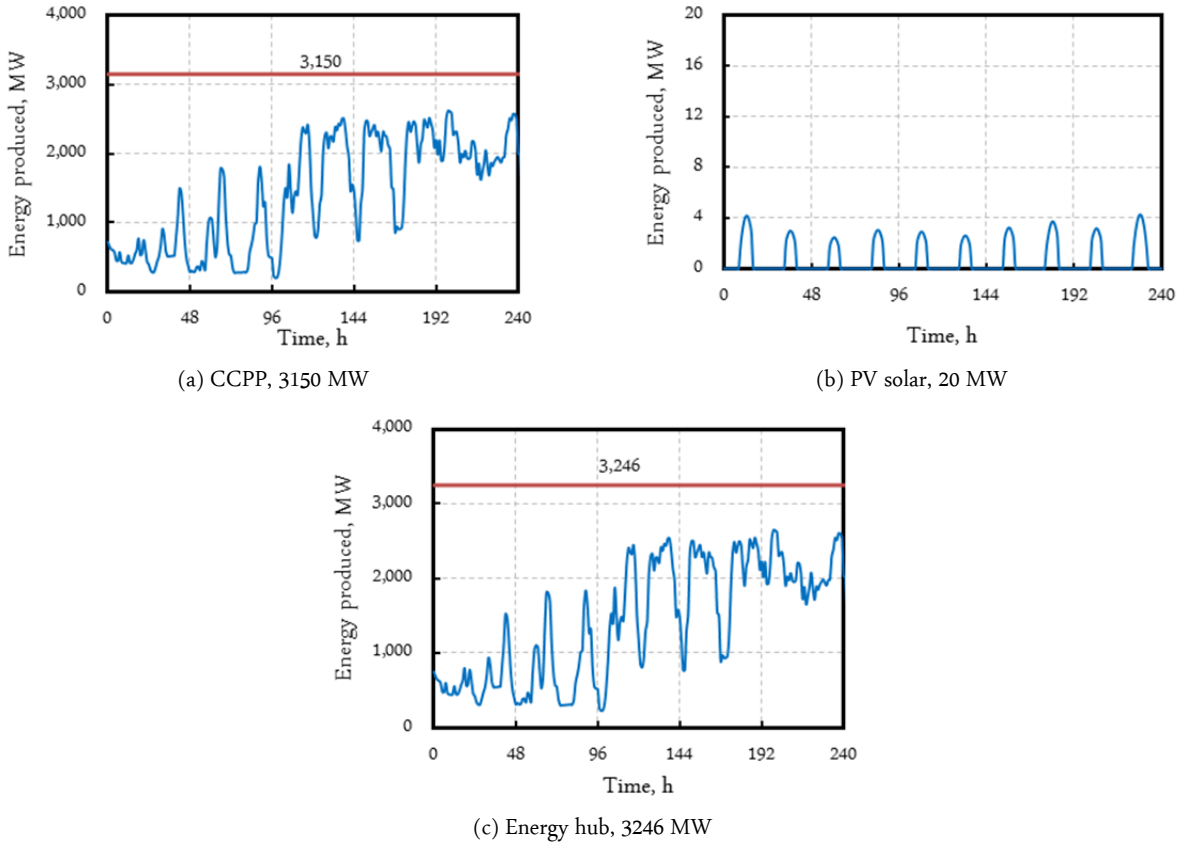
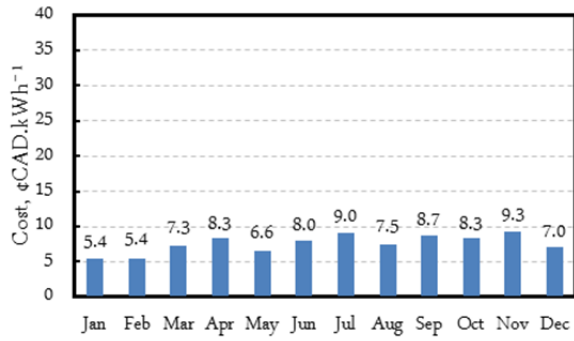
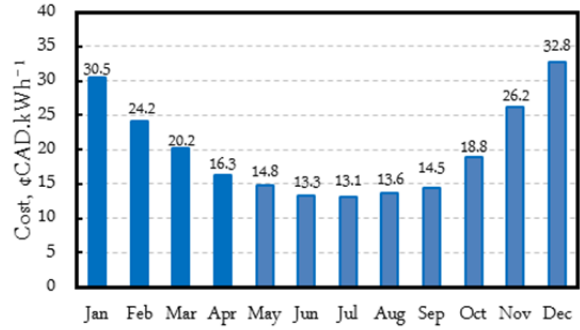


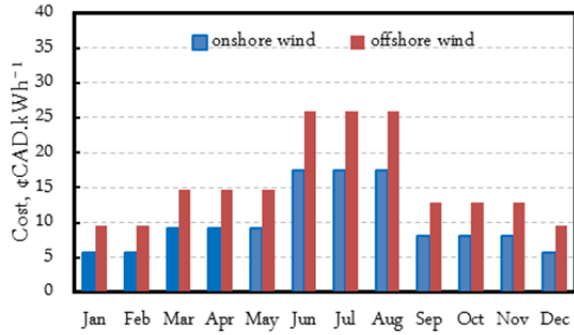
Figure A.18 Energy produced from the hub, a ten-day sample, 1-10 January.



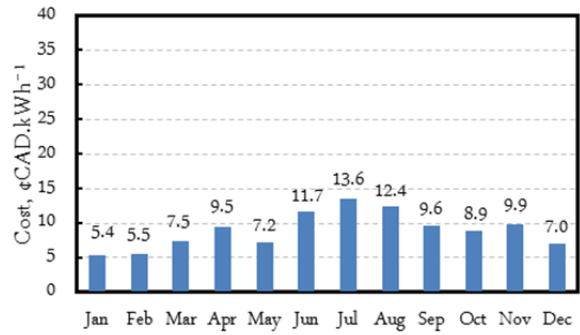
(a) CCPP, 3150 MW



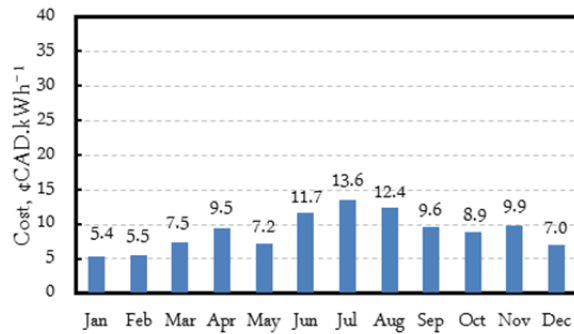
(b) PV solar farm, 20 MW



(c) Wind farm, 30 and 46 MW

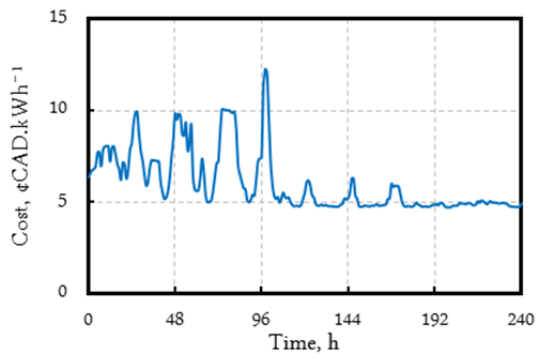


(d) Electrolysers, 2677 kg_{H2}/h

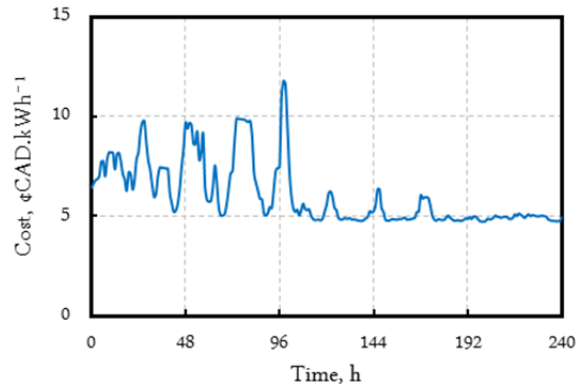


(e) Energy hub, 3246 MW

Figure A.19 Monthly average cost of energy produced and consumed by the hub, Scenario C.



(a) CCPP electricity cost: A ten-day sample, 1-10 January



(b) EH electricity cost: A ten-day sample, 1-10 January

Figure A.20 Hourly cost of electricity, a ten-day sample, 1-10 January.

APPENDIX C

GAMS® Code

GAMS IDE®

Version : 23.6.5

Release date : December 13th, 2010

```
*=====
*=====          OPTIMIZATION OF NG-BASED CLEAN ENERGY HUB          =====
*=====
*BY ABDUSLAM M. SHARIF, EMAIL: a6sharif@uwaterloo.ca

*CHEMICAL ENGINEERING DEPARTMENT, UNIVERSITY OF WATERLOO, 200 UNIVERSITY AVE
W, WATERLOO, ON

$TITLE OPTIMIZATION OF NG-BASED CLEAN ENERGY HUB

*=====

$ONTEXT
VERSION: V2.0
DATE: 4-JAN-2012
*DESIGN POINTS: T0_GT, P0_GT, rc=p2/p1, Zet_c, Zet_t, W_SC, AIR-FUEL RATIO.
1. NG TURBINE UNIT
2. Steam Turbine Unit:
$OFFTEXT

*=====
*TYPE THIS "a=c rf=NGT.ref" IN THE UPPER RIGHT SIDE BAR TO LIST VARIABLES,
*PARAMETERS, EQUATIONS, etc.
*=====

SCALARS
*ENTER THESE SCALARS
Np_PP          '**nominal power of the PP, MW'           /393.70/
rc             'pressure ratio, P2/P1'                   /15.6/
Zet_t         'polytropic efficiency of GT'              /0.90/
Zet_ST       'polytropic efficiency of ST'               /0.92/
Zet_c        'polytropic efficiency of the compressor' /0.92/
Z_PMP        'pump isentropic efficiency'                /0.84/
Zet_gen      'generator efficiency'                      /0.98/
U_COND       'overall heat transfer coefficient, condenser-VOLUME:6,P.637
              [kW/(m2.K)]'                               /1.250/

B_GT          'installation cost factor'                 /1.0/
EX_rate      '$CAD exchange rate, Sep-2011'             /1.03/
LS_GT        'life span of the GT, y'                    /25/
Omf_GT       'O&M factor, xIC'                           /1.1/

*PROPERTIES
```

```

k1      'cp/cv, at air comp.'           /1.4/
k2      'cp/cv, at expander'          /1.4/
k3      'cp/cv of steam'              /1.4/
LHV_CH4 'lower heating value of CH4, H2O(g), kJ/kmol' /802279/
HHV_CH4 'higher heating value of CH4, H2O(l), kJ/kmol' /890225/
den_H2O 'density of water [kg/m3]'      /1000/
CpH2O   'heat capacity of water [kJ/(kmol.K)]' /75.33/
HvH2O   'heat of vaporisation of water [kJ/kmol]' /40905/
MW_O2   'molecular weight of O2,kg/kmol' /32.00/
MW_N2   'molecular weight of N2,kg/kmol' /28.01/
MW_CH4  'molecular weight of CH4,kg/kmol' /16.04/
MW_CO2  'molecular weight of CO2,kg/kmol' /44.01/
MW_H2O  'molecular weight of H2O,kg/kmol' /18.02/
MW_Air  'Air avg. molecular weight, kg/kmol' /28.97/

```

**ESTIMATED SCALARS*

```

N_GT    'no. of gas turbines'
Np_GT   'nominal power of GT [MW]'
Np_ST   'nominal power of ST [MW]'
Am_COND 'max heat transfer area, condenser [m2]'
Qm_T67  'rated kW for HRSG [kW]'
LMTDm67 'rated LMTD for HRSG [C]'
Np_PMP  'required nominal power of the pump [MW]'
NGkgyt_GT 'Total NG consumed per year, kg/y'
Airkgyt_GT 'Total air consumed per year, kg/y'

ICoGT_GT 'installed capital(IC) costs of the GT [$CAD]'
ICogenA_GT 'IC costs of the gen-A [$CAD]'
ICoST_GT  'IC costs of the ST [$CAD]'
ICogenB_GT 'IC costs of the gen-B [$CAD]'
ICoHRSG_GT 'IC costs of the HRSG [$CAD]'
ICoCon_GT 'IC costs of the cond. [$CAD]'
ICoPMP_GT 'IC costs of the pump [$CAD]'
ICoEQP_GT 'total initial equipment costs [$CAD]'
CkWh_GT  'avg annual cost per kWh, ¢CAD/kWh'

```

```

m1      'polytropic temp. coefficient'
n1      'expansion/compression index'
m2      'polytropic temp. coefficient'
n2      'expansion/compression index'
m3      'polytropic temp. coefficient'
n3      'expansion/compression index';

```

```

=====
SETS          IT 'temp iteration' /IT1*IT50/, IEH/IEH1*IEH8760/, JEH /JEH1/;
=====

```

```

PARAMETERS   Taff(IT), fTaff(IT), fdTaff(IT), T3aa(IT), fT3aa(IT),
fdT3aa(IT);

```

PARAMETERS

**ENTER THESE PARAMETERS*

```

Tf(IEH,JEH) 'fuel supply temperature, oC'
T0_GT(IEH,JEH) 'ambient air temp, oC'
P0_GT(IEH,JEH) 'ambient air pressure, Pa'
T5(IEH,JEH) '**GT inlet temp, oC'
W_EXN(IEH,JEH) 'total work from the SCPP (expander), MW'
Edemand_GT(IEH,JEH) 'hourly electricity demand, MWh/h'
CNGh(IEH,JEH) 'hourly NG market price, $CAD/kg'

```

**ESTIMATED PARAMETERS*

Ni_GT(IEH,JEH)	'hourly no. of GTs in operation'
W_ACp(IEH,JEH)	'polytropic work required by air comp., MW'
W_AC(IEH,JEH)	'actual work required by air comp., MW'
W_EXp(IEH,JEH)	'polytropic ideal work output from the expander, MW'
W_SC(IEH,JEH)	'net work of the simple cycle, MW'
W_STp(IEH,JEH)	'polytropic work of ST [MW]'
W_STg(IEH,JEH)	'gross work of ST [MW]'
W_PMP(IEH,JEH)	'actual work of the pump [MW]'
Eh_GT(IEH,JEH)	'net electricity produced per turbine per hour, MWh/h'
Eht_GT(IEH,JEH)	'Total net electricity produced per hour,MWh/h'
Eh_ST(IEH,JEH)	'hourly net electricity produced per ST [MWh/h]'
Eht_ST(IEH,JEH)	'total hourly net electricity of ST [MWh/h]'
Eh_PMP(IEH,JEH)	'electricity consumed per pump per hour [MWh/h]'
Eht_PMP(IEH,JEH)	'total electricity consumed per hour [MWh/h]'
Eh_PP(IEH,JEH)	'electricity from the power plant per GT [MWh/h]'
Eht_PP(IEH,JEH)	'total electricity from the power plant [MWh/h]'
A_COND(IEH,JEH)	'heat transfer area, condenser [m2]'
effh_SC(IEH,JEH)	'hourly eff. of the simple cycle, %'
effh_PP(IEH,JEH)	'hourly eff. of the whole power plant, %'
Airkgh_GT(IEH,JEH)	'hourly air required per turbine, kg/h'
Airkght_GT(IEH,JEH)	'total hourly air required, kg/h'
NGkgh_GT(IEH,JEH)	'Hourly NG consumed per turbine, kg/h'
NGkght_GT(IEH,JEH)	'Total hourly NG consumed, kg/h'
CNGht_GT(IEH,JEH)	'Total hourly cost of fuel consumed, \$CAD/h'
OMcht_GT(IEH,JEH)	'total O&M costs per hour, \$CAD/h'
ICEQPht_GT(IEH,JEH)	'total hourly installed capital costs, \$CAD/h'
Cht_PP(IEH,JEH)	'total hourly costs of the PP [\$CAD/h]'
CkWhh_GT(IEH,JEH)	'**hourly cost of kWh, ¢CAD/kWh'
T1(IEH,JEH)	'compressor inlet temp, oC'
T2(IEH,JEH)	'compressor outlet temp, oC'
T3a(IEH,JEH)	'air temp.@ combustor inlet, oC'
Taf(IEH,JEH)	'avg temp of air-fuel@ combustor inlet, oC'
T3b(IEH,JEH)	'by-pass cooling air temp, oC'
T4(IEH,JEH)	'combustion chamber outlet temp, oC'
T6(IEH,JEH)	'GT outlet temp, oC'
T7(IEH,JEH)	'HRSG outlet temp.[oC]'
T8(IEH,JEH)	'ST inlet/HRSG superheated steam outlet temp.[oC]'
T9(IEH,JEH)	'ST outlet/cond. inlet temp.[oC]'
T10(IEH,JEH)	'cond. outlet/pump inlet temp.[oC]'
T11(IEH,JEH)	'pump outlet temp.[oC]'
T12(IEH,JEH)	'backup water temp.[oC]'
T13(IEH,JEH)	'HRSG inlet water temp.[oC]'
Tcw1(IEH,JEH)	'temp. of cw to condenser inlet[oC]'
Tcw2(IEH,JEH)	'temp. of cw from condenser outlet[oC]'
P1(IEH,JEH)	'compressor inlet pressure, Pa'
P2(IEH,JEH)	'compressor outlet pressure, Pa'
P3a(IEH,JEH)	'combustion chamber inlet pressure, Pa'
P3b(IEH,JEH)	'by-pass cooling air pressure, Pa'
P4(IEH,JEH)	'combustion chamber outlet pressure, Pa'
P5(IEH,JEH)	'GT inlet pressure, Pa'
P6(IEH,JEH)	'GT outlet pressure, Pa'
P7(IEH,JEH)	'HRSG outlet pres.[Pa]'

P8(IEH,JEH)	'ST inlet/HRS superheated steam outlet pres.[Pa]'
P9(IEH,JEH)	'ST outlet/cond. inlet pres.[Pa]'
P10(IEH,JEH)	'cond. outlet/pump inlet pres.[Pa]'
P11(IEH,JEH)	'pump outlet pres.[Pa]'
P12(IEH,JEH)	'backup water pres.[Pa]'
P13(IEH,JEH)	'HRS inlet water pres.[Pa]'
del_P01(IEH,JEH)	'pressure loss at compressor entrance, Pa'
del_P3a4(IEH,JEH)	'pressure loss at combustion chamber, Pa'
H_T4(IEH,JEH)	'enthalpy of @ T4, kJ/s'
H_Taf(IEH,JEH)	'enthalpy of @ Taf, kJ/s'
H_CH4Tf(IEH,JEH)	'enthalpy of CH4@combustor input,kJ/s'
H_T67(IEH,JEH)	'enthalpy of gases@ T6-T7 [kJ/s]'
H_T813(IEH,JEH)	'enthalpy of steam@ T8-T13 [kJ/kmol]'
H_T109(IEH,JEH)	'enthalpy of steam@ T10-T9 [kJ/kmol]'
LMTD67(IEH,JEH)	'LMTD T6-T7 [oC]'
LMTD910(IEH,JEH)	'LMTD T9-T10 [oC]'
Q_T67(IEH,JEH)	'heat flow T6-T7 [kJ/s]'
Q_T910(IEH,JEH)	'heat flow T9-T10 [kJ/s]'
nCH4_f(IEH,JEH)	'Total CH4 moles@combustor entrance, kmol/s'
nO2_1(IEH,JEH)	'no. of O2 moles@point 1, kmol/s'
nN2_1(IEH,JEH)	'no. of N2 moles@point 1, kmol/s'
nO2_2(IEH,JEH)	'no. of O2 moles@point 2, kmol/s'
nN2_2(IEH,JEH)	'no. of N2 moles@point 2, kmol/s'
nO2_3a(IEH,JEH)	'no. of O2 moles@point 3a, kmol/s'
nN2_3a(IEH,JEH)	'no. of N2 moles@point 3a, kmol/s'
nO2_3b(IEH,JEH)	'no. of O2 moles@point 3b, kmol/s'
nN2_3b(IEH,JEH)	'no. of N2 moles@point 3b, kmol/s'
nO2_af(IEH,JEH)	'no. of O2 moles right before the combustor, kmol/s'
nN2_af(IEH,JEH)	'no. of N2 moles right before the combustor, kmol/s'
nCH4_af(IEH,JEH)	'no. of CH4 moles right before the combustor, kmol/s'
nO2_4(IEH,JEH)	'no. of O2 moles@point 4, kmol/s'
nN2_4(IEH,JEH)	'no. of N2 moles@point 4, kmol/s'
nCO2_4(IEH,JEH)	'no. of CO2 moles@point 4, kmol/s'
nH2O_4(IEH,JEH)	'no. of H2O moles@point 4, kmol/s'
nCH4_4(IEH,JEH)	'no. of unburned CH4 moles@point 4, kmol/s'
nO2_5(IEH,JEH)	'no. of O2 moles@point 5, kmol/s'
nN2_5(IEH,JEH)	'no. of N2 moles@point 5, kmol/s'
nCH4_5(IEH,JEH)	'no. of CH4 moles@point 5, kmol/s'
nCO2_5(IEH,JEH)	'no. of CO2 moles@point 5, kmol/s'
nH2O_5(IEH,JEH)	'no. of H2O moles@point 5, kmol/s'
nO2_6(IEH,JEH)	'no. of O2 moles@point 6, kmol/s'
nN2_6(IEH,JEH)	'no. of N2 moles@point 6, kmol/s'
nCH4_6(IEH,JEH)	'no. of CH4 moles@point 6, kmol/s'
nCO2_6(IEH,JEH)	'no. of CO2 moles@point 6, kmol/s'
nH2O_6(IEH,JEH)	'no. of H2O moles@point 6, kmol/s'
Nmol_t4(IEH,JEH)	'Total # of moles@point 4, kmol/s'
Nmol_t5(IEH,JEH)	'Total # of moles@point 5, kmol/s'
Nmol_t6(IEH,JEH)	'Total # of moles@point 6, kmol/s'
Nmol_8(IEH,JEH)	'molar flow of steam-water [kmol/s]'
mass_8(IEH,JEH)	'mass flow of steam-water [kg/s]'
EmN2ht_GT(IEH,JEH)	'hourly N2 in exhaust, kg/h'
EmO2ht_GT(IEH,JEH)	'hourly O2 in exhaust, kg/h'

```

EmH2Oht_GT( IEH,JEH)      'hourly H2O in exhaust, kg/h'
EmCO2ht_GT( IEH,JEH)      'hourly CO2 emissions, kg/h'
EmCOht_GT( IEH,JEH)       'hourly CO emissions, kg/h'
EmNOxht_GT( IEH,JEH)      'hourly NOx emissions, kg/h'
EmCH4ht_GT( IEH,JEH)      'hourly CH4 emissions, kg/h'
EmUHChT_GT( IEH,JEH)      'hourly UHC emissions, kg/h'
EmPMht_GT( IEH,JEH)       'hourly PM emissions, kg/h'
ER( IEH,JEH)              'operation check factor [0,1]';
*=====

*IMPORTING HOURLY DATA FROM NGTData SHEET
$LIBINCLUDE XLIMPORT T0_GT      D:\EHInput.XLSX EHData!P4:Q8764 COL
$LIBINCLUDE XLIMPORT P0_GT      D:\EHInput.XLSX EHData!R4:S8764 COL
$LIBINCLUDE XLIMPORT Edemand_GT D:\EHInput.XLSX EHData!V4:W8764 COL
$LIBINCLUDE XLIMPORT CNGh       D:\EHInput.XLSX EHData!X4:Y8764 COL
*=====

PARAMETERS Nfr_GT(IEH,JEH), Ni_GT(IEH,JEH), TURNDOWN(IEH,JEH);

Edemand_GT(IEH,JEH)      $ (Edemand_GT(IEH,JEH) LT 10) = 0;
ER(IEH,JEH)              = 1$(Edemand_GT(IEH,JEH) GE 10)+0;

Nfr_GT(IEH,JEH)          = Edemand_GT(IEH,JEH)/Np_PP;
Ni_GT(IEH,JEH)           = CEIL(Nfr_GT(IEH,JEH));

TURNDOWN(IEH,JEH)        $ Ni_GT(IEH,JEH) = (Ni_GT(IEH,JEH) - 1 +
FRAC(Nfr_GT(IEH,JEH)))/Ni_GT(IEH,JEH)*100;

TURNDOWN(IEH,JEH)        $ (Ni_GT(IEH,JEH) EQ 0)          = 0;

TURNDOWN(IEH,JEH)        $ (FRAC(Nfr_GT(IEH,JEH)) EQ 0)   = 100;

TURNDOWN(IEH,JEH)        $ (Ni_GT(IEH,JEH) EQ 0)          = 0;

TURNDOWN(IEH,JEH)        $ ((TURNDOWN(IEH,JEH) GT 1) AND (TURNDOWN(IEH,JEH) LT
40)) = 40;

N_GT                      = SMAX((IEH,JEH),Ni_GT(IEH,JEH));
*=====

*ENTER TOTAL WORK [MW]
W_EXN(IEH,JEH) = 600*TURNDOWN(IEH,JEH)/100;

*[oC]
T5(IEH,JEH) = 2151.591;
Tf(IEH,JEH) = 25;

*CHECK COULSON & RICHARDSON. VOL-6. p.85
m2          = (k2-1)/k2*Zet_t;
n2          = 1/(1-m2);

*POLYTROPIC, IDEAL WORK PRODUCED BY THE EXPANDER [MW].
W_EXp(IEH,JEH) = W_EXN(IEH,JEH)/Zet_t;

*[kmol/s]

```

```

*W_EXP = Nmol_t5*8.314*(T5+273)*n2/(n2-1)*((P5/P6)**((n2-1)/n2)-1);
Nmol_t5(IEH,JEH) = W_EXP(IEH,JEH)*1000*(n2-1)/(8.314*(T5(IEH,JEH)
+273)*n2*(rc**((n2-1)/n2)-1));

T6(IEH,JEH) = (T5(IEH,JEH)+273)*(1/rc)**m2-273;
Nmol_t6(IEH,JEH) = Nmol_t5(IEH,JEH);

T4(IEH,JEH) = T5(IEH,JEH);
Nmol_t4(IEH,JEH) = Nmol_t5(IEH,JEH);

*SPECIAL CASE: CH4 + 2O2 + 7.52N2--> CO2 + 2H2O + 7.52N2 (stoichiometric air).
nCO2_4(IEH,JEH) $ Nmol_t4(IEH,JEH) = 1 / (1+2+7.52) *Nmol_t4(IEH,JEH) ;
nCO2_4(IEH,JEH) $ (Nmol_t4(IEH,JEH) EQ 0) = 0;

nH2O_4(IEH,JEH) $ Nmol_t4(IEH,JEH) = 2 / (1+2+7.52) *Nmol_t4(IEH,JEH) ;
nH2O_4(IEH,JEH) $ (Nmol_t4(IEH,JEH) EQ 0) = 0;

nN2_4(IEH,JEH) $ Nmol_t4(IEH,JEH) = 7.52 / (1+2+7.52) *Nmol_t4(IEH,JEH) ;
nN2_4(IEH,JEH) $ (Nmol_t4(IEH,JEH) EQ 0) = 0;

nO2_4(IEH,JEH) $ Nmol_t4(IEH,JEH) = 0 / (1+2+7.52) *Nmol_t4(IEH,JEH) ;
nO2_4(IEH,JEH) $ (Nmol_t4(IEH,JEH) EQ 0) = 0;

nCH4_4(IEH,JEH) $ Nmol_t4(IEH,JEH) = 0 / (1+2+7.52) *Nmol_t4(IEH,JEH) ;
nCH4_4(IEH,JEH) $ (Nmol_t4(IEH,JEH) EQ 0) = 0;

*MOLE FLOW OF SIDE COOLING STREAM @ POINT 3b [kmol/s]
nN2_3b(IEH,JEH) = 0;
nO2_3b(IEH,JEH) = 0;

*MOLE FLOW @ POINT 5 [kmol/s]
nCO2_5(IEH,JEH) = nCO2_4(IEH,JEH);
nH2O_5(IEH,JEH) = nH2O_4(IEH,JEH);
nN2_5(IEH,JEH) = nN2_3b(IEH,JEH) + nN2_4(IEH,JEH);
nO2_5(IEH,JEH) = nO2_3b(IEH,JEH) + nO2_4(IEH,JEH);
nCH4_5(IEH,JEH) = nCH4_4(IEH,JEH);

nCO2_6(IEH,JEH) = nCO2_5(IEH,JEH);
nH2O_6(IEH,JEH) = nH2O_5(IEH,JEH);
nN2_6(IEH,JEH) = nN2_5(IEH,JEH);
nO2_6(IEH,JEH) = nO2_5(IEH,JEH);
nCH4_6(IEH,JEH) = nCH4_5(IEH,JEH);

*MOLE FLOW OF AIR-FUEL MIX [kmol/s]
nCH4_af(IEH,JEH) = nCO2_4(IEH,JEH);
nN2_af(IEH,JEH) = nN2_4(IEH,JEH);
nO2_af(IEH,JEH) = 2*nCH4_af(IEH,JEH);

*MOLE FLOW BEFORE ENTERING TO THE COMBUSTION CHAMBER [kmol/s]
nCH4_f(IEH,JEH) = nCH4_af(IEH,JEH);
nN2_3a(IEH,JEH) = nN2_af(IEH,JEH);
nO2_3a(IEH,JEH) = nO2_af(IEH,JEH);

```

*=====

*CALCULATING THE AVG TEMP.(Taf,oC)OF REACTANTS [CH4 + nO2_af*O2 + nN2_af*N2]
 *=====

*ENTHALPY OF GASES LEAVING THE COMBUSTION CHAMBER @ T4 [kJ/s = kW].
 H_T4(IEH,JEH) = (nCO2_4(IEH,JEH) *22.257 + nH2O_4(IEH,JEH) *32.2384 +
 nN2_4(IEH,JEH) *28.9015 + nO2_4(IEH,JEH) *25.4767)
 *((T4(IEH,JEH)+273)-298)+(nCO2_4(IEH,JEH) *5.981E-02 +
 nH2O_4(IEH,JEH) *1.923E-03 - nN2_4(IEH,JEH) *1.571E-03 +
 nO2_4(IEH,JEH)*1.52E-02)/2 *((T4(IEH,JEH)+273)**2-298**2) +(-
 nCO2_4(IEH,JEH) *3.501E-05 + nH2O_4(IEH,JEH) *1.055E-05 +
 nN2_4(IEH,JEH) *8.081E-06 - nO2_4(IEH,JEH) *7.155E-06) /3
 *((T4(IEH,JEH)+273)**3-298**3) +(nCO2_4(IEH,JEH) *7.469E-09
 - nH2O_4(IEH,JEH) *3.595E-09 - nN2_4(IEH,JEH) *2.873E-09 +
 nO2_4(IEH,JEH) *1.312E-09) /4 *((T4(IEH,JEH)+273)**4-298**4);

LOOP((IEH,JEH),
 *INITIAL GUESS(VALUE), C
 Taff('IT1') = 100;

LOOP(IT,
 fTaff(IT) = (nCH4_af(IEH,JEH) *19.8873 + nO2_af(IEH,JEH) *25.4767+
 nN2_af(IEH,JEH) *28.9015)*ABS(((Taff(IT)+273)-298)) + (nCH4_af(IEH,JEH)
 *5.0242E-02 + nO2_af(IEH,JEH) *1.5202E-02 - nN2_af(IEH,JEH) *1.571E-03)
 /2 *ABS((POWER((Taff(IT)+273),2)-298**2))+
 (nCH4_af(IEH,JEH) *1.2686E-05 - nO2_af(IEH,JEH) *7.155E-06 +
 nN2_af(IEH,JEH) *8.081E-06) /3 *ABS((POWER((Taff(IT)+273),3)-298**3))+
 (-nCH4_af(IEH,JEH)*1.101E-08 + nO2_af(IEH,JEH) *1.3117E-09 -
 nN2_af(IEH,JEH) *2.8726E-09)/4 *ABS((POWER((Taff(IT)+273),4)-298**4))+
 802279*nCH4_af(IEH,JEH) - H_T4(IEH,JEH) ;

fdTaff(IT) = (nCH4_af(IEH,JEH) *19.8873 + nO2_af(IEH,JEH) *25.4767 +
 nN2_af(IEH,JEH) *28.9015) + (nCH4_af(IEH,JEH) *5.0242E-02 +
 nO2_af(IEH,JEH) *1.5202E-02 - nN2_af(IEH,JEH) *1.571E-03)
 *(Taff(IT)+273) + (nCH4_af(IEH,JEH) *1.2686E-05 - nO2_af(IEH,JEH)
 *7.155E-06 + nN2_af(IEH,JEH) *8.081E-06) *POWER((Taff(IT)+273),2) + (-
 nCH4_af(IEH,JEH) *1.101E-08 + nO2_af(IEH,JEH) *1.3117E-09 -
 nN2_af(IEH,JEH) *2.8726E-09)*POWER((Taff(IT)+273),3) ;

Taff(IT+1) \$ fdTaff(IT) = Taff(IT)-fTaff(IT)/fdTaff(IT);

Taff(IT+1) \$ (fdTaff(IT) EQ 0) = 0;

);

Taf(IEH,JEH) = Taff('IT50');
);

*=====

* CALCULATION OF THE AIR TEMP. @ POINT 3

*ENTHALPY OF FUEL@ Tf(IEH,JEH), O2& N2 @(T3a) [kJ/s = kW].
 H_CH4Tf(IEH,JEH) = nCH4_f(IEH,JEH) *(19.8873*ABS(((Tf(IEH,JEH)+273)-298)) +
 5.0242E-02/2*ABS((POWER((Tf(IEH,JEH)+273),2)-298**2)) + 1.2686E-
 05/3*ABS((POWER((Tf(IEH,JEH)+273),3)-298**3))- 1.10113E-
 08/4*ABS((POWER((Tf(IEH,JEH)+273),4)-298**4)));

*ENTHALPY OF CH4, O2& N2 @(Taf) [kJ/s = kW].

```

H_Taf(IEH,JEH) = (nCH4_af(IEH,JEH) *19.8873 + nO2_af(IEH,JEH)
*25.4767 + nN2_af(IEH,JEH) *28.9015) *ABS(((Taf(IEH,JEH)+273)-298))
+ (nCH4_af(IEH,JEH) *5.0242E-02 + nO2_af(IEH,JEH) *1.5202E-02 -
nN2_af(IEH,JEH) *1.571E-03) /2 *ABS((POWER((Taf(IEH,JEH)+273),2)-298**2)) +
(nCH4_af(IEH,JEH) *1.2686E-05 - nO2_af(IEH,JEH) *7.155E-06 +
nN2_af(IEH,JEH) *8.081E-06) /3 *ABS((POWER((Taf(IEH,JEH)+273),3)-298**3)) +
(-nCH4_af(IEH,JEH) *1.10113E-08 + nO2_af(IEH,JEH) *1.3117E-09 -
nN2_af(IEH,JEH) *2.8726E-09)/4 *ABS((POWER((Taf(IEH,JEH)+273),4)-298**4)) ;

```

```

LOOP( ( IEH,JEH) ,
*INITIAL GUESS, oC
*T3aa('IT1') = Taf;
T3aa('IT1') = 100;

```

```

LOOP(IT,
fT3aa(IT) = (nO2_3a(IEH,JEH) *25.4767 + nN2_3a(IEH,JEH) *28.9015)
*((T3aa(IT)+273)-298) + (nO2_3a(IEH,JEH) *1.5202E-02 - nN2_3a(IEH,JEH)
*1.571E-03)/2 *(POWER((T3aa(IT)+273),2)-298**2) + (-nO2_3a(IEH,JEH)
*7.155E-06 + nN2_3a(IEH,JEH) *8.081E-06)/3 *(POWER((T3aa(IT) +273),3)-
298**3) + (nO2_3a(IEH,JEH) *1.3117E-09 - nN2_3a(IEH,JEH) *2.8726E-09)/4
*(POWER((T3aa(IT)+273),4)-298**4) + H_CH4Tf(IEH,JEH)- H_Taf(IEH,JEH) ;

```

```

fdT3aa(IT) = (nO2_3a(IEH,JEH) *25.4767 + nN2_3a(IEH,JEH) *28.9015)
+ (nO2_3a(IEH,JEH) *1.5202E-02 - nN2_3a(IEH,JEH) *1.571E-03)
*(T3aa(IT)+273)+(-nO2_3a(IEH,JEH)*7.155E-06 + nN2_3a(IEH,JEH) *8.081E-
06) *POWER((T3aa(IT)+273),2) +(nO2_3a(IEH,JEH) *1.3117E-09 -
nN2_3a(IEH,JEH) *2.8726E-09) *POWER((T3aa(IT)+273),3) ;

```

```

T3aa(IT+1) $ fdT3aa(IT) = T3aa(IT) - fT3aa(IT)/fdT3aa(IT);

```

```

T3aa(IT+1) $ (fdT3aa(IT) EQ 0) = 0;

```

```

);

```

```

T3a(IEH,JEH) = T3aa('IT50');

```

```

);

```

```

*=====

```

```

*[oC]
T2(IEH,JEH) = T3a(IEH,JEH);
T3b(IEH,JEH) = T2(IEH,JEH);
T1(IEH,JEH) = T0_GT(IEH,JEH);

```

```

*CHECK COULSON & RICHARDSON. VOL-6. p.85. PLANT DESIGN & ECOMOMICS, 5TH ED,
p.528

```

```

m1 = (k1-1)/(k1*Zet_c);
n1 = 1/(1-m1);

```

```

*[N/m2]
del_P01(IEH,JEH) = 0.02*P0_GT(IEH,JEH);
P1(IEH,JEH) = P0_GT(IEH,JEH) - del_P01(IEH,JEH);
P2(IEH,JEH) = P1(IEH,JEH)*((T2(IEH,JEH)+273)/(T1(IEH,JEH)+273))**(1/m1);

```

```

*[kmol/s]

```



```
nN2_2(IEH,JEH) = nN2_3a(IEH,JEH);
nO2_2(IEH,JEH) = nO2_3a(IEH,JEH);
```

```
*=====
*          CALCULATION OF THE ACTUAL WORK REQUIRED BY COMPRESSOR (W_AC)
*=====
```

```
*[kmol/s]
nN2_1(IEH,JEH) = nN2_2(IEH,JEH);
nO2_1(IEH,JEH) = nO2_2(IEH,JEH);
```

```
*[kg/h]
Airkgh_GT(IEH,JEH) = nN2_1(IEH,JEH)/0.79*MW_Air*3600;
Airkght_GT(IEH,JEH) = Ni_GT(IEH,JEH)*nN2_1(IEH,JEH)/0.79*MW_Air*3600;
```

```
*POLYTROPIC(IDEAL) WORK REQUIRED BY AIR COMPRESSOR [MW].
W_ACp(IEH,JEH) = (nO2_1(IEH,JEH) + nN2_1(IEH,JEH))*8.314* (T1(IEH,JEH)+273)
                *n1/(n1-1)*((P2(IEH,JEH)/P1(IEH,JEH))**((n1-1)/n1)-1)/1000;
```

```
*ACTUAL WORK REQUIRED BY AIR COMPRESSOR [MW].
W_AC(IEH,JEH) = W_ACp(IEH,JEH)/Zet_c*13;
```

```
*[N/m2]
P3a(IEH,JEH) = P2(IEH,JEH);
P3b(IEH,JEH) = P2(IEH,JEH);
del_P3a4(IEH,JEH) = 0.03*P3a(IEH,JEH);
P4(IEH,JEH) = P3a(IEH,JEH) - del_P3a4(IEH,JEH);

P5(IEH,JEH) = P4(IEH,JEH);
P6(IEH,JEH) = P5(IEH,JEH)/rc;
```

```
*=====
*          STEAM CYCLE CALCULATIONS
*=====
```

```
m3 = (k3-1)/k3*Zet_ST;
n3 = 1/(1-m3);
```

```
*[oC]
T7(IEH,JEH) = 105;
T8(IEH,JEH) = T6(IEH,JEH)-10;
```

```
*LAZZARETTO et al. 2004
T9(IEH,JEH) = 120;
T10(IEH,JEH) = 100;
T11(IEH,JEH) = T10(IEH,JEH);
T13(IEH,JEH) = T11(IEH,JEH);
Tcw1(IEH,JEH) = 15.5;
Tcw2(IEH,JEH) = 90;
```

```
*[N/m2]
P11(IEH,JEH) = 15000000;
P13(IEH,JEH) = P11(IEH,JEH);
P8(IEH,JEH) = P13(IEH,JEH);
```

```
*T9/T8=(P9/P8)^m3
```

P9(IEH,JEH) = P8(IEH,JEH)*((T9(IEH,JEH)+273)/(T8(IEH,JEH)+273))**(1/m3);
P10(IEH,JEH) = P9(IEH,JEH);

*HRSG

*[kW]

H_T67(IEH,JEH) = (nCO2_6(IEH,JEH) *22.257+ nH2O_6(IEH,JEH) *32.2384 +
nN2_6(IEH,JEH) *28.9015 + nO2_6(IEH,JEH) *25.4767)*((T6(IEH,JEH)+273) -
(T7(IEH,JEH)+273)) + (nCO2_6(IEH,JEH) *5.981E-02 + nH2O_6(IEH,JEH)
*1.923E-03 - nN2_6(IEH,JEH) *1.571E-03 + nO2_6(IEH,JEH) *1.52E-02) /2
*((T6(IEH,JEH)+273)**2 - (T7(IEH,JEH)+273)**2) + (-nCO2_6(IEH,JEH)*3.501E-
05 + nH2O_6(IEH,JEH) *1.055E-05 + nN2_6(IEH,JEH) *8.081E-06 -
nO2_6(IEH,JEH) *7.155E-06) /3 *((T6(IEH,JEH)+273)**3 - (T7(IEH,JEH)
+273)**3) +(nCO2_6(IEH,JEH) *7.469E-09 - nH2O_6(IEH,JEH) *3.595E-09 -
nN2_6(IEH,JEH) *2.873E-09 + nO2_6(IEH,JEH) *1.312E-09) /4
*((T6(IEH,JEH)+273)**4 - (T7(IEH,JEH)+273)**4) ;

*[kW]

Q_T67(IEH,JEH) = H_T67(IEH,JEH);
Qm_T67 = SMAX((IEH,JEH),Q_T67(IEH,JEH));
LMTD67(IEH,JEH) = ((T6(IEH,JEH)-T8(IEH,JEH)) - (T7(IEH,JEH)-T13(IEH,JEH))
)/LOG((T6(IEH,JEH)-T8(IEH,JEH)) / (T7(IEH,JEH)-T13(IEH,JEH))) ;

LMTDm67 = SMAX((IEH,JEH),LMTD67(IEH,JEH));

*ENTHALPY CHANGE [kJ/kmol] ||STEAM FLOW [kmol/s],[kg/s]

H_T813(IEH,JEH) = 32.2384*(T8(IEH,JEH)- T13(IEH,JEH)) +1.92E-03/2
*((T8(IEH,JEH)+273)**2 - (T13(IEH,JEH)+273)**2) + 1.06E-05/3
*((T8(IEH,JEH)+273)**3 - (T13(IEH,JEH)+273)**3) - 3.60E-09/4
*((T8(IEH,JEH)+273)**4 - (T13(IEH,JEH)+273)**4);

Nmol_8(IEH,JEH) = Q_T67(IEH,JEH)/(HvH2O + H_T813(IEH,JEH));
mass_8(IEH,JEH) = MW_H2O*Nmol_8(IEH,JEH);

*STEAM TURBINE

*IDEAL GROSS WORK OF ST [MW] || ACTUAL GROSS WORK [MW]

W_STp(IEH,JEH) = Nmol_8(IEH,JEH)*8.314*(T8(IEH,JEH)+273)*n3/(n3-1)
*((P8(IEH,JEH)/P9(IEH,JEH))**((n3-1)/n3)-1)/1000;
W_STg(IEH,JEH) = Zet_gen*Zet_ST*W_STp(IEH,JEH)*0.75;

*CONDENSER

* ENTHALPY [kJ/kmol] ||TOTAL HEAT [kW] ||AREA [m2] ||MAX AREA [m2]

H_T109(IEH,JEH) = 32.2384*(T10(IEH,JEH) - T9(IEH,JEH)) + 1.92E-03/2
*((T10(IEH,JEH)+273)**2 - (T9(IEH,JEH)+273)**2) +1.06E-05/3 *
((T10(IEH,JEH)+273)**3 - (T9(IEH,JEH)+273)**3) - 3.60E-09/4
*((T10(IEH,JEH)+273)**4 - (T9(IEH,JEH)+273)**4);

Q_T910(IEH,JEH) = Nmol_8(IEH,JEH)*(H_T109(IEH,JEH) + HvH2O);

LMTD910(IEH,JEH) = ((T9(IEH,JEH)-Tcw2(IEH,JEH)) - (T10(IEH,JEH)-
Tcw1(IEH,JEH))) / LOG((T9(IEH,JEH)-Tcw2(IEH,JEH)) / (T10(IEH,JEH)-
Tcw1(IEH,JEH)));

A_COND(IEH,JEH) = Q_T910(IEH,JEH)/(U_COND*LMTD910(IEH,JEH));
Am_COND = SMAX((IEH,JEH),A_COND(IEH,JEH));

*PUMP

```

*ACTUAL WORK REQUIRED [MW] ||(Eh_PMP)HOURLY ELECTRICITY CONSUMED BY PUMP
[MWh/h] ||(Eht_PMP)HOURLY TOTAL ELECTRCITY [MWh/h]
W_PMP(IEH,JEH) = Nm01_8(IEH,JEH)*MW_H2O*(P11(IEH,JEH)-P10(IEH,JEH))/den_H2O
                /1000/Z_PMP/1000*10;
Eh_PMP(IEH,JEH) = W_PMP(IEH,JEH);
Eht_PMP(IEH,JEH) = Ni_GT(IEH,JEH)*Eh_PMP(IEH,JEH);

*PUMP NOMINAL POWER [MW]
Np_PMP          = SMAX((IEH,JEH),W_PMP(IEH,JEH));

*(Eh_ST)HOURLY NET ELECTRICITY PRODUCED BY ST[MWh/h] ||(Eht_ST)HOURLY TOTAL
NET ELECTRCITY [MWh/h]
Eh_ST(IEH,JEH)  = W_STg(IEH,JEH) - W_PMP(IEH,JEH);
Eht_ST(IEH,JEH) = Ni_GT(IEH,JEH)*Eh_ST(IEH,JEH);
Np_ST           = SMAX((IEH,JEH),W_STg(IEH,JEH));

*=====

*NET ACTUAL WORK OF THE SIMPLE CYCLE [MW]
W_SC(IEH,JEH)   = (W_EXN(IEH,JEH) - W_AC(IEH,JEH))*Zet_gen;
Np_GT           = SMAX((IEH,JEH),W_SC(IEH,JEH));

*(Eh_GT)HOURLY ELECTRICITY PRODUCED [MWh/h] || (Eht_GT)HOURLY TOTAL
ELECTRCITY [MWh/h]
Eh_GT(IEH,JEH)   = W_SC(IEH,JEH);
Eht_GT(IEH,JEH)  = Eh_GT(IEH,JEH)*Ni_GT(IEH,JEH);

*(Eh_PP)HOURLY ELECTRICITY PRODUCED [MWh/h] || (Eht_PP)HOURLY TOTAL
ELECTRCITY [MWh/h]
Eh_PP(IEH,JEH)   = Eh_GT(IEH,JEH) + Eh_ST(IEH,JEH);
Eht_PP(IEH,JEH)  = Eh_PP(IEH,JEH)*Ni_GT(IEH,JEH);

*HOURLY EFFICIENCY OF THE SIMPLE CYCLE BASED ON LHV [%]|| EFFICEINCY OF GT+ST
effh_SC(IEH,JEH) $ nCH4_f(IEH,JEH) = Eh_GT(IEH,JEH)/(LHV_CH4/1000
                *nCH4_f(IEH,JEH))*100;
effh_SC(IEH,JEH) $ (nCH4_f(IEH,JEH) EQ 0) = 0;

effh_PP(IEH,JEH) $ nCH4_f(IEH,JEH = Eh_PP(IEH,JEH)/(LHV_CH4/1000*
                nCH4_f(IEH,JEH))*100;
effh_PP(IEH,JEH) $ (nCH4_f(IEH,JEH) EQ 0) = 0;

*(NGkgh_GT)HOURLY FUEL CONSUMED PER TURBINE [kg/h] || (NGkght_GT) TOTAL
HOURLY FUEL CONSUMED
NGkgh_GT(IEH,JEH) = MW_CH4*nCH4_f(IEH,JEH)*3600;
NGkght_GT(IEH,JEH) = NGkgh_GT(IEH,JEH)*Ni_GT(IEH,JEH);

*TOTAL NG CONSUMED PER YEAR(kg/y)||TOTAL AIR CONSUMED PER YEAR(kg/y)
NGkgyt_GT          = SUM ((IEH,JEH), NGkght_GT(IEH,JEH));
Airkgyt_GT         = SUM ((IEH,JEH), Airkght_GT(IEH,JEH));

*INITIAL INSTALLED CAPITAL COSTS [$CAD]
*UNITS USED: Np[MW], Qm[kW], A[m2]. MUST CONVERTED TO: Np[kW], Q[kW], A[m2].
ICoGT_GT           = EX_rate*3832*((Np_GT*1000)**0.71);
ICogenaA_GT        = EX_rate*3082*((Np_GT*1000)**0.58);

*CHECK Mansouri et. al, 58(2012), 540.6 USD/kW

```

ICoST_GT = EX_rate*540.6*1000*Np_ST;
 ICogenB_GT = EX_rate*3082*((Np_ST*1000)**0.58) ;
 ICoHRSG_GT = EX_rate*17000*(Qm_T67*1/LMTDm67)**0.6 ;
 ICoCon_GT = EX_rate*162*(Am_COND**1.01) ;
 ICoPMP_GT = EX_rate*1293.44*(Np_PMP*1000)**0.8*(1+(0.3/(1-Z_PMP))**(-0.46));

ICoEQP_GT = (ICoGT_GT + ICogenA_GT + ICoST_GT + ICogenB_GT + ICoHRSG_GT + ICoCon_GT + ICoPMP_GT);

**NOTE O&M COSTS ARE NOT FUNCTION IN PRODUCTION HERE.*

**TOTAL HOURLY INSTALLED CAPITAL COSTS [\$CAD/h]|| TOTAL HOURLY O&M COSTS \$CAD/h|| HOURLY FUEL COST [\$CAD/h]*

ICEQPht_GT(IEH,JEH) = ICoEQP_GT*B_GT*N_GT*0.05*1.05**LS_GT/(1.05**LS_GT-1)/8760;

**CONSULT Mansouri et al. 58(2012), O&M fixed=20, O&M variable=0.002*

OMChT_GT(IEH,JEH) = EX_rate*(20/8760*1000*Np_PP*N_GT + 0.002*1000*Eht_PP(IEH,JEH));

CNGht_GT(IEH,JEH) = NGkght_GT(IEH,JEH)*cNGh(IEH,JEH);
 Cht_PP(IEH,JEH) = (ICEQPht_GT(IEH,JEH) + OMChT_GT(IEH,JEH) + CNGht_GT(IEH,JEH));

**HOURLY ENERGY COST [¢CAD/kWh]*

CkWhh_GT(IEH,JEH) = (Cht_PP(IEH,JEH)/Eht_PP(IEH,JEH)/1000*100) \$(Eht_PP(IEH,JEH) GT 0) + 0;

**AVG ENERGY COST [¢CAD/kWh]*

CkWh_GT = SUM((IEH,JEH), CkWhh_GT(IEH,JEH))/ SUM((IEH,JEH),ER(IEH,JEH));

**TOTAL HOURLY GASES EMISSIONS [kg/h]*

EmN2ht_GT(IEH,JEH) = (MW_N2 *nN2_5(IEH,JEH) *3600)*Ni_GT(IEH,JEH) ;
 EmO2ht_GT(IEH,JEH) = (MW_O2 *nO2_5(IEH,JEH) *3600)*Ni_GT(IEH,JEH) ;
 EmH2Oht_GT(IEH,JEH) = (MW_H2O *nH2O_5(IEH,JEH)*3600)*Ni_GT(IEH,JEH) ;
 EmCO2ht_GT(IEH,JEH) = (MW_CO2 *nCO2_5(IEH,JEH)*3600)*Ni_GT(IEH,JEH) ;

**CONSULT (RIZK & MONGIA, 1993)*

**[tao=0.002 s], [tao_ev=0 s]*

EmCOht_GT(IEH,JEH) \$ P3a(IEH,JEH) = (0.179E9*EXP(7800/(T4(IEH,JEH)+273)))/(P3a(IEH,JEH)**2*0.002*(0.03)**0.5)/1000*NGkght_GT(IEH,JEH);

EmCOht_GT(IEH,JEH) \$ (P3a(IEH,JEH) EQ 0) = 0;

EmNOxht_GT(IEH,JEH)\$ P3a(IEH,JEH) = (0.15E16*0.002**0.5*EXP(-71100/(T4(IEH,JEH)+273)))/(P3a(IEH,JEH)**0.05*0.03**0.5)/1000*NGkght_GT(IEH,JEH);

EmNOxht_GT(IEH,JEH) \$ (P3a(IEH,JEH) EQ 0) = 0;

EmCH4ht_GT(IEH,JEH) = (MW_CH4*nCH4_5(IEH,JEH)*3600)*Ni_GT(IEH,JEH);

EmUHChT_GT(IEH,JEH) \$ P3a(IEH,JEH) = (0.755E11*EXP(9756/(T4(IEH,JEH)+273)))/(P3a(IEH,JEH)**2.3*0.002**0.1*0.03**0.6)/1000*NGkght_GT(IEH,JEH);

EmUHChT_GT(IEH,JEH) \$ (P3a(IEH,JEH) EQ 0) = 0;

EmPMht_GT(IEH,JEH) = 0;

*DISPLAY ZERO VALUES

W_EXN(IEH,JEH)	\$ (Not W_EXN(IEH,JEH))	= EPS ;
W_AC(IEH,JEH)	\$ (Not W_AC(IEH,JEH))	= EPS ;
W_SC(IEH,JEH)	\$ (Not W_SC(IEH,JEH))	= EPS ;
W_PMP(IEH,JEH)	\$ (Not W_PMP(IEH,JEH))	= EPS ;
W_STg(IEH,JEH)	\$ (Not W_STg(IEH,JEH))	= EPS ;
Eh_GT(IEH,JEH)	\$ (Not Eh_GT(IEH,JEH))	= EPS ;
Eh_PMP(IEH,JEH)	\$ (Not Eh_PMP(IEH,JEH))	= EPS ;
Eh_ST(IEH,JEH)	\$ (Not Eh_ST(IEH,JEH))	= EPS ;
Eh_PP(IEH,JEH)	\$ (Not Eh_PP(IEH,JEH))	= EPS ;
Eht_GT(IEH,JEH)	\$ (Not Eht_GT(IEH,JEH))	= EPS ;
Eht_PMP(IEH,JEH)	\$ (Not Eht_PMP(IEH,JEH))	= EPS ;
Eht_ST(IEH,JEH)	\$ (Not Eht_ST(IEH,JEH))	= EPS ;
Eht_PP(IEH,JEH)	\$ (Not Eht_PP(IEH,JEH))	= EPS ;
effh_SC(IEH,JEH)	\$ (Not effh_SC(IEH,JEH))	= EPS ;
effh_PP(IEH,JEH)	\$ (Not effh_PP(IEH,JEH))	= EPS ;
Airkgh_GT(IEH,JEH)	\$ (Not Airkgh_GT(IEH,JEH))	= EPS ;
mass_8(IEH,JEH)	\$ (Not mass_8(IEH,JEH))	= EPS ;
NGkght_GT(IEH,JEH)	\$ (Not NGkght_GT(IEH,JEH))	= EPS ;
CNGht_GT(IEH,JEH)	\$ (Not CNGht_GT(IEH,JEH))	= EPS ;
ICEQPht_GT(IEH,JEH)	\$ (Not ICEQPht_GT(IEH,JEH))	= EPS ;
OMCht_GT(IEH,JEH)	\$ (Not OMCht_GT(IEH,JEH))	= EPS ;
Cht_PP(IEH,JEH)	\$ (Not Cht_PP(IEH,JEH))	= EPS ;
CkWhh_GT(IEH,JEH)	\$ (Not CkWhh_GT(IEH,JEH))	= EPS ;
EmCO2ht_GT(IEH,JEH)	\$ (Not EmCO2ht_GT(IEH,JEH))	= EPS ;
EmCOht_GT(IEH,JEH)	\$ (Not EmCOht_GT(IEH,JEH))	= EPS ;
EmNOxht_GT(IEH,JEH)	\$ (Not EmNOxht_GT(IEH,JEH))	= EPS ;
EmUHChht_GT(IEH,JEH)	\$ (Not EmUHChht_GT(IEH,JEH))	= EPS ;
EmPMht_GT(IEH,JEH)	\$ (Not EmPMht_GT(IEH,JEH))	= EPS ;
Nfr_GT(IEH,JEH)	\$ (Not Nfr_GT(IEH,JEH))	= EPS ;
Ni_GT(IEH,JEH)	\$ (Not Ni_GT(IEH,JEH))	= EPS ;
TURNDOWN(IEH,JEH)	\$ (Not TURNDOWN(IEH,JEH))	= EPS ;

*=====

* *VARIABLES & EQUATIONS*

*=====

VARIABLES Eyt_GT,ICEQP_GT, OMCyt_GT, CNGyt_GT,Ct_GT, EmCO2yt_GT, EmCOyt_GT, EmNOxyt_GT, EmUHcyt_GT, CF_GT;

EQUATIONS eq100, eq101, eq102, eq103, eq104, eq105, eq106, eq107, eq108, eq109;

* *total net electricity produced per year, MWh/y*
 eq100.. Eyt_GT =E= SUM ((IEH,JEH), Eht_PP(IEH,JEH));

* *equipment cost per year [\$CAD/y]*
 eq101.. ICEQP_GT =E= ICoEQP_GT*B_GT*N_GT*0.05*1.05**LS_GT/
 (1.05**LS_GT-1);

```

* total O&M costs of the PP [$CAD/y]
eq102..  OMCyt_GT          =E= SUM ((IEH,JEH), OMChT_GT(IEH,JEH));

* total fuel cost of PP [$CAD/y]
eq103..  CNGyt_GT          =E= SUM ((IEH,JEH), CNGht_GT(IEH,JEH));

* total annual costs of PP [$CAD/y]
eq104..  Ct_GT             =E= ICEQP_GT + OMCyt_GT + CNGyt_GT ;

* Total CO2 emissions [kg/y]
eq105..  EmCO2yt_GT        =E= SUM ((IEH,JEH), EmCO2ht_GT(IEH,JEH));

* Total CO emissions [kg/y]
eq106..  EmCOyt_GT         =E= SUM ((IEH,JEH), EmCOht_GT(IEH,JEH));

* Total NOx emissions [kg/y]
eq107..  EmNOxyt_GT        =E= SUM ((IEH,JEH), EmNOxht_GT(IEH,JEH));

* Total UHCs emissions [kg/y]
eq108..  EmUHCyt_GT        =E= SUM ((IEH,JEH), EmUHChT_GT(IEH,JEH));

* capacity factor of NGT turbine [%]
eq109..  CF_GT             =E= Eyt_GT/(N_GT*Np_PP*8760)*100;

*=====

MODEL NGT    GAS TURBINE WITH NG FEED /eq100, eq101, eq102, eq103, eq104,
                                         eq105, eq106, eq107, eq108, eq109/;

SOLVE NGT USING MCP;

*EQUATIONS & VARIABLES LISTINGS WILL NOT APPEAR IN THE SOLUTION
OPTIONS LIMROW=0, LIMCOL=0;

*NO OF DECIMALS DISPLAYED, DEFAULT IS (4).
OPTIONS DECIMALS=4;

*CHECK IF THE MODEL NORMALLY COMPLETED WITH OPTIMAL SOLUTION [1 1] LINEAR, [1
2] NONLINEAR
DISPLAY NGT.MODELSTAT, NGT.SOLVESTAT;
*=====

```

\$ONTEXT

VERSION: V2.0
DATE: 26-OCT-2011
1.2 WIND TURBINES
1.2.1 ONSHORE WIND TURBINES
- MODEL (GE 1.5 SLE); NOMINAL POWER [1.5 MW]; MANUFACTURER [GE ENERGY CORP.]
- WIND SPEED RANGE [3.5-25m/s]; LIFESPAN [20 y].

\$OFFTEXT

*SCALARS FOR WIND

SCALARS

*ENTER THESE SCALARS

N_WTON	'No. of onshore WTs'	/20/
A_WTON	'swept area of GE1.5SLE Model, m2'	/4657/
Cp_WTON	'coef. of performance, onshore WT'	/0.35/
NP_WTON	'nominal power, onshore MW'	/1.5/
OMC_MWhON	'O&M costs onshore, \$USD/MWh produced'	/7/
LS_WTON	'life span of WTON, y'	/20/
Cins_WTON	'onshore wind cost per installed capacity, \$USD/MW'	/1700000/
eff_WTGN	'generator efficiency, onshore WT'	/0.90/
eff_WTME	'mechanical eff. of (gearbox & bearings)'	/0.95/
EX_rate	'\$CAD exchange rate, Sep-2011'	/1.03/
Air_den	'air density, kg/m3 @ 15.5 oC & 1atm'	/1.225/;

SCALARS

Pmax_WTON	'max. onshore wind power can be produced, MW'
Avail_WTON	'availability of onshore wind, %'
WH_WTON	'working hours of onshore wind turbines per year, h'
CkWh_WTON	'avg cost of energy produced per year, \$CAD/kWh';

SETS IEH /IEH1*IEH8760/, JEH /JEH1/;

PARAMETERS

WS_ON(IEH,JEH)	'hourly onshore wind speed, m/s'
WSNR(IEH,JEH)	'wind speed range check factor[0,1]'
Eh_WTON(IEH,JEH)	'electricity produced, MWh/h per turbine'
Eht_WTON(IEH,JEH)	'total electricity produced, MWh/h'
Ph_WTON(IEH,JEH)	'power produced, MW per turbine'
Pht_WTON(IEH,JEH)	'total power produced, MW'
OMCh_WTON(IEH,JEH)	'hourly O&M costs, \$CAD/h'
FCh_WTON(IEH,JEH)	'hourly FC costs, \$CAD/h'
CkWhh_WTON(IEH,JEH)	'hourly energy costs per kWh, \$CAD/kWh';

*IMPORTING HOURLY WIND SPEED [m/s]

\$LIBINCLUDE XLIMPORT WS_ON D:\EHInput.XLSX EHData!D4:E8764 COL

*WIND SPEED RANGE CHECK FACTOR [1] IN RANGE, [0] OUT OF RANGE

WSNR(IEH,JEH) = 1\$((WS_ON(IEH,JEH) GE 3.5) AND (WS_ON(IEH,JEH) LE 25));

*(Ph_WTON) POWER PRODUCED PER TURBINE [MW]

*CHECK: (WIZELIUS, 2007). "WIND POWER PROJECTS"

Ph_WTON(IEH,JEH) = WSNR(IEH,JEH)*(0.5*Air_den * A_WTON * Cp_WTON * eff_WTGN
* eff_WTME *(WS_ON(IEH,JEH))**3)/(1000*1000);

*PRODUCTION LIMIT PER TURBINE [1.5 MW] | (Pht_WTON) TOTAL POWER PRODUCED [MW]

Ph_WTON(IEH,JEH) \$ (Ph_WTON(IEH,JEH) GT NP_WTON) = NP_WTON;

Pht_WTON(IEH,JEH) = N_WTON*Ph_WTON(IEH,JEH);

```

*(Eh_WTON) ENERGY PRODUCED PER TURBINE [MWh/h] || (Eht_WTON) TOTAL ENERGY
PRODUCED [MWh/h]
Eh_WTON(IEH,JEH) = Ph_WTON(IEH,JEH);
Eht_WTON(IEH,JEH) = N_WTON*Eh_WTON(IEH,JEH);

*(WH_WTON)WORKING HOURS OF ONSHORE WIND TURBINES PER YEAR [h]
WH_WTON = SUM ((IEH,JEH), WSONR(IEH,JEH));

*HOURLY O&M COSTS [$CAD/h] || HOURLY FIXED COSTS [$CAD/h] || HOURLY ENERGY
COST [¢CAD/kWh]

OMCh_WTON(IEH,JEH) = OMC_MWhON*EX_rate*Eht_WTON(IEH,JEH);

FCh_WTON(IEH,JEH) = NP_WTON*N_WTON*Cins_WTON*EX_rate*0.05*1.05**LS_WTON
/(1.05**LS_WTON-1)/8760;

CkWhh_WTON(IEH,JEH) = (OMCh_WTON(IEH,JEH) + FCh_WTON(IEH,JEH))
/Eht_WTON(IEH,JEH) /1000*100;

*AVG ENERGY COST [¢CAD/kWh]
CkWh_WTON = SUM ((IEH,JEH), CkWhh_WTON(IEH,JEH))/8760;

*MAX FARM CAPACITY [MW] || AVAILABILITY OF ONSHORE WIND [%]
Pmax_WTON = N_WTON*NP_WTON;
Avail_WTON = WH_WTON/8760*100;

*FORCING GAMS TO DISPLAY ZERO VALUES
WSONR(IEH,JEH) $ (Not WSONR(IEH,JEH)) = EPS ;
Ph_WTON(IEH,JEH) $ (Not Ph_WTON(IEH,JEH)) = EPS ;
Pht_WTON(IEH,JEH) $ (Not Pht_WTON(IEH,JEH)) = EPS ;
Eh_WTON(IEH,JEH) $ (Not Eh_WTON(IEH,JEH)) = EPS ;
Eht_WTON(IEH,JEH) $ (Not Eht_WTON(IEH,JEH)) = EPS ;
OMCh_WTON(IEH,JEH) $ (Not OMCh_WTON(IEH,JEH)) = EPS ;
FCh_WTON(IEH,JEH) $ (Not FCh_WTON(IEH,JEH)) = EPS ;
CkWhh_WTON(IEH,JEH) $ (Not CkWhh_WTON(IEH,JEH)) = EPS ;

VARIABLES Ey_WTON, Eyt_WTON, CF_WTON, OMC_WTON, FC_WTON, Ct_WTON, FL_WTON;

EQUATIONS eq200, eq201, eq202, eq203, eq204, eq205, eq206;

*onshore electricity produced per year, MWh/y per turbine
eq200.. Ey_WTON =E= SUM ((IEH,JEH), Eh_WTON(IEH,JEH));

*total onshore electricity produced per year, MWh/y
eq201.. Eyt_WTON =E= SUM ((IEH,JEH), Eht_WTON(IEH,JEH));

*capacity factor WTON, %
eq202.. CF_WTON =E= Ey_WTON/(NP_WTON*8760)*100;

*O&M costs onshore, $CAD/y
eq203.. OMC_WTON =E= OMC_MWhON*EX_rate*Eyt_WTON;

*FC costs onshore, $CAD/y

```



```
eq204.. FC_WTON =E= NP_WTON*N_WTON*Cins_WTON*EX_rate *0.05*1.05**LS_WTON/  
(1.05**LS_WTON-1);
```

```
*total onshore power cost,$CAD/y
```

```
eq205.. Ct_WTON =E= OMC_WTON + FC_WTON;
```

```
*WTON full load hours per year, h/y
```

```
eq206.. FL_WTON =E= Ey_WTON/NP_WTON;
```

```
MODEL WTON ONSHORE WIND TURBINES /eq200, eq201, eq202, eq203, eq204, eq205,  
eq206/;
```

```
SOLVE WTON USING MCP;
```

```
*DISPLAY 4 DIGITS AFTER THE DECIMAL POINT
```

```
OPTION decimals=4;
```

```
*CHECK IF THE MODEL IS EXECUTED WITH OPTIMAL SOLUTION
```

```
*[1 1] LINEAR, [1 2] NON-LINEAR
```

```
DISPLAY WTON.MODELSTAT, WTON.SOLVESTAT;
```

```
*=====
```

```

$ONTEXT
VERSION: V2.0
DATE: 26-OCT-2011
1.2 WIND TURBINES
1.2.2 OFFSHORE WIND TURBINES
- MODEL (SWT 2.3-93); NOMINAL POWER [2.3 MW]; MANUFACTURER [SIEMENS AG
CORP.].
- WIND SPEED RANGE [4-25m/s]; LIFESPAN [20 y].
$OFFTEXT

*SCALARS FOR WIND
SCALARS
*ENTER THESE SCALARS
N_WTOF          'No. of offshore WTs'                /20/
A_WTOF          'swept area of SWT2.3-93 Model, m2'   /6800/
Cp_WTOF         'coef. of performance, offshore WT'   /0.35/
NP_WTOF         'nominal power, offshore MW'          /2.3/
OMC_MWhOF      'O&M costs offshore, $USD/MWh produced' /20/
LS_WTOF         'life span, WTOF, y'                 /20/
Cins_WTOF      'offshore wind cost per installed capacity, $USD/MW'
                                                    /2924000/
eff_WTGN        'generator efficiency, offshore WT'   /0.90/
eff_WTME        'mechanical eff. of (gearbox & bearings)' /0.95/
EX_rate         '$CAD exchange rate, Sep-2011'       /1.03/
Air_den         'air density, Kg/m3 @ 15.5 oC & 1atm' /1.225/;

SCALARS
Pmax_WTOF      'max. offshore wind power can be produced, MW'
Avail_WTOF     'availability of offshore wind, %'
WH_WTOF        'working hours of offshore wind turbines per year, h'
CkWh_WTOF      'avg cost of energy produced per year, ¢CAD/kWh';

SETS IEH /IEH1*IEH8760/, JEH /JEH1/;

PARAMETERS
WS_OF(IEH,JEH) 'hourly offshore wind speed, m/s'
WSOFR(IEH,JEH) 'wind speed reange check factor[0,1]'
Eh_WTOF(IEH,JEH) 'electricity produced, MWh/h per turbine'
Eht_WTOF(IEH,JEH) 'total electricity produced, MWh/h'
Ph_WTOF(IEH,JEH) 'power produced, MW per turbine'
Pht_WTOF(IEH,JEH) 'total power produced, MW'
OMCh_WTOF(IEH,JEH) 'hourly O&M costs, $CAD/h'
FCh_WTOF(IEH,JEH) 'hourly FC costs, $CAD/h'
CkWhh_WTOF(IEH,JEH) 'hourly energy costs per kWh, ¢CAD/kWh';

*IMPORTING HOURLY WIND SPEED DATA [m/s]
$LIBINCLUDE XLIMPORT WS_OF D:\EHInput.XLSX EHData!F4:G8764 COL

*WIND SPEED RANGE CHECK FACTOR [1] IN RANGE, [0] OUT OF RANGE
WSOFR(IEH,JEH)= 1$( (WS_OF(IEH,JEH) GE 4) AND (WS_OF(IEH,JEH) LE 25));

*(Ph_WTOF)POWER PRODUCED PER TURBINE [MW]
* CHECK: (WIZELIUS, 2007). "WIND POWER PROJECTS"
Ph_WTOF(IEH,JEH) = WSOFR(IEH,JEH)*(0.5*Air_den * A_WTOF * Cp_WTOF *
eff_WTGN * eff_WTME *(WS_OF(IEH,JEH))**3)/(1000*1000);

```

**PRODUCTION LIMIT PER TURBINE [2.3 MW] || (Pht_WTOF) TOTAL POWER PRODUCED [MW]*
 Ph_WTOF(IEH,JEH) \$ (Ph_WTOF(IEH,JEH) GT NP_WTOF) = NP_WTOF;
 Pht_WTOF(IEH,JEH) = N_WTOF*Ph_WTOF(IEH,JEH);

**(Eh_WTOF) ENERGY PRODUCED PER TURBINE [MWh/h] || (Eht_WTOF) TOTAL ENERGY PRODUCED [MWh/h]*
 Eh_WTOF(IEH,JEH) = Ph_WTOF(IEH,JEH);
 Eht_WTOF(IEH,JEH) = N_WTOF*Eh_WTOF(IEH,JEH);

**(WH_WTOF)WORKING HOURS OF OFFSHORE WIND TURBINES PER YEAR [h]*
 WH_WTOF = SUM ((IEH,JEH), WSOFR(IEH,JEH));

**HOURLY O&M COSTS [\$CAD/h] || HOURLY FIXED COSTS [\$CAD/h] || HOURLY ENERGY COST [¢CAD/kWh]*
 OMCh_WTOF(IEH,JEH) = OMC_MWhOF*EX_rate*Eht_WTOF(IEH,JEH);
 FCh_WTOF(IEH,JEH) = NP_WTOF*N_WTOF*Cins_WTOF*EX_rate*0.05*1.05**LS_WTOF / (1.05**LS_WTOF-1)/8760;

CkWhh_WTOF(IEH,JEH) = (OMCh_WTOF(IEH,JEH) + FCh_WTOF(IEH,JEH))/ Eht_WTOF(IEH,JEH)/1000*100;

**AVG ENERGY COST [¢CAD/kWh]*
 CkWh_WTOF = SUM ((IEH,JEH), CkWhh_WTOF(IEH,JEH))/8760;

**MAX FARM CAPACITY [MW] || AVAILABILITY OF OFFSHORE WIND [%]*
 Pmax_WTOF = N_WTOF*NP_WTOF;
 Avail_WTOF = WH_WTOF/8760*100;

**FORCING GAMS TO DISPLAY ZERO VALUES*
 WSOFR(IEH,JEH) \$ (Not WSOFR(IEH,JEH)) = EPS ;
 Ph_WTOF(IEH,JEH) \$ (Not Ph_WTOF(IEH,JEH)) = EPS ;
 Pht_WTOF(IEH,JEH) \$ (Not Pht_WTOF(IEH,JEH)) = EPS ;
 Eh_WTOF(IEH,JEH) \$ (Not Eh_WTOF(IEH,JEH)) = EPS ;
 Eht_WTOF(IEH,JEH) \$ (Not Eht_WTOF(IEH,JEH)) = EPS ;
 OMCh_WTOF(IEH,JEH) \$ (Not OMCh_WTOF(IEH,JEH)) = EPS ;
 FCh_WTOF(IEH,JEH) \$ (Not FCh_WTOF(IEH,JEH)) = EPS ;
 CkWhh_WTOF(IEH,JEH) \$ (Not CkWhh_WTOF(IEH,JEH)) = EPS ;

VARIABLES Ey_WTOF, Eyt_WTOF, CF_WTOF, OMC_WTOF, FC_WTOF, Ct_WTOF, FL_WTOF;

EQUATIONS eq250, eq251, eq252, eq253, eq254, eq255, eq256;

** offshore electricity produced per year, MWh/y per turbine*
 eq250.. Ey_WTOF =E= SUM ((IEH,JEH), Eh_WTOF(IEH,JEH));

** total offshore electricity produced per year, MWh/y*
 eq251.. Eyt_WTOF =E= SUM ((IEH,JEH), Eht_WTOF(IEH,JEH));

** capacity factor WTOF, %*
 eq252.. CF_WTOF =E= Ey_WTOF/(NP_WTOF*8760)*100;

** O&M costs offshore, \$CAD/y*
 eq253.. OMC_WTOF =E= OMC_MWhOF*EX_rate*Eyt_WTOF;

** FC costs offshore, \$CAD/y*
 eq254.. FC_WTOF =E= NP_WTOF*N_WTOF*Cins_WTOF*EX_rate * 0.05*1.05**LS_WTOF/(1.05**LS_WTOF-1);

```

* total offshore power cost,$CAD/y
eq255.. Ct_WTOF          =E=      OMC_WTOF + FC_WTOF;

* offshore WTOF full load hours per year, h/y
eq256.. FL_WTOF          =E=      Ey_WTOF/NP_WTOF;

MODEL WTOF OFFSHORE WIND TURBINES /eq250, eq251, eq252, eq253, eq254, eq255,
eq256/;

SOLVE WTOF USING MCP;

*DISPLAY 4 DIGITS AFTER THE DECIMAL POINT
OPTION decimals=4;

*CHECK IF THE MODEL IS EXECUTED WITH OPTIMAL SOLUTION
*[1 1] LINEAR, [1 2] NON-LINEAR
DISPLAY WTOF.MODELSTAT, WTOF.SOLVESTAT;
*=====

```

\$ONTEXT

VERSION: V2.0

DATE: 26-OCT-2011

1.3 PV SOLAR CELLS

-MODEL [SPR-400]; MANUFACTURER [SUNPOWER CORP.]; TYPE [ALL-BACK MONOCRYSTALLINE]

-No. OF CELLS IN ONE MODULE [128(8*16)]; MAX POWER [400W]; DIMENSIONS [1046x2067x54 mm]

-NOCT [45oC @ G=800 w/m2], Tair [20oC], WIND SPEED [1m/s], OPERATING TEMPERATURE [-45 to 85 oC]

-Life cycle emission from NG-fired combined cycle is (0.493 kg-CO2/kWhe), GHG from PV solar is (0.217 kg-CO2/kWhe) (Kannan et al., 2006)

\$OFFTEXT

*SCALARS FOR PV SOLAR CELLS

SCALARS

*ENTER THESE SCALARS

WS_PV	'**avg. wind speed, m/s'	/5/
Np_PV	'nominal power of PV module, W'	/400/
N_PV	'**No. of PV solar panels (modules)'	/50000/
LS_PV	'life span of PV cells, y'	/25/
LS_PVin	'life span of the inverter (PV cells), y'	/8/
Area_PV	'area of 1 PV panel (1.046x2.067), m2'	/2.162/
eff_PV	'module efficiency'	/0.185/
eff_PVin	'inverter efficiency, PV cells'	/0.95/
eff_PVtrns	'transformer efficiency, PV cells'	/0.99/
T_NOCT	'the nominal operating cell temp, oC'	/45/
Ta_NOCT	'the ambient air temp. @ NOCT, oC'	/20/
G_NOCT	'reference solar irradiance @ NOCT,W/m2'	/800/
alpha_PV	'temp-power coefficient'	/-0.0038/
IC400_PV	'installed capital cost per SPR400 module, CAD/MODULE'	/1324/
InvCW_PV	'invertor cost per watt, USD/W'	/0.714/
OMckWh_PV	'O&M cost per kWh, USD/kWh'	/0.01/
EX_rate	'\$CAD exchange rate, Sep-2011'	/1.03/;

SCALARS

Areat_PV	'total area covered by PV cells, m2'
Pmax_PV	'max. power can be produced, MW'
InvCh_PV	'hourly cost of inverter, \$CAD/h'
CkWh_PV	'avg cost of energy produced per year, ¢CAD/kWh';

SETS IEH /IEH1*IEH8760/, JEH /JEH1/;

PARAMETERS

Ta_PV(IEH,JEH)	'hourly ambient air temp. , oC'
G_PV(IEH,JEH)	'hourly solar irradiance/m2'
T_PV(IEH,JEH)	'hourly cell operating temp, oC'
TR(IEH,JEH)	'temp range check factor (1) in range,(0) out of range'
GR(IEH,JEH)	'radiation range check factor (1)in range,(0)out of range'
PVR(IEH,JEH)	'PV operation check,(1) ON, (0) OFF'
effp_PV(IEH,JEH)	'effective solar irradiance efficiency'
Eh_PV(IEH,JEH)	'net electricity produced per hour, MWh/h per module'
Eht_PV(IEH,JEH)	'total electricity produced per hour, MWh/h'
Ph_PV(IEH,JEH)	'power produced, MW per module'
Pht_PV(IEH,JEH)	'total power produced, MW'
OMCh_PV(IEH,JEH)	'hourly O&M costs, \$CAD/h'

```

FCh_PV(IEH,JEH)      'hourly FC costs, $CAD/h'
CkWhh_PV(IEH,JEH)   'hourly energy costs per MWh, ¢CAD/kWh';

*IMPORTING HOURLY AMBIENT AIR TEMP (oC) AND SOLAR IRRADIANCE (W/m2)
$LIBINCLUDE XLIMPORT Ta_PV      D:\EHInput.XLSX EHData!H4:I8764 COL
$LIBINCLUDE XLIMPORT G_PV      D:\EHInput.XLSX EHData!J4:K8764 COL

*[m2] || [MW]
Areat_PV              = Area_PV*N_PV;
Pmax_PV              = Np_PV*N_PV/1000/1000;

*HOURLY CELL OPERATING TEMP. [oC]
T_PV(IEH,JEH)       = G_PV(IEH,JEH)/G_NOCT*(T_NOCT-Ta_NOCT)+ Ta_PV(IEH,JEH) ;

*TEMP. & RADIATION CHECK FACTOR:[0] OUT OF RANGE,OR [1] INRANGE
TR(IEH,JEH)         = 1$( (T_PV(IEH,JEH) GE -40) AND (T_PV(IEH,JEH) LE 85) ) ;
GR(IEH,JEH)         = 1$(G_PV(IEH,JEH) GE 100) + 0;

*PV CELL OPERATION FACTOR CHECK: [0] OFF, [1] ON
PVR(IEH,JEH)= TR(IEH,JEH)*GR(IEH,JEH);

*EFFECTIVE SOLAR IRRADIANCE EFF.
effp_PV(IEH,JEH)$(T_PV(IEH,JEH) GT T_NOCT) = (eff_PV*(1 + alpha_PV*
(T_PV(IEH,JEH)-T_NOCT)));
effp_PV(IEH,JEH)$(T_PV(IEH,JEH) LE T_NOCT) = (eff_PV*(1 + alpha_PV*(T_NOCT-
T_PV(IEH,JEH))));

*(Eh_PV) NET ELECTRICITY PRODUCED PER MODULE [MWh/h] || (Et_PV) TOTAL NET
ELECTRCICITY PRODUCED [MWh/h]
Eh_PV(IEH,JEH)      = TR(IEH,JEH)*GR(IEH,JEH)*effp_PV(IEH,JEH)*eff_PVinv
*eff_PVtrns * G_PV(IEH,JEH)/(1000*1000)* Area_PV;

*PRODUCTION LIMIT PER PV MODULE [400 Wh/h]
Eh_PV(IEH,JEH)      $ (Eh_PV(IEH,JEH) GT (Np_PV/1000/1000)) =
(Np_PV/1000/1000);
Eht_PV(IEH,JEH)     = Eh_PV(IEH,JEH)*N_PV;

*(Ph_PV) POWER PRODUCED PER MODULE [MW] || (Pht_PV) TOTAL POWER PRODUCED [MW]
Ph_PV(IEH,JEH)      = Eh_PV(IEH,JEH);
Pht_PV(IEH,JEH)     = Ph_PV(IEH,JEH)*N_PV;

*HOURLY O&M COSTS [$CAD/h] || HOURLY FIXED COSTS [$CAD/h] || HOURLY INVERTER
COST [$CAD/h] ||HOURLY ENERGY COST [¢CAD/kWh]

OMCh_PV(IEH,JEH)    = OMckWh_PV*1000*EX_rate*Eht_PV(IEH,JEH);
FCh_PV(IEH,JEH)     = IC400_PV*N_PV*0.05*1.05**LS_PV/(1.05**LS_PV-
1)/8760;

InvCh_PV            = InvCW_PV*Np_PV*N_PV*EX_rate*0.05*1.05**LS_PVinv
/(1.05**LS_PVinv-1)/8760;

CkWhh_PV(IEH,JEH)  = ((OMCh_PV(IEH,JEH) + FCh_PV(IEH,JEH) + InvCh_PV)/
Eht_PV(IEH,JEH)/1000*100)$(Eht_PV(IEH,JEH) GT 0)+0;

*AVG ENERGY COST [¢CAD/kWh]
CkWh_PV             = SUM ((IEH,JEH), CkWhh_PV(IEH,JEH))/SUM ((IEH,JEH),
PVR(IEH,JEH));

```

```

*FORCING GAMS TO DISPLAY ZERO VALUES
T_PV(IEH,JEH)    $ (Not T_PV(IEH,JEH))    = EPS ;
TR(IEH,JEH)     $ (Not TR(IEH,JEH))      = EPS ;
GR(IEH,JEH)     $ (Not GR(IEH,JEH))      = EPS ;
PVR(IEH,JEH)    $ (Not PVR(IEH,JEH))     = EPS ;
Eh_PV(IEH,JEH)  $ (Not Eh_PV(IEH,JEH))   = EPS ;
Eht_PV(IEH,JEH) $ (Not Eht_PV(IEH,JEH))  = EPS ;
OMCh_PV(IEH,JEH) $ (Not OMCh_PV(IEH,JEH)) = EPS ;
FCh_PV(IEH,JEH) $ (Not FCh_PV(IEH,JEH))  = EPS ;
CkWhh_PV(IEH,JEH) $ (Not CkWhh_PV(IEH,JEH)) = EPS ;

VARIABLES Ey_PV, Eyt_PV, FC_PV, OMC_PV, InvC_PV, Ct_PV, GHG_PV, CF_PV;

EQUATIONS eq300, eq301, eq302, eq303, eq304, eq305, eq306, eq307;

* net electricity produced per year, MWh/y per module
eq300.. Ey_PV    =E=    SUM ((IEH,JEH), Eh_PV(IEH,JEH));

* total net electricity produced per year, MWh/y
eq301.. Eyt_PV   =E=    SUM ((IEH,JEH), Eht_PV(IEH,JEH));

* FC of PV cells, $CAD/y
eq302.. FC_PV    =E=    IC400_PV*N_PV*0.05*1.05**LS_PV/(1.05**LS_PV-1);

* O&M costs of PV cells, $CAD/y
eq303.. OMC_PV   =E=    OMckWh_PV*1000*EX_rate* Eyt_PV;

* inverter replacement cost,$CAD/y
eq304.. InvC_PV  =E=    InvCW_PV*Np_PV*N_PV*EX_rate*0.05*1.05**LS_PVinv
                        /(1.05**LS_PVinv-1);

* total PV costs, $CAD/y
eq305.. Ct_PV    =E=    OMC_PV + FC_PV + InvC_PV;

* total GHGs in term of CO2 saved, kg/y
eq306.. GHG_PV   =E=    0.493-0.217)* Eyt_PV*1000;

* capacity factor of PV module, %
eq307.. CF_PV    =E=    Ey_PV/(Np_PV/1000/1000*8760)*100;

MODEL PVSolar PV SOLAR CELLS /eq300, eq301, eq302, eq303, eq304, eq305,
                                eq306, eq307/;

SOLVE PVSolar USING MCP;

*DISPLAY 4 DIGITS AFTER THE DECIMAL POINT
OPTION decimals=4;

*CHECK IF THE MODEL IS EXECUTED WITH OPTIMAL SOLUTION
*[1 1] LINEAR, [1 2] NON-LINEAR
DISPLAY PVSolar.MODELSTAT, PVSolar.SOLVESTAT;
*=====

```

\$ONTEXT

VERSION: V2.0

DATE: 26-OCT-2011

1.4 ELECTROLYZERS:

- MODEL [HySTAT-60]; MANUFACTURER (HYDROGENICS Cor.).
- MAX H2 CAPACITY [60 Nm3/h @ 273 K & 1.013 bar]; POWER CONSUMPTION [5.2 kWh/Nm3]
- H2 OUTLET PRESSURE [10 bar= 1 MPa]; LIFESPAN [10y].
- ELZ OPERATION RANGE [40-100%].

\$OFFTEXT

*SCALARS FOR ELECTROLYZERS

SCALARS

*ENTER THESE SCALARS

PNm3_ELZ	'power cons, kWh/Nm3'	/5.2/
H2Cap_ELZ	'electrolyzer max capacity Nm3/h'	/60/
IC60_ELZ	'ELZ total installed capital cost, USD/60Nm3 of H2'	/634678/
LS_ELZ	'life span of the Elz, y'	/10/
EX_rate	'\$CAD exchange rate, Sep-2011'	/1.03/
HHV_H2	'higher heating value of H2 MJ/kg'	/141.9/
LHV_H2	'lower heating value of H2 MJ/kg'	/120.1/
CH2O_ELZ	'cost of demineralized water, \$CAD/1000kg'	/1.04/
eff_ELZinv	'inverter efficiency, PV cells'	/0.95/
InvCW_ELZ	'invertor cost per watt, USD/W'	/0.714/
LS_ELZinv	'life span on the inverter, y'	/8/;

SCALARS

eff_ELZ	'efficiency of the ELZ based on HHV of H2, %'
H2kgh_ELZ	'hourly H2 produced per Elz, kg/h'
H2Nm3h_ELZ	'hourly H2 produced per Elz, Nm3/h'
O2kgh_ELZ	'hourly O2 produced per Elz, kg/h'
O2Nm3h_ELZ	'hourly O2 produced per Elz, Nm3/h'
H2Okgh_ELZ	'hourly H2O consumed per Elz, kg/h'
Ph_ELZ	'power consumed per Elz, MW'
Eh_ELZ	'energy consumed per Elz, MWh/h'
Nmax_ELZ	'max. # of electrolyzers required'
CH2kgy_ELZ	'avg cost of H2, \$CAD/kg'
CO2kgy_ELZ	'avg cost of O2, \$CAD/kg'
SUMH2t_ELZ	'total H2 produced, kg/y'
SUMO2t_ELZ	'total O2 produced, kg/y'
InvCh_ELZ	'hourly inv. cost, \$CAD/h';

SETS IEH /IEH1*IEH8760/, JEH /JEH1/;

PARAMETERS

Eexch_ELZ(IEH,JEH)	'**hourly excess electricity, MWh/h'
Nh_ELZ(IEH,JEH)	'No of electrolyzer units in operation per hour'
H2kght_ELZ(IEH,JEH)	'total H2 produced per hour, kg/h'
H2Nm3ht_ELZ(IEH,JEH)	'total H2 produced per hour, Nm3/h'
O2kght_ELZ(IEH,JEH)	'total O2 produced per hour, kg/h'
O2Nm3ht_ELZ(IEH,JEH)	'total O2 produced per hour, Nm3/h'
H2Okght_ELZ(IEH,JEH)	'total H2O consumed per hour, kg/h'
Eht_ELZ(IEH,JEH)	'total energy consumed per hour, MWh/h'
Pht_ELZ(IEH,JEH)	'total power consumed, MW'
FCh_ELZ(IEH,JEH)	'FC per h per ELZ, \$CAD/h'
Fcht_ELZ(IEH,JEH)	'FC per h, \$CAD/h'
ELZF(IEH,JEH)	'ELZ operation check [0]OFF, [1]ON'

CkWhh_ELZ(IEH,JEH) 'hourly cost of electricity per kWh, ¢CAD/kWh'
 CkWhht_ELZ(IEH,JEH) 'total cost of consumed electricity per hour, \$CAD/h'
 CH2Oh_ELZ(IEH,JEH) 'total hourly cost of water consumed, \$CAD/h'
 FCh_ELZ(IEH,JEH) 'hourly fixed costs, \$CAD/h'
 OMCh_ELZ(IEH,JEH) 'hourly O&M costs, \$CAD/h'
 CH2kgh_ELZ(IEH,JEH) 'hourly H2 cost, \$CAD/kg'
 CO2kgh_ELZ(IEH,JEH) 'hourly O2 cost, \$CAD/kg';

*IMPORTING HOURLY EXCESS ELECTRICITY (MWh/h) & HOURLY ELECTRICITY PRICE
 (\$CAD/MWh)

\$LIBINCLUDE XLIMPORT Eexch_ELZ D:\EHInput.XLSX EHData!L4:M8764 COL
 \$LIBINCLUDE XLIMPORT CkWhh_ELZ D:\EHInput.XLSX EHData!N4:O8764 COL

eff_ELZ = HHV_H2*0.09015/(PNm3_ELZ*3600/1000)*100;
 Ph_ELZ = PNm3_ELZ*H2Cap_ELZ/1000;
 Eh_ELZ = Ph_ELZ;

*ELZ OPERATION CHECK FACTOR [0]OFF, [1]ON

ELZF(IEH,JEH) =1\$((Eexch_ELZ(IEH,JEH)/eff_ELZinv) GT (Eh_ELZ*0.40))+0;

*ELZ PRODUCTION CAPACITIES [kg/h, Nm3/h]

H2kgh_ELZ = H2Cap_ELZ*(101.3*2.02/(8.314*273));
 O2kgh_ELZ = (32/2.02)/2*H2kgh_ELZ;
 H2Okgh_ELZ = (18.02/2.02)*H2kgh_ELZ;
 H2Nm3h_ELZ = H2Cap_ELZ;
 O2Nm3h_ELZ = (8.314*273/32/101.3)*O2kgh_ELZ;

*NO. OF ELZs REQUIRED PER HOUR

Nh_ELZ(IEH,JEH)= eff_ELZinv*Eexch_ELZ(IEH,JEH)/Ph_ELZ;

*CHECK IF THE ELZ OPERATION IN RANGE [40-100%]

Nh_ELZ(IEH,JEH) \$ (FRAC(Nh_ELZ(IEH,JEH)) LT 0.40) = FLOOR(Nh_ELZ(IEH,JEH))
 ;
 Nmax_ELZ = SMAX((IEH,JEH),Nh_ELZ(IEH,JEH));

*H2,O2,H2O MASS FLOW [kg/h]

H2kght_ELZ(IEH,JEH) = Nh_ELZ(IEH,JEH)*H2kgh_ELZ;
 O2kght_ELZ(IEH,JEH) = Nh_ELZ(IEH,JEH)*O2kgh_ELZ;
 H2Okght_ELZ(IEH,JEH) = Nh_ELZ(IEH,JEH)*H2Okgh_ELZ;

*H2,O2,H2O VOL. FLOW RATE [Nm3/h]

H2Nm3ht_ELZ(IEH,JEH) = Nh_ELZ(IEH,JEH)*H2Nm3h_ELZ;
 O2Nm3ht_ELZ(IEH,JEH) = Nh_ELZ(IEH,JEH)*O2Nm3h_ELZ;

*(Pht_ELZ)TOTAL POWER [MW] | |(Eht_ELZ)TOTAL HOURLY ENERGY CONSUMED [MWh/h]

Pht_ELZ(IEH,JEH) = Nh_ELZ(IEH,JEH)*Ph_ELZ;
 Eht_ELZ(IEH,JEH) = Nh_ELZ(IEH,JEH)*Eh_ELZ;

*TOTAL HOURLY COST OF ELECTRICITY [\$CAD/h]

CkWhht_ELZ(IEH,JEH) = CkWhh_ELZ(IEH,JEH)/100*1000*Eht_ELZ(IEH,JEH);

*TOTAL HOURLY COST OF WATER CONSUMED [\$CAD/h]

CH2Oh_ELZ(IEH,JEH) = (CH2O_ELZ/1000)* H2Okght_ELZ(IEH,JEH);

*HOURLY FIXED COSTS [\$CAD/h]

FCh_ELZ(IEH,JEH) = IC60_ELZ*Nmax_ELZ*EX_rate*0.05*1.05**LS_ELZ
 /(1.05**LS_ELZ-1)/8760;

**HOURLY O&M COSTS [\$CAD/h]*

$$\text{OMCh_ELZ(IEH,JEH)} = 0.05 * \text{FCh_ELZ(IEH,JEH)} + \text{CkWhht_ELZ(IEH,JEH)} + \text{CH2Oh_ELZ(IEH,JEH)} ;$$

**HOURLY INVERTER COST [\$CAD/h]*

$$\text{InvCh_ELZ} = \text{InvCW_ELZ} * (\text{Ph_ELZ} * 1000 * 1000) * \text{Nmax_ELZ} * \text{EX_rate} * 0.05 * 1.05 ** \text{LS_ELZinv} / (1.05 ** \text{LS_ELZinv} - 1) / 8760 ;$$

**HOURLY H2 COST [\$CAD/kg]*

$$\text{SUMH2t_ELZ} = \text{SUM}((\text{IEH,JEH}), \text{H2kght_ELZ(IEH,JEH)}) ;$$

$$\text{SUMO2t_ELZ} = \text{SUM}((\text{IEH,JEH}), \text{O2kght_ELZ(IEH,JEH)}) ;$$

$$\text{CH2kgh_ELZ(IEH,JEH)} = 0.70 * (\text{FCh_ELZ(IEH,JEH)} + \text{OMCh_ELZ(IEH,JEH)} + \text{InvCh_ELZ}) / \text{H2kght_ELZ(IEH,JEH)} ;$$

$$\text{CO2kgh_ELZ(IEH,JEH)} = (1 - 0.70) * (\text{FCh_ELZ(IEH,JEH)} + \text{OMCh_ELZ(IEH,JEH)} + \text{InvCh_ELZ}) / \text{O2kght_ELZ(IEH,JEH)} ;$$

**AVG H2 & O2 COSTS [\$CAD/kg]*

$$\text{CH2kgy_ELZ} = \text{SUM}((\text{IEH,JEH}), \text{CH2kgh_ELZ(IEH,JEH)}) / 8760 ;$$

$$\text{CO2kgy_ELZ} = \text{SUM}((\text{IEH,JEH}), \text{CO2kgh_ELZ(IEH,JEH)}) / 8760 ;$$

**DISPLAY ZERO VALUES*

ELZF(IEH,JEH)	\$ (Not ELZF(IEH,JEH))	= EPS ;
Nh_ELZ(IEH,JEH)	\$ (Not Nh_ELZ(IEH,JEH))	= EPS ;
Eht_ELZ(IEH,JEH)	\$ (Not Eht_ELZ(IEH,JEH))	= EPS ;
Pht_ELZ(IEH,JEH)	\$ (Not Pht_ELZ(IEH,JEH))	= EPS ;
H2kght_ELZ(IEH,JEH)	\$ (Not H2kght_ELZ(IEH,JEH))	= EPS ;
H2Nm3ht_ELZ(IEH,JEH)	\$ (Not H2Nm3ht_ELZ(IEH,JEH))	= EPS ;
O2kght_ELZ(IEH,JEH)	\$ (Not O2kght_ELZ(IEH,JEH))	= EPS ;
O2Nm3ht_ELZ(IEH,JEH)	\$ (Not O2Nm3ht_ELZ(IEH,JEH))	= EPS ;
H2Okght_ELZ(IEH,JEH)	\$ (Not H2Okght_ELZ(IEH,JEH))	= EPS ;
CkWhht_ELZ(IEH,JEH)	\$ (Not CkWhht_ELZ(IEH,JEH))	= EPS ;
CH2Oh_ELZ(IEH,JEH)	\$ (Not CH2Oh_ELZ(IEH,JEH))	= EPS ;
FCh_ELZ(IEH,JEH)	\$ (Not FCh_ELZ(IEH,JEH))	= EPS ;
OMCh_ELZ(IEH,JEH)	\$ (Not OMCh_ELZ(IEH,JEH))	= EPS ;
CH2kgh_ELZ(IEH,JEH)	\$ (Not CH2kgh_ELZ(IEH,JEH))	= EPS ;

SCALARS Ct_ELZ, FC_ELZ, OMC_ELZ, InvCy_ELZ, CkWhyt_ELZ, CH2Oy_ELZ;

**Total cost of electricity consumed per year, \$CAD/y*

$$\text{CkWhyt_ELZ} = \text{SUM}((\text{IEH,JEH}), \text{CkWhht_ELZ(IEH,JEH)}) ;$$

** INVERTERS COST*

$$\text{InvCy_ELZ} = \text{InvCW_ELZ} * (\text{Ph_ELZ} * 1000 * 1000) * \text{Nmax_ELZ} * \text{EX_rate} * 0.05 * 1.05 ** \text{LS_ELZinv} / (1.05 ** \text{LS_ELZinv} - 1) ;$$

**FIXED COSTS*

$$\text{FC_ELZ} = \text{Nmax_ELZ} * \text{IC60_ELZ} * \text{EX_rate} * 0.05 * 1.05 ** \text{LS_ELZ} / (1.05 ** \text{LS_ELZ} - 1) ;$$

**total cost of H2O consumed per year, \$CAD/y*

$$\text{CH2Oy_ELZ} = \text{SUM}((\text{IEH,JEH}), \text{CH2Oh_ELZ(IEH,JEH)}) ;$$

**O&M costs of Elzs, \$CAD/y*

$$\text{OMC_ELZ} = 0.05 * \text{FC_ELZ} + \text{CkWhyt_ELZ} + \text{CH2Oy_ELZ} ;$$

```

*TOTAL COSTS OF ELZS, $CAD/y
Ct_ELZ          =      OMC_ELZ + FC_ELZ + InvCy_ELZ;

VARIABLES  H2kgyt_ELZ, H2Nm3yt_ELZ, O2kgyt_ELZ, O2Nm3yt_ELZ, H2Okgyt_ELZ,
            Eyt_ELZ, Z, X1, X2;

EQUATIONS eq400, eq401, eq402, eq403,eq404, eq405,eq406, eq407,eq408, eq409;

eq400..  Z                      =E=      X1*Ct_ELZ + X2*Ct_ELZ;

*total H2 produced by Elzs, kg/y
eq401..  H2kgyt_ELZ            =E=      SUM ((IEH,JEH), H2kght_ELZ(IEH,JEH));

* total H2 produced by Elzs, Nm3/y
eq402..  H2Nm3yt_ELZ          =E=      SUM ((IEH,JEH), H2Nm3ht_ELZ(IEH,JEH));

* total O2 produced by Elzs, kg/y
eq403..  O2kgyt_ELZ           =E=      SUM ((IEH,JEH), O2kght_ELZ(IEH,JEH));

* total O2 produced by Elzs, Nm3/y
eq404..  O2Nm3yt_ELZ          =E=      SUM ((IEH,JEH), O2Nm3ht_ELZ(IEH,JEH));

* total water consumed per year, kg/y
eq405..  H2Okgyt_ELZ          =E=      SUM ((IEH,JEH), H2Okght_ELZ(IEH,JEH));

* total energy consumed by Elzs per year, MWh/y
eq406..  Eyt_ELZ              =E=      SUM ((IEH,JEH), Eht_ELZ(IEH,JEH));

eq407..  X1 + X2              =E= 1;

eq408..  X1                   =G= 0.1;

eq409..  X2                   =G= 0.1;

MODEL ELZ THE ELECTROLYZER MODEL /eq400, eq401, eq402, eq403, eq404,
            eq405, eq406, eq407, eq408, eq409/;

SOLVE ELZ USING LP MINIMIZING Z;

*DISPLAY 4 DIGITS AFTER THE DECIMAL POINT
OPTION decimals=4;

*CHECK IF THE MODEL IS EXECUTED WITH OPTIMAL SOLUTION
*[1 1] LINEAR, [1 2] NON-LINEAR
DISPLAY ELZ.MODELSTAT, ELZ.SOLVESTAT;
*=====

```